

University of Alberta

Characterization of bacteriophage receptors in the *Burkholderia cepacia*
complex (Bcc)

by

Gerardo R. Juárez-Lara

A thesis submitted to the Faculty of Graduate Studies and Research
in partial fulfillment of the requirements for the degree of

Master of Science

in

Microbiology and Biotechnology

Biological Sciences

©Gerardo Rubén Juárez-Lara

Spring 2013

Edmonton, Alberta

Permission is hereby granted to the University of Alberta Libraries to reproduce single copies of this thesis and to lend or sell such copies for private, scholarly or scientific research purposes only. Where the thesis is converted to, or otherwise made available in digital form, the University of Alberta will advise potential users of the thesis of these terms.

The author reserves all other publication and other rights in association with the copyright in the thesis and, except as herein before provided, neither the thesis nor any substantial portion thereof may be printed or otherwise reproduced in any material form whatsoever without the author's prior written permission.

DEDICATION

I would like to dedicate this research to my parents Miguel. A. Juárez Perez and Aurora Lara Flores. My sisters Aurora A. Juárez Lara and Brenda I. Juárez Lara.

To my uncle Miguel Angel Juárez Perez and my aunt Dolores Valdés Romero who I consider my second parents.

And finally to my best friends Enrique A. Rodriguez Galvan, Andrea Estevez, Sandra I. Pinedo Leyva and Paz C. Gutierrez Rosas.

ABSTRACT

Because of their ability to infect bacterial cells, bacteriophages or phages (viruses that infect and kill bacteria) show promise in treating diseases caused by multidrug resistant bacteria like the *Burkholderia cepacia* complex (Bcc). In order to carry out their lifecycle, phages must recognize, adsorb to, and inject their genetic material into the host. Host recognition is a crucial stage during phage infection and is divided in two main stages: a) reversible binding, characterized by low affinity binding of the phage to a secondary receptor in the outermost membrane of the host, and b) irreversible binding, characterized by a high affinity binding of the phage to its primary receptor. A wide variety of phage receptors have been characterized including lipopolysaccharide, pili, flagella, porins, capsules, and ligand-gated porins. Two random transposon insertion libraries were screened against a collection of Bcc specific phages. Bacterial mutants resistant to phage infection were then isolated and the disrupted genes and proteins involved in phage adherence were characterized.

ACKNOWLEDGEMENT

I would like to acknowledge the people that helped me and supported me during my Masters degree. Firstly, I would like to thank Dr. Jonathan Dennis for taking me as a grad student into your lab, and taking a chance on someone from a non-English speaking country with a Bachelors in Biology with perhaps not enough experience in Molecular Biology and Genetics.

I would like to thank too to my committee members Dr. Stefan Pukatzki and Dr. Christine Szymanski for all their support and advice and to Dr. Mario Feldman and people from the Feldman lab, for helping me with an appropriate LPS extraction protocol.

I would also like to thank all my family. They all made a huge sacrifice helping me to move to Canada. Special thanks go to Mom and Dad who never prevented me from following my dreams, even though it meant moving to a different country.

Finally, I would like to thank all my Canadian friends. Especially Euan Thomson, Megan Goudie, Mandi Goudie, Leslie Bush, and Shannon Leblanc. You guys are what I consider to be my Canadian family, and made my transition from México to Canada less difficult. Thank you all!

TABLE OF CONTENTS

INTRODUCTION.....	1
The <i>Burkholderia cepacia</i> complex (Bcc).....	2
Antibiotic resistance mechanisms of the Bcc.....	3
Bacteriophages (Phages).....	4
Phage therapy.....	5
Bacteriophages life cycle.....	7
Bacteriophage host recognition and adsorption.....	9
Bacterial cells walls and their potential receptors for bacteriophages.....	12
Bacteriophage host recognition and adsorption to the Gram-negatives cell wall.....	12
Porins, Porin-like and Ligand-gated porins (LGP) as bacteriophage Receptors.....	14
Bacteriophages utilizing OmpA as a receptor.....	16
Bacteriophages utilizing enzymes (OmpT & OmpX) as receptors.....	17
Bacteriophages utilizing Lipopolysaccharide (LPS) as a receptor.....	17
Other potential receptors for bacteriophage adsorption (Flagella, pili and capsules).....	23
Bacteriophages utilizing flagella as receptors.....	24
Bacteriophages utilizing pili as a receptor.....	25
Bacteriophages utilizing capsular polysaccharides (CPS) as a receptor...	27
Tailless phages: Host recognition and adsorption.....	30

MATERIALS & METHODS.....	37
Bacterial strains & growth conditions.....	38
Bacteriophage propagation.....	40
Plasposon mutant library construction.....	40
Identification of phages able to clear bacterial liquid cultures.....	40
Plasposon mutant library screening.....	41
DNA manipulation, plasposon isolation and DNA sequencing.....	43
Bacteriophage infection assays vs. LPS truncated mutants [Liquid culture clearing assays].....	45
Bacteriophage infection assays vs. LPS truncated mutants [Efficiency of plating (EOPs)].....	45
Molecular Cloning.....	45
Plasmid Conjugation.....	53
Bacteriophage infection assays vs. LPS complemented mutants [Liquid culture clearing assays].....	54
LPS extraction & SDS-polyacrylamide gel electrophoresis.....	55
Western Blots.....	56
Transmission electron microscopy (TEM).....	57
Swarming and Twitching Motility Assays.....	58
RESULTS & DISCUSSION.....	60
Towards the identification of phages able to clear liquid cultures.....	61
Plasposon mutant library screening.....	72
Plasposon mutant library screening confirmatory assays [Solid media].....	102

Plasposon mutant library screening in minimal media (MM).....	104
Plasposon isolation and sequencing of disrupted genes.....	104
Genes <i>wbxD</i> & <i>wbcE</i> and their function.....	119
Bacteriophage infection assays vs. LPS truncated mutants [Liquid culture clearing assays].....	120
Bacteriophage infection assays vs. LPS truncated mutants [Efficiency of plating (EOP)].....	138
Molecular cloning of <i>wbxD</i> & <i>wbcE</i> into pSCRhaB3 Tp-Tc and modification of pXO3 into pXO3 Tp-Tc.....	142
Complementation of pXO3 Tp-Tc, pXO4 Tp-Tc, pXO7 Tp-Tc and pSCRhaB3 Tp-Tc into the K56-2::pTnMod-OTp' KS4-M & KS12 resistant mutant 16 E1 (<i>wbxD-wbcE</i> ::Tp ^R) and into K56-2 wt.....	149
Bacteriophage infection assays vs. K56-2::pTnModOTp' mutant 16 E1 (<i>wbxD-wbcE</i> ::Tp ^R) complemented with pXO3 Tp-Tc, pXO4 Tp-Tc, pXO7 Tp-Tc and pSCRhaB3 Tp-Tc [Liquid culture clearing assays].....	151
LPS extraction, purification and visualization from mutant 16 E1 complemented with pXO3 Tp-Tc, pXO4 Tp-Tc, pXO7 Tp-Tc and pSCRhaB3 Tp-Tc and from K56-2 wt complemented with same set of plasmids.....	168
Molecular cloning and modification of pSCRhaB2 into pSCRhaB2-Tc.....	172
Molecular cloning of <i>waaC</i> & <i>wabO</i> into pSCRhaB2-Tc.....	176
Complementation of pSC <i>wabO</i> -Tc, pSC <i>waaC</i> -Tc and pSCRhaB2-Tc into the K56-2 LPS truncated mutants XOA8 (<i>wabO</i> ::pGPΩTp Tp ^R) and CCB1	

(<i>waaC</i> ::pGPΩTp Tp ^R).....	179
Bacteriophage infection assays vs. K56-2 LPS truncated mutants XOA8 (<i>wabO</i> ::pGPΩTp Tp ^R) complemented with pSC <i>wabO</i> -Tc and pSCRhaB2- Tc and CCB1 (<i>waaC</i> ::pGPΩTp Tp ^R) complemented with pSC <i>waaC</i> -Tc and pSCRhaB2-Tc [Liquid culture clearing assays].....	181
LPS extraction, purification and visualization from XOA8 (<i>wabO</i> ::pGPΩTp Tp ^R) complemented with pSC <i>wabO</i> -Tc and pSCRhaB2-Tc and from CCB1 (<i>waaC</i> ::pGPΩTp Tp ^R) complemented with pSC <i>waaC</i> -Tc and pSCRhaB2-Tc.....	194
Western Blots from mutant 16 E1 complemented with pXO4 Tp-Tc, pXO7 Tp-Tc and pSCRhaB3 Tp-Tc and from K56-2 LPS mutants XOA8 (<i>wabO</i> ::pGPΩTp Tp ^R) complemented with pSC <i>wabO</i> -Tc and pSCRhaB2- Tc and from CCB1 (<i>waaC</i> ::pGPΩTp Tp ^R) complemented with pSC <i>waaC</i> - Tc and pSCRhaB2-Tc.....	197
Transmission electron microscopy (TEM) from PC184 pTn <i>ModluxO</i> Tp' DC1 resistant mutant 72 C12 (<i>pulO</i> ::Tp ^R), PC184 wt and 72 C12 (<i>pulO</i> ::Tp ^R) incubated with phage DC1.....	202
Swarming and Twitching Motility assays from PC184::pTn <i>ModluxO</i> Tp' DC1 resistant mutants, PC184 wt and <i>Pseudomonas aeruginosa</i> strain PAO1.....	207
CONCLUSION.....	214
Bacteriophage receptors and their implications in phage therapy.....	215
LITERATURE CITED.....	219

LIST OF TABLES

Table 1: Phages that require at least two receptors in order to infect the host.....	35
Table 2: Bacterial species and strains used in this research.....	39
Table 3: <i>B. cenocepacia</i> K56-2 LPS truncated mutants used in this research.....	39
Table 4: Plasmids used in this research.....	51
Table 5: PCR specifications and primers used in this research.....	52
Table 6: Bcc specific bacteriophages tested to determine if bacterial liquid cultures are cleared.....	62
Table 7: Ten <i>B. cenocepacia</i> K56-2::TnModOTp' KS4-M resistant mutants....	109
Table 8: Six <i>B. cenocepacia</i> PC184::pTnModluxOTp' DC1 resistant mutants..	115
Table 9: Two <i>B. cenocepacia</i> PC184::pTnModluxOTp' KS10 and SR1 resistant Mutants.....	118
Table 10: Bcc specific bacteriophages tested in this study and their receptors..	213

LIST OF FIGURES

Figure 1: Bacteriophages' lytic lifecycle.....	8
Figure 2: The Gram-negative cell wall depicting all potential phage receptors...	13
Figure 3: Simplified LPS structure from <i>B. cenocepacia</i> strain K56-2.....	19
Figure 4: Growth curve of <i>B. cenocepacia</i> PC184 wt exposed to phage DC1.....	63
Figure 5: Growth curve of <i>B. cenocepacia</i> K56-2 wt exposed to phage KS5.....	64
Figure 6: Growth curve of <i>B. cenocepacia</i> K56-2 wt exposed to phage KS9.....	65
Figure 7: Growth curve of <i>B. cenocepacia</i> PC184 wt exposed to phage KS10....	66
Figure 8: Growth curve of <i>B. cenocepacia</i> K56-2 wt exposed to phage KS12....	67
Figure 9: Growth curve of <i>B. cenocepacia</i> PC184 wt exposed to phage KS14....	68
Figure 10: Growth curve of <i>B. cenocepacia</i> K56-2 wt exposed to phage KL1...	69
Figure 11: Growth curve of <i>B. cenocepacia</i> K56-2 wt exposed to phage AH2...	70
Figure 12: Growth curve of <i>B. cenocepacia</i> PC184 wt exposed to phage SR.....	71
Figure 13: Growth curve of <i>B. cenocepacia</i> K56-2::pTnModOTp' mutant 15 E11 (Glycosyltransferase::Tp ^R) exposed to phage KS4-M.....	73
Figure 14: Growth curve of <i>B. cenocepacia</i> K56-2::pTnModOTp' mutant 16 E1 (<i>wbxD-wbcE</i> ::Tp ^R) exposed to phage KS4-M.....	74
Figure 15: Growth curve of <i>B. cenocepacia</i> K56-2::pTnModOTp' mutant 20 A12 (<i>wbxD-wbcE</i> ::Tp ^R) exposed to phage KS4-M.....	75
Figure 16: Growth curve of <i>B. cenocepacia</i> K56-2::pTnModOTp' mutant 21 C7 (Glycosyltransferase::Tp ^R) exposed to phage KS4-M.....	76
Figure 17: Growth curve of <i>B. cenocepacia</i> K56-2::pTnModOTp' mutant 22 G8 (ESA_02316::Tp ^R) exposed to phage KS4-M.....	77

Figure 18: Growth curve of <i>B. cenocepacia</i> K56-2::pTnModOTp' mutant 32 F4 (Putative phage membrane protein BCAM1921::Tp ^R) exposed to phage KS4-M.....	78
Figure 19: Growth curve of <i>B. cenocepacia</i> K56-2::pTnModOTp' mutant 67 B4 (Glycosyltransferase::Tp ^R) exposed to phage KS4-M.....	79
Figure 20: Growth curve of <i>B. cenocepacia</i> K56-2::pTnModOTp' mutant 67 F1 (Hypothetical protein BCAS0773A::Tp ^R) exposed to phage KS4-M.....	80
Figure 21: Growth curve of <i>B. cenocepacia</i> K56-2::pTnModOTp' mutant 72 D1 (<i>wbxD-wbcE</i> ::Tp ^R) exposed to phage KS4-M.....	81
Figure 22: Growth curve of <i>B. cenocepacia</i> K56-2::pTnModOTp' mutant 73 F6 (<i>wbxD-wbcE</i> ::Tp ^R) exposed to phage KS4-M.....	82
Figure 23: Growth curve of <i>B. cenocepacia</i> K56-2::pTnModOTp' mutant 20 A12 (<i>wbxD-wbcE</i> ::Tp ^R) exposed to phage KS12.....	83
Figure 24: Growth curve of <i>B. cenocepacia</i> K56-2::pTnModOTp' mutant 67 B4 (Glycosyltransferase::Tp ^R) exposed to phage KS12.....	84
Figure 25: Growth curve of <i>B. cenocepacia</i> K56-2 pTnMod-OTp' mutant 67 F1 (Hypothetical protein BCAS0773A::Tp ^R) exposed to phage KS12.....	85
Figure 26: Growth curve of <i>B. cenocepacia</i> K56-2::pTnModOTp' mutant 22 G8 (ESA_02316::Tp ^R) exposed to phage KS9.....	86
Figure 27: Growth curve of <i>B. cenocepacia</i> K56-2::pTnModOTp' mutant 67 B4 (Glycosyltransferase::Tp ^R) exposed to phage KS9.....	87
Figure 28: Growth curve of <i>B. cenocepacia</i> K56-2::pTnModOTp' mutant 72 D1 (<i>wbxD-wbcE</i> ::Tp ^R) exposed to phage KS9.....	88

Figure 29: Growth curve of <i>B. cenocepacia</i> K56-2::pTnModOTp' mutant 73 F6 (<i>wbxD-wbcE</i> ::Tp ^R) exposed to phage KS9.....	89
Figure 30: Growth curve of <i>B. cenocepacia</i> K56-2::pTnModOTp' mutant 32 F4 (Putative phage membrane protein BCAM1921::Tp ^R) exposed to phage KS5.....	90
Figure 31: Growth curve of <i>B. cenocepacia</i> K56-2 pTnModOTp' mutant 67 F1 (Hypothetical protein BCAS0773A::Tp ^R) exposed to phage KS5.....	91
Figure 32: Growth curve of <i>B. cenocepacia</i> PC184::pTnModluxOTp' mutant 49 B12 (<i>gspM</i> ::Tp ^R) exposed to phage DC1.....	92
Figure 33: Growth curve of <i>B. cenocepacia</i> PC184::TnModluxOTp' mutant 54 H3 (<i>gspM</i> ::Tp ^R) exposed to phage DC1.....	93
Figure 34: Growth curve of <i>B. cenocepacia</i> PC184::TnModluxOTp' mutant 72 C12 (<i>pulO</i> ::Tp ^R) exposed to phage DC1.....	94
Figure 35: Growth curve of <i>B. cenocepacia</i> PC184::TnModluxOTp' mutant 76 B3 (Hypothetical protein BCPG_02344::Tp ^R) exposed to phage DC1.....	95
Figure 36: Growth curve of <i>B. cenocepacia</i> PC184::TnModluxOTp' mutant 76 D2 (<i>gspJ</i> ::Tp ^R) exposed to phage DC1.....	96
Figure 37: Growth curve of <i>B. cenocepacia</i> PC184::TnModluxOTp' mutant 76 H8 (<i>gspM?</i> ::Tp ^R) exposed to phage DC1.....	97
Figure 38: Growth curve of <i>B. cenocepacia</i> PC184::pTnModluxOTp' mutant 30 D1 (UDP-glucose LOS-beta-1,4 Glucosyltransferase <i>Bcenmc03_2331</i> ::Tp ^R) exposed to phage KS10.....	98

Figure 39: Growth curve of <i>B. cenocepacia</i> PC184::pTn <i>Modlux</i> OTp' mutant 30 F7 (ADP-L-glycero-D-manno-heptose-6-epimerase? <i>Bcenmc03_1012</i> ::Tp ^R) exposed to phage KS10.....	99
Figure 40: Growth curve of <i>B. cenocepacia</i> PC184::pTn <i>Modlux</i> OTp' mutant 30 D1 (UDP-glucose LOS-beta-1,4 Glucosyltransferase <i>Bcenmc03_2331</i> ::Tp ^R) exposed to phage SR1.....	100
Figure 41: Growth curve of <i>B. cenocepacia</i> PC184::pTn <i>Modlux</i> OTp' mutant 30 F7 (ADP-L-glycero-D-manno-heptose-6-epimerase? <i>Bcenmc03_1012</i> ::Tp ^R) exposed to phage SR1.....	101
Figure 42: NCBI genomic context and organization of the <i>B. cenocepacia</i> J2315 region containing the disrupted genes from the KS4-M resistant mutants (16 E1, 20 A12, 72 D1 and 73 F6).....	106
Figure 43: NCBI genomic context and organization of the <i>Cronobacter sakazakii</i> ATCC BAA-894 region containing the disrupted gene from the KS4-M resistant mutant (22 G8).....	107
Figure 44: NCBI genomic context and organization of the <i>B. cenocepacia</i> J2315 region containing the disrupted gene from the KS4-M resistant mutant (32 F4).....	108
Figure 45: NCBI genomic context and organization of the <i>B. cenocepacia</i> J2315 region containing the disrupted gene from the KS4-M resistant mutant (67 F1).....	108
Figure 46: Schematic comparison between the T2SS and type IV pili biogenesis.....	112

Figure 47: NCBI genomic context and organization of the <i>B. cenocepacia</i> J2315 region containing the disrupted gene from the DC1 resistant mutants (49 B12, 54 H3 and 76 H8?).....	113
Figure 48: NCBI genomic context and organization of the <i>B. cenocepacia</i> MC0-3 region containing the disrupted gene from the KS10, SR1 resistant mutant (30 D1).....	116
Figure 49: NCBI genomic context and organization of the <i>B. cenocepacia</i> AU 1054 region containing the disrupted genes from the KS10, SR1 resistant mutant (30 F7).....	117
Figure 50: Genetic organization of the <i>B. cenocepacia</i> K56-2 region containing genes for core oligosaccharide OS and O-antigen biosynthesis (Adapted from Ortega et al., 2009).....	120
Figure 51: Structural assignments of the core OS and O-antigen subunit from <i>B. cenocepacia</i> K56-2 LPS truncated mutants (Adapted from Ortega et al., 2009).....	122
Figure 52: Growth curve of <i>B. cenocepacia</i> K56-2 LPS mutant XOA7 (<i>waaL</i> ::pGPΩTp Tp ^R) exposed to phage KS12.....	124
Figure 53: Growth curve of <i>B. cenocepacia</i> K56-2 LPS mutant XOA8 (<i>wabO</i> ::pGPΩTp Tp ^R) exposed to phage KS12.....	125
Figure 54: Growth curve of <i>B. cenocepacia</i> K56-2 LPS mutant RSF19 (<i>wbxE</i> ::pRF201 Tp ^R) exposed to phage KS12.....	126
Figure 55: Growth curve of <i>B. cenocepacia</i> K56-2 LPS mutant CCB1 (<i>waaC</i> ::pGPΩTp Tp ^R) exposed to phage KS12.....	127

Figure 56: Growth curve of <i>B. cenocepacia</i> K56-2 LPS mutant XOA15 (<i>wabR</i> ::pGPΩTp Tp ^R) exposed to phage KS12.....	128
Figure 57: Growth curve of <i>B. cenocepacia</i> K56-2 LPS mutant XOA17 (<i>wabS</i> ::pGPApTp Tp ^R) exposed to phage KS12.....	129
Figure 58: Growth curve of <i>B. cenocepacia</i> K56-2 LPS mutant XOA7 (<i>waaL</i> ::pGPΩTp Tp ^R) exposed to phage KS4-M.....	130
Figure 59: Growth curve of <i>B. cenocepacia</i> K56-2 LPS mutant XOA7 (<i>waaL</i> ::pGPΩTp Tp ^R) exposed to phage KS5.....	132
Figure 60: Growth curve of <i>B. cenocepacia</i> K56-2 LPS mutant XOA8 (<i>wabO</i> ::pGPΩTp Tp ^R) exposed to phage KS5.....	133
Figure 61: Growth curve of <i>B. cenocepacia</i> K56-2 LPS mutant RSF19 (<i>wbxE</i> ::pRF201 Tp ^R) exposed to phage KS5.....	134
Figure 62: Growth curve of <i>B. cenocepacia</i> K56-2 LPS mutant CCB1 (<i>waaC</i> ::pGPΩTp Tp ^R) exposed to phage KS5.....	135
Figure 63: Growth curve of <i>B. cenocepacia</i> K56-2 LPS mutant XOA15 (<i>wabR</i> ::pGPΩTp Tp ^R) exposed to phage KS5.....	136
Figure 64: Growth curve of <i>B. cenocepacia</i> K56-2 LPS mutant XOA17 (<i>wabS</i> ::pGPApTp Tp ^R) exposed to phage KS5.....	137
Figure 65: Efficiency of plating (EOP) of phage KS4 vs. <i>B. cenocepacia</i> K56-2 LPS mutants XOA7 (<i>waaL</i> ::pGPΩTp Tp ^R), XOA8 (<i>wabO</i> ::pGPΩTp Tp ^R), RSF19 (<i>wbxE</i> ::pRF201 Tp ^R), CCB1 (<i>waaC</i> ::pGPΩTp Tp ^R), XOA15 (<i>wabR</i> ::pGPΩTp Tp ^R) and XOA17 (<i>wabS</i> ::pGPApTp Tp ^R).....	139

Figure 66: Efficiency of plating (EOP) of phage KS4-M vs. <i>B. cenocepacia</i> K56-2 LPS mutants XOA7 (<i>waaL</i> ::pGPΩTp Tp ^R), XOA8 (<i>wabO</i> ::pGPΩTp Tp ^R), RSF19 (<i>wbxE</i> ::pRF201 Tp ^R), CCB1 (<i>waaC</i> ::pGPΩTp Tp ^R), XOA15 (<i>wabR</i> ::pGPΩTp Tp ^R) and XOA17 (<i>wabS</i> ::pGPAPTp Tp ^R).....	140
Figure 67: Efficiency of plating (EOP) of phage KS12 vs. <i>B. cenocepacia</i> K56-2 LPS mutants XOA7 (<i>waaL</i> ::pGPΩTp Tp ^R), XOA8 (<i>wabO</i> ::pGPΩTp Tp ^R), RSF19 (<i>wbxE</i> ::pRF201 Tp ^R), CCB1 (<i>waaC</i> ::pGPΩTp Tp ^R), XOA15 (<i>wabR</i> ::pGPΩTp Tp ^R) and XOA17 (<i>wabS</i> ::pGPAPTp Tp ^R).....	141
Figure 68: pDNA from <i>E. coli</i> DH5-α cells (Invitrogen). (A) Plasmid map of pXO3 (<i>wbxD-wbcE</i>), (B) Plasmid map of pSCRhaB3, (C) Gel image.....	143
Figure 69: pDNA from <i>E. coli</i> DH5-α cells (Invitrogen). (A) Plasmid map from pSCRhaB3 Tp-Tc. (B) Gel image.....	144
Figure 70: pDNA from <i>E. coli</i> DH5-α cells (Invitrogen). (A) Plasmid map from pXO3 Tp-Tc (<i>wbxD-wbcE</i>). (B) Gel image.....	145
Figure 71: TopTaq PCR from DNA fragment <i>wbxD-wbcE</i> extracted from pXO3 Tp-Tc. (A) <i>wbcE</i> . (B) <i>wbxD</i>	146
Figure 72: pDNA from <i>E. coli</i> DH5-α cells (Invitrogen): (A) Gel image pJET1.2/blunt- <i>wbcE</i> . (B) Gel image pJET1.2/blunt- <i>wbxD</i>	147
Figure 73: pDNA from <i>E. coli</i> DH5-α cells (Invitrogen): (A) Gel image pXO4 Tp- Tc. (B) pXO7 Tp-Tc.....	148
Figure 74: Colony PCR from mutant 16 E1 (<i>wbxD-wbcE</i>) complemented with pXO3 Tp-Tc.....	149

Figure 75: Colony PCR from mutant 16 E1 (<i>wbxD-wbcE</i>) complemented with pXO4 Tp-Tc and pXO7 Tp-Tc.....	150
Figure 76: Colony PCR from mutant 16 E1 (<i>wbxD-wbcE</i>) complemented with pSCRhaB3 Tp-Tc.....	150
Figure 77: Growth curve of <i>B. cenocepacia</i> K56-2::pTnModOTp' mutant 16 E1 (<i>wbxD-wbcE</i> ::Tp ^R) complemented with pXO3 Tp-Tc (<i>wbxD-wbcE</i>) exposed to phage KS4-M.....	153
Figure 78: Growth curve of <i>B. cenocepacia</i> K56-2::pTnModOTp' mutant 16 E1 (<i>wbxD-wbcE</i> ::Tp ^R) complemented with pSCRhaB3 Tp-Tc (empty vector) exposed to phage KS4-M.....	154
Figure 79: Growth curve of <i>B. cenocepacia</i> K56-2::pTnModOTp' mutant 16 E1 (<i>wbxD-wbcE</i> ::Tp ^R) complemented with pXO3 Tp-Tc (<i>wbxD-wbcE</i>) exposed to phage KS12.....	155
Figure 80: Growth curve of <i>B. cenocepacia</i> K56-2::pTnModOTp' mutant 16 E1 (<i>wbxD-wbcE</i> ::Tp ^R) complemented with pSCRhaB3 Tp-Tc (empty vector) exposed to phage KS12.....	156
Figure 81: Growth curve of <i>B. cenocepacia</i> K56-2::pTnModOTp' mutant 16 E1 (<i>wbxD-wbcE</i> ::Tp ^R) complemented with pXO4 Tp-Tc (<i>wbcE</i>) exposed to phage KS4-M.....	158
Figure 82: Growth curve of <i>B. cenocepacia</i> K56-2::pTnModOTp' mutant 16 E1 (<i>wbxD-wbcE</i> ::Tp ^R) complemented with pSCRhaB3 Tp-Tc (empty vector) exposed to phage KS4-M.....	159

Figure 83: Growth curve of <i>B. cenocepacia</i> K56-2::pTnModOTp' mutant 16 E1 (<i>wbxD-wbcE</i> ::Tp ^R) complemented with pXO4 Tp-Tc (<i>wbcE</i>) exposed to phage KS12.....	160
Figure 84: Growth curve of <i>B. cenocepacia</i> K56-2::pTnModOTp' mutant 16 E1 (<i>wbxD-wbcE</i> ::Tp ^R) complemented with pSCRhaB3 Tp-Tc (empty vector) exposed to phage KS12.....	161
Figure 85: Growth curve of <i>B. cenocepacia</i> K56-2::pTnModOTp' mutant 16 E1 (<i>wbxD-wbcE</i> ::Tp ^R) complemented with pXO7 Tp-Tc (<i>wbxD</i>) exposed to phage KS4-M.....	163
Figure 86: Growth curve of <i>B. cenocepacia</i> K56-2::pTnModOTp' mutant 16 E1 (<i>wbxD-wbcE</i> ::Tp ^R) complemented with pSCRhaB3 Tp-Tc (empty vector) exposed to phage KS4-M.....	164
Figure 87: Growth curve of <i>B. cenocepacia</i> K56-2::pTnModOTp' mutant 16 E1 (<i>wbxD-wbcE</i> ::Tp ^R) complemented with pXO7 Tp-Tc (<i>wbxD</i>) exposed to phage KS12.....	165
Figure 88: Growth curve of <i>B. cenocepacia</i> K56-2::pTnModOTp' mutant 16 E1 (<i>wbxD-wbcE</i> ::Tp ^R) complemented with pSCRhaB3 Tp-Tc (empty vector) exposed to phage KS12.....	166
Figure 89: LPS diagram from four LPS truncated mutants. (Adapted from Kotränge et al., 2011).....	167
Figure 90: LPS electrophoretic profiles from <i>B. cenocepacia</i> K56-2 wt.....	169
Figure 91: LPS electrophoretic profiles from <i>B. cenocepacia</i> K56- 2::pTnModOTp' mutant 16 E1 (<i>wbxD-wbcE</i> ::Tp ^R).....	170

Figure 92: pDNA from <i>E. coli</i> DH5- α cells (Invitrogen): (A) Gel image pSCRhaB2. (B) Gel image p34S-Tc.....	173
Figure 93: pDNA from <i>E. coli</i> DH5- α cells (Invitrogen): (A) Plasmid map from pSCRhaB2-Tc (empty vector). (B) Gel image pSCRhaB2-Tc.....	174
Figure 94: (A) <i>E. coli</i> DH5- α cells (Invitrogen) complemented with pSCRhaB2-Tc (empty vector) plated on LB + 10 μ g of Tc/mL. (B) plated on LB + 100 μ g of Tp/mL.....	175
Figure 95: TopTaq PCR from <i>B. cenocepacia</i> K56-2 cDNA: (A) Gel image <i>wabO</i> . (B) Gel image <i>waaC</i>	176
Figure 96: pDNA from <i>E. coli</i> DH5- α cells (Invitrogen): (A) Gel image pJET1.2/blunt- <i>waaC</i> . (B) Gel image pJET1.2/blunt- <i>wabO</i>	176
Figure 97: pDNA from <i>E. coli</i> DH5- α cells (Invitrogen): (A) Gel image pSC <i>wabO</i> -Tc. (B) Gel image pSC <i>waaC</i> -Tc.....	178
Figure 98: Colony PCR from mutant XOA8 (<i>wabO</i> ::pGP Ω Tp Tp ^R) complemented with pSC <i>wabO</i> -Tc and pSCRhaB2-Tc.....	179
Figure 99: Colony PCR from mutant CCB1 (<i>waaC</i> ::pGP Ω Tp Tp ^R) complemented with pSC <i>waaC</i> -Tc and pSCRhaB2-Tc.....	180
Figure 100: Growth curve of <i>B. cenocepacia</i> K56-2 LPS mutant XOA8 (<i>wabO</i> ::pGP Ω Tp Tp ^R) complemented with pSC <i>wabO</i> -Tc exposed to phage KS5.....	182
Figure 101: Growth curve of <i>B. cenocepacia</i> K56-2 LPS mutant XOA8 (<i>wabO</i> ::pGP Ω Tp Tp ^R) complemented with pSCRhaB2-Tc exposed to phage KS5.....	184

Figure 102: Growth curve of <i>B. cenocepacia</i> K56-2 LPS mutant XOA8 (<i>wabO</i> ::pGPΩTp Tp ^R) complemented with pSC <i>wabO</i> -Tc exposed to phage KS9.....	185
Figure 103: Growth curve of <i>B. cenocepacia</i> K56-2 LPS mutant XOA8 (<i>wabO</i> ::pGPΩTp Tp ^R) complemented with pSCRhaB2-Tc exposed to phage KS9.....	186
Figure 104: Growth curve of <i>B. cenocepacia</i> K56-2 LPS mutant CCB1 (<i>waaC</i> ::pGPΩTp Tp ^R) complemented with pSC <i>waaC</i> -Tc exposed to phage KS5.....	187
Figure 105: Growth curve of <i>B. cenocepacia</i> K56-2 LPS mutant CCB1 (<i>waaC</i> ::pGPΩTp Tp ^R) complemented with pSCRhaB2-Tc exposed to phage KS5.....	188
Figure 106: Growth curve of <i>B. cenocepacia</i> K56-2 LPS mutant CCB1 (<i>waaC</i> ::pGPΩTp Tp ^R) complemented with pSC <i>waaC</i> -Tc exposed to phage KS5.....	190
Figure 107: Growth curve of <i>B. cenocepacia</i> K56-2 LPS mutant CCB1 (<i>waaC</i> ::pGPΩTp Tp ^R) complemented with pSCRhaB2-Tc exposed to phage KS5.....	191
Figure 108: Growth curve of <i>B. cenocepacia</i> K56-2 LPS mutant CCB1 (<i>waaC</i> ::pGPΩTp Tp ^R) complemented with pSC <i>waaC</i> -Tc exposed to phage KS5.....	192

Figure 109: Growth curve of <i>B. cenocepacia</i> K56-2 LPS mutant CCB1 (<i>waaC</i> ::pGPΩTp Tp ^R) complemented with pSCRhaB2-Tc exposed to phage KS5.....	193
Figure 110: LPS electrophoretic profiles from <i>B. cenocepacia</i> K56-2 wt and K56- 2 LPS truncated mutant XOA8 (<i>wabO</i> ::pGPΩTp Tp ^R).....	195
Figure 111: LPS electrophoretic profiles from <i>B. cenocepacia</i> K56-2 wt and K56- 2 LPS truncated mutant CCB1 (<i>waaC</i> ::pGPΩTp Tp ^R).....	196
Figure 112: Western blot from <i>B. cenocepacia</i> K56-2 wt and mutant 16 E1 (<i>wbxD-wbcE</i> ::Tp).....	198
Figure 113: Coomassie blue-stained gel from <i>B. cenocepacia</i> K56-2 wt and mutant 16 E1 (<i>wbxD-wbcE</i> ::Tp).....	199
Figure 114: Western blot from <i>B. cenocepacia</i> K56-2 wt and K56-2 LPS truncated mutants XOA8 (<i>wabO</i> :: pGPΩTp Tp ^R) and CCB1 (<i>waaC</i> ::pGPΩTp Tp ^R).....	200
Figure 115: Coomassie blue-stained gel from <i>B. cenocepacia</i> K56-2 wt and K56-2 LPS truncated mutants XOA8 (<i>wabO</i> :: pGPΩTp Tp ^R) and CCB1 (<i>waaC</i> ::pGPΩTp Tp ^R).....	201
Figure 116: Electron micrographs of negatively stained (2% PTA) <i>B. cenocepacia</i> PC184 wt (A) and mutant 72 C12 (<i>pulO</i> ::Tp ^R) (B).....	203
Figure 117: Electron micrographs of negatively stained (2% PTA) <i>B. cenocepacia</i> PC184 wt (A) and mutant 72 C12 (<i>pulO</i> ::Tp ^R) (B).....	204

Figure 118: Electron micrographs of negatively stained (2% PTA) <i>B. cenocepacia</i> PC184 wt + phage DC1 (A) and mutant 72 C12 (<i>pulO</i> ::Tp ^R) + phage DC1 (B).....	206
Figure 119: Stab assay for twitching motility on 1% agar plates.....	208
Figure 120: Swarming motility on 0.5% agar plates.....	211

LIST OF ABBREVIATIONS

α	alpha
β	beta
Φ	phi
AA	Aminoacid
Amp	Ampicillin
Bcc	<i>Burkholderia cepacia</i> complex
BLAST	Basic local alignment search tool
bp	base pair
CGD	Chronic Granulomatous Disease
CF	Cystic Fibrosis
Cm	Chloramphenicol
dd	Double stranded
DNA	Deoxyribonucleic acid
EOP	Efficiency of plating
ET12	Enzyme electrophoretic type 12
IM	Inner membrane
Kdo	3-Deoxy-D-manno-oct-2-ulosonic acid
Kb	Kilo base pair
Km	Kanamycin
LB	Luria-Bertani media
LGP	Ligand-gated porin
LPS	Lipopolysaccharide
MIC	minimum inhibitory concentration
NCBI	National Center for Biotechnology Information
OD	Optical density
OS	Oligosaccharide
OM	Outer membrane
PCR	Polymerase chain reaction
PFU	Plaque forming units
PTA	Phosphotungstic acid
R-type LPS	Rough LPS phenotype
RNA	Ribonucleic acid
ss	Single stranded
S-type LPS	Smooth LPS phenotype
T2SS	Type II secretion system
TEM	Transmission electron micrograph
Tp	Trimethoprim
Tc	Tetracycline
TSA	Tryptic soy agar
wt	Wild type

INTRODUCTION

The *Burkholderia cepacia* complex (Bcc)

B. cepacia was isolated and identified by W. H. Burkholder during the 50's as a phytopathogen of onions. The Bcc is widely distributed in water, soils and in the rhizosphere interacting with plants. This bacterial group has beneficial effects in the environment as a symbiotic organism in plant roots increasing the productivity of crops; it also can be used as a biocontrol agent against fungi, and as a bioremediation agent with an incredible capacity to degrade more than 200 compounds. The Bcc is a group of bacilli-shaped Gram-negative bacteria with high phenotypic similarity but markedly genetic differences. Bcc bacteria are members of the β -subgroup of the Proteobacteria and at least seventeen species exist, including *Burkholderia cepacia*, *Burkholderia multivorans*, *Burkholderia cenocepacia*, *Burkholderia stabilis*, *Burkholderia vietnamiensis*, *Burkholderia dolosa*, *Burkholderia ambifaria*, *Burkholderia anthina* and *Burkholderia pyrrocinia* (Coenye et al., 2001; Mahenthiralingam et al., 2005; Parke & Gurian-Sherman, 2001).

Nevertheless, in recent years, the detrimental effects of this bacterial group have also been identified and studied. Some species are phytopathogens of onions causing decay. During the last three decades, strains of the Bcc have been demonstrated to be opportunistic human pathogens of immunocompromised patients and/or individuals with cystic fibrosis (CF) or chronic granulomatous disease (CGD). Luckily, less than 20% of CF individuals infected with a member of the Bcc will develop the disease known as "cepacia syndrome", which is characterized by a decrease in pulmonary function, necrotizing pneumonia and

septicemia, that eventually results in death (Frangolias et al., 1999). Alarming, the number of patients infected with members of the Bcc has increased because Bcc bacteria are highly resistant to chemical antibiotic therapy, which causes major problems when treating Bcc infections (Coenye et al., 2001; Parke & Gurian-Sherman, 2001). Thus alternative therapies are needed. One example of an alternative therapy is phage therapy (the therapeutic use of phages) to treat infectious diseases.

Antibiotic resistance mechanisms of the Bcc

The Bcc is a highly problematic group of bacteria to treat due to its naturally high antibiotic resistance. Some of the mechanisms by which this bacterial group inactivates some of the most common antibiotics include the production of antibiotic efflux pumps and the production of β -lactamases that inactivate β -lactams (Chiesa et al., 1986; Vinion-Dubiel & Goldberg 2003). Resistance to trimethoprim is conferred by the production of dihydrofolate reductases, as described by Burns and collaborators (1989a). Surprisingly, some strains have minimum inhibitory concentrations (MICs) of 1000 $\mu\text{g}/\text{mL}$. A second study by Burns et al., (1989b) revealed that a decreased permeability in the outer membrane (OM) provides increased resistance to chloramphenicol. The unusual structure of the lipopolysaccharide (LPS) in members of the Bcc inhibits the attachment of cationic antibiotics like polymyxin. Some of these unusual structures include reduced levels of phosphate in the core oligosaccharide (OS) and the presence of 4-amino-4-deoxyarabinose (Ara4N) residues attached to the phosphate of the lipid

A backbone. In addition, spontaneous mutations in the Bcc LPS, as detected by LPS extractions electrophoresed on polyacrylamide gels, were also linked to resistance to trimethoprim, sulphamethoxazol and chloramphenicol. Chloramphenicol resistant mutants lacked O-antigens, as observed on LPS silver stained gels (Vinion-Dubiel & Goldberg, 2003).

Biofilms have also been proposed as an alternative way in which bacteria increase their resistance to antibiotics and host antimicrobial defenses. It is hypothesized that availability of the drug is decreased in a biofilm and penetration is dependent on the thickness and density of the biofilm. For instance, it is known that members of the Bcc are able to form biofilms; in fact, it is hypothesized that Bcc form biofilms in the lungs of individuals with CF (Conway et al., 2002) thus biofilms formed by Bcc in the lungs enhance the resistance to antibiotics. A study by Desai and collaborators (1998) revealed that members of the Bcc were 15 times more resistant to ciprofloxacin and ceftazidime when living in a biofilm as compared to planktonic Bcc cells. Thus, it is also probable that biofilms provide resistance not only to these two antibiotics, but also to a wide variety of drugs.

Bacteriophages (Phages)

Phages are considered to be one of the most abundant “life” forms on Earth. Bergh et al. (1989) reported that 1 mL of ocean water contained approximately 2.5×10^8 viral particles, including phages. More recent estimations propose a number of around 4×10^{30} viral particles in the biosphere (Casjens, 2008; Suttle, 2005; Hanlon, 2007).

Phages were independently discovered early in the 20th century by Felix d'Herelle while traveling in Mexico and Frederick Twort in England. The antibacterial potential of these organisms was rapidly appreciated; observations of zones of clearing on bacterial lawns suggested to Twort and d'Herelle that bacteria were being killed in these areas. Early experiments using phages as antibiotic agents were carried out. In some cases, the use of phages was successful. In fact, the first promising trials were reported by d'Herelle in 1917 when a patient with dysentery recovered his health after being treated with phages. However, with the development a few years later of broad-spectrum antibiotics effective against a wide variety of bacteria and less selective than phages, the medical community in western countries lost interest in phage therapy, which was rapidly supplanted by chemical antibiotic therapy. Nevertheless, in Eastern Europe phage therapy continued to be a common way to treat bacterial infections diseases, and some of these promising results were published in Eastern Europe. Unfortunately, the western scientific community has criticized these results because the vast majority are anecdotal rather than scientific, thus discrediting the effectiveness of phages (Duckworth & Gulig, 2002; Summers, 2001). In addition, many of the past failures relating to phage therapy are mainly due to a poor understanding of phage biology and how phages interact with their bacterial hosts (O'Flaherty et al., 2009).

Phage therapy

Because the increasing prevalence of infectious diseases are caused by highly antibiotic resistant bacteria, a new opportunity for phage therapy has arisen (O'Flaherty et al., 2009; Nishikawa, 2008; Das, 2001). Experiments using animal models have demonstrated the ability of phages to cure infectious diseases. In a study using *E. coli* infected mice and calves, results revealed that both prophylactic and therapeutic use of phages showed high levels of effectiveness in clearing the bacteria; higher levels than those obtained using antibiotics (Barrow, 1997). Years later, experiments were performed in order to demonstrate the ability of phages to treat antibiotic-resistant bacterial infections in human burn injures. These results revealed the effectiveness of phages against *Pseudomonas aeruginosa* infections in pig skin, which is commonly used as a substitute of skin in human burns (Barrow, 1997). These early experiments provided scientific evidence that perhaps phage therapy was a potential alternative in the treatment of infectious diseases. Similarly, Biaswas et al., (2002) treated vancomycin-resistant *Enterococcus faecium* infections in mice, and Matsuzaki et al., (2005) demonstrated the ability of phage Φ MR11 to rescue mice from an infection with *Staphylococcus aureus*.

However like any other therapy, disadvantages have also been proposed for the use of phages. One of these is the risk of a strong immune response reaction in mammalian cells, based on the fact that phages are foreign to the human body. However, so far, a negative immune response by phages in animal or even human models has not been reported (Hanlon, 2007; Matsuzaki et al., 2005; Ochs et al., 1971). In addition, phages are in continuous contact with all kinds of life without

causing adverse effects, thus the utilization of phages for therapeutic purposes seems feasible (Carlton, 1994; Merrill et al., 1996).

Because phages have a very specific host range and in general only infect a few species of bacteria, phage therapy seems limited in its ability to treat an infection broadly. However, the utilization of “phage cocktails” (the combination of distinct phage species targeting distinct hosts) has been proposed as a solution to overcome this problem (McVay et al., 2007; Tanji et al., 2004). In addition, an obvious advantage of phage specificity is the fact that the host’s natural and beneficial bacterial flora will not be affected by phages.

Bacteriophages life cycle

Phages, like other viruses, are obligate parasites. Thus, in order to continue their “life cycle” they need to hijack and control the natural and biological functions of their bacterial hosts. In the majority of cases, only the viral genome will be delivered into the host. Subsequently, the newly injected nucleic acid will be expressed which then alters the bacterial biosynthetic apparatus to produce new phage particles, phage nucleic acids, etc. This interaction is highly regulated and it follows an ordered pathway (Figure 1, Campbell et al., 2003).

In general, four intracellular main steps have been identified: 1. nucleic acid (single (ss) or double stranded (ds) DNA or RNA) replication, 2. synthesis of new structural viral particles, mainly made of proteins, 3. newly synthesized particles and nucleic acid assembly, and finally, 4. lysis and subsequent release into the medium of fully functional phages (Campbell et al., 2003). Interestingly, two of

the key stages during phage infection occur outside of the host cell. These are: 1. host recognition and phage adsorption onto the host cell surface followed by, 2. the “injection” of the phage nucleic acid into the cell. Unfortunately, our understanding of both phages’ nucleic acid transport mechanisms and phages’ interaction with host receptors are still poorly understood.

Attempts to describe global mechanisms of phage adsorption and nucleic acid injection have been put forth. Results have revealed that such a “global mechanism” of infection is in fact, inapplicable to all phages. Phage adsorption and nucleic acid release are very specific, and yet diverse depending upon the phage species. However, modern technologies (like protein-protein interactions, genetics, and molecular biology) may increase our understanding of phage biology, in order to ensure successful use of these marvelous entities as therapeutic agents.

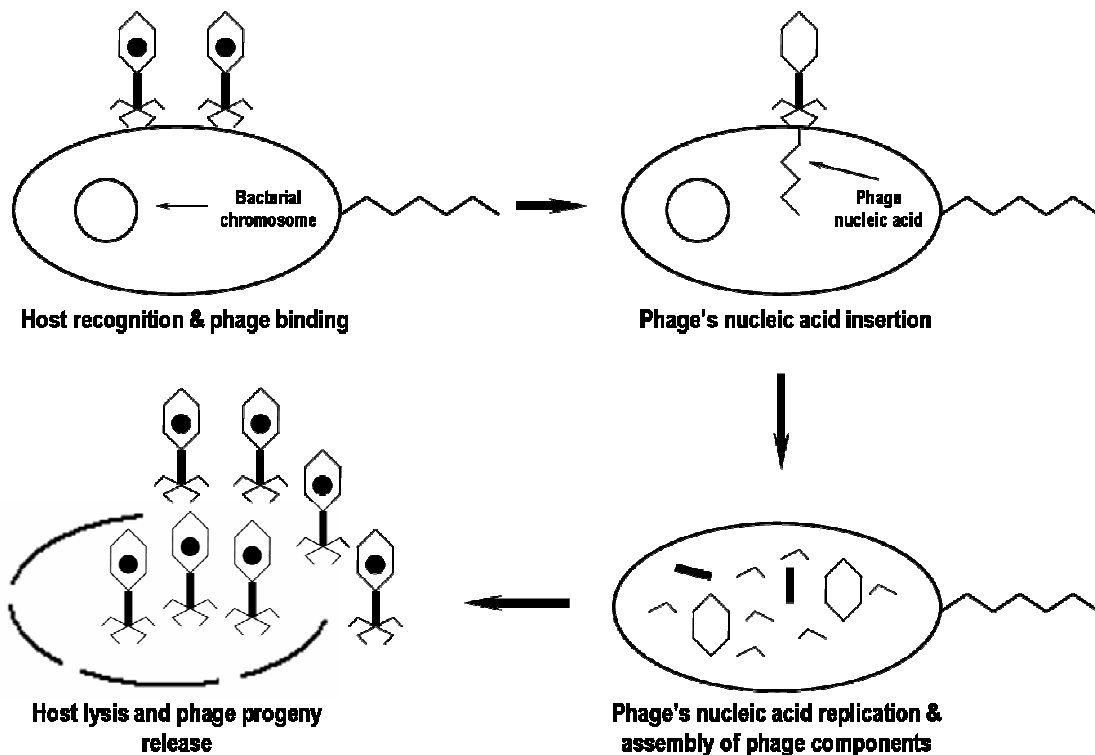


Figure 1: Bacteriophages' lytic lifecycle.

Bacteriophage host recognition and adsorption

Bacteriophage infection follows a “general” pattern independent of the bacterial host. A complex and well-organized cascade of events occurs during infection. Phage host recognition and adsorption is perhaps the pinnacle of all phages' lifecycle because it ensures the successful delivery of the nucleic acid into the host allowing propagation, and hence the preservation of the phage population in the environment (Zayas & Villafane, 2007). Because host recognition is a probability event, variables like the concentration of phage/host or the presence of specific elements in the surrounding media can affect the chance and effectiveness of phages during host infection. The randomness of a phage binding to a host is somehow confirmed by the fact that the presence of motility structures in bacteriophages has never been reported. This is one reason why phages cannot move independently as bacteria do. Instead, the process of phage host recognition and adsorption results from the random collision of phages with a cell. From this point of view, it can be assumed that higher concentrations of phage and bacteria will increase the chance of random collisions, thereby producing higher adsorption rates (Rakhuba et al., 2010). However and surprisingly, this isn't always the case.

For example some of the phages in our collection seem to contradict this “logical” hypothesis. When plating phages AH2 or KL1 with their susceptible hosts by the soft agar overlay method, a set of serial dilutions is required in order

to detect plaques on the plates. Higher numbers of phages (10^5 and above) will not result in bacterial cell infection. Additionally, incubation of the plate must be extended up to 48 hrs. in order to detect any plaques. The reason behind this phenomenon is still unknown (Lynch, personal communication).

As previously mentioned, the rate of adsorption is also governed by other factors besides phage/host concentration. Elements like pH, temperature, host physiological state, culture conditions and growth phase, and the presence of specific molecules like ions (e.g. calcium) may affect the efficiency of phage infection and entry into the host (Sillankorva et al., 2004; Cvirkaite-Krupovic et al., 2010). Previous examples provide some information as to how different and complex phage-bacteria interactions can be.

The general consensus is that phage host recognition and adsorption onto the bacterial cell surface is divided in two steps or stages. The phage first recognizes and adsorbs in a reversible manner onto the cell surface of the bacterium. It is hypothesized that this first stage of binding is transient because it allows the phage to “move” over the surface until it finds its primary receptor. Because phages cannot move actively as bacteria do, it is hypothesized that phages first bind to secondary receptors, and that this binding is characterized by its low affinity, reversibility, permitting a “binding-unbinding without dissociation” cycle. This cycle allows the phage to “scan” the surface of its host to find its primary receptor. How exactly this reversible binding works is still not fully understood. It should be mentioned that there are marked differences during phage

adsorption onto the host surface (and phage infection in general) in Tailed (*Caudovirales*) and Tailless (Pleomorphic, filamentous and polyhedral) phages, and that these are very specific differences and with significant variation. Specific examples will be discussed in the following sections. Research has mainly focused on tailed phages, perhaps because they represent 96% of the total known phages (Ackermann & Kropinski, 2007).

Subsequently, phages will interact and in an irreversible manner attach to their specific or primary receptor. Elements such as porins, ligand gated porins (LGP), capsules, flagella, pili and LPS may serve as the primary receptor. For some phages, the secondary and primary receptors are the same. An example is the case of phage T7. The presence of LPS serves as the secondary and primary receptor during phage infection. Even though the exact mechanism of adsorption to LPS has not yet been elucidated, it is assumed that it may follow a similar pattern to that observed in other tailed phages because of the close similarity in its morphology and structures (Molineux, 2001).

How specific is this second binding step? The specificity of the irreversible binding stage has been assessed by *in vitro* and *in vivo* experiments through the analysis of the interaction between the purified receptors of bacteria (OM proteins or structural components that serve as phage receptors) and phages (receptor binding proteins) (Letellier et al., 2004). Once the phage has irreversibly bound to its primary receptor, signals trigger conformational changes throughout the phage (mainly in the phage tail and tail neck) leading to the insertion of the nucleic acid into the host (Letellier et al., 2004).

Bacterial cells walls and their potential receptors for bacteriophages

Bacterial cell walls are complex structures with several functions essential for the survival of the bacterium. In general, it can be said that cell walls help bacteria to overcome the lower pressure of their surrounding medium, they give bacteria their shape and rigidity, but also serve as a permeability barrier between the environment and the bacteria. Two large groups of bacteria are differentiated by the variations in the chemical composition and structure of their cell wall: Gram-positive and Gram-negative bacteria (Madigan & Martinko, 2006). Phages infecting both Gram-positive and Gram-negative bacteria have been isolated and studied, however, only phages infecting the Gram-negative bacteria will be discussed herein.

Bacteriophage host recognition and adsorption into the Gram-negatives cell wall

The cell wall of Gram-negative bacteria is considered a “richer” binding site compared to that of Gram-positive bacteria due the diversity and large amount of potential phage binding receptors. To mention an example, it was estimated that the number of transport channels in Gram-negative bacteria is approximately 20,000 per cell (Rakhuba et al., 2010), and these channels are utilized by some phages as binding receptors. In Gram-negative bacteria, the peptidoglycan layer represents only a small portion of the total cellular barrier (Nikaido, 1996). In addition to the peptidoglycan (PP) and the inner membrane (IM), Gram-negative bacteria present an additional outer membrane (OM), which is composed of

phospholipids, proteins, and LPS [Fig. 2]. The major function of the OM is to form a barrier against noxious elements in the surrounding medium (Nikaido, 1996). For example, it was reported that approximately 95% of recently developed antibiotics are only active against Gram-positive bacteria, thus the importance of this extra membrane for the protection of the microbial cell in Gram-negative bacteria is obvious. Nevertheless, the protection provided by the OM does not affect the influx of essential or efflux of detrimental compounds.

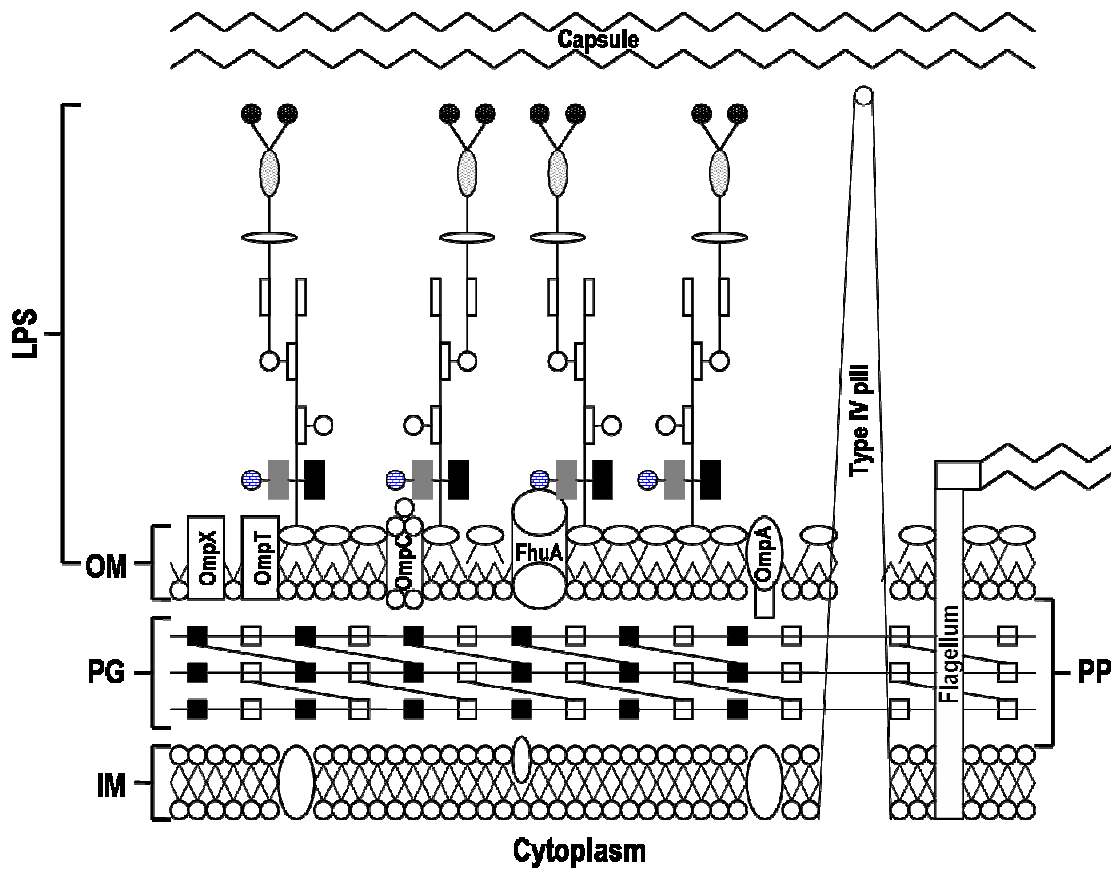


Figure 2: The Gram-negative cell wall depicting all the potential phage receptors described unto date. These include: Porins (ex. OmpC, F and PhoE), porin-like proteins (ex. LamB and Tsx), ligand-gated porins (ex. siderophore receptors [FhuA] and vitamin B12 transporter [BtuB]), surface proteins (ex. OmpA), surface proteolytic enzymes (ex. OmpX or T), lipopolysaccharide (LPS), flagella, pili (ex. type IV pili) and capsular polysaccharide or capsule. Legends: inner membrane (IM), periplasm (PP), peptidoglycan (PG) and outer membrane (OM).

Porins, Porin-like and Ligand-gated porins (LGP) as bacteriophage receptors

Permeability in the OM is conferred by the presence of several proteins that serve as channels for the transport of molecules, and as surface exposed proteins can function as phage receptors. These proteins or protein complexes are typically classified into three main groups. However, these groups will not be discussed in depth because none of the 10 Bcc specific phages examined in this research appear to bind to these groups of proteins.

Classical porins: A large open water-filled channel in the OM composed of protein subunits, their main function being the non-specific passive diffusion of ions and small nutrient molecules. Classical examples of this group include the *E. coli* strain K12 OmpC (outer membrane protein C), OmpF and PhoE. Phages such as TuIb and T4 bind to OmpC (Heller, 1992; Yu & Mizushima, 1982; Arisaka, 2005; Leiman et al., 2003). In the case of phage T4, the primary receptor was determined to be the LPS core OS region. OmpF has been discovered as a secondary binding receptor for phage T2, whose primary receptor is the LPS heptose residues to which the phage binds irreversibly (Rakhuba et al., 2010; Yoichi et al., 2005). Phage K20 binds to both of these receptors as well, LPS core OS and OmpF (Traurig & Misra, 1999). Other phages binding to OmpF include TuIa, TP1 and TP2 (Heller, 1992).

Porin-like specific proteins: This type of porins contain a specific binding site for specific molecules, thus they are selective in what type of molecule is transported. A narrow water-filled channel is formed through the protein(s) allowing passive and slow diffusion of nutrients. A classical example is

the *E. coli* LamB protein, its main function is the transport of maltose and maltodextrans into the cell. Recent studies have demonstrated that LamB takes up other kinds of sugars as well (Nikaido, 1993; Nikaido, 2003). Another example is the *E. coli* Tsx protein characterized as a nucleoside-specific channel, its main function is the transport of nucleotides (Rakhuba et al., 2010; Nikaido, 2003; Heller, 1992). Phage lambda (λ) binds to LamB, and evidence suggests that no other receptor is required. The mere presence of LamB is enough to allow phage adsorption and λ DNA transport through the OM (Wang et al., 1998; 2000; Berkane et al., 2006). Other phages utilizing LamB as a receptor include K10, TP1, SS1 (Heller, 1992). Tsx and its utilization by phage T6 as a binding receptor was first described in the 1970's. Tsx is also a target for the antibiotic albicidin (Nikaido, 2003). Other phages that bind to Tsx include phage H3 and Ox1 (Heller, 1992).

Ligand-gated proteins (LGPs): These highly specific transport proteins get activated only when they interact with their specific substrate. Typical examples in *E. coli* strain K12 include the proteins involved in the transport of siderophores (iron chelators). Six LGPs have been identified: FepA for Fe³⁺-enterobactin, FhuA for Fe³⁺-ferrichrome, FecA for Fe³⁺-citrate, FhuE for Fe³⁺-coprogen, Cir for Fe³⁺-catecholates and Fiu for Fe³⁺-dihydroxybenzoyl-serine. The transport of vitamin B₁₂ is mediated by the LPG BtuB (Nikaido, 2003). It is known that LGPs actively transport nutrients into the cell, because the sizes of the molecules being transported are too large to be introduced by passive diffusion. As the OM is unenergized, a source of energy is required. The TonB complex

transduces the energy produced by the IM proton motive force to the OM, and this energy transduction is required for the correct function of LGPs (Nikaido, 2003; Cascales et al., 2001). As far as is known, only three LGPs are known to be used by phages as receptors; these include FhuA, FepA and BtuB.

FhuA is an OM protein that transports ferric iron-ferrichrome complexes inside the bacterium. Despite its main function, phages like T1, T5, UC-1 and phi80 bind to FhuA in order to infect and replicate within the host (Letellier et al., 2004; Heller, 1992). Interestingly, phages T1 and phi80 also require the presence and correct functioning of TonB (thus an energized IM is required) in order to successfully infect the host, while phage T5 does not (Letellier et al., 2004; Bonhivers et al., 1996). Additionally, phage T5 also requires the presence of secondary receptor LPS O-antigen subunits, and therefore the primary receptor is logically FhuA (Heller, 1992; Plançon et al., 2002). To date, only one phage has been reported to utilize FepA as a binding receptor. Rabsch and collaborators (2007) named this phage H8. Phage H8 infection is TonB-dependent (thus an IM source of energy is required). Finally, phage BF23 binds to BtuB (Heller, 1992).

Bacteriophages utilizing OmpA as a receptor

A second group of proteinaceous phage receptors found in the OM are similar to OmpA, a structural transmembrane protein that interacts with the OM, periplasm, and peptidoglycan (Rakhuba et al., 2010). Some of the main functions of OmpA include maintenance of the structural integrity of the OM, involvement in bacterial conjugation, cell growth, and a role in mammalian cell invasion

(Power et al., 2006; Jeannin et al., 2002). Colicins and several *E. coli* phage species use OmpA as a receptor (Power et al., 2006; Jeannin et al., 2002). As above, since none of the Bcc-specific phages examined in this study appear to utilize OmpA as a receptor, this OM protein will not be discussed in depth. Phage K3 binds to OmpA (Rakhuba et al., 2010). Phage TuIb requires in addition the presence of LPS (Datta et al., 1977). Other phages utilizing OmpA include Ox4, Ox5, Ox2, TuIi, and M1 (Heller, 1992).

Bacteriophages utilizing enzymes (OmpT & OmpX) as receptors

Finally, the third group of proteinaceous phage receptors found in the OM of bacteria is proteolytic enzymes, such as OmpT and OmpX (Nikaido, 2003; Hashemolhosseini et al., 1994). Phages exclusively utilizing these enzymes as receptors have not been isolated, however early in the 1990's researchers were able to modify phages Ox2, K3, and M1 in order to change their host range and permit them to bind to either OmpT (phage M1) or OmpX (phages Ox2 and K3) (Hashemolhosseini et al., 1994).

Bacteriophages utilizing Lipopolysaccharide (LPS) as receptor

Exclusively found in Gram-negative bacteria, the LPS appears to play an essential role during phage adsorption, and some phages only require the presence of this structural element in order to infect their host. It is hypothesized that perhaps this is because LPS is the first element phages may encounter when making contact with a potential host (Nikaido, 2003; Bos & Tommassen, 2004).

The LPS structure is a complex polymer composed of monosaccharides and fatty acids. It has three clearly distinguishable parts [Fig. 3] (Nikaido, 2003; Bos & Tommassen, 2004). The first component is a hydrophobic membrane anchor layer, termed Lipid A. This first section is usually a short chain of disaccharides composed of two D-glycosamine moieties linked by β -1,6-bonds attached to acyl groups (fatty acids) and represents the innermost region of the LPS.

The second section comprised of inner and outer core oligosaccharide (OS) of LPS is composed of short chain sugar residues, one of the inner core oligosaccharides is attached directly to the lipid A and it contains a sugars such as KDO (3-deoxy-D-*manno*-oct-2-ulosonic acid) or heptoses. The outer core oligosaccharide is mainly composed of hexoses. Because many LPS core oligosaccharides (particularly the outer core) contain non-carbohydrate components such as phosphate, amino acids, and ethanolamine substituents, this region is more diverse among strains of the same bacterial species. However, these variations are not as marked as those seen in the O-antigen region (Nikaido, 2003; Bos & Tommassen, 2004).

The third and final component of the LPS is the O-antigen (O-polysaccharide or O-side chain), a repetitive glycan polymer attached to the outer core OS. It is the outermost region of the LPS. Highly variable in its composition from strain to strain, this variability has been analyzed extensively. To cite an example, approximately 160 distinct O-antigens are found in different strains of *E. coli* (Raetz & Whitfield, 2002).

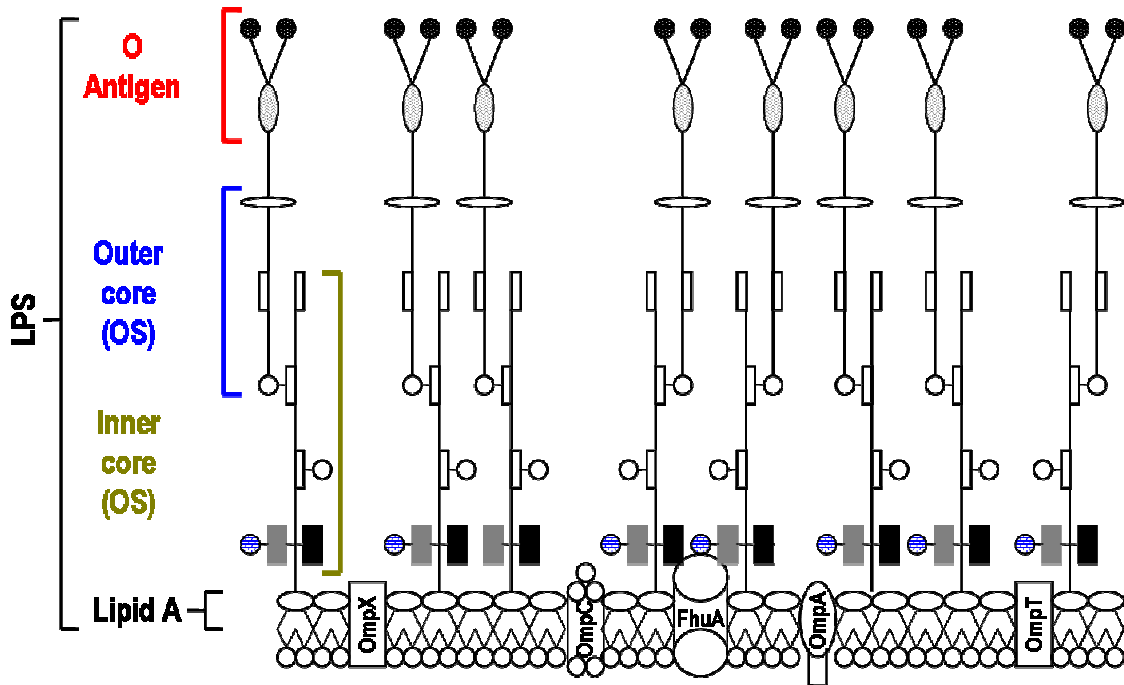


Figure 3: Simplified LPS structure from *B. cenocepacia* strain K56-2. Legends:

- Lipid A
- D-glycero-D-talo-octulosonic acid (KO)
- 3-deoxy-D-manno-oct-2-ulosonic acid (KDO)
- 4-amino-4-deoxyarabinose (Ara4N)
- Heptose (Hep)
- Glucose (Glc)
- QuiNAc
- Rhamnose
- N-Acetylgalactosamine (GalNAc)

Due to differences in the LPS components, two broad types of LPS have been described; this variation depends on the presence or absence of the O-antigen. The presence of the O-antigen will produce a smooth LPS phenotype (S-type LPS), while the absence of the O-chain will produce a rough LPS phenotype (R-type LPS). These phenotypes have several implications relative to bacterial virulence, resistance to antibiotics, and recognition by host antibodies (Nikaido, 2003; Bos & Tommassen, 2004).

A well-studied model of binding to an S-type LPS is phage P22. In the 1970's important discoveries regarding phage P22 adsorption and host recognition were made. From these studies, Eriksson & Lindberg (1977) determined that phage P22 recognizes and adsorbs to the O-antigen of *S. typhimurium*. Interestingly, an enzyme with an endorhamnosidase activity was discovered in the phage tail. This enzyme revealed an ability to specifically cleave and hydrolyze the Rha $\alpha(1 \rightarrow 3)$ Gal linkage of the O-antigen repeating units. A hypothetical advantage for phages carrying this type of enzymes was proposed. The enzyme allows the phage to degrade the sugars of the O-antigen and subsequently permits the phage to find a proper receptor on the OM of its host. In subsequent years, the structure of P22's tail spike protein (TSP) was elucidated and its receptor binding and rhamnose degrading activities were confirmed. This specific P22 protein is protein gp9. Six of these proteins are attached to the "neck" of the phage, which is also connected to the head. Results revealed that, similar to other phages, each one of the TSPs binds rapidly and reversibly, thus allowing the phage to "move" over the surface of bacteria and partially destroy sections of the LPS by the endorhamnosidase activity of the TSP. Only two O-antigen molecules are required for P22 binding (Letellier et al., 2004; Steinbacher et al., 1997). Another phage that binds to the O-antigen and hydrolyses the Rha $\alpha(1 \rightarrow 3)$ Gal linkage is phage ϵ^{15} , thus it is possible that this phage behaves in a similar way to phage P22.

Phage HK620 also requires an S-type LPS to infect its host. The crystal structure of its TSP, its affinity for the O-antigen, and its endoglycosidase activity

has been elucidated. Size exclusion chromatography revealed that phage HK620 TSP has a trimeric structure (similar to phage Sf6). Subsequent experiments utilizing recombinant HK620 TSP and the LPS of a specific *E. coli* strain TD2158 (in which HK620 was propagated) revealed that HK620's TSP recognizes and binds to the O-antigen. Photometric detection revealed the presence of *N*-acetyl-D-glucosamine moieties in the short oligosaccharides degraded by the recombinant HK620 TSP, thus revealing its enzymatic specificity as an endo-*N*-acetylglucosaminidase. Interestingly, this phage was only active on S-type LPS (Barbirz et al., 2008). Due to its morphological similarity to the *Podoviridae* (short non-contractile tails) phages P22 and Sf6, a similar pattern of phage adsorption and subsequent infection may be observed for phage HK620. Other phages requiring a full LPS or S-type LPS include ϕ 1 with a endo-1,2-*N*-galactoseaminidase activity, Ω 8 with a endorhamnosidase activity breaking down the Man-1 \rightarrow 3-Man linkage in *E. coli*, phage Sf6 hydrolyzing the Rha-1 \rightarrow 3-Rha linkage in the *S. flexneri* O-antigen (Rakhuba et al., 2010).

Some of the phages infecting bacteria with a R-type LPS include the well-studied phage T7. Similar to T4 or T5 phages, the tail fibers of phage T7 play an important role during host recognition and subsequent adsorption. Phage T7 initiates the infection of host *E. coli* by the interaction of its tail fibers (gp17) with the LPS core OS, specifically the galactose residues bound to glucose. Similar to other phages, each one of the six tail fibers is totally capable of binding to LPS in an independent manner; this binding is characterized as weak and reversible thus

permitting the phage to move over the cell surface, allowing the “bind-unbind without dissociation” cycle. However, when all of the tail fibers interact with LPS at the same time, the position of the phage is oriented in a way such that the tail faces the OM thus ensuring correct positioning for subsequent steps of infection (Molineux, 2001; Kemp et al., 2005). It is hypothesized that a series of signals are sent from the cell surface to the phage. The internal head protein (gp13) seems to play an important role in this signaling pathway because phages lacking this protein were unable to irreversibly bind to the cell surface, and no infection was observed because these phages dissociated from the host. Surprisingly, some gp13 homology has been found in the tail fiber protein gp17, phage tail proteins gp11 and gp12, and the head-tail connector protein gp8. Molineux (2001) hypothesized that two signals are transmitted, one from the cell surface to the tail fibers and subsequently to the phage head-tail connector, and the second one through the tail to the head-tail connector. These separate signals might inform the phage that it’s correctly positioned on the cell surface before it irreversibly binds to the OM. The degradation of T7 phage proteins gp7.3 and gp13 is known to be important to the irreversible binding step. This triggers the subsequent release of three core proteins from the phage capsid, which have been found in the OM and IM of the infected cell. More recently, Kemp et al. (2005) hypothesized that gp7.3 along with either gp11 or gp12 (or both) make contact with a specific receptor in the cell surface and irreversibly bind to it. Unfortunately, this receptor has not yet been identified.

Other phages infecting R-type LPS bacteria include bacteriophages F0, which binds to the α -1,2-bond at the N-acetylglucosamine residue in *Salmonella* strains, phage S13, which infects its host with or without expression of the terminal glucosamine residues, phage 6SR, which requires a complete core OS in order to infect *S. typhimurium* and *S. flexneri* cells, and the tailless phage phiX174, which requires a complete core OS (Rakhuba et al., 2010).

Other potential receptors for bacteriophage adsorption (Flagella, pili and capsules)

Bacteriophages are the most diverse and ubiquitous entities on Earth. Such diversity is mainly driven by the ability of phages to evolve and mutate just like any other living organism. Bacteria are in continuous exposure to harsh conditions and elements that may affect their survivability. Phages are one of the elements bacteria must survive, thus it is not unexpected that at some point bacteria have developed different mechanisms to protect themselves from phage infection. As a defense, bacteria mutate and become resistant to phages. Subsequently, phages must overcome these bacterial defensive mechanisms by means of mutation, allowing them to infect again their specific host. This ability of phages to evolve in order to overcome bacterial mutation is considered an advantage over chemical antibiotics (Labrie et al., 2010).

Interestingly, and perhaps part of an evolving warfare, almost every bacterial external structure has been exploited as a potential receptor by phages. In the previous section, porins, structural proteins, enzymes, and LPS were

mentioned as potential receptors, and these are the most common receptors for a wide variety of bacteriophages. However, these are not the only structures utilized by phages. Because none of the Bcc specific phages used in this study utilize any of these other binding receptors, in the following section the less common phage receptors will be only briefly discussed.

Bacteriophages utilizing flagella as receptors

Flagella-dependent phages reversibly bind to any section of the flagella (as a secondary receptor) using their tail fibers (for tailed phages) and subsequently move closer to the cell where they irreversibly attach to their primary receptor, commonly the baseplate of the flagella (Rakhuba et al., 2010). The utilization of flagella as a phage receptor was first described during the 1970's by the group of Lindberg. In fact, the first flagellatropic phage was discovered in 1936 (Coward et al., 2006; Evans et al., 2010). Some of the flagellatropic phages previously described include phage χ (chi) that binds to the flagella of *E. coli*, *Salmonella*, and *Serratia* species. Phage Φ CbK exclusively binds to functional flagella in *Caulobacter crescentus* bacteria (Rakhuba et al., 2010; Coward et al., 2006). Interestingly, in all cases flagella is not the primary receptor. Instead, phages reversibly adsorb to flagella and subsequently, by means of the flagellar rotation, move closer to the bacterial cell surface where irreversible binding at a primary receptor can take place (typically the flagellar baseplate). Zhilenkov et al., (2006) reported that PV22 reversibly adsorbs to *C. jejuni*'s flagella. A study by Coward and collaborators (2006) reveals that phages Φ 3, Φ 4, Φ 8, Φ 10, Φ 12, Φ 14 and Φ 15

bind to flagella. Similarly, phage Φ AT1 binds to flagella of the phytopathogen *Erwina carotovora* ssp. *atroseptica* (Eca) (Evans et al., 2010).

Bacteriophages utilizing pili as a receptor

Different types of pili have been described as bacteriophage receptors, even though pili-dependent phages are less common as compared to LPS or porin-dependent phages. Type IV pili are among those pili-like receptors most common for phage adsorption. This type of pili has been mainly studied in *P. aeruginosa*. It is now well known that this pilus is involved in bacterial motility (twitching motility), which is totally independent and distinct from flagellar motility. Twitching motility is present in several bacterial species (Chibeu et al., 2009; Mattick, 2002). Generally, it occurs by the extension, tethering, and retraction of polar type IV pili. Interestingly, these pili (and twitching motility) are important for host colonization in plants and animals, and the formation of biofilms on abiotic and biotic surfaces (Chibeu et al., 2009). *P. aeruginosa* type IV pili biogenesis and function is heavily regulated by a large number of genes (around 40), signal transduction systems such as two-component systems, and a chemosensory system (Mattick, 2002). Somewhat surprisingly, the gene clusters controlling type IV pili are randomly spread throughout the *P. aeruginosa* genome (Chibeu et al., 2009).

Type IV pili has been exploited by the Φ KMV-like bacteriophage Φ KMV. These phages comprise a subgroup of the *Podoviridae* family, along with two extra members: LKA1 and LKD16. Chibeu's research (2009) demonstrated the

importance of the type IV pili during phage adsorption. Genetic experiments utilizing a Φ KMV-resistant *P. aeruginosa* mutant (named PAO1KR) revealed that phage sensitivity was fully restored when a cosmid carrying the operon *pilMNOPQ* (which is responsible for type IV pili biogenesis) was conjugated into the mutant. As expected, twitching motility was also restored to wild type levels. However, the exact mechanism of phage Φ KMV adsorption remains unsolved. Interestingly it is known that Φ KMV-like bacteriophages (or at least phages Φ KMV and LKD16) adsorb poorly to the OM of their host cells, and rapidly stimulate the rise of phage-resistant mutants. These phage-resistant mutants are typically pili-less. Chibeu et al. (2009) highlighted this fact as a possible disadvantage when using this virus in phage therapy. However, this may be a beneficial side-effect as unpiliated bacteria cannot produce mature biofilms, thus reducing their virulence and antibiotic resistance. Other phages known to bind to type IV pili include PO4, PP7, Pf, F116, D3112, DMS3 and B3 (Chibeu et al., 2009).

On the other hand, sex pili (or fertility- or F-pili) are also utilized by some bacteriophages as a receptor. F-pili is expressed only in those bacterial strains carrying an F conjugative plasmid. Bacterial conjugation occurs when the tips of F-pili make contact with an adjacent receptive cell, and a mating bridge is formed establishing cell-cell contact. A pore is formed between the cytoplasm of both bacteria, which is used to transfer plasmid DNA from the donor bacterium (F+) to the recipient bacterium (F-). It has been determined that F-pili are also involved

in early stages of biofilm formation (May et al., 2011). Phages utilizing F-pili will be discussed below in the tailless phage section.

Bacteriophages utilizing capsular polysaccharides (CPS) as a receptor

Labrie et al. (2010) extensively and comprehensively reviewed the many different mechanisms bacteria have created in order to overcome bacteriophage infection. One of those mechanisms (not solely restricted to phage protection) is the production of a slimy protective layer in the form of a capsule or capsular polysaccharide (CPS). The production of this polymer gives the bacterium several advantages, including increased survivability by protecting the bacteria from harsh environmental conditions like desiccation, or phagocytosis. CPS also can serve as a virulence factor, and as mentioned previously, as a barrier blocking phage access to its primary receptor on the bacterial surface (Labrie et al., 2010; Srivastava et al., 2009). Interestingly, although the production of CPS will impair the attachment of some phages to its specific receptor, other bacteriophages have evolved to recognize these polymers and bind to them. Variations in CPS have produced different groups of CPS-dependent phages (Rakhuba et al., 2010; Labrie et al., 2010).

Briefly, some phages utilize the antigens found in the capsule as receptors; phages will specifically recognize some of these antigens, like K antigens or Vi-antigen. Other phages can utilize their CPS depolymerase activity or polysaccharide-degrading enzymes in order to degrade the CPS and subsequently attach to their primary receptor on the host cell surface. These enzymes can be

found either attached to the phage tails or as free soluble enzymes that are released into the medium when bacteria are lysed by phages (Rakhuba et al., 2010; Labrie et al., 2010; Nimmich et al., 1991).

Coward et al. (2006) isolated phage-resistant mutants where CPS was involved as a receptor. After a series of experiments, they determined that phages $\Phi 1$, $\Phi 2$, $\Phi 6$ and $\Phi 16$ recognize the antigen found in CPS. Perhaps a surprising feature of some phages attaching to CPS is the presence of capsular polysaccharide degrading enzymes, which help the phage to degrade the capsule sugars to allow the phage to reach the OM and attach to its specific receptor. A key characteristic of phages with a CPS-degrading activity is the presence of halos surrounding the plaques (or the production of haloed plaques), when phages are propagated by the top agar overlay method.

Some of the first descriptions of bacteriophages with capsular depolymerase enzymes were published in the 1970's. For example, phages K29 and K11 carry an enzyme with an endoglycosidase activity. Similarly, phage K2 hydrolyzes the *Aerobacter aerogenes* capsule by means of its glucan hydrolase, breaking the $\alpha 1,3$ links in the galactose residues. In all previous examples, the CPS serves as a secondary receptor for phage adsorption, and thus reversible binding is common at this stage of infection (Rakhuba et al., 2010).

Two bacteriophages that recognize and attach to the K antigens (K5 and K20) found in the capsule of *E. coli* are $\Phi K5$ and $\Phi K20$. Early studies revealed the presence of CPS degrading enzymes through the interaction between phages and isolated polysaccharides, and the finding of the reduced sugars in the

degradation products. In the case of phage Φ K5, its depolymerase enzyme was able to degrade the *E. coli* K5 and K95 polysaccharides. Conversely, phage Φ K20 enzyme degraded antigens K5 and K20. The enzymatic activity of phage Φ K20 was attributed to a glycanase, cleaving the β -keto-pyranosidic KDO linkages present in K20, K13 and K23 capsular antigens. Additionally, because phage Φ K20 was also able to degrade the K5 antigen, it was hypothesized that a second CPS degrading enzyme could be present in the phage, as this putative second enzyme showed an endo- α -N-acetylglucosaminidase activity. It was proposed that phage Φ K5 carried a glycanase, breaking down the β -furanosidic linkages of the K95 capsular antigen, based on the finding that the exact enzyme (glycanase) was previously described in the K95 specific phage Φ K95. Unfortunately, the authors did not test whether phage adsorption to these antigens was reversible (Nimmich et al., 1991).

A more recent study carried out by Glonti and colleagues (2010) identified a putative phage-attached depolymerase degrading the alginic acid capsule of *P. aeruginosa*. As previously mentioned, the presence of haloed plaques suggested to the authors the possible presence of a CPS degrading enzyme. Phages PT-1, PT-7, PT-6 and PT-12 all produced haloed plaques. Further characterization of the putative enzyme revealed that it was active against alginic acid from three different *P. aeruginosa* strains. In addition, the enzyme degraded alginic acid extracted from algae. A reduction of 62-66% of viscosity was observed after 15 minutes of interaction between the alginate degrading enzyme and the four distinct alginic acids, proving its high efficiency at degrading sugars. CPS-

specific phages have been investigated for the possibility of employing their depolymerases in conjunction with classical antibiotics to treat biofilms or perhaps reduce the colonization during bacterial infections. Molecular interactions between the bacterial receptors and these phages have not been totally elucidated, however, assumptions can be made due to similarities in phage morphology with other phages.

Tailless phages: Host recognition and adsorption

There are evident morphological differences between tailed and tailless phages. The latter resemble eukaryotic viruses, in which the DNA or RNA is enclosed in a membrane-capsid complex. No tail structures are found in this group of phages. When delivering nucleic acid into the host the phage capsid fuses with the host membranes, protecting the nucleic acid from external damage, nucleases, etc., and subsequently delivering it directly into the cytoplasm (Letellier et al., 2004). This group of phages represents only 4% of all known phages (Ackermann & Kropinski, 2007).

A well-studied model is bacteriophage PRD1, a member of the *Tectiviridae* family. Its dsDNA is enclosed in a capsid-like membrane that is additionally protected by an icosahedral protein shell. The proteins forming several structures of this phage family have been characterized, including a set of three proteins (P2, P5 and P31) that form the spike-penton complex, which is essential during host recognition and subsequent adsorption. These complexes are found in the phage proteinaceous shell. Through years of investigation and the

discovery of P2 nonsense mutants, it was revealed that the P2 protein is the receptor binding protein because phages mutated in P2 were unable to attach to the host cell surface. P2 complementation and competition experiments between the phage and the purified P2 protein also confirmed this previous finding. In addition, it was determined that P2 is present in at least 11 of the phage vertices as proved by P2-specific antibodies.

It is known that phage PRD1 infects Gram-negative bacteria carrying the IncP conjugative plasmid RP4, which encodes a cell envelope structure (mating bridge) that connects the OM and IM during bacterial conjugation. Reversible binding occurs when P2 first interacts with this mating bridge, however, after 15 minutes of interaction this adsorption becomes irreversible due conformational changes in the spike-penton complex. These changes lead to the release of other proteins that assist in the delivery of the DNA into the cell's cytoplasm via fusion of the capsid-like membrane into the host IM (Gowen et al., 2003; Grahn et al., 1999; 2002).

PM2 is an interesting bacteriophage; the only member of the *Corticoviridae* family, it infects members of the *Pseudoalteromonas* species. Morphologically similar to PRD1, it is composed of a lipid-membrane that encloses the dsDNA. Protecting the lipid-membrane is an icosahedral protein shell that contains several vertices, each one carrying a pentameric receptor binding structure that is composed of protein P1. Phage infection is triggered by the recognition and subsequent adsorption of P1 to its receptor. Unfortunately, its specific receptor has not been identified. However, high-resolution X-ray images

have provided some insight about the putative receptor. Because the structure of P1 resembles the Ca^{2+} -dependent carbohydrate-binding proteins from the marine bacterium *Saccharophagus degradans*, it has been suggested that LPS moieties may serve as the phage PM2 receptor. Interestingly, phage PM2 adsorption depends upon the intracellular ATP concentrations of the host. Experiments with specific compounds affecting either the proton motive force or ATP revealed that phage adsorption was reduced between 24 and 40% (depending on the substance used) when the intracellular ATP level was reduced. This finding poses a question; how can the phage adsorb to LPS in an energy-dependent manner if the OM is a non-energized membrane? The authors proposed that LPS may serve as a secondary receptor (reversible binding) and that a transmembrane protein or protein-complex serves as the primary receptor, thus explaining why ATP is essential for phage irreversible adsorption. In addition, results demonstrate that phage PM2 genome delivery depends upon the presence of calcium ions (Cvirkaite-Krupovic, 2010a).

RNA bacteriophage $\phi 13$ also adsorbs to LPS moieties, although this phage was only able to infect bacteria with an R-Type LPS. Bacteriophage $\phi 6$ recognizes and adsorbs to type IV pili of *P. syringae* cells. Interestingly, contrary to what is observed with filamentous phages where the attachment occurs at the tip of pili, the icosahedral phage $\phi 6$ adsorbs to the sides of the pilus by means of its spike protein P3. When the pilus retracts, it brings the phage close to the host OM and subsequently the phage binds irreversibly to its primary receptor allowing fusion with the OM. At that time, a series of proteins are expressed that

degrade periplasmic components and peptidoglycan, finally permitting the nucleocapsid (capsid-membrane) to make contact with the host's IM and be internalized in an energy-dependent manner with release of the RNA into the cytoplasm (Cvirkaite-Krupovic, 2010b; Daugelavicius et al., 2005).

As previously mentioned, F-pili is also an uncommon target for phages. Some of the tailless phages bind to F-pili including the well-studied filamentous non-lytic phage f1. This was confirmed when early biofilm formation was totally abolished by the addition of phage f1. Phage f1 binds to the tip of the F-pilus (similar to phages fd and M13). When phage f1 was added to a "mature" (24 hr old) biofilm, the phage was unable to degrade it. Interestingly, this phage does not lyse its host or affect planktonic cell growth, rather it exclusively appears to reduce biofilm formation at early developmental stages. Biofilm formation was greatly affected by phage f1, as compared to phage M2 (which was used as a control phage that also utilizes F-pili to infect its host). However, phage M2 (and phage Q β) bind to the sides of the pili and cause host cell lysis contrary to phage f1 (May et al., 2011).

Another well-studied model phage is bacteriophage fd. The interaction between phage fd and its receptors in the OM of bacteria have been elucidated to some extent. Phage fd utilizes its gene 3 protein (G3P) to attach to its host. Studies have demonstrated the presence of three to five copies of G3P at one end of the phage. G3P consists of different domains: the C-terminal domain links G3P to the phage particle, the N2 (middle) domain makes contact in a reversible

manner to the tip of the F-pili (its secondary receptor), and the N1-terminal domain adsorbs to the TolA-C complex in an irreversible manner (the primary receptor). G3P is a very stable protein; this stability is provided by the tight interaction between domains N1 and N2. However, when the N2 domain makes contact with the F-pilus, a signal is sent to a connector that links N2 with the N1 domain. Structural conformational changes occur destabilizing the N1-N2 interaction exposing the TolA binding site in the N1 domain of G3P (Lorenz et al., 2011)

Bacteriophage M13 also behaves similarly to phage fd. Lorenz and collaborators (2011) also performed a comparative study between phages fd and IF1. Bacteriophage IF1's G3P also consists of three domains. A C-terminal domain anchors G3P to the phage, the N2 domain interacts with the I-pili, and finally, the N1 domain makes contact with the TolA-C complex. Spectroscopy analyses revealed that the N1 domain of both phages interacts with the same region in the TolA-C complex, and that they can be functionally exchanged without loss of function. However, the N1 domain is not essential for phage infection. Observations confirmed that IF1 phages lacking the N1-domain were still able to infect their target host but 1000-fold less efficiently, and dependent upon the presence of CaCl_2 . Interestingly, opposite to what is seen with phage fd, there is no interaction between domains N1 and N2 in phage IF1. Thus, the N1 domain is always accessible to interact with its primary receptor TolA-C. Furthermore, experiments with chimera phages where the IF1-N2 domain was replaced with the fd-N2 domain produced host variable phages that changed the

host recognition and attachment from I-pilus to F-pilus respectively. As expected, a phage N2 deleted domain was no longer able to infect *E. coli* carrying either I or F-pili (Lorenz et al., 2011). Other phages that recognize and attach to pili include P17, M12, fr, f2 and f4 (Rakhuba et al., 2010).

Table 1: Phages that require at least two receptors in order to infect the host. ? symbols indicate putative receptor.

Phage	Secondary receptor (Reversible binding)	Primary receptor (Irreversible binding)	Reference
Tu1b	LPS?	OmpC?	Heller et al. (1992)
T4	OmpC LPS?	Core oligosaccharide (LPS)	Yu & Mizushima, (1982); Leiman et al. (2003)
T2	OmpF?	LPS (Heptose)	Rakhuba et al. (2010); Yoichi et al. (2005)
K20	LPS? (Glucose-Galactose)	OmpF?	Traurig & Misra, (1999)
T5	LPS O-antigen	FhuA	Letellier et al. (2004); Bonhivers et al. (1996); Heller, (1992); Plançon et al. (2002)
T1	Similar to phage T5?	FhuA	Letellier et al. (2004); Heller, (1992)
UC-1	Similar to phage T5?	FhuA?	Letellier et al. (2004); Heller, (1992)
φ 80	Similar to phage T5?	FhuA	Letellier et al. (2004); Heller, (1992)
Tu1b	LPS? (OmpA-LPS complex required for full phage)	OmpA	Rakhuba et al. (2010); Datta et al. (1977)

	infection)		
P22	LPS O-antigen (Rhamnose-Galactose)	LPS?	Letellier et al. (2004); Steinbacher et al. (1997)
ϵ^{15}	LPS O-antigen (Rhamnose-Galactose)	LPS?	Letellier et al. (2004)
$\phi 1$	LPS O-antigen? (endo-1,2-N-galactoseaminidase)	LPS?	Rakhuba et al. (2010)
$\Omega 8$	LPS O-antigen? (Endorhamnosidase)	LPS?	Rakhuba et al. (2010)
Sf6	LPS O-antigen (Rha-1 \rightarrow 3-Rha)	LPS?	Rakhuba et al. (2010)
HK620	LPS O-antigen (endo-N-acetylglucosaminidase)	LPS?	Barbirz et al. (2008)
χ (chi)	Flagella	Flagella baseplate?	Rakhuba et al. (2010)
Φ CbK	Flagella	Flagella baseplate?	Rakhuba et al. (2010); Coward et al. (2006)
PV22	Flagella	Flagella baseplate?	Zhilenkov et al. (2006)
K29	Capsular polysaccharide	?	Rakhuba et al. (2010)
K11	Capsular polysaccharide	?	Rakhuba et al. (2010)
K2	Capsular polysaccharide	?	Rakhuba et al. (2010)
PM2	LPS?	?	Cvirkaite-Krupovic, 2010a
PRD1	Mating bridge (IncP conjugative plasmid)	Mating bridge (After 15 mins. of interaction?)	Gowen et al. (2003); Grahn et al. (1999; 2002)
fd	F-pili (tip of pili)	TolA-C complex	Lorenz et al. (2011)
M13	F-pili (tip of pili)	TolA-C complex	Lorenz et al. (2011)
IF1	I-Pili	TolA-C complex	Lorenz et al. (2011)

MATERIALS & METHODS

Bacterial strains & growth conditions

The *B. cenocepacia* complex (Bcc) strains used in this study have been grouped by Coenye et al., (2001) and Mahenthiralingam et al., (2000). Strains K56-2 and PC184 belong to the *Burkholderia cenocepacia* ET12 clonal lineage [Table 2]. Different strains were isolated from different sources and provided by the Canadian *Burkholderia cepacia* complex Research and Referral Repository. Bcc bacteria were grown aerobically in ½ and/or full Luria-Bertani (LB) medium at 37°C for approximately 16 hrs. with shaking (225 rpm) or in solid agar and supplemented if required with antibiotics, 300 µg of trimethoprim (Tp)/mL (for plasposon mutants) and 100 µg of trimethoprim (Tp)/mL and 100 µg of tetracycline (Tc)/mL plus 0.2% or 0.02% rhamnose (for plasmid induction) for complemented Bcc mutants.

For cloning experiments, commercially obtained chemically competent *E. coli* DH5-α [F⁻ φ80*lacZ* M15 *endA recA hsdR(rK⁻mK⁻) supE thi gyrA relA Δ(lacZYA-argF)U169*] cells (Invitrogen, Carlsbad, CA) were used. Bacteria were grown aerobically on LB agar medium at 37°C for approximately 16 hrs. and supplemented with appropriate antibiotics, 100 to 300 µg of trimethoprim/mL, 10 µg of tetracycline/mL, 50 µg of kanamycin/mL (*E. coli* HB101 tri-parental matings helper strain) and 100 µg of ampicillin/mL.

K56-2 lipopolysaccharide mutants were kindly provided by Miguel Valvano (University of Western Ontario, London, Ontario, Canada). These strains were grown at 37°C for approximately 16 hrs. with shaking (225 rpm) or in solid agar and supplemented with 100 µg of trimethoprim/mL [Table 3].

All strains were stored at -80°C in LB medium supplemented with 20% glycerol.

Table 2: Bacterial species and strains used in this research. Legend abbreviations: CF-e, cystic fibrosis epidemic isolate, NA, not applicable (Adapted from Routier, 2010).

Species	Strain	Source & Location	Reference
<i>B. cenocepacia</i>	K56-2	CF-e, Canada	Mahenthiralingam et al., (2000)
<i>B. cenocepacia</i>	PC184	CF-e, USA	Mahenthiralingam et al., (2000)
<i>E. coli</i>	HB101 (pRK2013)	NA	Figurski and Helinski (1979)
<i>E. coli</i>	DH5- α	NA	Invitrogen
<i>E. coli</i>	JM109 (p34S-Tc)	NA	Dennis & Zylstra (1998)

Table 3: *B. cenocepacia* K56-2 LPS truncated mutants used in this research.

Species	Parental Strain	Disrupted genes and new strain name	Reference
<i>B. cenocepacia</i>	K56-2	XOA7 (<i>waaL</i> ::pGP Ω Tp Tp ^R)	Ortega et al., (2009)
<i>B. cenocepacia</i>	K56-2	XOA8 (<i>wabO</i> ::pGP Ω Tp Tp ^R)	Ortega et al., (2009)
<i>B. cenocepacia</i>	K56-2	RSF19 (<i>wbxE</i> ::pRF201 Tp ^R)	Loutet et al., (2006)
<i>B. cenocepacia</i>	K56-2	XOA15 (<i>wabR</i> ::pGP Ω Tp Tp ^R)	Ortega et al., (2009)
<i>B. cenocepacia</i>	K56-2	XOA17 (<i>wabS</i> ::pGP Δ pTp Tp ^R)	Ortega et al., (2009)
<i>B. cenocepacia</i>	K56-2	CCB1 (<i>waaC</i> ::pGP Ω Tp Tp ^R)	Ortega et al., (2009)

Bacteriophage propagation

Bacteriophages KS4-M, KS5, KS9, KS12, KL1 and AH2 were all propagated on host *B. cenocepacia* strain K56-2 while phages KS14, DC1, SR1 and KS10 were all propagated on host *B. cenocepacia* strain PC184 by the soft agar overlay method. Briefly, 100 μ L of phage were mixed with 100 μ L of host liquid culture and incubated for 20 minutes at room temperature, 3 mL of soft $\frac{1}{2}$ LB agar was added to previous mixture and poured onto a $\frac{1}{2}$ LB agar plate, and the plate was incubated overnight at 30°C. Phage-bacteria mixture was resuspended on sterile mQH₂O water, centrifuged at 11,000 rpm for 15 minutes and filter sterilized using a 0.45 μ m pore-size filter. To determine the plaque forming units (PFU) per mL on the phage stocks, a series of serial dilutions were performed with the original phage stock and plated on the appropriate host using the previously described soft agar overlay method. Plaques were counted the next day and the phage concentration determined for each phage stock.

Plasposon mutant library construction

The construction of the K56-2 pTn*Mod*OTp' and the PC184 pTn*Modlux*-OTp' plasposon insertion mutant libraries has been described elsewhere (Routier, 2010).

Identification of phages able to clear bacterial liquid cultures

Overnight cultures of either *B. cenocepacia* K56-2 or PC184 were grown in $\frac{1}{2}$ LB broth at 37°C with continuous shaking (225 rpm) for ~16 hrs. prior to the

assays. In a 96-well plate, a blank control group (200 μ L of $\frac{1}{2}$ LB broth), a positive control (190 μ L of $\frac{1}{2}$ LB broth, 10 μ L of host either K56-2 or PC184), and a test group (150 μ L of $\frac{1}{2}$ LB broth, 10 μ L of host K56-2 or PC184 and 50 μ L of high titer phage stock) were mixed. Plates were incubated for a period of six hours at 37°C with shaking (225 rpm) and the absorbance ($A_{600\text{nm}}$) was measured every two hours during this six hour period in a Victor X3 2030 multilabel reader spectrophotometer. Absorbance readings between the control (no phage) and the test groups (phage added) wells were compared. Data was analyzed with A-Nova plus Tukey Post Hoc tests with 95% reliability.

Plasposon mutant library screening

A high-throughput liquid clearing assay was performed in order to detect phage resistant mutants. Briefly, the original 96-well plates stored at -80°C were subcultured in a new 96-well plate with fresh $\frac{1}{2}$ LB broth and incubated overnight at 37°C with shaking (225 rpm) to allow for homogeneous growth. Two 96-well plates with fresh $\frac{1}{2}$ LB broth (150 μ L per well) were then stamp inoculated from the previous overnight plate, one served as control (no phage added) and one served as test (phage added) with 50 μ L of high titer phage stock per well. Plates were incubated for a period of six hours at 37°C with shaking (225 rpm) and the A_{600} was measured every three hours during the six hour period in a Victor X3 2030 multilabel reader spectrophotometer. Absorbance readings between the control and the test plates were compared; bacteria from wells with high Abs

readings (phage unable to lyse the host) were subsequently isolated to confirm their resistance to phage infection.

A second confirmatory screening was performed similar to the previously described test, however only the putative resistant mutants were cultured in a 96-well plate with fresh $\frac{1}{2}$ LB broth and incubated overnight at 37°C with shaking (225 rpm). A new 96-well plate was then inoculated with 200 μ L of $\frac{1}{2}$ LB broth (negative control), 10 μ L of the putative phage resistant mutant plus 190 μ L of $\frac{1}{2}$ LB broth (positive control), and 10 μ L of the putative phage resistant mutant, 50 μ L of high titer phage stock and 150 μ L of $\frac{1}{2}$ LB broth (test group). Plates were incubated for a period of six hours at 37°C with shaking (225 rpm). A_{600} was taken every two hours during this six hour period in the spectrophotometer. High A_{600} readings confirmed phage KS4-M resistance. Data was analyzed with A-Nova plus Tukey Post Hoc tests with 95% reliability. A total of ten phage KS4-M resistant mutants were isolated and stored accordingly for further analysis.

Other bacteriophages in our collection were then tested against the KS4-M bacterial resistant mutants. These were phages KS5, KS9 and KS12, which all infect strain K56-2 (Seed & Dennis, 2005; 2009). A similar approach was used, but an additional control was included in the assay; 10 μ L of a K56-2 wt liquid overnight, 50 μ L of high titer phage stock were mixed in 150 μ L of $\frac{1}{2}$ LB broth. This control group proves that the phage stocks were active at the time the assay was performed. From this third screening, it was determined that phages KS9 and KS12 shared a common receptor as that for phage KS4-M. Only phage KS5 was

able to infect the KS4-M bacterial resistant mutants, thus suggesting a different receptor.

A similar approach was used to screen the PC184::pTn*Modlux*OTp' plasposon mutant library, however phages DC1, KS10 and SR1 were selected to screen this second library because their natural host is the strain PC184 (which can't be infected by phages KS4-M, KS5, KS9 and KS12 phages).

Finally, a third screening was performed on both libraries and using the same phages, however the media ½ LB was substituted with minimal media (MM) [K₂HPO₄, 6 g; KH₂PO₄, 3 g; (NH₄)₂SO₄, 1 g; MgSO₄·7H₂O, 0.2 g; succinic acid, 4 g; adjusted to 1 L with dH₂O. pH was adjusted to 7.0 before sterilization]. This media provides the minimum nutrients required for a bacterium to grow thus in theory it better emulates the conditions bacteria will face in the soils or in an *in vivo* environment.

DNA manipulation, plasposon isolation and DNA sequencing

Bacterial DNA from ten K56-2::pTn*Mod*OTp' KS4-M, KS9 and KS12 resistant mutants, six PC184::pTn*Modlux*OTp' DC1 resistant mutants and two PC184::pTn*Modlux*OTp' KS10 and SR1 resistant mutants was isolated and purified by the CTAB DNA precipitation method (Wilson, 1997). After purification, the DNA was digested with Fast Digest *Pst*I (Fermentas) in order to determine the plasposon insertion sites, as has been previously described (Dennis & Zylstra, 1998). DNA digestions were ligated using T4 DNA ligase (Promega, CA) and subsequently transformed into *E. coli* DH5-*a* cells, transformants were

selected on LB agar + 100 µg of Tp/mL. The plasposon's insertion site was determined by isolating the recombinant plasmid from the clones and subsequently sequencing them with specific primers JD28 5' Ori: 5'-GGGGAAACGCCTGGTATC and JD47 3' Tp: 5'-TTTATCCTGTGGCTGC, which anneal to sequences inside the plasposon.

DNA sequencing was performed using the Big Dye kit (Applied Biosciences, Warrington, UK). Briefly, 3 µL of 5x Big Dye sequencing buffer, 2 µL of Big Dye, 1 µL of each primer and 6 µL of pDNA template adjusted to a final volume of 20 µL with mQH₂O were combined on a PCR tube on ice and runned in the standard sequencing reaction. PCR reaction included 35 cycles of a 20 second denaturation at 95°C, primer annealing at 50°C for 15 s and a 1 minute extension at 60°C. Following this, the sequencing reaction was maintained at 4°C. To stop and clean up the sequencing reactions, 2 µL of sodium acetate/EDTA and 80 µL of 95% ethanol were added and the mixture was incubated at 4°C for 15 minutes. To precipitate DNA, the DNA was pelleted by centrifugation at 14,000 rpm for 15 minutes, the supernatant was removed and the pellet was washed a second time with 500 µL of 50% EtOH. DNA was pelleted by centrifugation at 14,000 rpm for 5 minutes and dried in a vacuum for 5-10 minutes. Sequences were electrophoresed on an ABI 3100 genetic analyzer (Applied Biosystems, Foster City, CA) by the University of Alberta Department of Biological Sciences Molecular Biology Service Unit. Sequences were then analyzed using the software packages 4peaks, DynamoDNA, and the Basic Local Alignment Search Tool (BLAST) with the NCBI database (blast.ncbi.nlm.nih.gov/Blast.cgi).

Bacteriophage infection assays vs. LPS truncated mutants [Liquid culture clearing assays]

A similar approach to that used for screening was used, and similar controls were included. The six K56-2 LPS truncated mutants (kindly provided by Dr. Miguel Valvano) were tested against phages KS4-M, KS5, KS9 and KS12 on liquid cultures. K56-2 LPS truncated mutants are listed in Table 2.

Bacteriophage infection assays vs. LPS truncated mutants [Efficiency of plating (EOPs)]

Briefly, bacteria were grown on ½ LB broth + 100 µg of Tp/mL for 16 hrs. at 37°C with shaking (225 rpm). The A₆₀₀ was measured for previous overnights and standardized to ~2.0. 100 µL of high titer phage stock was serially diluted (up to 10⁻⁷) and mixed with 100 µL of host liquid culture and incubated for 20 minutes at room temperature. 3 mL of soft ½ LB agar was added to the previous mixture and poured into a ½ LB + 100 µg of Tp/mL agar plate, and plates were incubated overnight at 30°C. Plaques (if present) were counted the next day and the EOP determined for phages KS4, KS4-M and KS12.

Molecular Cloning

Plasmid pXO3 (*wbxD-wbcE*) was kindly provided by Dr. Valvano and collaborators; the construction of this plasmid has been previously described (Ortega et al., 2005). However, this plasmid in its original form was unable to be used because a Tp^R marker was used for plasmid selection. Our K56-

2::pTnModOTp' phage resistant mutants are also Tp resistant. In order to modify pXO3 with a new resistance cassette, the plasmid was digested with fast digest *NdeI* and *XbaI* enzymes (Fermentas) eliminating the insert and leaving pSCRhaB3 (empty vector). The fragments were separated and visualized using 0.7% agarose gel electrophoresis. Fragments were purified using the GeneClean III Kit (Q-Biogene, Irvine, CA) following the manufacturer's instructions. Subsequently, Bcc gene 6466 was cloned into the vector with *NdeI* and *XbaI* ends, forming pSCRha6466. The Tc^R marker was extracted from p34S-Tc (Dennis & Zylstra, 1998) with fast digest *SmaI* (Fermentas) and inserted into the *EcoRV* site of pSCRha6466. Once the Tc^R cassette was inserted, genes *wbxD-wbcE* were cloned back into the plasmid using *NdeI* and *XbaI*.

To create the empty vector, the plasmid was treated with Mung Bean Nuclease following the manufacturer's instructions. To ligate the DNA, 4 µL of insert were mixed with 1 µL of T4 DNA ligase, 2 µL of ligase T4 buffer (Promega, Madison WI), 0.5 µL of pSCRhaB3 Tp-Tc and adjusted to a final volume of 20 µL with mQH₂O, the mixture was incubated overnight at 16°C.

The resulting plasmid was named pXO3 Tp-Tc (*wbxD-wbcE*). 5 µL of plasmid DNA was transformed into chemically competent subcloning efficiency *E. coli* DH5-α (Invitrogen) cells by the heat shock method with a slight modification. Briefly, cells were incubated on ice for 30 seconds following the heat shock, instead of the regular 2 minutes. 500 to 900 µL of SOC (in 990 mL dH₂O: 20 g Bactotryptone, 5 g yeast extract, 0.5g NaCl, 2.5 mL 1 M KCl, 10 mL 1 M MgCl₂ and 20 mL 1 M glucose, pH 7.0 using 10 M NaOH) (Sambrook et al.,

1989) was used to allow for cell recovery after heat shock and cells were incubated for 1 hour at 37° with shaking (225 rpm). Subsequently, cells were plated on LB + 10 µg of Tc/mL. Transformants carrying recombinant plasmids with the DNA insert were screened by pDNA digestion with the appropriate restriction enzymes and also by DNA sequencing, as previously described, using primers pSCRha R1 5'-GCTTCTGCGTTCTGA and pSCRha F2 5'-GGCCATTTTCCTGTC, which anneal to vector sequences flanking the MCS of pSCRhaB3.

Top Taq (Qiagen) polymerase chain reaction (PCR) was used to amplify genes *wbcE* and *wbxD*. These were amplified from the *B. cenocepacia* K56-2 DNA fragment *wbcE-wbxD* extracted from pXO3 Tp-Tc.

Primers P1163-*XbaI* 6 His-Tag (2) 5'-ATTCTAGATCAGTGGTGATGGTGATGATGGCCGTGCCGCTCTGGCG and *wbxD-NdeI* (1) 5'-GCGGGCGCATATGGAGTTTGACCGACAAA were used to amplify gene *wbxD*. The amplification conditions were 3 min at 94°C, 30 cycles of 94°C for 30 s, 64°C for 30 s, and 72 °C for 3 min, and a final extension of 10 min at 72°C.

Primers P1164-*NdeI* 6 His Tag (2) 5'-GGAATTCCATATGCATCATCACCATCACCACCCGCGATACCAAAAATT TTTGTTCTTT and *wbcE-XbaI* (1) 5'-AATTCTAGATCAAACCTCCATAACCTTCCAACCTCCC were used to amplify *wbcE*. The amplification conditions were 3 min at 94°C, 30 cycles of 94°C for 30 s, 60°C for 30 s, and 72 °C for 3 min, and a final extension of 10 min at 72°C.

Two of the primers (P1163 and P1164) were used as a template to create the same primers with a His tag, and these primers have been previously described (Ortega et al., 2005). Previously obtained PCR amplification products were cloned into pJET1.2/blunt (Fermentas) using the blunt end protocol and following the manufacturer's instructions. Resulting plasmids were then transformed into chemically competent *E. coli* DH5- α cells as previously described and plated on LB + 100 μ g of Amp/mL.

Plasmid DNA from previous clones was isolated and digested with fast digest *Nde*I and *Xba*I (Fermentas) to confirm the correct insertion of the product. Products were visualized on 0.7% agarose gels by electrophoresis. These products were excised from gels and purified using the GeneClean III Kit following the manufacturer's instructions. To ligate DNA, 1.66 μ L of insert (*wbxD*) and 3.84 μ L of (*wbcE*) were mixed with 1 μ L of T4 DNA ligase, 2 μ L of ligase T4 buffer (Promega, Madison WI), 2 μ L of pSCRhaB3 Tp-Tc and adjusted to a final volume of 20 μ L with mQH₂O, the mixture was incubated at 22°C for 1 hr.

Resulting plasmids were named pXO4 Tp-Tc (*wbcE*) and pXO7 Tp-Tc (*wbxD*) and were similar to plasmids previously described (Ortega et al., 2005). 5 μ L of previous plasmid DNA was transformed into *E. coli* DH5- α (Invitrogen) cells as previously described and plated on the appropriate media. Transformants carrying recombinant plasmids with the DNA insert were screened by pDNA digestion with the appropriate restriction enzymes and also by DNA sequencing using primers pSCRha R1 and pSCRha F2, which anneal to vector sequences flanking the MCS of pSCRhaB3.

The original plasmid pSCRhaB2, which carries a Tp^R marker for plasmid selection (Cardona & Valvano, 2005) was modified with a Tc cassette prior the transformation of the LPS truncated mutants XOA8 (*wabO*::pGPΩTp Tp^R) and CCB1 (*waaC*::pGPΩTp Tp^R). pSCRhaB2 was first digested with fast digest *SacI* (Fermentas) to eliminate a region that contains part of the Tp^R promoter, which disrupts the function of the cassette. Similarly, the Tc^R marker was extracted by digesting p34S-Tc (Dennis & Zylstra, 1998) cloned in *E. coli* strain JM109 with fast digest *SacI* (Fermentas). Products were visualized on 0.7% agarose gels by electrophoresis. These bands were excised from gels and purified using the GeneClean III Kit following the manufacturer's instructions. To ligate DNA, 2.16 μ L of insert (Tc^R) was mixed with 1 μ L of T4 DNA ligase, 2 μ L of ligase T4 buffer (Promega, Madison WI), 5 μ L of pSCRhaB2 (No Tp^R) and adjusted to a final volume of 20 μ L with mQH₂O, then the mixture was incubated at 16°C for 8 hrs. The resulting plasmid was named pSCRhaB2-Tc. Five μ L of the previous plasmid DNA was transformed into *E. coli* DH5- α (Invitrogen) cells as previously described and plated on LB + 10 μ g of Tc/mL agar plates and incubated at 37°C for ~16 hrs. Transformants carrying recombinant plasmids with the DNA insert were screened by pDNA digestion with fast digest *EcoRV* (Fermentas) to determine the orientation of the insert (Tc^R) on the plasmid. Clones with the antibiotic marker oriented in the opposite direction (reverse) of the multiple cloning site (MCS) were stored at -80°C on LB broth + 20% glycerol.

Genes *wabO* and *waaC* were also amplified from *B. cenocepacia* K56-2 chromosomal DNA using TopTaq (Qiagen) in a polymerase chain reaction (PCR).

Primers *wabO-NdeI* (XOA8) 5'-

AAGATCGCATATGGCTGAACCTACGCTCGG and *wabO-XbaI* 10 His-Tag

(XOA8) 5'-

ATTTCTAGACTAGTGATGGTGATGATGGTGATGGTGATGATGGCGGCG

CGATGCGGG were used to amplify gene *wabO*. The amplification conditions

were 3 min at 94°C, 30 cycles of 94°C for 30 s, 69.5°C for 30 s, and 72 °C for 1

min, and a final extension time of 10 min at 72°C.

Primers *waaC-NdeI* 10 His-Tag (CCB1) 5'-

CAATTAACATATGCATCATCACCATCACCATCATCACCATCACCAAAA

GATCCTGATCGTGC and *waaC-BamHI* 10 His-Tag (CCB1) 5'-

TAGGATCCTTAGTGATGGTGATGATGGTGATGGTGATGATGCAGGAGG

CCGAAGCCCG were used to amplify *waaC*. The amplification conditions were

3 min at 94°C, 30 cycles of 94°C for 30 s, 56.5°C for 30 s, and 72 °C for 1:20

min, with a final extension time of 10 min at 72°C. Previous PCR amplification

products were cloned into pJET1.2/blunt (Fermentas) as previously described and

transformed into chemically competent *E. coli* DH5- α cells as previously

described. Plasmid DNA from previous clones was isolated and digested with fast

digest *NdeI* and *XbaI* or *NdeI* and *BamHI* (Fermentas) to confirm the correct

insertion of the product. Products were excised from gels and purified using the

GeneClean III Kit following the manufacturer's instructions. To ligate DNA, 6.92

μ L of insert (*wabO*) and 0.64 μ L of (*waaC*) were mixed with 1 μ L of T4 DNA

ligase, 2 μ L of ligase T4 buffer (Promega, Madison WI), 8 μ L of pSCRhaB2-Tc

and adjusted to a final volume of 20 μ L with mQH₂O, then the mixture was incubated at 16°C for 8 hr.

Resulting plasmids were named pSC*wabO*-Tc and pSC*waaC*-Tc. Five μ L of the previous plasmid DNA was transformed into *E. coli* DH5- α (Invitrogen) cells as previously described and plated on the appropriate media. Transformants carrying recombinant plasmids with the DNA insert were screened by pDNA digestion with the appropriate restriction enzymes and also by DNA sequencing PCR using primers pSCRha R1 and pSCRha F2, which anneal to vector sequences flanking the MCS of pSCRhaB2-Tc.

Table 4: Plasmids used in this research.

Plasmid	Description	Reference
pXO3	pSCRhaB3, <i>wbxD-wbcE</i> under the control of P _{RHA}	Ortega et al., (2005)
pSC6466 Tp-Tc	pSCRhaB3, 6466 under the control of P _{RHA} with a Tc ^R and a Tp ^R cassettes	This study. Thomson, unpublished
pSCRhaB3 Tp-Tc	pSCRhaB3, with a Tc ^R and a Tp ^R cassettes	This study
pXO3 Tp-Tc	pSCRhaB3 Tp-Tc, <i>wbxD-wbcE</i> under the control of P _{RHA} with a Tc ^R and a Tp ^R cassettes	This study
pXO4 Tp-Tc	pSCRhaB3 Tp-Tc, <i>wbcE</i> under the control of P _{RHA} with a Tc ^R and a Tp ^R cassettes	This study
pXO7 Tp-Tc	pSCRhaB3 Tp-Tc, <i>wbxD</i> under the control of P _{RHA} with a Tc ^R and a Tp ^R cassettes	This study
pSCRhaB2	pSCRhaB1, opposite orientation of the <i>dhfr</i> cassette	Cardona & Valvano (2005)
pSCRhaB2-Tc	pSCRhaB2, with a Tc ^R cassette	This study
pSC <i>wabO</i> -Tc	pSCRhaB2-Tc, <i>wabO</i> under the control of P _{RHA} with a Tc ^R cassette	This study
pSC <i>waaC</i> -Tc	pSCRhaB2-Tc, <i>waaC</i> under the control of P _{RHA} with a Tc ^R cassette	This study

p34S-Tc	P34E, with a Tc ^R cassette	Dennis & Zylstra, (1998)
pJET1.2/blunt- <i>wbcE</i>	pJET1.2/blunt, <i>wbcE</i> with a N-terminus 6 His Tag	This study
pJET1.2/blunt- <i>wbxD</i>	pJET1.2/blunt, <i>wbxD</i> with a C-terminus 6 His Tag	This study
pJET1.2/blunt- <i>wabO</i>	pJET1.2/blunt, <i>wabO</i> with a C-terminus 10 His Tag	This study
pJET1.2/blunt- <i>waaC</i>	pJET1.2/blunt, <i>waaC</i> with a N and C-termini 10 His Tag	This study

Table 5: PCR specifications and primers used in this research. Bold letters represent restriction sites, Legend abbreviation: NA, not applicable.

Primer set & sequence	Amplified region	Annealing temperature (°C)	Amplicon size (bp)
JD28 5' Ori: 5'-GGGAAACGCCTGGTATC JD47 3' Tp: 5'-TTTATCCTGTGGCTGC	Variable	50°	NA
pSCRha R1: 5'-GCTTCTGCGTTCTGA pSCRha F2: 5'-GGCCATTTCTCTGTC	Insert at MCS	60°	Variable Pending on insert size
P1163- <i>XbaI</i> 6 His-Tag (2): 5'- ATTCTAGATCAGTGGTGATGGTGATGAT GGCCGTGCCGCTCTGGCG <i>wbxD-NdeI</i> (1): 5'- GCGGGCGCATATGGAGTTTGACCGACA AA	<i>wbxD</i> 3,414,875 to 3,416,842	64°	1968
P1164- <i>NdeI</i> 6 His Tag (2): 5'- GGAATTCCATATGCATCATCACCATCAC CACCCGCGATACCAAAAATTTTGTCTT T <i>wbcE-XbaI</i> (1): 5'- AATTCTAGATCAAACCTCATAACCTTCC AACTCCC	<i>wbcE</i> 3,416,832 to 3,419,119	60°	1470
<i>wabO-NdeI</i> (XOA8): 5'- AAGATCGCATATGGCTGAACCTACGCTC GG <i>wabO-XbaI</i> 10 His-Tag (XOA8): 5'- ATTTCTAGACTAGTGATGGTGATGATGG TGATGGTGATGATGGCGCGGATGCGG G	<i>wabO</i> 2,657,099 to 2,657,869	69.5°	771
<i>waaC-NdeI</i> 10 His-Tag (CCB1): 5'- CAATTAACATATGCATCATCACCATCAC CATCATCACCATCACAAAAGATCCTGA TCGTGC <i>waaC-BamHI</i> 10 His-Tag (CCB1): 5'- TAGGATCCTTAGTGATGGTGATGATGGT	<i>waaC</i> 3,400,803 to 3,401,798	56.5°	996

GATGGTGATGATGCAGGAGGCCGAAGC CCG			
------------------------------------	--	--	--

Plasmid Conjugation

Plasmids pXO3 Tp-Tc, pXO4 Tp-Tc, pXO7 Tp-Tc and pSCRhaB3 Tp-Tc were all mobilized into the K56-2::pTnModOTp' mutant 16 E1 (*wbxD-wbcE*::Tp^R) and into the K56-2 wt by triparental matings. Briefly, the helper strain, *E. coli* HB101 pRK2013 (Figurski & Helinski, 1979), the *E. coli* DH5- α with the appropriate plasmid, and the Bcc strain of interest were all mixed in 1 mL of 10% glycerol. The cell mixture was then centrifuged at 4,000 rpm for 4 minutes. Cells were resuspended in 100 μ L of 10% glycerol, and spotted onto a 1/2 LB agar plate and incubated at 30°C for approximately 16 h rightside-up. Following this incubation, cells were resuspended in 1 mL of 10% glycerol and the mixture was spread on the appropriate media. Exconjugants were selected on LB agar plates + 300 μ g of Tp/mL + 100 μ g of Tc/mL + 25 μ g of Amp/mL and incubated for 16 to 48 hrs at 30°C.

To confirm correct transformation of the plasmids, complemented clones were subject to colony PCR. Briefly, the colony is resuspended in the appropriate PCR solution containing the buffers, dNTPs, primers pSCRha R1 and pSCRha F2, and mQH₂O before the PCR reaction is run. This mixture is incubated for 5 minutes at 99.9°C, cooled to room temperature (22°C), and 0.25 μ L of Taq DNA polymerase is added. The amplification conditions were 3 min at 94°C, 30 cycles of 94°C for 30 s, 60°C for 30 s, and 72 °C for 3 min for pXO3 Tp-Tc, 2:30 min for pXO4 Tp-Tc and pXO7 Tp-Tc and 30 s for pSCRhaB3 Tp-Tc, with a final extension time of 10 min at 72°C.

Plasmids pSC*wabO*-Tc, pSC*waaC*-Tc and pSCRhaB2-Tc were all mobilized into the K56-2 LPS truncated mutants XOA8 (*wabO*::pGPΩTp Tp^R) and CCB1 (*waaC*::pGPΩTp Tp^R) by triparental matings as previously described. Exconjugants were selected on similar media and incubated for 16 to 48 hrs at 30°C. To confirm the correct insertion of the plasmids, complemented clones were subject to colony PCR as previously described. The amplification conditions were 3 min at 94°C, 30 cycles of 94°C for 30 s, 60°C for 30 s, and 72 °C for 2 min for pSC*wabO*-Tc, pSC*waaC*-Tc and 30 s for pSCRhaB2-Tc, with a final extension time of 10 min at 72°C.

Bacteriophage infection assays vs. LPS complemented mutants [Liquid culture clearing assays]

In order to test restoration of wt phenotype in the K56-2::pTn*ModOTp*' mutant, 16 E1 (*wbxD-wbcE*::Tp^R) was complemented with the appropriate plasmids and tested vs. phages KS4-M and KS12. An approach similar to the plasposon mutant library screening was used. Briefly, mutant 16 E1 complemented with different plasmids was grown on ½ LB broth + 100 µg of Tp/mL + 100 µg of Tc/mL for 16 hrs. at 37°C with shaking (225 rpm). The plasmid containing cells were induced with 0.2% rhamnose while a second set was grown in non-inducing conditions. The assay was performed in a 96-well plate with the appropriate controls. Blank, (200 µL of ½ LB broth supplemented with appropriate antibiotics and with or without rhamnose), Wt control (150 µL of ½ LB broth + 10 µL of *B. cenocepacia* K56-2 wt + 50 µL of KS4-M or KS12),

Positive control (190 μ L of $\frac{1}{2}$ LB broth supplemented with antibiotics and with or without Rha + 10 μ L of K56-2::pTnModOTp' mutant 16 E1 (*wbxD-wbcE*::Tp^R) complemented with pXO3, pXO4, pXO7 or pSCRhaB3 Tp-Tc) finally Test group (150 μ L of $\frac{1}{2}$ LB broth supplemented with antibiotics and with or without Rha + 10 μ L of K56-2::pTnModOTp' mutant 16 E1 (*wbxD-wbcE*::Tp^R) complemented with pXO3, pXO4, pXO7 or pSCRhaB3 Tp-Tc + and 50 μ L of KS4-M or KS12.)

Plates were incubated for a period of six hours at 37°C with shaking (225 rpm) and A₆₀₀ taken every two hours for a period of six hours in the multilabel spectrophotometer. Abs readings between the positive control and the test group were compared and graphs constructed with this data. Data was analyzed with A-Nova plus Tukey Post Hoc tests with 95% reliability. The same method was used to test complemented mutants XOA8 and CCB1 vs. phages KS5 and KS9.

LPS extraction & SDS-polyacrylamide gel electrophoresis

LPS from different strains was extracted by a short Proteinase K method. A₆₀₀ from all the overnights was standardized to 2.0. Briefly, 500 μ L from induced and non-induced overnight cultures was centrifuged, pellets were resuspended in 30 μ L of 1x PBS buffer. 2.5 μ L of 50 mg/mL proteinase K was added to tubes and vortexed for a few seconds and incubated at 55°C. Six hours later another 2.5 μ L of 50 mg/mL proteinase K was added. Tubes were incubated on a Isotemp 125D heat block machine for 16 hrs. After 16 hrs of incubation tubes were centrifuged at 15,000 rpm for 1 min and the supernatant was transferred to a new tube, this supernatant containing the LPS.

LPS was resolved by electrophoresis in 16.5% polyacrylamide gels with a Tris-Tricine system (Schägger & Jagow, 1987; Schägger, 2006) or a Tris-Glycine system. Samples were run for 180 minutes at 90 V on a Power Pac 200 (Bio-Rad) apparatus. Gels were subsequently visualized by silver staining (Marolda et al., 1990; Fomsgaard et al., 1990).

Western Blots

200 μ L from overnight cultures of *B. cenocepacia* K56-2 Wt + pSCRhaB3 Tp-Tc, 16 E1 (*wbxD-wbcE::Tp*) + pSCRhaB3 Tp-Tc, 16 E1 + pXO4 Tp-Tc and 16 E1 + pXO7 Tp-Tc and from K56-2 Wt + pSCRhaB2-Tc, K56-2 LPS truncated mutants XOA8 (*wabO::pGP Ω Tp Tp^R*) + pSCRhaB2-Tc, CCB1 (*waaC::pGP Ω Tp Tp^R*) + pSCRhaB2-Tc, XOA8 (*wabO::pGP Ω Tp Tp^R*) + pSC*wabO*-Tc and CCB1 (*waaC::pGP Ω Tp Tp^R*) + pSC*waaC*-Tc were spun down and resuspended on 50 μ L of 5x sample buffer and 2.5 μ L of 2-Mercaptoethanol (Bio-Rad). Previous mixtures were then incubated at 99°C for 5 minutes and stored at -20°C.

10 μ L from previous preparations were runned on a 14% (XOA8 and CCB1 mutants) and 10% (16 E1 mutants) polyacrylamide gels on a Tris-Glycine system. For 140 minutes at 90 V on a Power Pac 200 (Bio-Rad) apparatus (same volumes for Commassie blue stained gels). Samples were transferred to nitrocellulose membranes soaked in electroblotting buffer, and runned in TAE buffer overnight at 10 V on the same apparatus. Membranes were blocked overnight with blocking solution + 0.4% skim milk at room temperature with continuous shake (225 rpm).

Western Blot was performed according to the Comparative Proteomics Kit II: Western Blot Module Quick Guide from Bio-Rad (www.bio-rad.com) with slight variations. The antibody solutions were made in TBS + 0.1% Tween (instead of TBS + 0.1% Tween + 0.1% skim milk). Membranes were incubated with a 1:2000 dilution of an Anti-6X his rabbit polyclonal antibody (Rockland, Gilbertsville, PA) ON at room temperature, followed with a 2 hr. incubation with an Anti-rabbit monoclonal antibody 1:10000 (Rockland).

Transmission electron microscopy (TEM)

Overnight cultures of *B. cenocepacia* PC184 and mutant 72 C12 (*pulO::Tp^R*) were incubated on a carbon grid for 5 min. at room temperature. Subsequently, the grids were negatively stained with 2% phosphotungstate. Images were visualized on a Philips/FEI (Morgagni) transmission electron microscope with a charge-coupled device camera with the assistance of University of Alberta Department of Biological Sciences Microscopy Service Unit.

Alternatively TEMs of bacteria from ½ LB (wt) and ½ LB + 100 µg of Tp/mL (*Tp^R* mutants) agar plates were also taken. In this case, a small amount of bacteria was resuspended in 1 mL of ½ LB broth with a sterile loop, the rest of the process was the same as previously described.

In the case of TEMs where host and phage were mixed together a small amount of bacteria from ½ LB (wt) and ½ LB + 100 µg of Tp/mL (*Tp^R* mutants) agar plates was resuspended on 1 mL of ½ LB broth with a sterile loop. Then 100 µL of phage (DC1) were mixed with 100 µL of the previous resuspended host and

incubated for 20 minutes at room temperature. TEMs were taken after this incubation period following the previously described protocol.

Swarming and Twitching Motility Assays

To assay twitching motility, an ON culture of *B. cenocepacia* PC184 wt (control) and the six PC184::Tn*Modlux*OTp' phage DC1 resistant mutants were stab inoculated with a sterile toothpick at the bottom of a ~5mm thick 1% and 1.5% agar ½ LB plate (wt) and ½ LB + 100 µg of Tp/mL plates (for Tp^R mutants). Plates were subsequently incubated at 37°C for a period of ~16-24 hrs. The zone of motility (hazy halo) formed at the agar/Petri dish interface surrounding the point of inoculation was measured and compared between the six DC1 resistant mutants and the wt strain (Rashid & Kornberg, 2000; Shan et al., 2004).

In addition to twitching motility assays, swarming motility and flagellum-dependent type of motility (Mattick, 2002; Rashid & Kornberg, 2000) was also tested on the six DC1 resistant mutants. To assay swarming motility, an ON culture of *Pseudomonas aeruginosa* strain PAO1 (positive swarm motility control), *B. cenocepacia* PC184 wt (control) and the six PC184::Tn*Modlux*OTp' phage DC1 resistant mutants were inoculated with a sterile toothpick on top of a ~5mm thick 0.5% agar ½ LB plate (wt) and ½ LB + 100 µg of Tp/mL plates (Tp^R mutants). Plates were subsequently incubated at 30°C for a period of ~16-24 hrs. The zone of motility was characterized by either a motility en masse at the colony edge, or as rafts of migrating cells leaving the colony behind (moving from the point of inoculation to the edges of the plate), and the characteristic production of

extracellular slime (polysaccharide and/or biosurfactant) and easily noticeable to the naked eye was measured, and compared between *P. aeruginosa* PAO1, *B. cenocepacia* PC184 and the six DC1 resistant mutants (Rashid & Kornberg, 2000).

RESULTS & DISCUSSION

Towards the identification of phages able to clear liquid cultures

A collection of nine Bcc specific phages (KS5, KS9, KS10, KS12, KS14, DC1, SR1, KL1 and AH2), have been isolated from different sources including soil and root material where onions were planted (phage KS5), soil from a botanical conservatory (phages KS12 isolated from soil planted to *Dietes grandiflora* wild iris, phages KS14 and DC1 both isolated from soil planted with *Dracaena* sp. also known as Dragon tree and phage AH2 isolated from *Nandina* sp. also known as heavenly bamboo), as lysogens of Bcc species (KS9 lysogen of *B. pyrrocinia* strain LMG 21824 and KS10 lysogen of *B. cenocepacia* strain K56-2), as phenotypic mutants (phages KS4-M, a variant of phage KS4 able to lyse liquid cultures of *B. cenocepacia* K56-2, and phage SR1, a variant of phage KS10 with an extended host range broader than that of KS10), and from sewage (phage KL1), by previous graduate and undergraduate students (Seed & Dennis, 2005; 2009; Routier, 2010; Lynch et al., 2012). Previous phages were all tested against *B. cenocepacia* strains K56-2 or PC184 depending upon the natural host for each phage. In addition, both mutant libraries were constructed in those two strains, so only phages infecting either K56-2 or PC184 were of importance. It is important to note that some phages cannot clear bacterial liquid cultures so it was imperative to determine which phages from our collection were able to clear hosts in liquid in order to perform a high-throughput liquid clearing assay. For this reason, a series of liquid culture clearing assays were carried in order to identify which phages were going to be used to screen the mutant libraries. [Table 6; Figs. 4-12].

Table 6: Bcc specific bacteriophages tested to determine if bacterial liquid cultures are cleared. Phages KS5, KS9, KS12, KL1 and AH2 were tested against *B. cenocepacia* K56-2 wt (one of their hosts), while phages DC1, KS10, KS14 and SR1 were tested against *B. cenocepacia* PC184 wt.

*Phage KS4-M was previously shown to clear liquid cultures, for this reason it was not tested again (Seed & Dennis, 2009).

Phage	Host	Liquid Culture Clearing
DC1	<i>B. cenocepacia</i> PC184	Cleared
KS4-M*	<i>B. cenocepacia</i> K56-2	Cleared
KS5	<i>B. cenocepacia</i> K56-2	Cleared
KS9	<i>B. cenocepacia</i> K56-2	Cleared
KS10	<i>B. cenocepacia</i> PC184	Cleared
KS12	<i>B. cenocepacia</i> K56-2	Cleared
KS14	<i>B. cenocepacia</i> PC184	No Clearing
KL1	<i>B. cenocepacia</i> K56-2	No Clearing
AH2	<i>B. cenocepacia</i> K56-2	No Clearing
SR1	<i>B. cenocepacia</i> PC184	Cleared

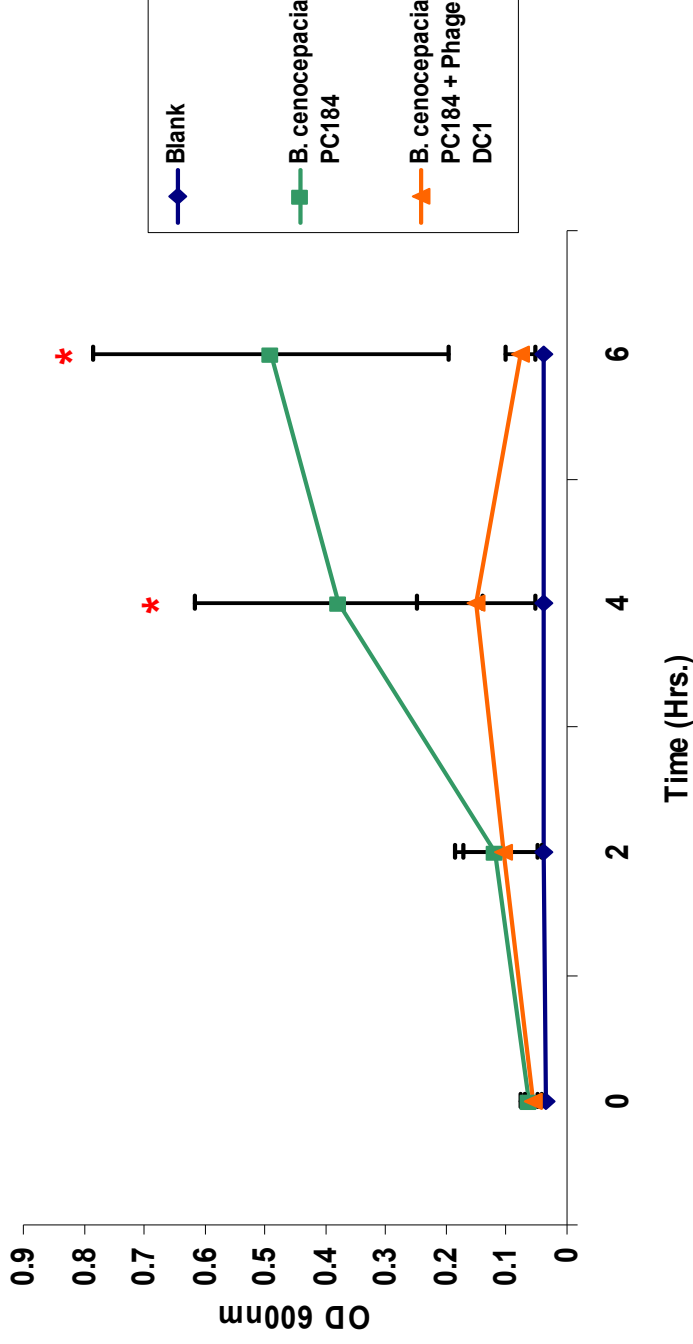


Figure 4: Growth curve of *B. cenocepacia* PC184 wt exposed to phage DC1: Blue, blank control (200 μ L of $\frac{1}{2}$ LB broth), Green, positive control (10 μ L of bacteria) and (190 μ L of $\frac{1}{2}$ LB broth) mixed together, Orange, test group (10 μ L of bacteria), (50 μ L of high titer phage stock) and (150 μ L of $\frac{1}{2}$ LB broth) were mixed together and incubated at 37°C with continuous shaking (225 rpm). A_{600} measured every 2 hrs. for a period of 6 hrs in the Victor X3 2030 multilabel reader spectrophotometer. Bacteria were previously grown on $\frac{1}{2}$ LB broth for ~16 hrs at 37°C with shaking (225 rpm). Each point represents the mean of three independent experiments in triplicate. Error bars indicate standard deviation. *Represents statistical significance between control (green) and test (orange) groups. A-Nova test (Tukey) ($P < 0.05$)

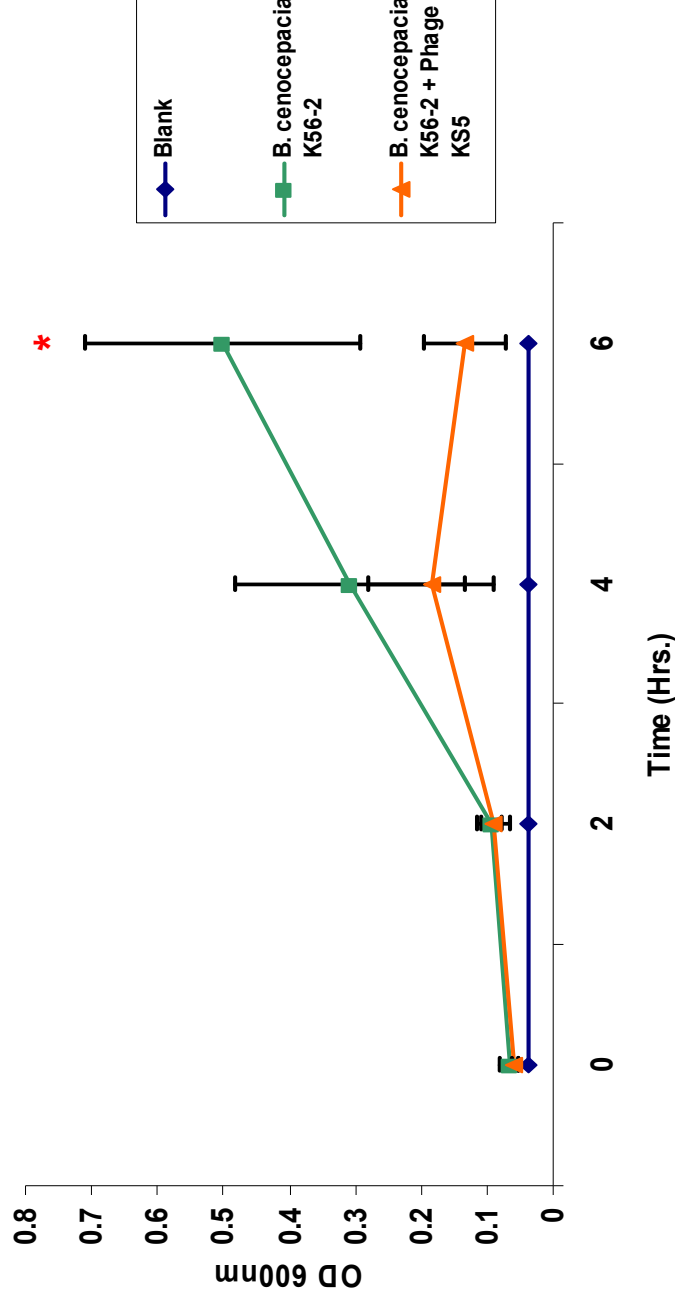


Figure 5: Growth curve of *B. cenocepacia* K56-2 wt exposed to phage KS5: Blue, blank control (200 μ L of $\frac{1}{2}$ LB broth), Green, positive control (10 μ L of bacteria) and (190 μ L of $\frac{1}{2}$ LB broth) mixed together, Orange, test group (10 μ L of bacteria), (50 μ L of high titer phage stock) and (150 μ L of $\frac{1}{2}$ LB broth) were mixed together and incubated at 37°C with continuous shaking (225 rpm). A_{600} measured every 2 hrs. for a period of 6 hrs in the Victor X3 2030 multilabel reader spectrophotometer. Bacteria were previously grown on $\frac{1}{2}$ LB broth for ~16 hrs at 37°C with shaking (225 rpm). Each point represents the mean of three independent experiments in triplicate. Error bars indicate standard deviation. *Represents statistical significance between control (green) and test (orange) groups. A-Nova test (Tukey) ($P < 0.05$)

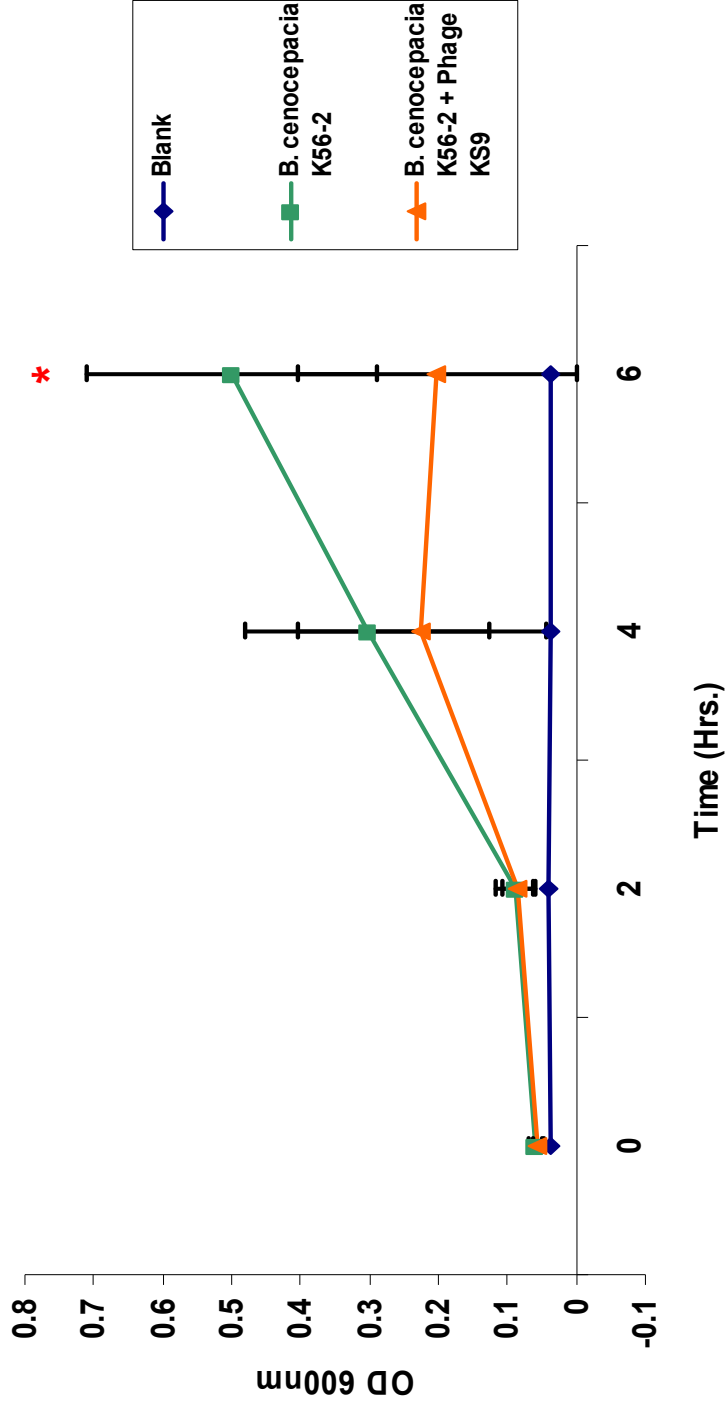


Figure 6: Growth curve of *B. cenocepacia* K56-2 wt exposed to phage KS9: Blue, blank control (200 μ L of $\frac{1}{2}$ LB broth), Green, positive control (10 μ L of bacteria) and (190 μ L of $\frac{1}{2}$ LB broth) mixed together, Orange, test group (10 μ L of bacteria), (50 μ L of high titer phage stock) and (150 μ L of $\frac{1}{2}$ LB broth) were mixed together and incubated at 37°C with continuous shaking (225 rpm). A_{600} measured every 2 hrs. for a period of 6 hrs in the Victor X3 2030 multilabel reader spectrophotometer. Bacteria were previously grown on $\frac{1}{2}$ LB broth for ~16 hrs at 37°C with shaking (225 rpm). Each point represents the mean of three independent experiments in triplicate. Error bars indicate standard deviation. *Represents statistical significance between control (green) and test (orange) groups. A-Nova test (Tukey) ($P < 0.05$)

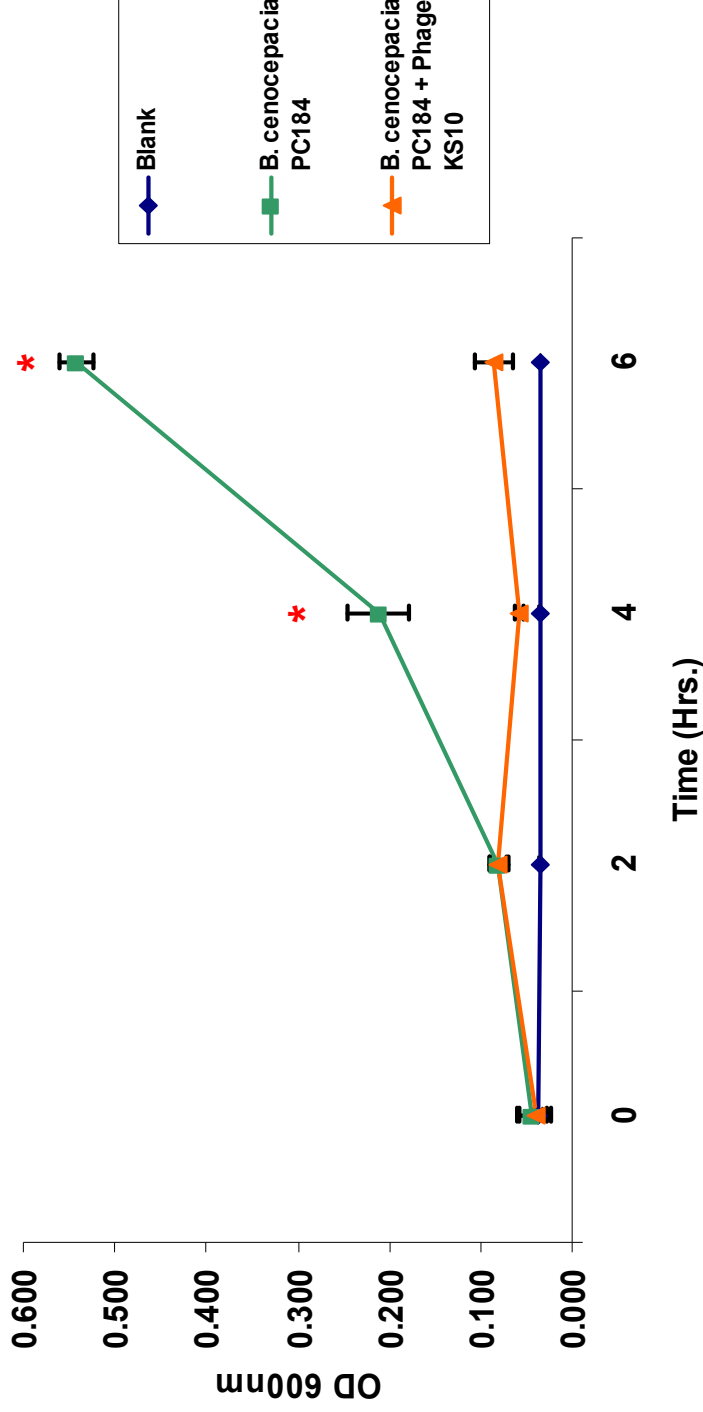


Figure 7: Growth curve of *B. cenocepacia* PC184 wt exposed to phage KS10: Blue, blank control (200 μ L of $\frac{1}{2}$ LB broth), Green, positive control (10 μ L of bacteria) and (190 μ L of $\frac{1}{2}$ LB broth) mixed together, Orange, test group (10 μ L of bacteria), (50 μ L of high titer phage stock) and (150 μ L of $\frac{1}{2}$ LB broth) were mixed together and incubated at 37°C with continuous shaking (225 rpm). A_{600} measured every 2 hrs. for a period of 6 hrs in the Victor X3 2030 multilabel reader spectrophotometer. Bacteria were previously grown on $\frac{1}{2}$ LB broth for ~16 hrs at 37°C with shaking (225 rpm). Each point represents the mean of three independent experiments in triplicate. Error bars indicate standard deviation. *Represents statistical significance between control (green) and test (orange) groups. A-Nova test (Tukey) ($P < 0.05$)

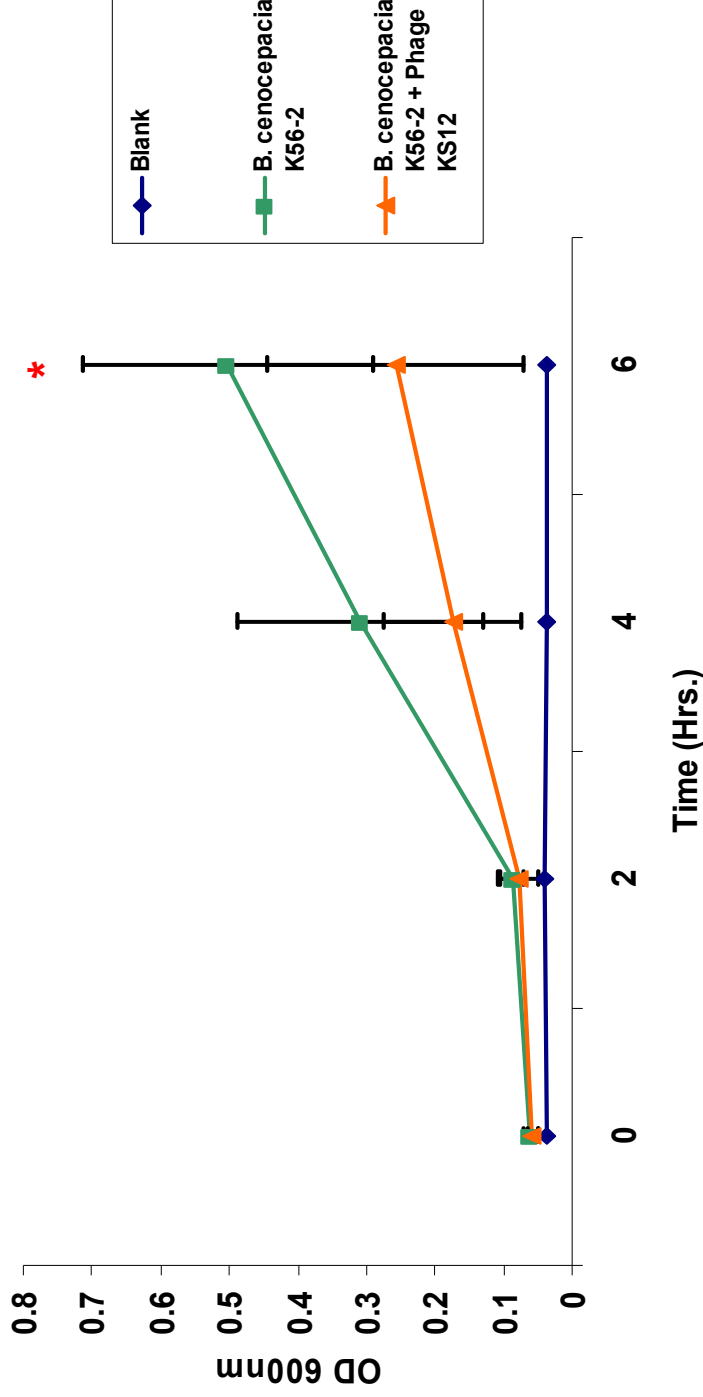


Figure 8: Growth curve of *B. cenocepacia* K56-2 wt exposed to phage KS12: Blue, blank control (200 μ L of $\frac{1}{2}$ LB broth), Green, positive control (10 μ L of bacteria) and (190 μ L of $\frac{1}{2}$ LB broth) mixed together and incubated at 37°C with continuous shaking (225 rpm). A₆₀₀ titer phage stock) and (150 μ L of $\frac{1}{2}$ LB broth) were mixed together and incubated at 37°C with continuous shaking (225 rpm). A₆₀₀ measured every 2 hrs. for a period of 6 hrs in the Victor X3 2030 multilabel reader spectrophotometer. Bacteria were previously grown on $\frac{1}{2}$ LB broth for ~16 hrs at 37°C with shaking (225 rpm). Each point represents the mean of three independent experiments in triplicate. Error bars indicate standard deviation. * Represents statistical significance between control (green) and test (orange) groups. A-Nova test (Tukey) (P < 0.05)

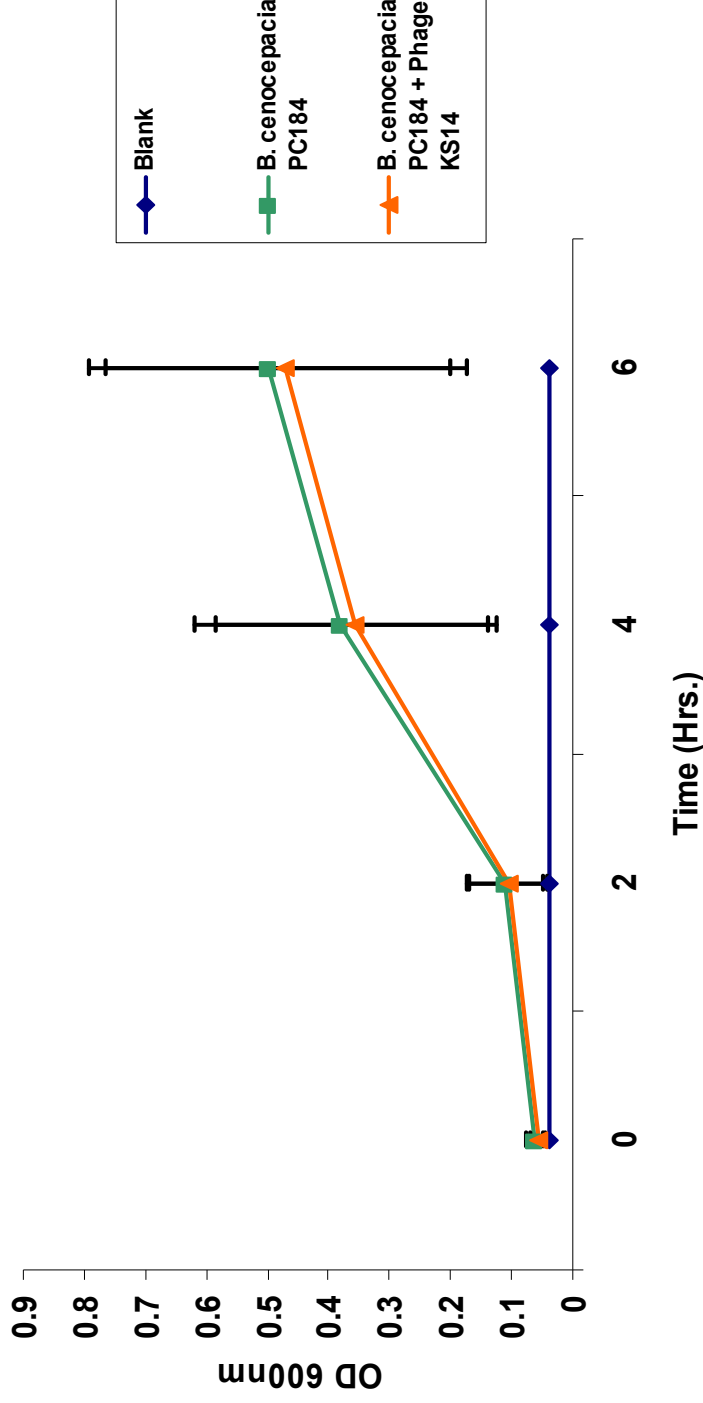


Figure 9: Growth curve of *B. cenocepacia* PC184 wt exposed to phage KS14: Blue, blank control (200 μ L of $\frac{1}{2}$ LB broth), Green, positive control (10 μ L of bacteria) and (190 μ L of $\frac{1}{2}$ LB broth) mixed together, Orange, test group (10 μ L of bacteria), (50 μ L of high titer phage stock) and (150 μ L of $\frac{1}{2}$ LB broth) were mixed together and incubated at 37°C with continuous shaking (225 rpm). A_{600} measured every 2 hrs. for a period of 6 hrs in the Victor X3 2030 multilabel reader spectrophotometer. Bacteria were previously grown on $\frac{1}{2}$ LB broth for ~16 hrs at 37°C with shaking (225 rpm). Each point represents the mean of three independent experiments in triplicate. Error bars indicate standard deviation. * Represents statistical significance between control (green) and test (orange) groups. A-Nova test (Tukey) ($P < 0.05$)

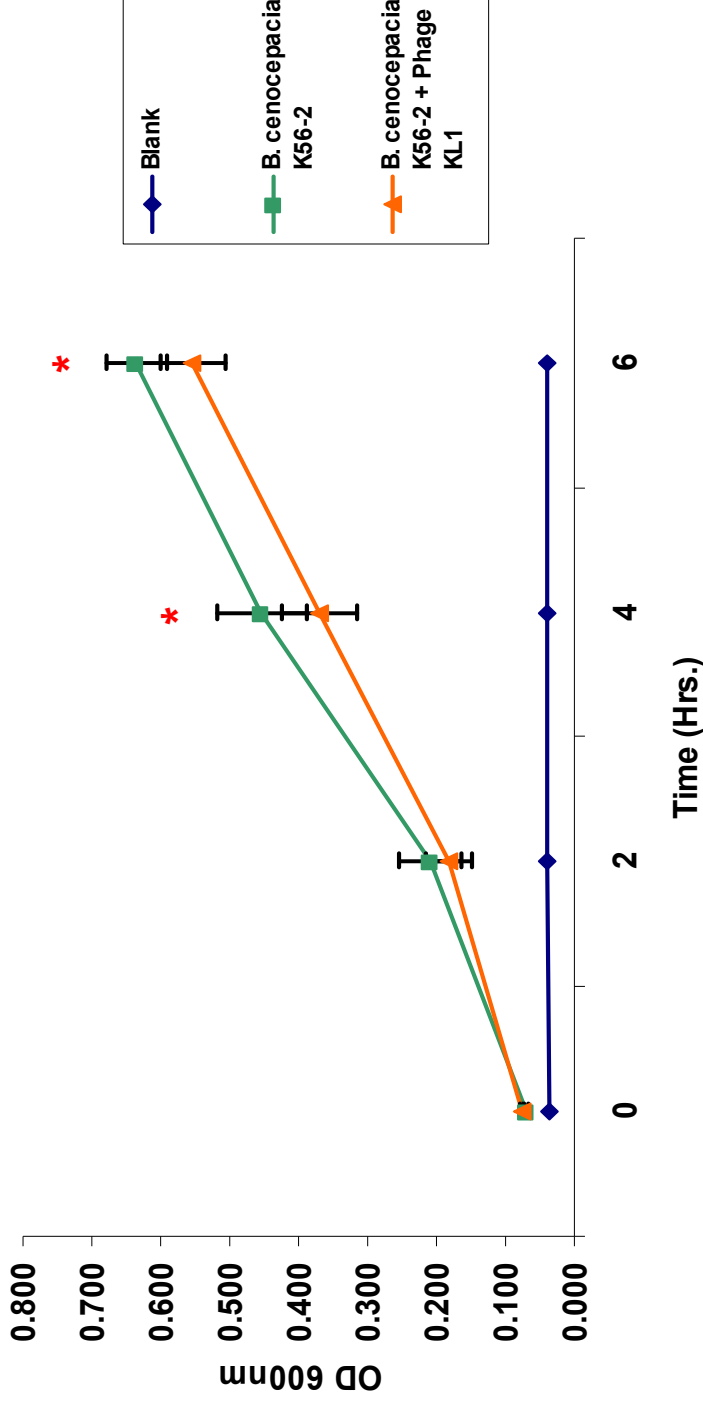


Figure 10: Growth curve of *B. cenocepacia* K56-2 wt exposed to phage KL1: Blue, blank control (200 μ L of $\frac{1}{2}$ LB broth), Green, positive control (10 μ L of bacteria) and (190 μ L of $\frac{1}{2}$ LB broth) mixed together, Orange, test group (10 μ L of bacteria), (50 μ L of high titer phage stock) and (150 μ L of $\frac{1}{2}$ LB broth) were mixed together and incubated at 37°C with continuous shaking (225 rpm). A_{600} measured every 2 hrs. for a period of 6 hrs in the Victor X3 2030 multilabel reader spectrophotometer. Bacteria were previously grown on $\frac{1}{2}$ LB broth for ~16 hrs at 37°C with shaking (225 rpm). Each point represents the mean of three independent experiments in triplicate. Error bars indicate standard deviation. * Represents statistical significance between control (green) and test (orange) groups. A-Nova test (Tukey) ($P < 0.05$)

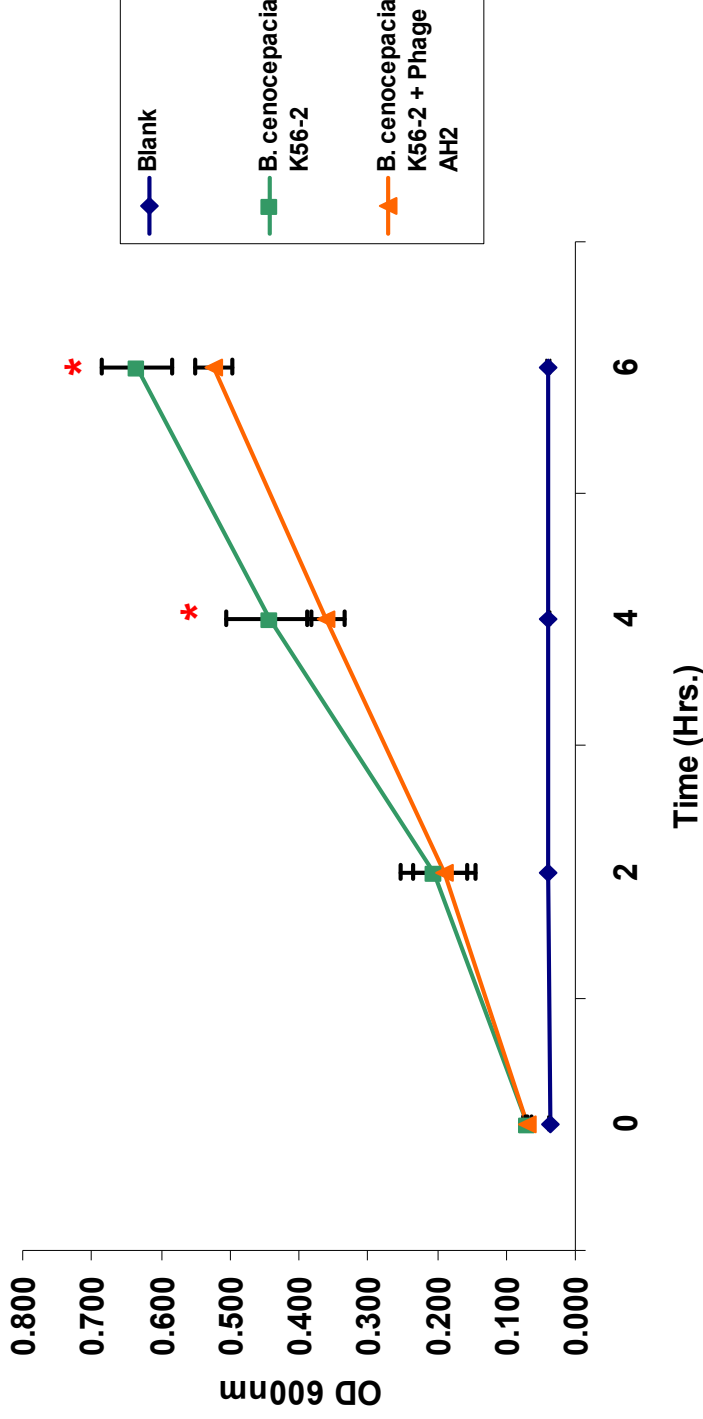


Figure 11: Growth curve of *B. cenocepacia* K56-2 wt exposed to phage AH2: Blue, blank control (200 μ L of $\frac{1}{2}$ LB broth), Green, positive control (10 μ L of bacteria) and (190 μ L of $\frac{1}{2}$ LB broth) mixed together, Orange, test group (10 μ L of bacteria), (50 μ L of high titer phage stock) and (150 μ L of $\frac{1}{2}$ LB broth) were mixed together and incubated at 37°C with continuous shaking (225 rpm). A_{600} measured every 2 hrs. for a period of 6 hrs in the Victor X3 2030 multilabel reader spectrophotometer. Bacteria were previously grown on $\frac{1}{2}$ LB broth for ~16 hrs at 37°C with shaking (225 rpm). Each point represents the mean of three independent experiments in triplicate. Error bars indicate standard deviation. * Represents statistical significance between control (green) and test (orange) groups. A-Nova test (Tukey) ($P < 0.05$)

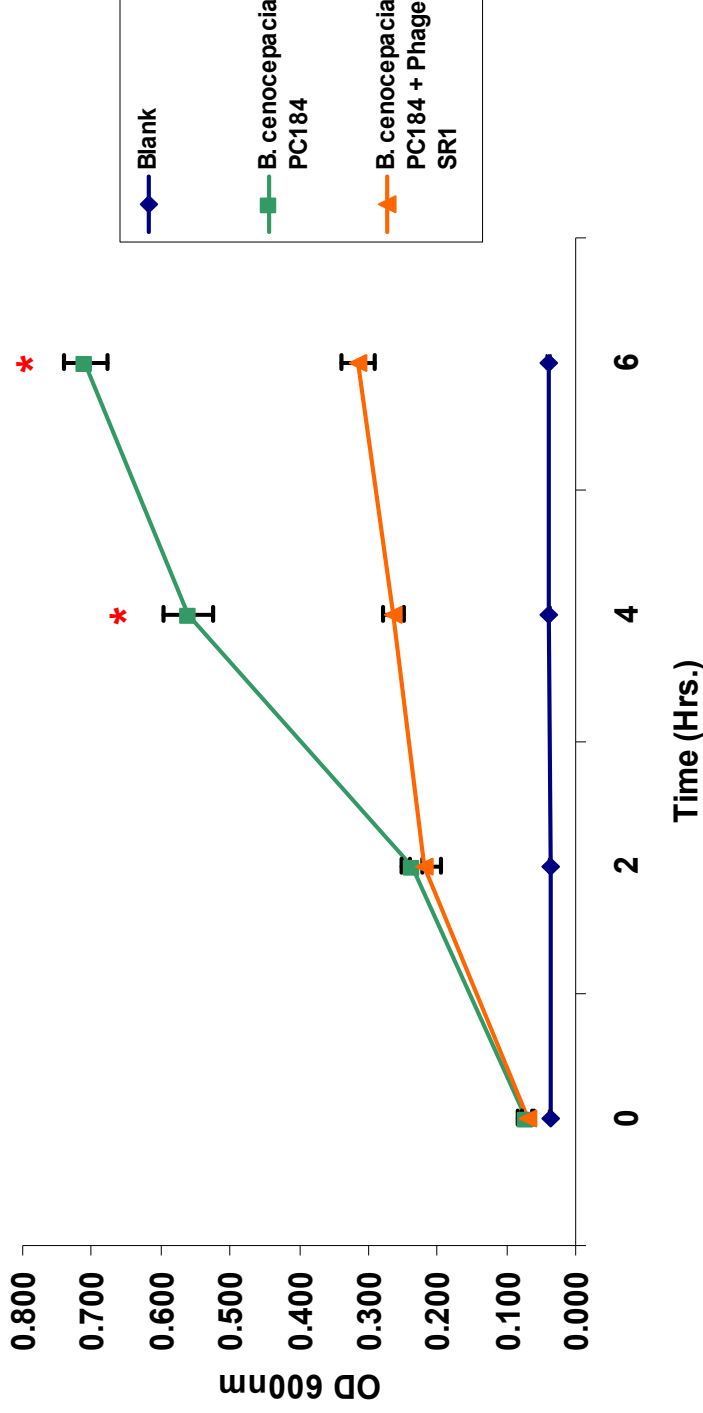


Figure 12: Growth curve of *B. cenocepacia* PC184 wt exposed to phage SR1: Blue, blank control (200 μ L of $\frac{1}{2}$ LB broth), Green, positive control (10 μ L of bacteria) and (190 μ L of $\frac{1}{2}$ LB broth) mixed together, Orange, test group (10 μ L of bacteria), (50 μ L of high titer phage stock) and (150 μ L of $\frac{1}{2}$ LB broth) were mixed together and incubated at 37°C with continuous shaking (225 rpm). A_{600} measured every 2 hrs. for a period of 6 hrs in the Victor X3 2030 multilabel reader spectrophotometer. Bacteria were previously grown on $\frac{1}{2}$ LB broth for ~16 hrs at 37°C with shaking (225 rpm). Each point represents the mean of three independent experiments in triplicate. Error bars indicate standard deviation. * Represents statistical significance between control (green) and test (orange) groups. A-Nova test (Tukey) ($P < 0.05$)

Plasposon mutant library screening

Similar to transposons, plasposons have been used as a molecular tool to randomly mutate the genomes of Gram-negative bacteria (Dennis & Zylstra, 1998). However, it has been demonstrated that plasposons have several advantages as mutation tools when compared to transposons. One example is the stability of plasposons when inserted into the genome of the target bacteria. This is because the transposase is not transferred as part of the inserted fragment, which makes the plasposon insertion more stable. Another advantage is the plasposon's self-cloning characteristic, which allows for several mutagenesis rounds. Also, plasposons are smaller than transposons making them particularly easy to use. Overall the advantages of plasposon insertion libraries are obvious, some of which include that they can be used to assay for a number of attributes including but not limited to phage receptors, antibiotic resistant determinants, and virulence factors. In the current project, two 9600 clone plasposon insertion libraries were used to screen and isolate phage resistant mutants. *B. cenocepacia* strain PC184 was mutagenized with the pTn*Modlux*-OTp' plasposon whereas strain K56-2 was mutagenized with the pTn*Mod*OTp' plasposon. These two strains were selected because of their prevalence in CF patients (Routier, 2010). The construction of the libraries has been described elsewhere (Routier, 2010).

After it was determined which phages were able to noticeably clear liquid cultures, we initially decided to select one phage to screen the K56-2::pTn*Mod*OTp' library. Bacteriophage KS4-M (a phenotypic variant of phage KS4) (Seed & Dennis, 2005) was selected. This phage variant is able to clear

bacterial liquid cultures in comparison to phage KS4; in addition, it is also easy to obtain high titer stocks thus the advantages of using this phage were obvious (Seed & Dennis, 2009). After screening a total of ~9600 K56-2 plasposon mutants it was confirmed that ten showed resistance to phage KS4-M [Figs. 13-22], these mutants were isolated and stored at -80°C for further analysis.

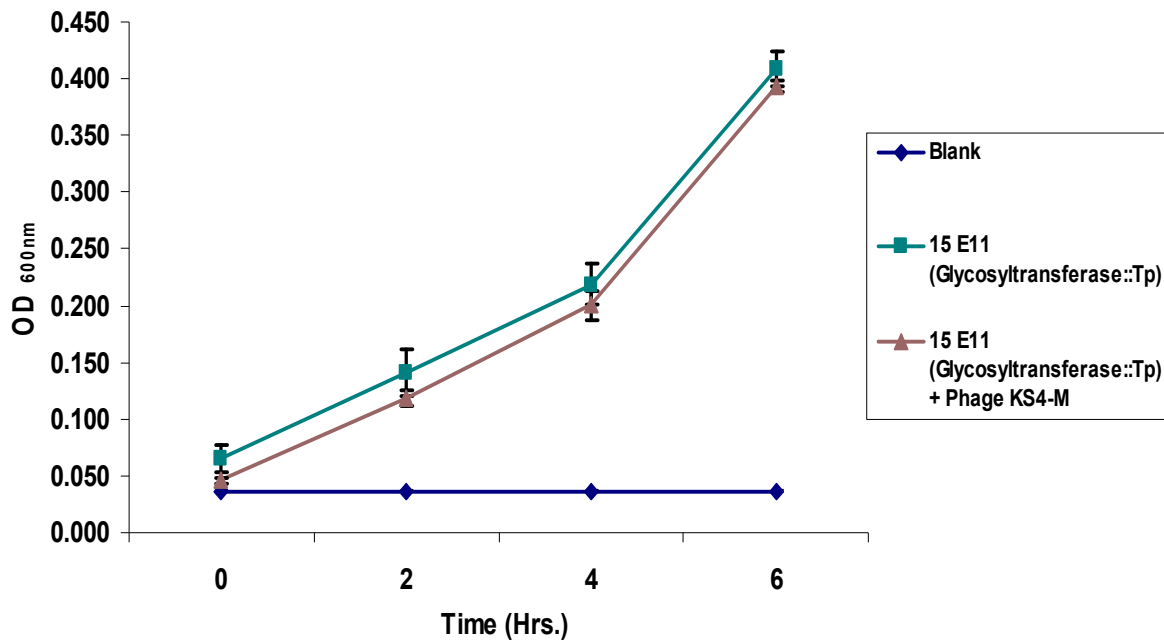


Figure 13: Growth curve of *B. cenocepacia* K56-2::pTnModOTp' mutant 15 E11 (Glycosyltransferase::Tp^R) exposed to phage KS4-M: Blue, blank control (200 μ L of $\frac{1}{2}$ LB broth), Green, positive control (10 μ L of bacteria) and (190 μ L of $\frac{1}{2}$ LB broth) mixed together, Orange, test group (10 μ L of bacteria), (50 μ L of high titer phage stock) and (150 μ L of $\frac{1}{2}$ LB broth) mixed together and incubated at 37°C with continuous shaking (225 rpm). A₆₀₀ measured every 2 hrs. for a period of 6 hrs in a Victor X3 2030 multilabel reader spectrophotometer. Mutant 15 E11 was previously grown on $\frac{1}{2}$ LB broth at 37°C with shaking (225 rpm) for ~16 hrs. Each point represents the mean of two independent experiments in triplicate; error bars indicate standard deviation. * Represents statistical significance between control (green) and test (orange) groups. A-Nova test (Tukey) (P < 0.05)

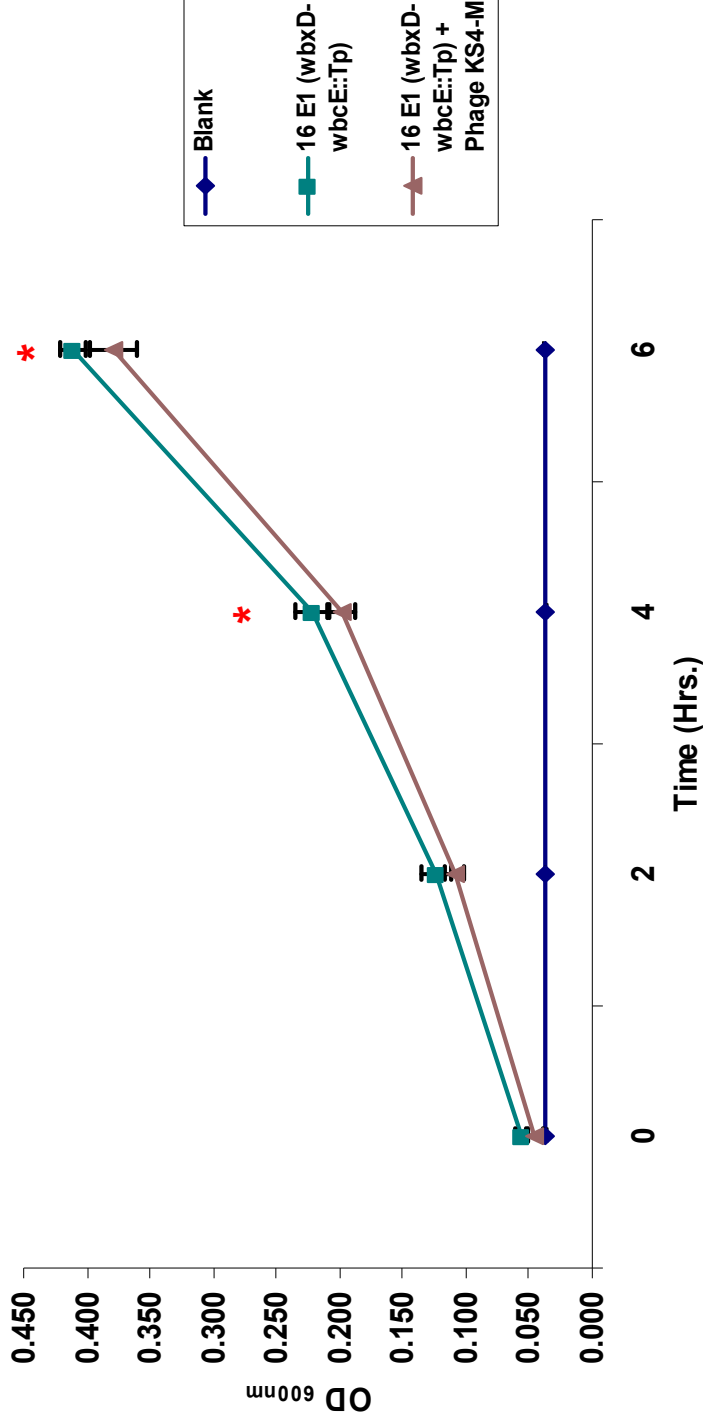


Figure 14: Growth curve of *B. cenocepacia* K56-2::pTnModOTp' mutant 16 E1 (*wbxD-wbcE::Tp^R*) exposed to phage KS4-M: Blue, blank control (200 μ L of $\frac{1}{2}$ LB broth), Green, positive control (10 μ L of bacteria) and (190 μ L of $\frac{1}{2}$ LB broth) mixed together, Orange, test group (10 μ L of bacteria), (50 μ L of high titer phage stock) and (150 μ L of $\frac{1}{2}$ LB broth) mixed together and incubated at 37°C with continuous shaking (225 rpm). A_{600} measured every 2 hrs. for a period of 6 hrs in a Victor X3 2030 multilabel reader spectrophotometer. Mutant 16 E1 was previously grown on $\frac{1}{2}$ LB broth at 37°C with shaking (225 rpm) for \sim 16 hrs. Each point represents the mean of two independent experiments in triplicate; error bars indicate standard deviation. * Represents statistical significance between control (green) and test (orange) groups. A-Nova test (Tukey) ($P < 0.05$)

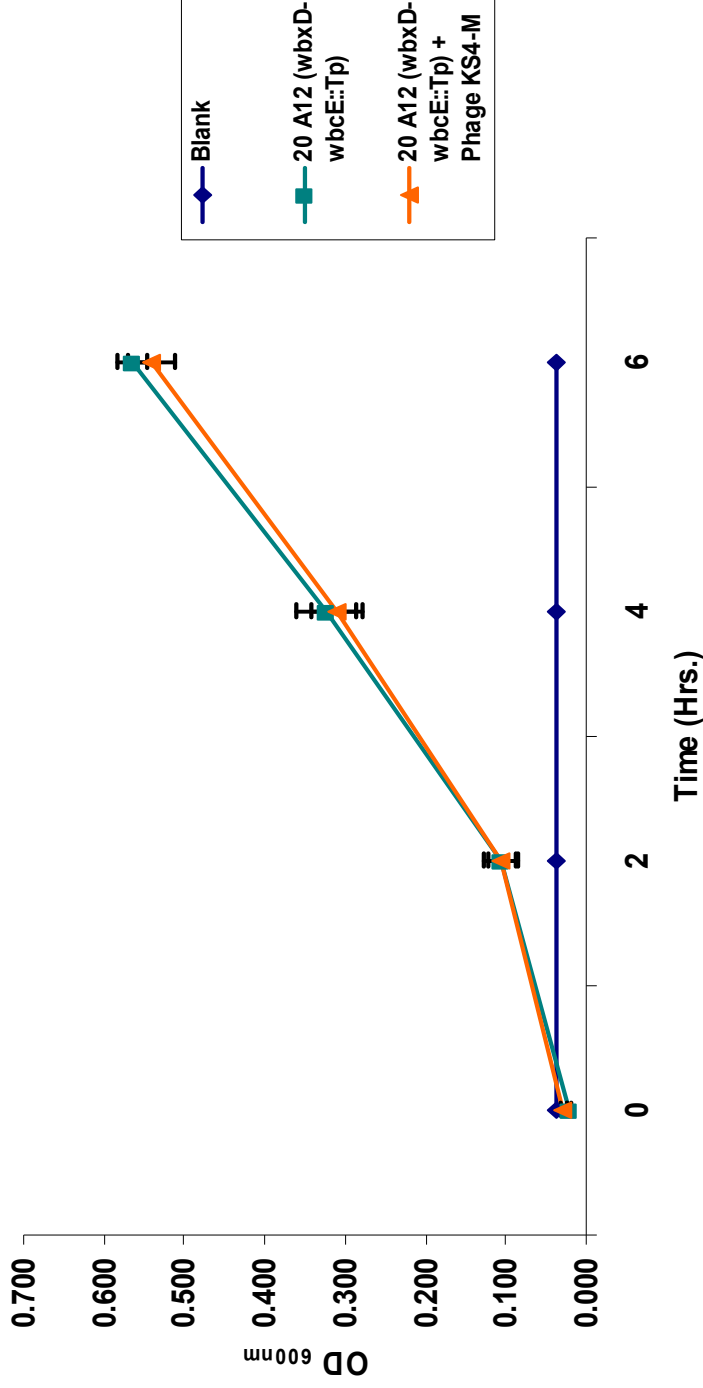


Figure 15: Growth curve of *B. cenocepacia* K56-2::pTnModOTp' mutant 20 A12 (*wbcD-wbcE::Tp*^R) exposed to phage KS4-M: Blue, blank control (200 μ L of $\frac{1}{2}$ LB broth), Green, positive control (10 μ L of bacteria) and (190 μ L of $\frac{1}{2}$ LB broth) mixed together, Orange, test group (10 μ L of bacteria), (50 μ L of high titer phage stock) and (150 μ L of $\frac{1}{2}$ LB broth) mixed together and incubated at 37°C with continuous shaking (225 rpm). A_{600} measured every 2 hrs. for a period of 6 hrs in a Victor X3 2030 multilabel reader spectrophotometer. Mutant 20 A12 was previously grown on $\frac{1}{2}$ LB broth at 37°C with shaking (225 rpm) for \sim 16 hrs. Each point represents the mean of two independent experiments in triplicate; error bars indicate standard deviation. * Represents statistical significance between control (green) and test (orange) groups. A-Nova test (Tukey) ($P < 0.05$)

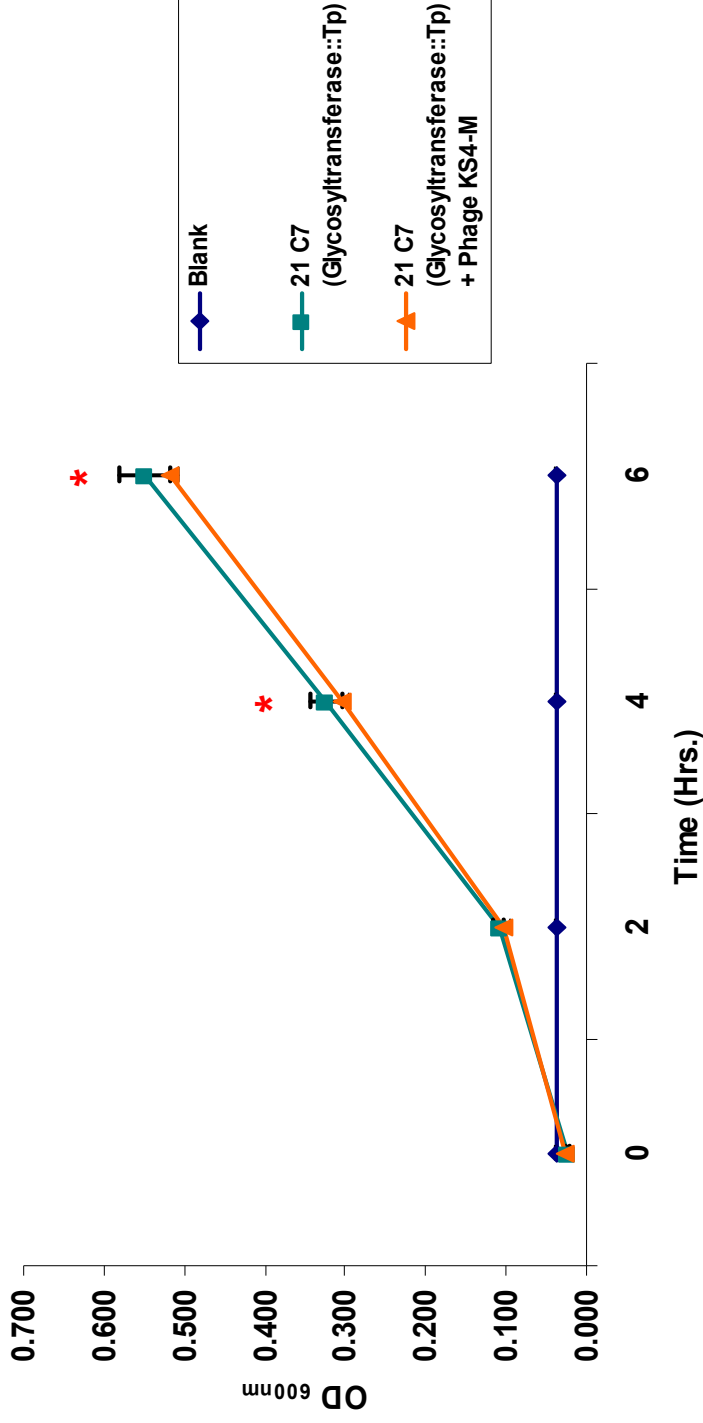


Figure 16: Growth curve of *B. cenocepacia* K56-2::pTnModOTp' mutant 21 C7 (Glycosyltransferase::Tp^R) exposed to phage KS4-M: Blue, blank control (200 μ L of $\frac{1}{2}$ LB broth), Green, positive control (10 μ L of bacteria) and (190 μ L of $\frac{1}{2}$ LB broth) mixed together, Orange, test group (10 μ L of bacteria), (50 μ L of high titer phage stock) and (150 μ L of $\frac{1}{2}$ LB broth) mixed together and incubated at 37°C with continuous shaking (225 rpm). A_{600} measured every 2 hrs. for a period of 6 hrs in a Victor X3 2030 multilabel reader spectrophotometer. Mutant 21 C7 was previously grown on $\frac{1}{2}$ LB broth at 37°C with shaking (225 rpm) for ~16 hrs. Each point represents the mean of two independent experiments in triplicate; error bars indicate standard deviation. * Represents statistical significance between control (green) and test (orange) groups. A-Nova test (Tukey) ($P < 0.05$)

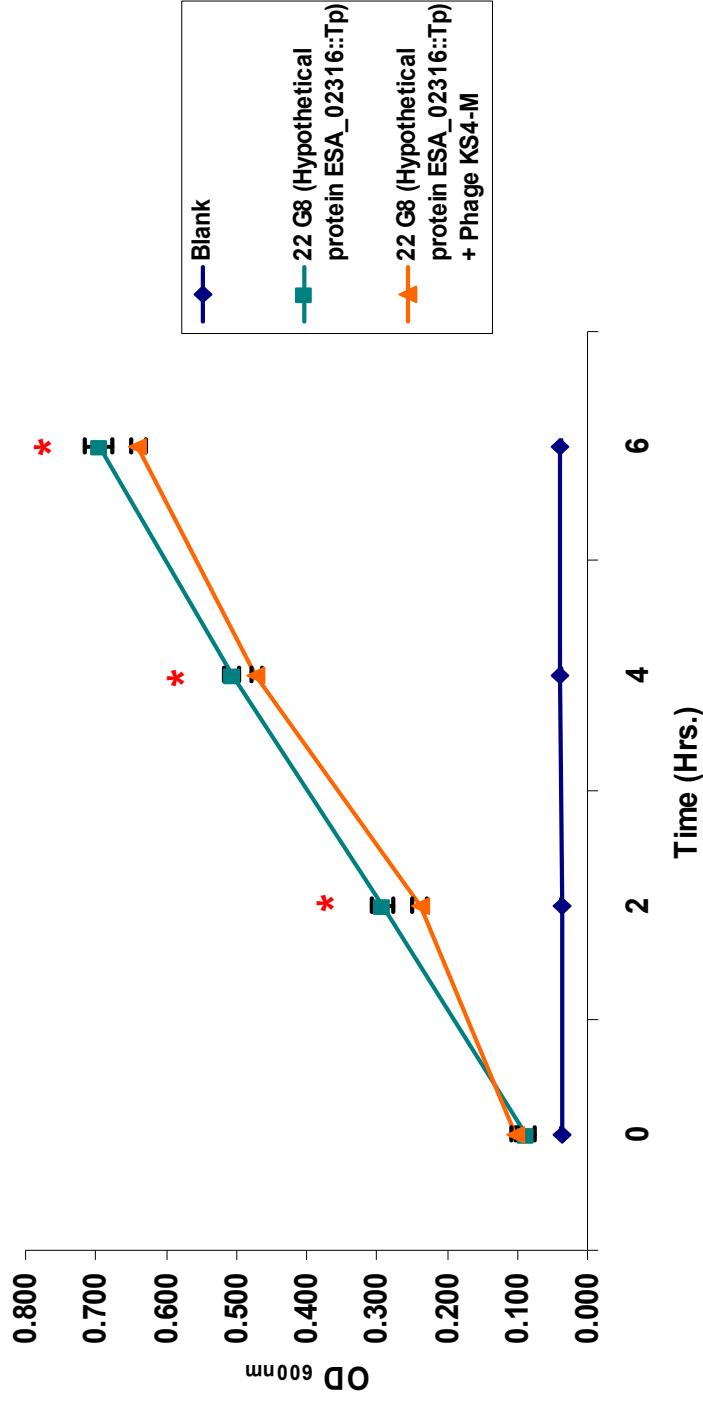


Figure 17: Growth curve of *B. cenocepacia* K56-2::pTnModOTp' mutant 22 G8 (ESA_02316::Tp^R) exposed to phage KS4-M: Blue, blank control (200 μ L of $\frac{1}{2}$ LB broth), Green, positive control (10 μ L of bacteria) and (190 μ L of $\frac{1}{2}$ LB broth) mixed together, Orange, test group (10 μ L of bacteria), (50 μ L of high titer phage stock) and (150 μ L of $\frac{1}{2}$ LB broth) mixed together and incubated at 37°C with continuous shaking (225 rpm). A₆₀₀ measured every 2 hrs. for a period of 6 hrs in a Victor X3 2030 multilabel reader spectrophotometer. Mutant 22 G8 was previously grown on $\frac{1}{2}$ LB broth at 37°C with shaking (225 rpm) for ~16 hrs. Each point represents the mean of two independent experiments in triplicate; error bars indicate standard deviation. * Represents statistical significance between control (green) and test (orange) groups. A-Nova test (Tukey) (P < 0.05)

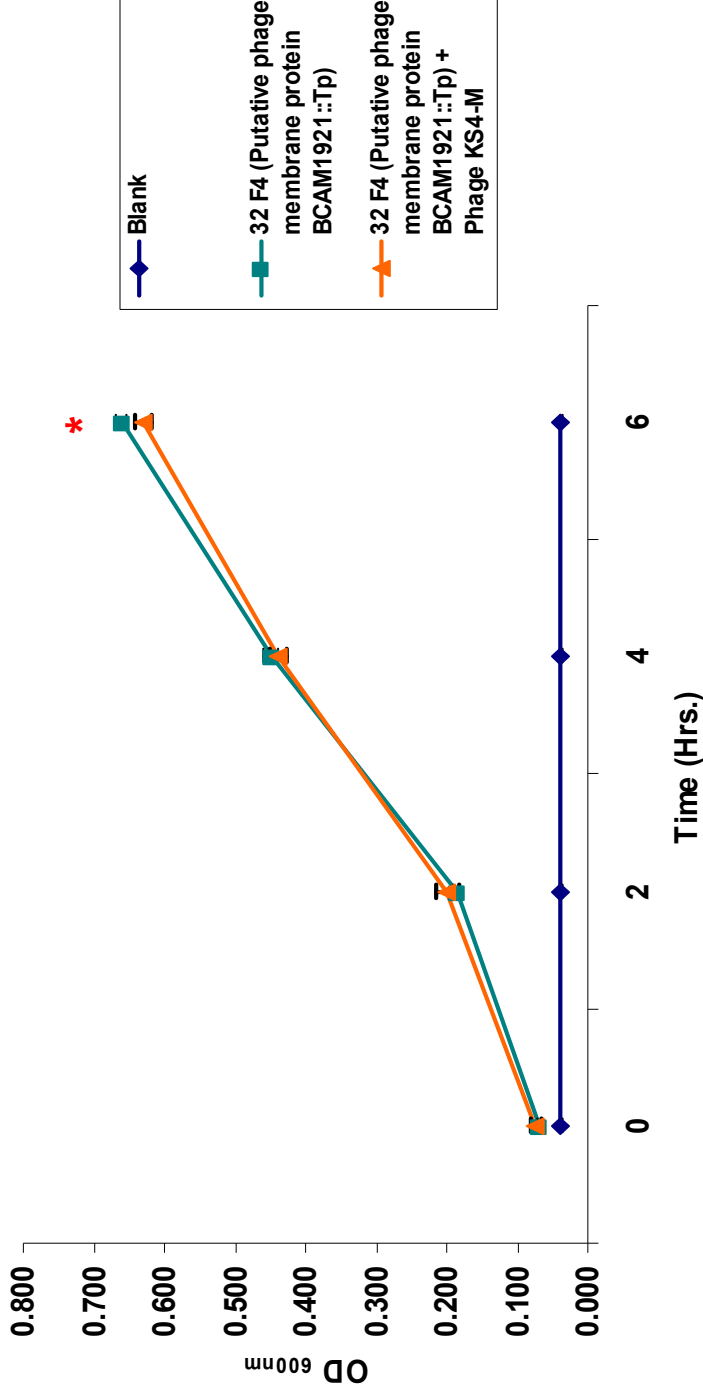


Figure 18: Growth curve of *B. cenocepacia* K56-2::pTnModOTp' mutant 32 F4 (Putative phage membrane protein BCAM1921::Tp^R) exposed to phage KS4-M: Blue, blank control (200 μ L of $\frac{1}{2}$ LB broth), Green, positive control (10 μ L of bacteria) and (190 μ L of $\frac{1}{2}$ LB broth) mixed together, Orange, test group (10 μ L of bacteria), (50 μ L of high titer phage stock) and (150 μ L of $\frac{1}{2}$ LB broth) mixed together and incubated at 37°C with continuous shaking (225 rpm). A₆₀₀ measured every 2 hrs. for a period of 6 hrs in a Victor X3 2030 multilabel reader spectrophotometer. Mutant 32 F4 was previously grown on $\frac{1}{2}$ LB broth at 37°C with shaking (225 rpm) for ~16 hrs. Each point represents the mean of two independent experiments in triplicate; error bars indicate standard deviation. * Represents statistical significance between control (green) and test (orange) groups. A-Nova test (Tukey) (P < 0.05)

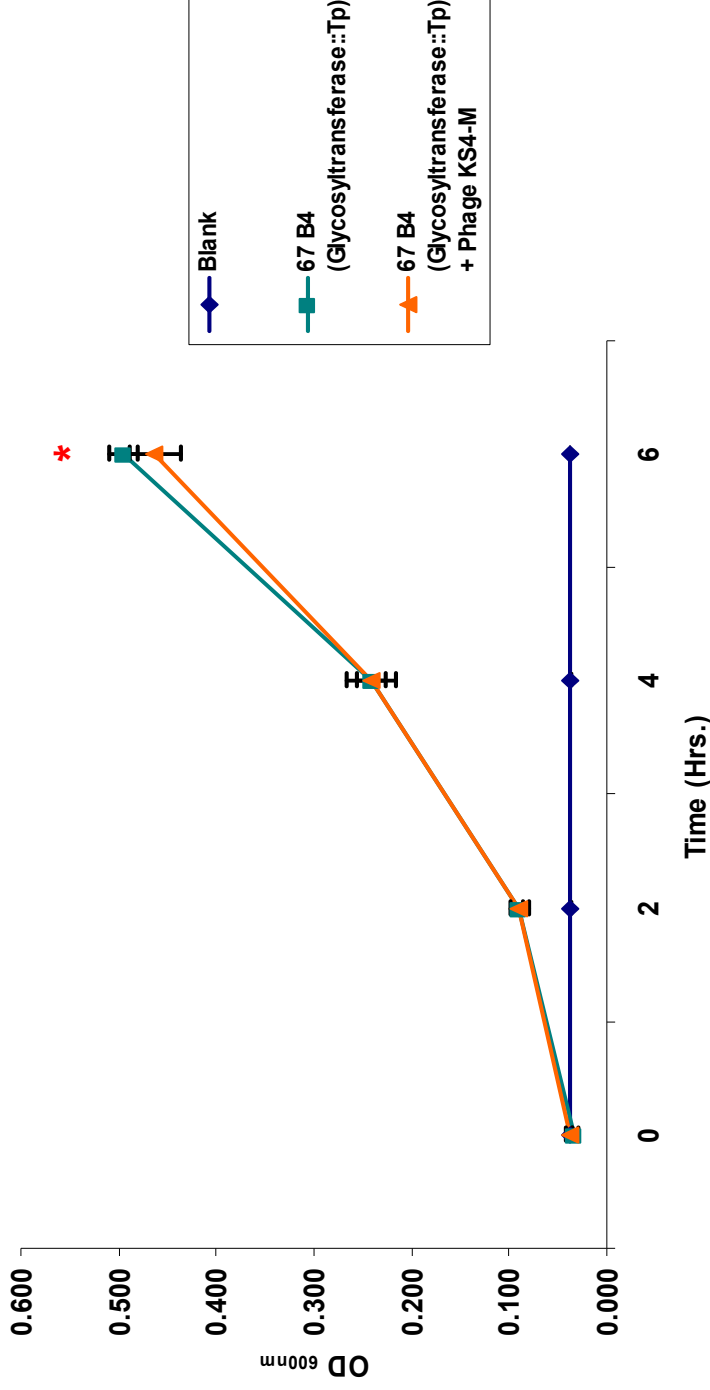


Figure 19: Growth curve of *B. cenocepacia* K56-2::pTnModOTp' mutant 67 B4 (Glycosyltransferase::Tp^R) exposed to phage KS4-M: Blue, blank control (200 μ L of $\frac{1}{2}$ LB broth), Green, positive control (10 μ L of bacteria) and (190 μ L of $\frac{1}{2}$ LB broth) mixed together, Orange, test group (10 μ L of bacteria), (50 μ L of high titer phage stock) and (150 μ L of $\frac{1}{2}$ LB broth) mixed together and incubated at 37°C with continuous shaking (225 rpm). A_{600} measured every 2 hrs. for a period of 6 hrs in a Victor X3 2030 multilabel reader spectrophotometer. Mutant 67 B4 was previously grown on $\frac{1}{2}$ LB broth at 37°C with shaking (225 rpm) for ~16 hrs. Each point represents the mean of two independent experiments in triplicate; error bars indicate standard deviation. * Represents statistical significance between control (green) and test (orange) groups. A-Nova test (Tukey) ($P < 0.05$)

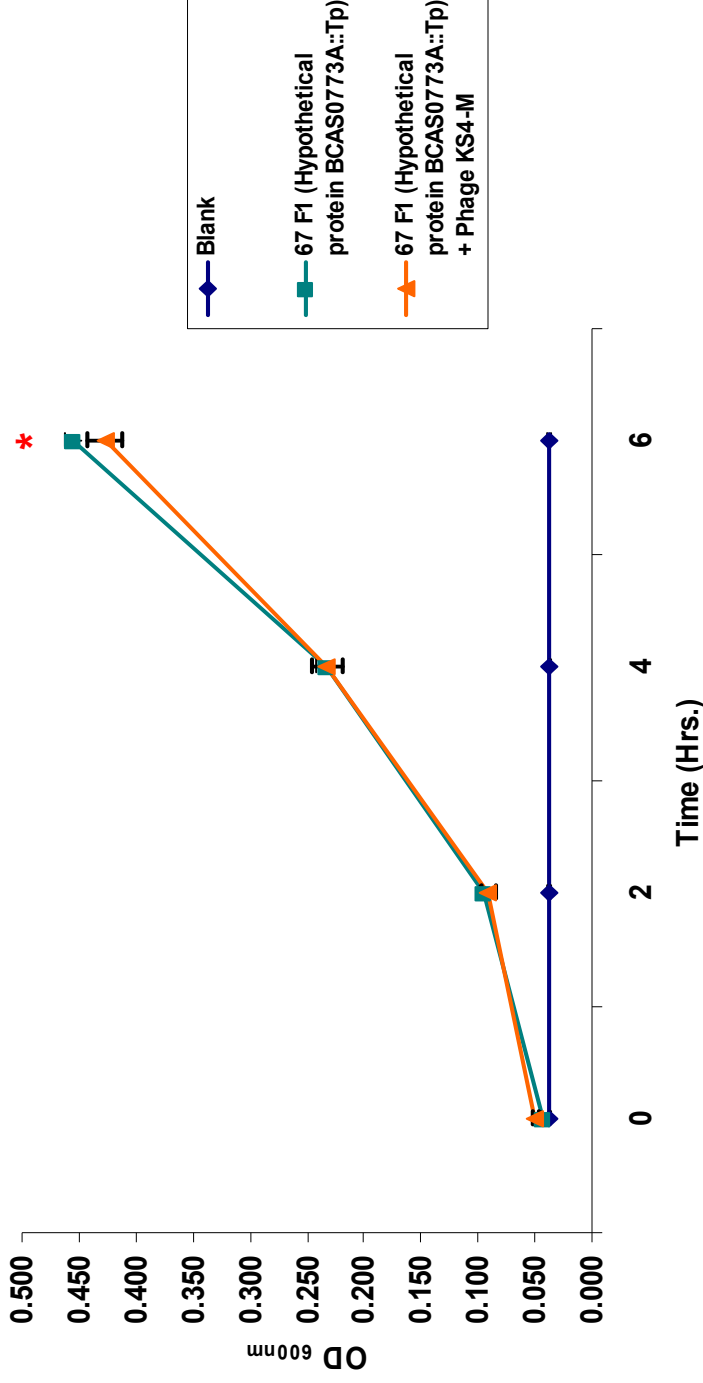


Figure 20: Growth curve of *B. cenocepacia* K56-2::pTnModOTp' mutant 67 F1 (Hypothetical protein BCAS0773A::Tp^R) exposed to phage KS4-M: Blue, blank control (200 μ L of $\frac{1}{2}$ LB broth), Green, positive control (10 μ L of bacteria) and (190 μ L of $\frac{1}{2}$ LB broth) mixed together, Orange, test group (10 μ L of bacteria), (50 μ L of high titer phage stock) and (150 μ L of $\frac{1}{2}$ LB broth) mixed together and incubated at 37°C with continuous shaking (225 rpm). A_{600} measured every 2 hrs. for a period of 6 hrs in a Victor X3 2030 multilabel reader spectrophotometer. Mutant 67 F1 was previously grown on $\frac{1}{2}$ LB broth at 37°C with shaking (225 rpm) for ~16 hrs. Each point represents the mean of two independent experiments in triplicate; error bars indicate standard deviation. * Represents statistical significance between control (green) and test (orange) groups. A-Nova test (Tukey) ($P < 0.05$)

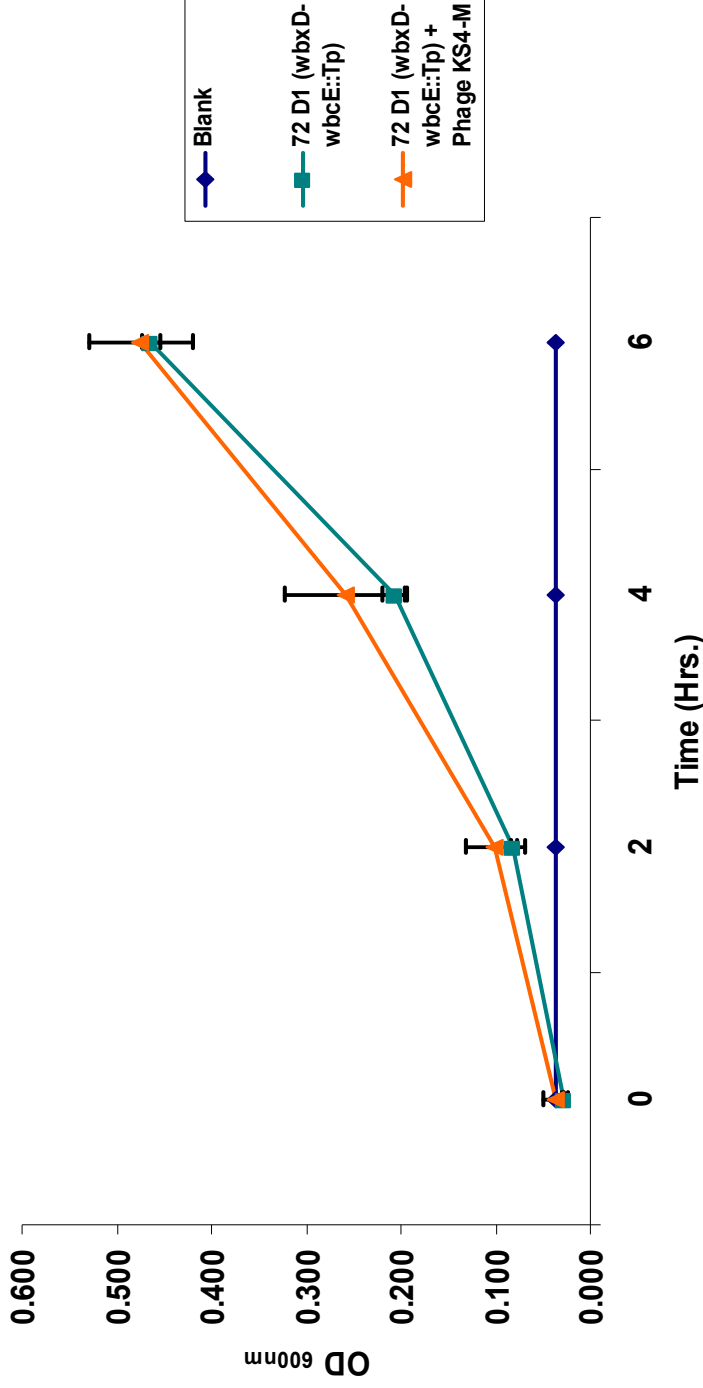


Figure 21: Growth curve of *B. cenocepacia* K56-2::pTnModOTp' mutant 72 D1 (*wbxD-wbcE::Tp^R*) exposed to phage KS4-M: Blue, blank control (200 μ L of $\frac{1}{2}$ LB broth), Green, positive control (10 μ L of bacteria) and (190 μ L of $\frac{1}{2}$ LB broth) mixed together, Orange, test group (10 μ L of bacteria), (50 μ L of high titer phage stock) and (150 μ L of $\frac{1}{2}$ LB broth) mixed together and incubated at 37°C with continuous shaking (225 rpm). A_{600} measured every 2 hrs. for a period of 6 hrs in a Victor X3 2030 multilabel reader spectrophotometer. Mutant 72 D1 was previously grown on $\frac{1}{2}$ LB broth at 37°C with shaking (225 rpm) for \sim 16 hrs. Each point represents the mean of two independent experiments in triplicate; error bars indicate standard deviation. * Represents statistical significance between control (green) and test (orange) groups. A-Nova test (Tukey) ($P < 0.05$)

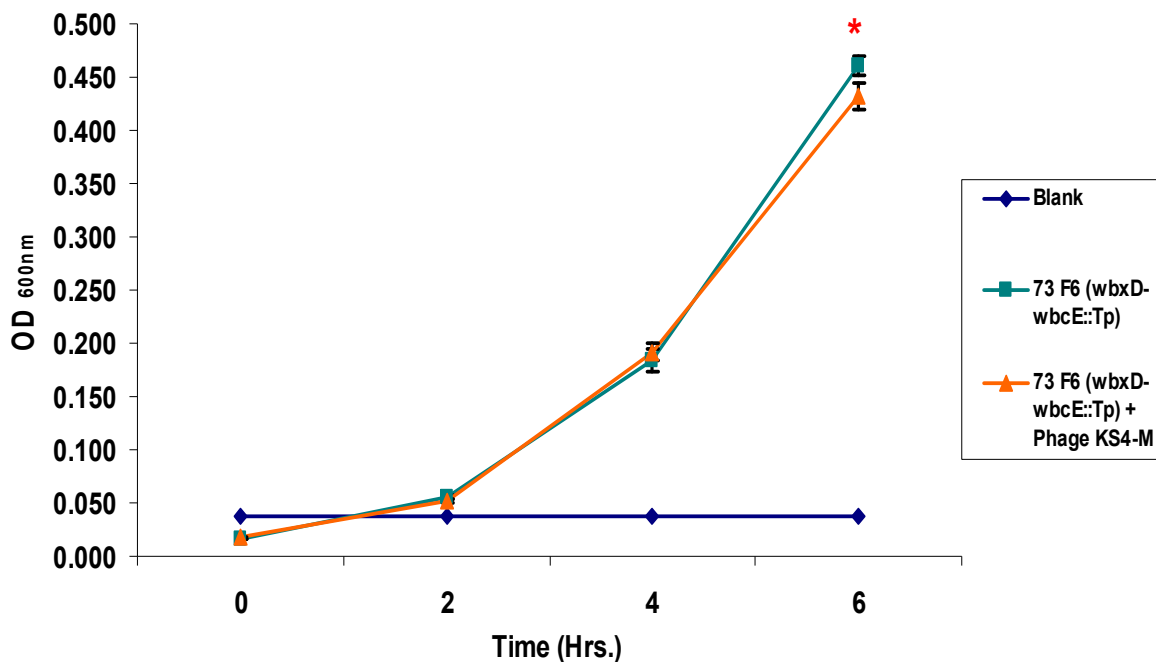


Figure 22: Growth curve of *B. cenocepacia* K56-2::pTnModOTp' mutant 73 F6 (*wbxD-wbcE::Tp^R*) exposed to phage KS4-M: Blue, blank control (200 μ L of $\frac{1}{2}$ LB broth), Green, positive control (10 μ L of bacteria) and (190 μ L of $\frac{1}{2}$ LB broth) mixed together, Orange, test group (10 μ L of bacteria), (50 μ L of high titer phage stock) and (150 μ L of $\frac{1}{2}$ LB broth) mixed together and incubated at 37°C with continuous shaking (225 rpm). A_{600} measured every 2 hrs. for a period of 6 hrs in a Victor X3 2030 multilabel reader spectrophotometer. Mutant 73 F6 was previously grown on $\frac{1}{2}$ LB broth at 37°C with shaking (225 rpm) for \sim 16 hrs. Each point represents the mean of two independent experiments in triplicate; error bars indicate standard deviation. * Represents statistical significance between control (green) and test (orange) groups. A-Nova test (Tukey) ($P < 0.05$)

Other bacteriophages in our collection were then tested against the KS4-M resistant mutants. These phages were KS5, KS9 and KS12, which all infect strain K56-2 (Seed & Dennis, 2005; 2009). A similar approach was used, but an additional control was included in the assay: 10 μ L of a K56-2 wt liquid overnight culture plus 50 μ L of high titer phage stock mixed in 150 μ L of $\frac{1}{2}$ LB broth. This positive control group proves that phage stocks are active when the assay was

performed. From this screening it was determined that phage KS12 produced similar results to those of phage KS4-M, with slight variations. Differences show that KS12 showed a slight capability to lyse mutants 20 A12, 67 B4 and 67 F1 [Figs. 23-25] as compared with no lysis by phage KS4-M. The remaining seven LPS mutants showed resistance to phage KS12, similar to that observed for phage KS4-M [data not shown].

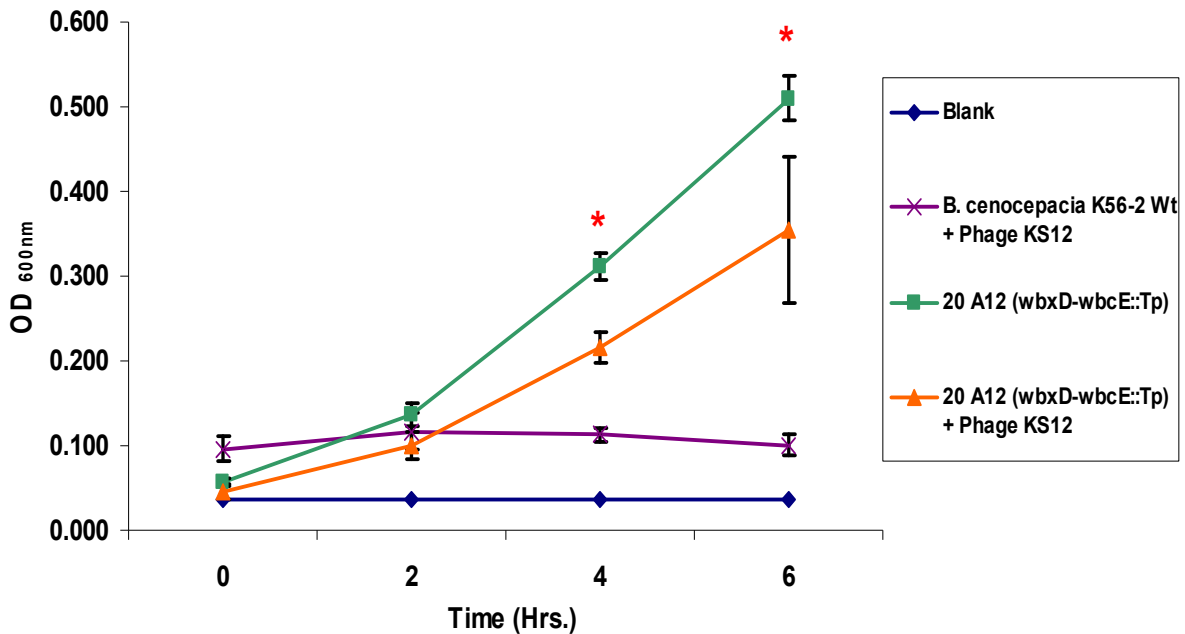


Figure 23: Growth curve of *B. cenocepacia* K56-2::pTnModOTp' mutant 20 A12 (*wbxD-wbcE::Tp^R*) exposed to phage KS12: Blue, blank control (200 μ L of $\frac{1}{2}$ LB broth), Purple, wt control (10 μ L of K56-2 wt), (50 μ L of high titer phage stock) and (150 μ L of $\frac{1}{2}$ LB broth) mixed, Green, positive control (10 μ L of bacteria) and (190 μ L of $\frac{1}{2}$ LB broth) mixed together, Orange, test group (10 μ L of bacteria), (50 μ L of high titer phage stock) and (150 μ L of $\frac{1}{2}$ LB broth) mixed together and incubated at 37°C with continuous shaking (225 rpm). A_{600} measured every 2 hrs. for a period of 6 hrs in a Victor X3 2030 multilabel reader spectrophotometer. Mutant 20 A12 was previously grown on $\frac{1}{2}$ LB broth at 37°C with shaking (225 rpm) for ~16 hrs. Each point represents the mean of two independent experiments in triplicate; error bars indicate standard deviation. * Represents statistical significance between control (green) and test (orange) groups. A-Nova test (Tukey) ($P < 0.05$)

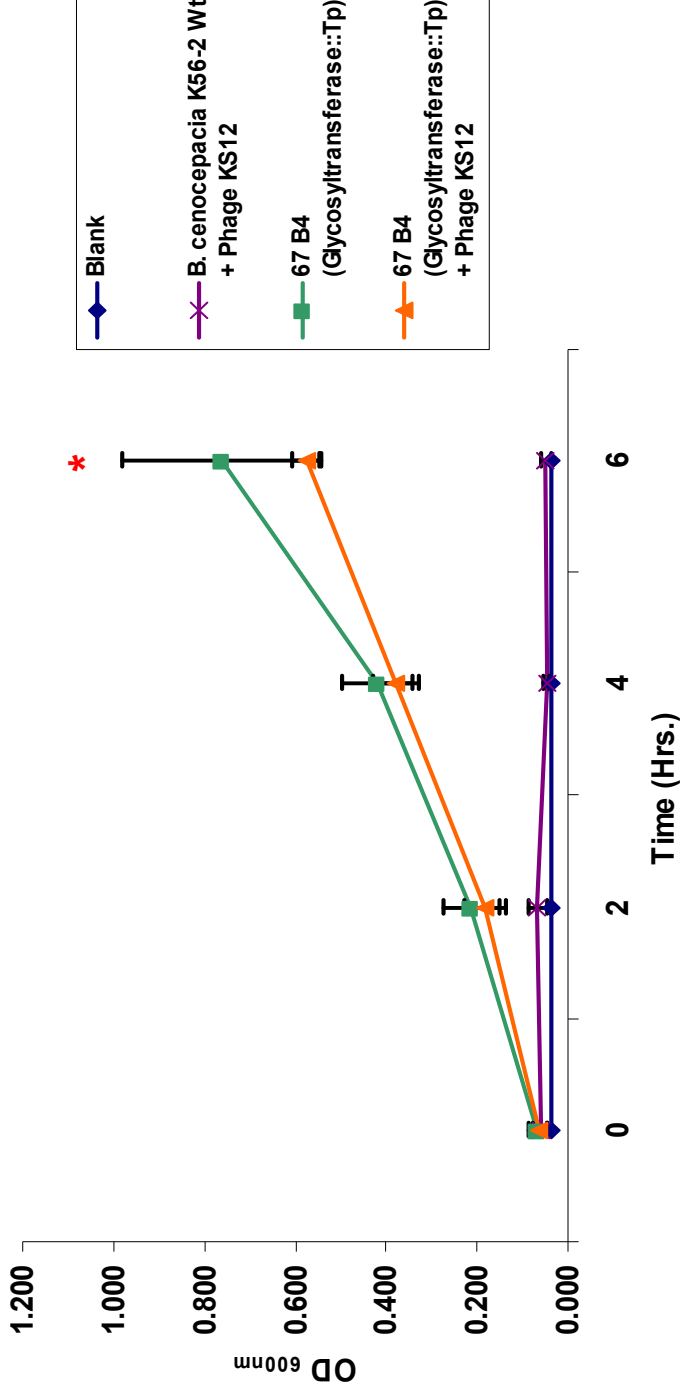


Figure 24: Growth curve of *B. cenocepacia* K56-2::pTnModOTp' mutant 67 B4 (Glycosyltransferase::Tp^R) exposed to phage KS12: Blue, blank control (200 μ L of $\frac{1}{2}$ LB broth), Purple, wt control (10 μ L of K56-2 wt), (50 μ L of high titer phage stock) and (150 μ L of $\frac{1}{2}$ LB broth) mixed, Green, positive control (10 μ L of bacteria) and (190 μ L of $\frac{1}{2}$ LB broth) mixed, Orange, test group (10 μ L of bacteria), (50 μ L of high titer phage stock) and (150 μ L of $\frac{1}{2}$ LB broth) mixed together and incubated at 37°C with continuous shaking (225 rpm). A₆₀₀ measured every 2 hrs. for a period of 6 hrs in a Victor X3 2030 multilabel reader spectrophotometer. Mutant 67 B4 was previously grown on $\frac{1}{2}$ LB broth at 37°C with shaking (225 rpm) for ~16 hrs. Each point represents the mean of two independent experiments in triplicate; error bars indicate standard deviation. * Represents statistical significance between control (green) and test (orange) groups. A-Nova test (Tukey) (P < 0.05)

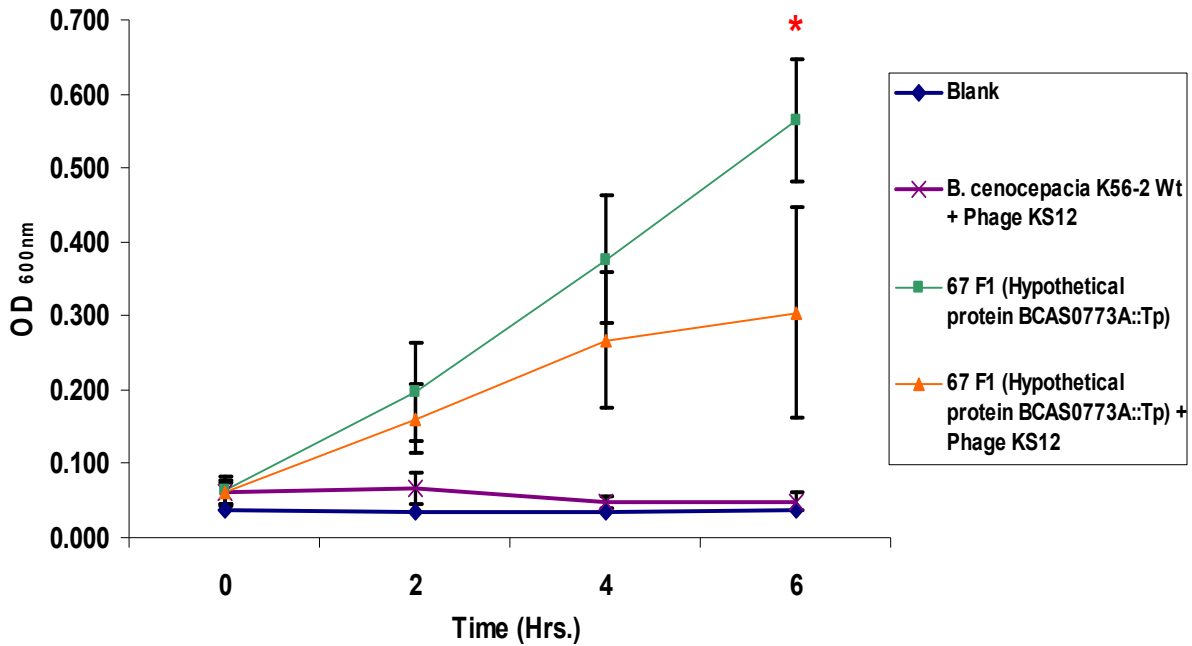


Figure 25: Growth curve of *B. cenocepacia* K56-2 pTnModOTp' mutant 67 F1 (Hypothetical protein BCAS0773A::Tp^R) exposed to phage KS12: Blue, blank control (200 μ L of $\frac{1}{2}$ LB broth), Purple, wt control (10 μ L of K56-2 wt), (50 μ L of high titer phage stock) and (150 μ L of $\frac{1}{2}$ LB broth) mixed, Green, positive control (10 μ L of bacteria) and (190 μ L of $\frac{1}{2}$ LB broth), Orange, test group (10 μ L of bacteria), (50 μ L of high titer phage stock) and (150 μ L of $\frac{1}{2}$ LB broth) incubated at 37°C with continuous shaking (225 rpm). A₆₀₀ measured every 2 hrs. for a period of 6 hrs in a Victor X3 2030 multilabel reader spectrophotometer. Mutant 67 F1 was previously grown on $\frac{1}{2}$ LB broth at 37°C with shaking (225 rpm) for ~16 hrs. Each point represents the mean of two independent experiments in triplicate; error bars indicate standard deviation. * Represents statistical significance between control (green) and test (orange) groups. A-Nova test (Tukey) (P < 0.05)

On the other hand, phage KS9 showed some interesting results. Plasposon mutant 22 G8 [Fig. 26] showed a slight sensitivity to KS9 infection compared to the full resistance observed for phage KS4-M. Mutants 67 B4, 72 D1 and 73 F6 [Figs. 27-29] showed full sensitivity to phage infection. Interestingly, two of these mutants 72 D1 and 73 F6 have a plasposon insertion in the same genes as mutant

16 E1, which is fully resistant to phage KS9 infection. We do not have an explanation for this discrepancy, other than perhaps the insertions are in different locations within the gene, and the gene product is still partially functional in mutant 16 E1. The remaining six mutants were resistant to phage KS9 infection, similar to the resistance observed for phage KS4-M [data not shown]. Data from phages KS9 and KS12 suggests that perhaps these phages use a similar receptor to that used by phage KS4-M to infect *B. cenocepacia* K56-2.

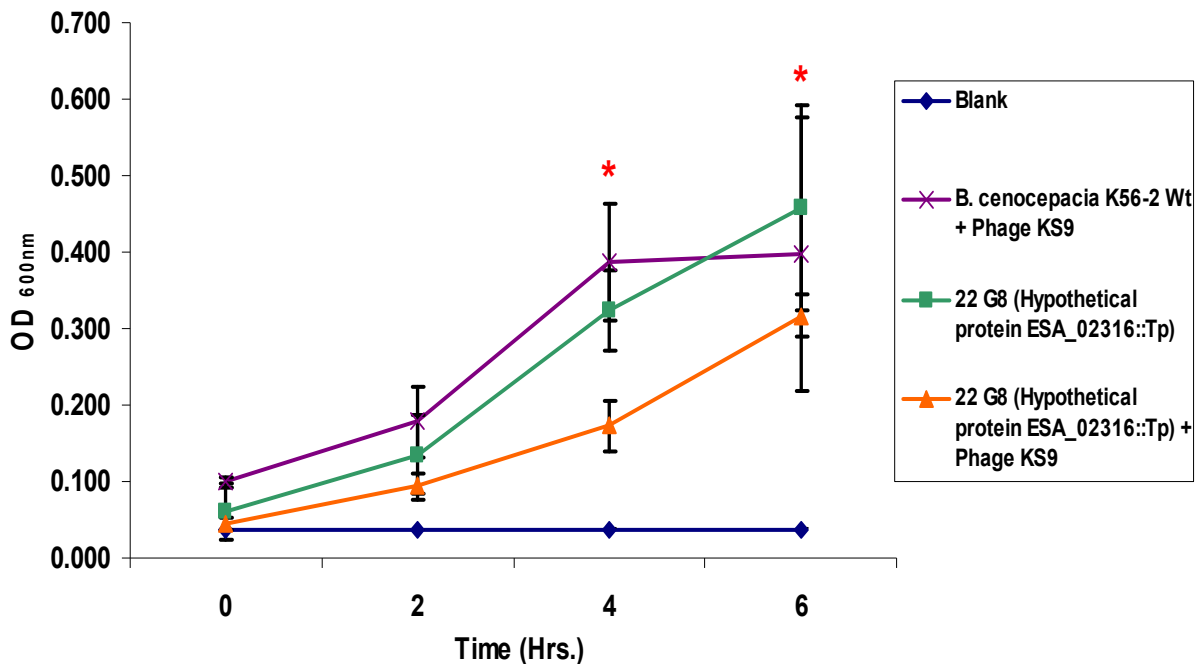


Figure 26: Growth curve of *B. cenocepacia* K56-2::pTnModOTp' mutant 22 G8 (ESA_02316::Tp^R) exposed to phage KS9: Blue, blank control (200 μ L of $\frac{1}{2}$ LB broth), Green, positive control (10 μ L of bacteria) and (190 μ L of $\frac{1}{2}$ LB broth), Orange, test group (10 μ L of bacteria), (50 μ L of high titer phage stock) and (150 μ L of $\frac{1}{2}$ LB broth) incubated at 37°C with continuous shaking (225 rpm). A₆₀₀ measured every 2 hrs. for a period of 6 hrs in a Victor X3 2030 multilabel reader spectrophotometer. Mutant 22 G8 was previously grown on $\frac{1}{2}$ LB broth at 37°C with shaking (225 rpm) for ~16 hrs. Each point represents the mean of two independent experiments in triplicate; error bars indicate standard deviation. * Represents statistical significance between control (green) and test (orange) groups. A-Nova test (Tukey) (P < 0.05)

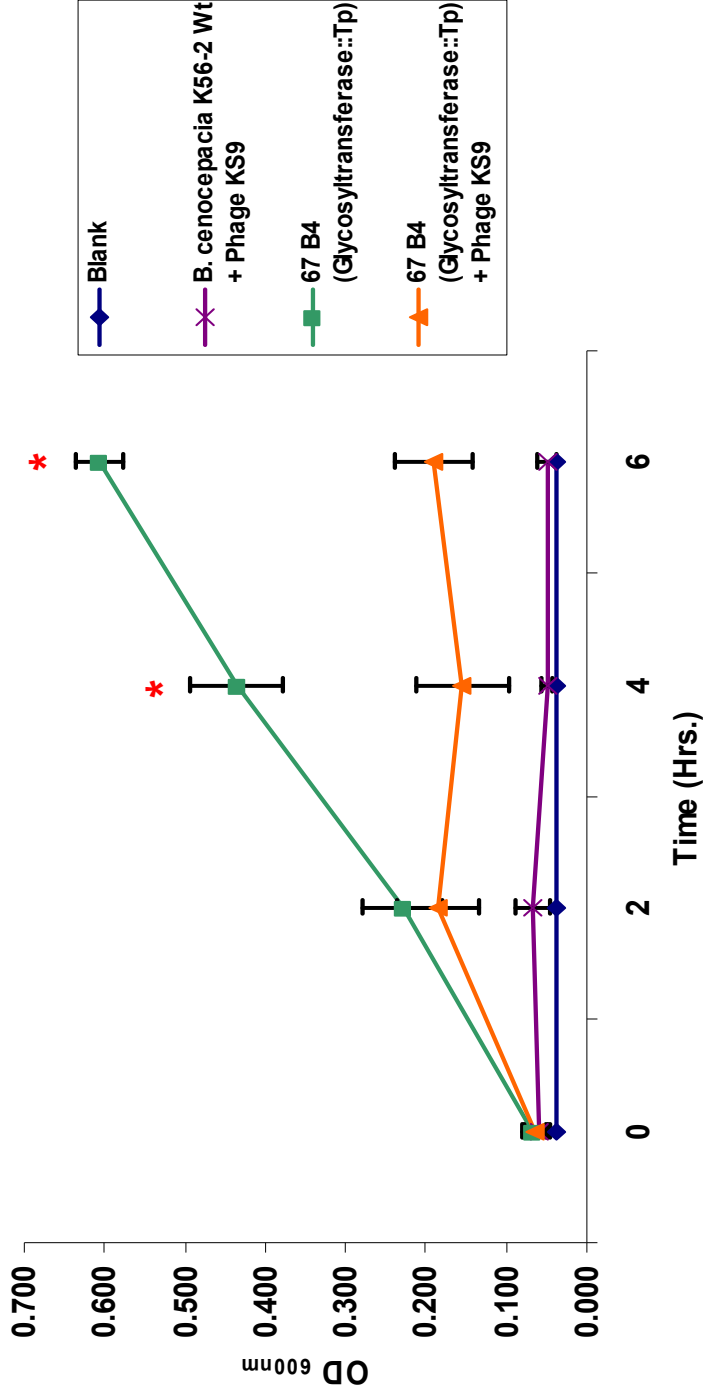


Figure 27: Growth curve of *B. cenocepacia* K56-2::pTnModOTp' mutant 67 B4 (Glycosyltransferase::Tp^R) exposed to phage KS9: Blue, blank control (200 μ L of $\frac{1}{2}$ LB broth), Green, positive control (10 μ L of bacteria) and (190 μ L of $\frac{1}{2}$ LB broth), Orange, test group (10 μ L of bacteria), (50 μ L of high titer phage stock) and (150 μ L of $\frac{1}{2}$ LB broth) incubated at 37°C with continuous shaking (225 rpm). A₆₀₀ measured every 2 hrs. for a period of 6 hrs in a Victor X3 2030 multilabel reader spectrophotometer. Mutant 67 B4 was previously grown on $\frac{1}{2}$ LB broth at 37°C with shaking (225 rpm) for ~16 hrs. Each point represents the mean of two independent experiments in triplicate; error bars indicate standard deviation. * Represents statistical significance between control (green) and test (orange) groups. A-Nova test (Tukey) (P < 0.05)

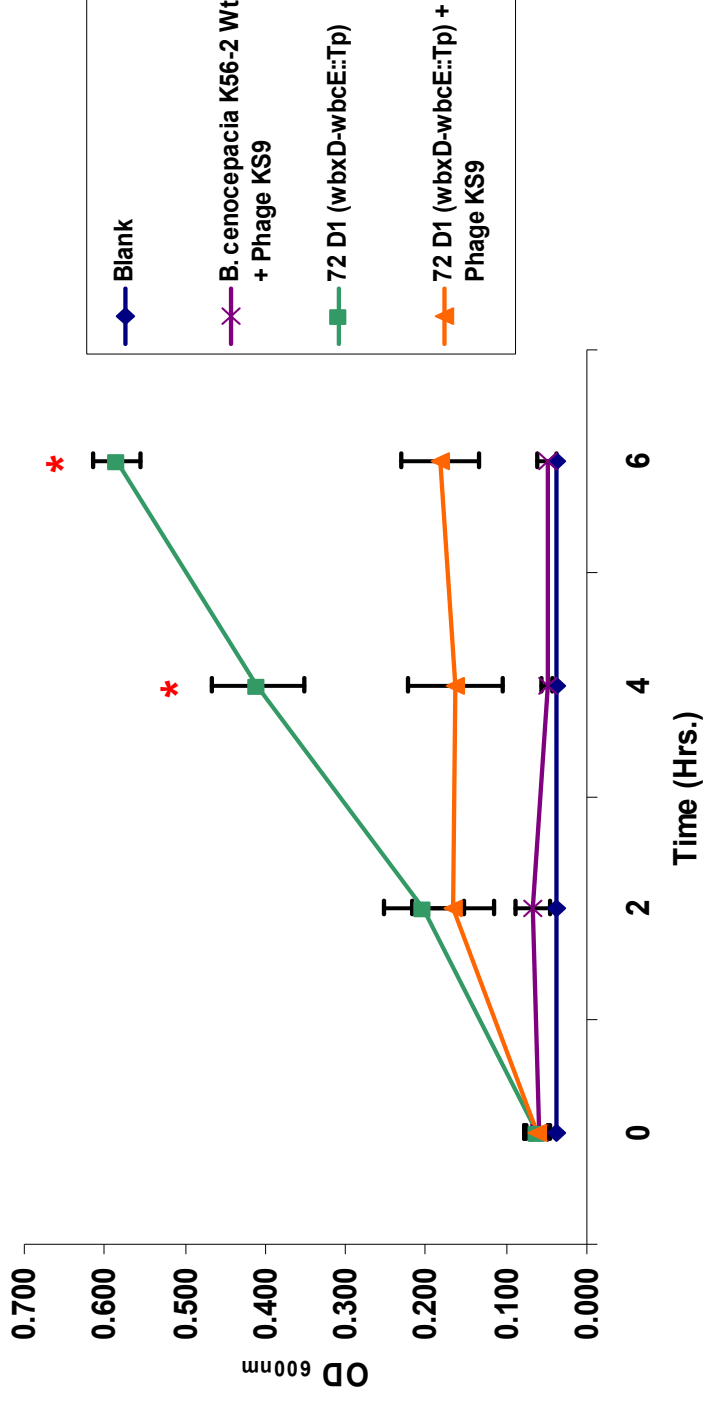


Figure 28: Growth curve of *B. cenocepacia* K56-2::pTnModOTp' mutant 72 D1 (*wbxD-wbcE::Tp^R*) exposed to phage KS9: Blue, blank control (200 μ L of $\frac{1}{2}$ LB broth), Green, positive control (10 μ L of bacteria) and (190 μ L of $\frac{1}{2}$ LB broth), Orange, test group (10 μ L of bacteria), (50 μ L of high titer phage stock) and (150 μ L of $\frac{1}{2}$ LB broth) incubated at 37°C with continuous shaking (225 rpm). A_{600} measured every 2 hrs. for a period of 6 hrs in a Victor X3 2030 multilabel reader spectrophotometer. Mutant 72 D1 was previously grown on $\frac{1}{2}$ LB broth at 37°C with shaking (225 rpm) for ~16 hrs. Each point represents the mean of two independent experiments in triplicate; error bars indicate standard deviation. * Represents statistical significance between control (green) and test (orange) groups. A-Nova test (Tukey) ($P < 0.05$)

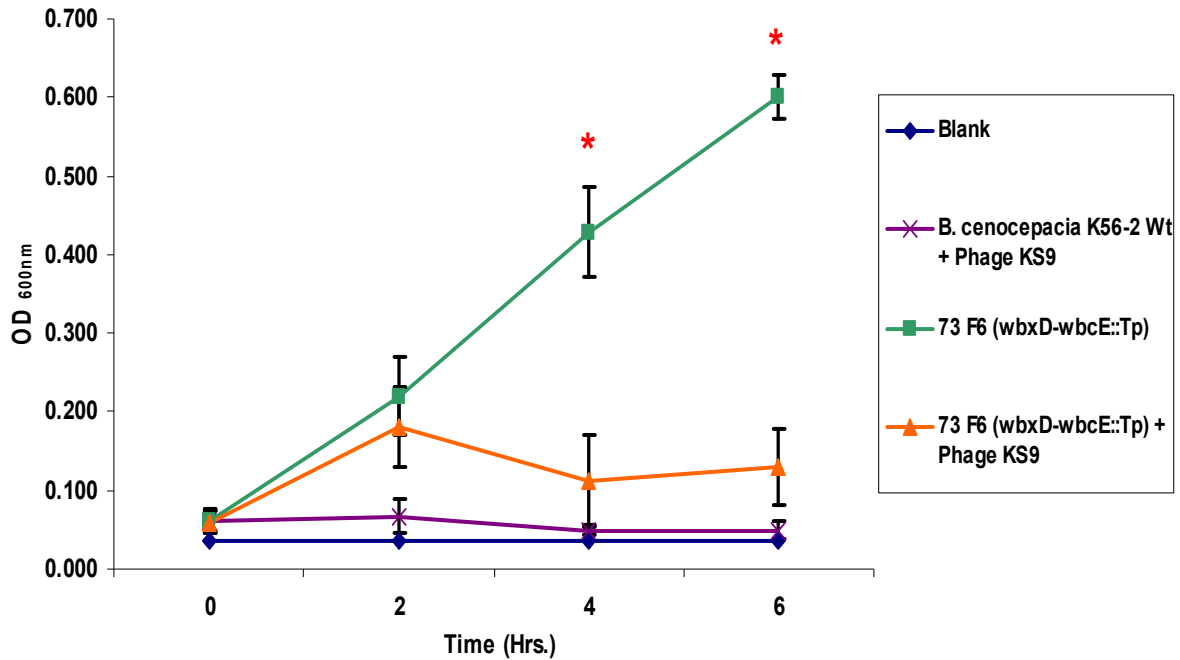


Figure 29: Growth curve of *B. cenocepacia* K56-2::pTnModOTp' mutant 73 F6 (*wbxD-wbcE::Tp^R*) exposed to phage KS9: Blue, blank control (200 μ L of $\frac{1}{2}$ LB broth), Green, positive control (10 μ L of bacteria) and (190 μ L of $\frac{1}{2}$ LB broth), Orange, test group (10 μ L of bacteria), (50 μ L of high titer phage stock) and (150 μ L of $\frac{1}{2}$ LB broth) incubated at 37°C with continuous shaking (225 rpm). A_{600} measured every 2 hrs. for a period of 6 hrs in a Victor X3 2030 multilabel reader spectrophotometer. Mutant 73 F6 was previously grown on $\frac{1}{2}$ LB broth at 37°C with shaking (225 rpm) for ~16 hrs. Each point represents the mean of two independent experiments in triplicate; error bars indicate standard deviation. * Represents statistical significance between control (green) and test (orange) groups. A-Nova test (Tukey) ($P < 0.05$)

Finally for the case of phage KS5, results revealed that this phage was able to clear eight out of the ten KS4-M resistant mutants [data not shown]. There was a slight similarity for the case of mutants 32 F4 and 67 F1 [Figs. 30 & 31], which showed a reduced level of sensitivity. However, the bacteria were still being cleared, but less efficiently than the rest of the KS4-M sensitive mutants. Data

from phage KS5 suggests that this is the only phage that seems to utilize a different receptor than that used by phages KS4-M, KS9 and KS12. This putative receptor is investigated in a series of experiments that will be discussed in following sections.

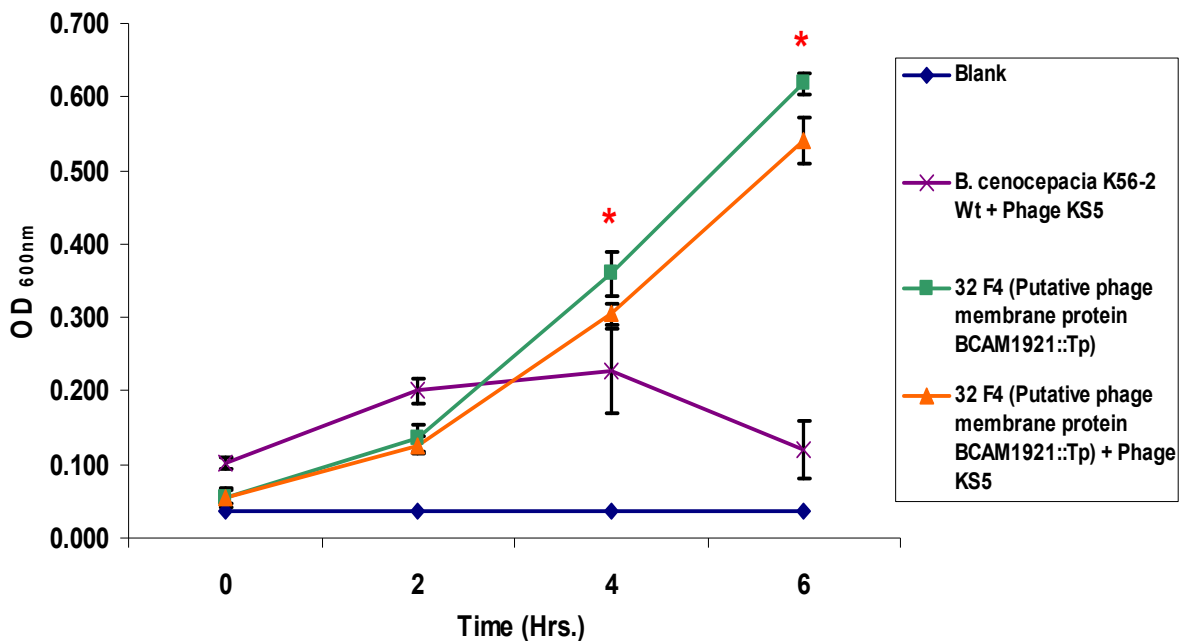


Figure 30: Growth curve of *B. cenocepacia* K56-2::pTnModOTp' mutant 32 F4 (Putative phage membrane protein BCAM1921::Tp^R) exposed to phage KS5: Blue, blank control (200 μ L of $\frac{1}{2}$ LB broth), Green, positive control (10 μ L of bacteria) and (190 μ L of $\frac{1}{2}$ LB broth), Orange, test group (10 μ L of bacteria), (50 μ L of high titer phage stock) and (150 μ L of $\frac{1}{2}$ LB broth) incubated at 37°C with continuous shaking (225 rpm). A₆₀₀ measured every 2 hrs. for a period of 6 hrs in a Victor X3 2030 multilabel reader spectrophotometer. Mutant 32 F4 was previously grown on $\frac{1}{2}$ LB broth at 37°C with shaking (225 rpm) for ~16 hrs. Each point represents the mean of two independent experiments in triplicate; error bars indicate standard deviation. * Represents statistical significance between control (green) and test (orange) groups. A-Nova test (Tukey) (P < 0.05)

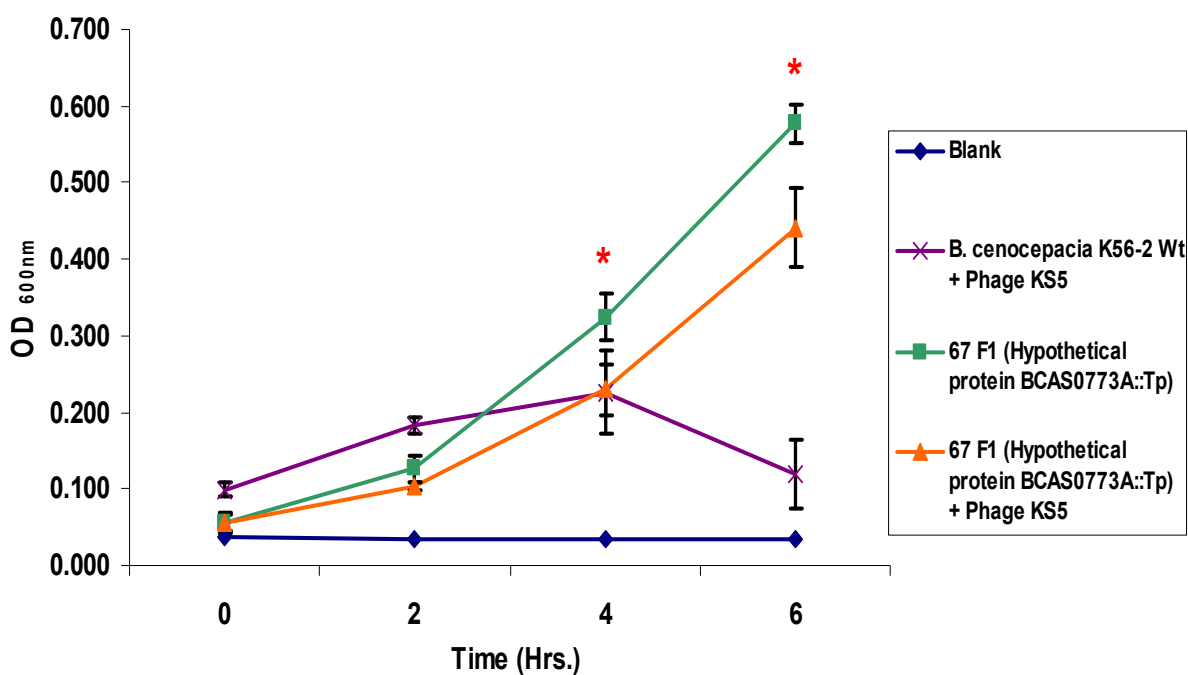


Figure 31: Growth curve of *B. cenocepacia* K56-2 pTnModOTp' mutant 67 F1 (Hypothetical protein BCAS0773A::Tp^R) exposed to phage KS5: Blue, blank control (200 μ L of $\frac{1}{2}$ LB broth), Purple, wt control (10 μ L of K56-2 wt), (50 μ L of high titer phage stock) and (150 μ L of $\frac{1}{2}$ LB broth) mixed, Green, positive control (10 μ L of bacteria) and (190 μ L of $\frac{1}{2}$ LB broth), Orange, test group (10 μ L of bacteria), (50 μ L of high titer phage stock) and (150 μ L of $\frac{1}{2}$ LB broth) incubated at 37°C with continuous shaking (225 rpm). A₆₀₀ measured every 2 hrs. for a period of 6 hrs in a Victor X3 2030 multilabel reader spectrophotometer. Mutant 67 F1 was previously grown on $\frac{1}{2}$ LB broth at 37°C with shaking (225 rpm) for ~16 hrs. Each point represents the mean of two independent experiments in triplicate; error bars indicate standard deviation. * Represents statistical significance between control (green) and test (orange) groups. A-Nova test (Tukey) (P < 0.05)

A similar approach was used to screen the *B. cenocepacia* PC184::pTnModluxOTp' library. Again, a total of ~9600 plasposon mutants were analyzed. Phages DC1, SR1 and KS10 were tested against this second library. For the case of phage DC1, six resistant mutants were isolated [Table 8] [Figs. 32-34].

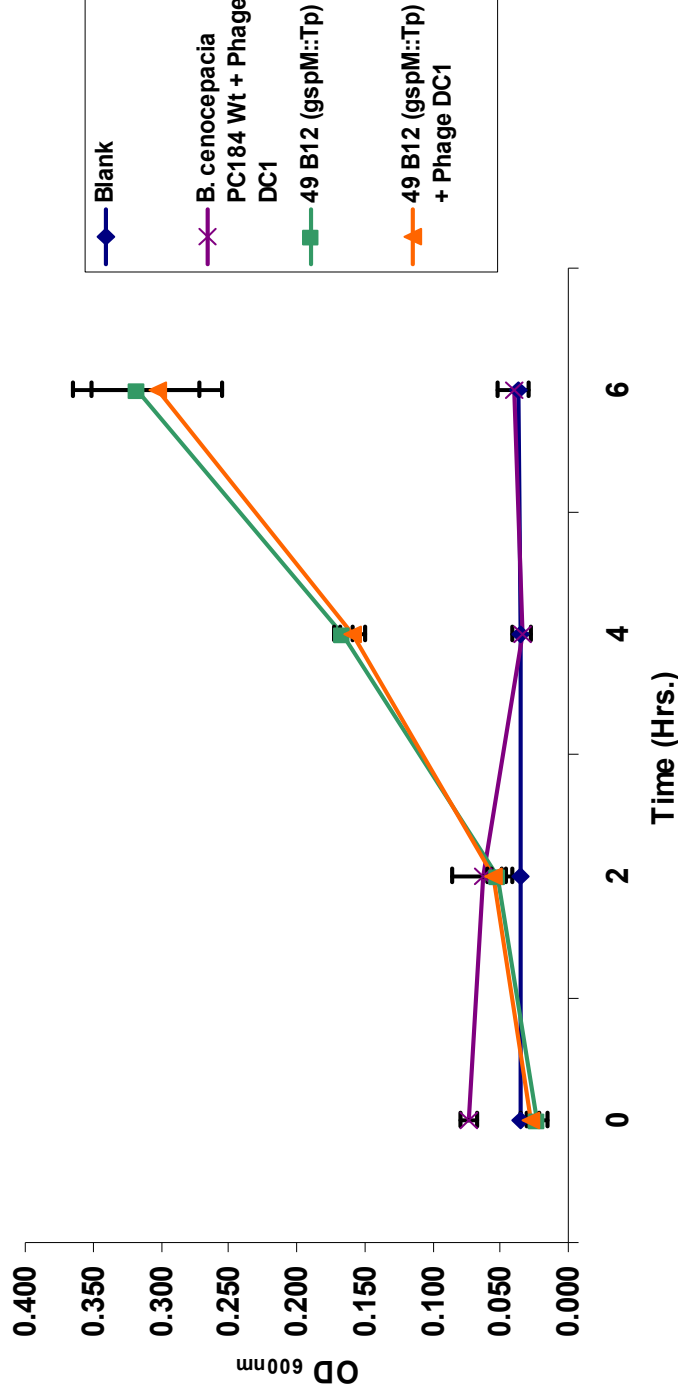


Figure 32: Growth curve of *B. cenocepacia* PC184:pTnModluxOTp^R mutant 49 B12 (*gspM::Tp*^R) exposed to phage DC1: Blue, blank control (200 μ L of $\frac{1}{2}$ LB broth), Purple, wt control (10 μ L of PC184 wt), (50 μ L of high titer phage stock) and (150 μ L of $\frac{1}{2}$ LB broth) mixed, Green, positive control (10 μ L of bacteria) and (190 μ L of $\frac{1}{2}$ LB broth), Orange, test group (10 μ L of bacteria), (50 μ L of high titer phage stock) and (150 μ L of $\frac{1}{2}$ LB broth) incubated at 37°C with continuous shaking (225 rpm). A_{600} measured every 2 hrs. for a period of 6 hrs in a Victor X3 2030 multilabel reader spectrophotometer. Mutant 49 B12 was previously grown on $\frac{1}{2}$ LB + 300 μ g of Tp/mL broth at 37°C with shaking (225 rpm) for ~16 hrs. Each point represents the mean of three independent experiments in triplicate; error bars indicate standard deviation. * Represents statistical significance between control (green) and test (orange) groups. A-Nova test (Tukey) ($P < 0.05$)

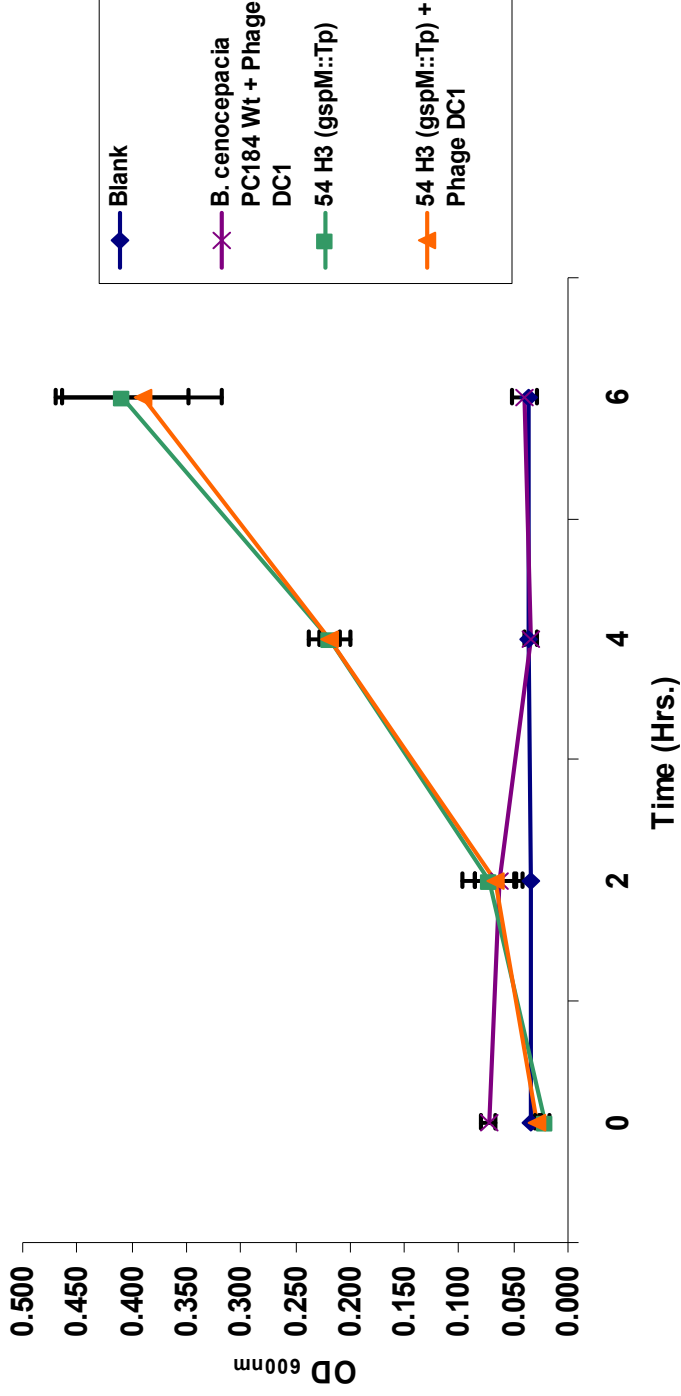


Figure 33: Growth curve of *B. cenocepacia* PC184::TnModluxOTp' mutant 54 H3 (*gspM::Tp^R*) exposed to phage DC1: Blue, blank control (200 μ L of $\frac{1}{2}$ LB broth), Purple, wt control (10 μ L of PC184 wt), (50 μ L of high titer phage stock) and (150 μ L of $\frac{1}{2}$ LB broth) mixed, Green, positive control (10 μ L of bacteria) and (190 μ L of $\frac{1}{2}$ LB broth), Orange, test group (10 μ L of bacteria), (50 μ L of high titer phage stock) and (150 μ L of $\frac{1}{2}$ LB broth) incubated at 37°C with continuous shaking (225 rpm). A_{600} measured every 2 hrs. for a period of 6 hrs in a Victor X3 2030 multilabel reader spectrophotometer. Mutant 54 H3 was previously grown on $\frac{1}{2}$ LB + 300 μ g of Tp/mL broth at 37°C with shaking (225 rpm) for ~16 hrs. Each point represents the mean of three independent experiments in triplicate; error bars indicate standard deviation. * Represents statistical significance between control (green) and test (orange) groups. A-Nova test (Tukey) ($P < 0.05$)

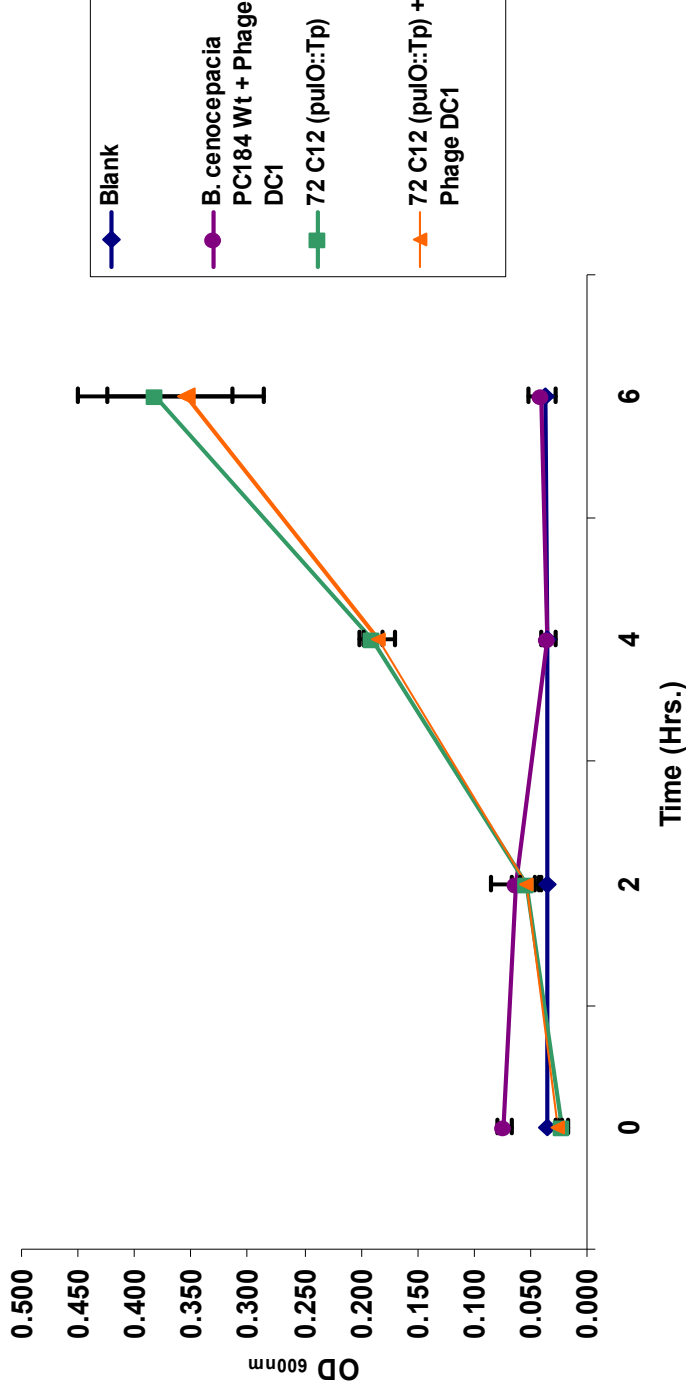


Figure 34: Growth curve of *B. cenocepacia* PC184::TnModluxOTp mutant 72 C12 (*pulO::Tp^R*) exposed to phage DC1: Blue, blank control (200 μ L of $\frac{1}{2}$ LB broth), Purple, wt control (10 μ L of PC184 wt), (50 μ L of high titer phage stock) and (150 μ L of $\frac{1}{2}$ LB broth) mixed, Green, positive control (10 μ L of bacteria) and (190 μ L of $\frac{1}{2}$ LB broth), Orange, test group (10 μ L of bacteria), (50 μ L of high titer phage stock) and (150 μ L of $\frac{1}{2}$ LB broth) incubated at 37°C with continuous shaking (225 rpm). A_{600} measured every 2 hrs. for a period of 6 hrs in a Victor X3 2030 multilabel reader spectrophotometer. Mutant 72 C12 was previously grown on $\frac{1}{2}$ LB + 300 μ g of Tp/mL broth at 37°C with shaking (225 rpm) for ~16 hrs. Each point represents the mean of three independent experiments in triplicate; error bars indicate standard deviation. * Represents statistical significance between control (green) and test (orange) groups. A-Nova test (Tukey) ($P < 0.05$)

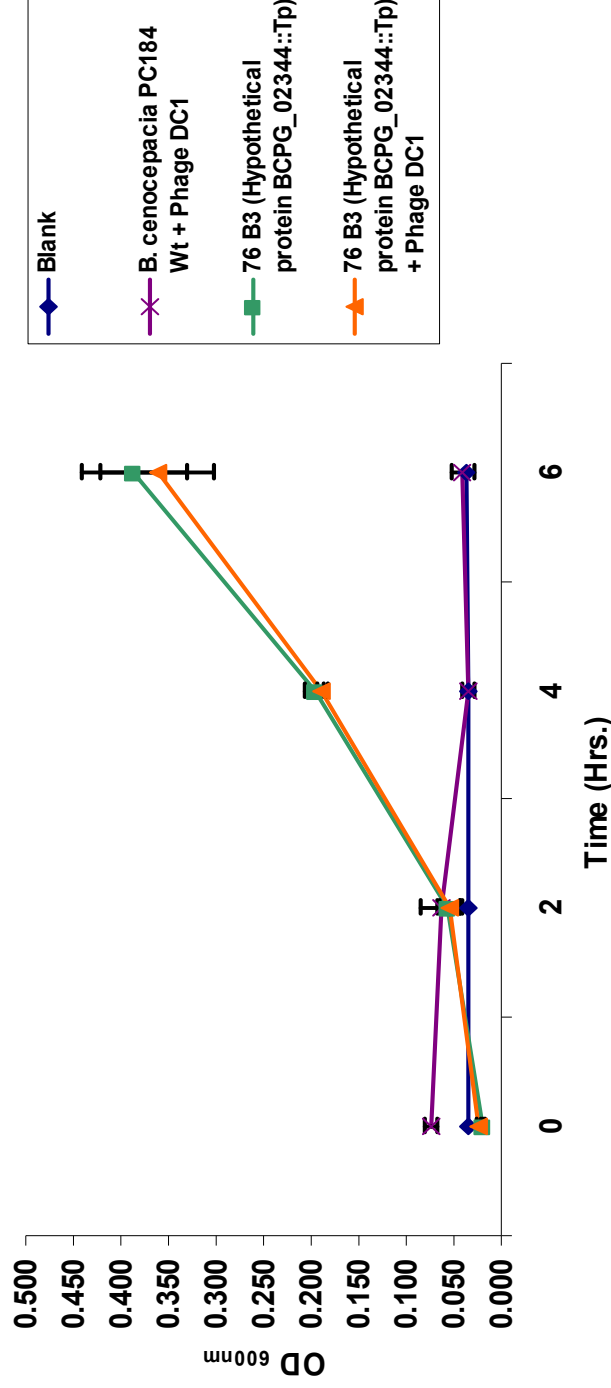


Figure 35: Growth curve of *B. cenocepacia* PC184::TnModluxOTp' mutant 76 B3 (Hypothetical protein BCPG_02344::Tp^R) exposed to phage DC1: Blue, blank control (200 μ L of $\frac{1}{2}$ LB broth), Purple, wt control (10 μ L of PC184 wt), (50 μ L of high titer phage stock) and (150 μ L of $\frac{1}{2}$ LB broth) mixed, Green, positive control (10 μ L of bacteria) and (190 μ L of $\frac{1}{2}$ LB broth), Orange, test group (10 μ L of bacteria), (50 μ L of high titer phage stock) and (150 μ L of $\frac{1}{2}$ LB broth) incubated at 37°C with continuous shaking (225 rpm). A₆₀₀ measured every 2 hrs. for a period of 6 hrs in a Victor X3 2030 multilabel reader spectrophotometer. Mutant 76 B3 was previously grown on $\frac{1}{2}$ LB + 300 μ g of Tp/mL broth at 37°C with shaking (225 rpm) for ~16 hrs. Each point represents the mean of three independent experiments in triplicate; error bars indicate standard deviation. * Represents statistical significance between control (green) and test (orange) groups. A-Nova test (Tukey) (P < 0.05)

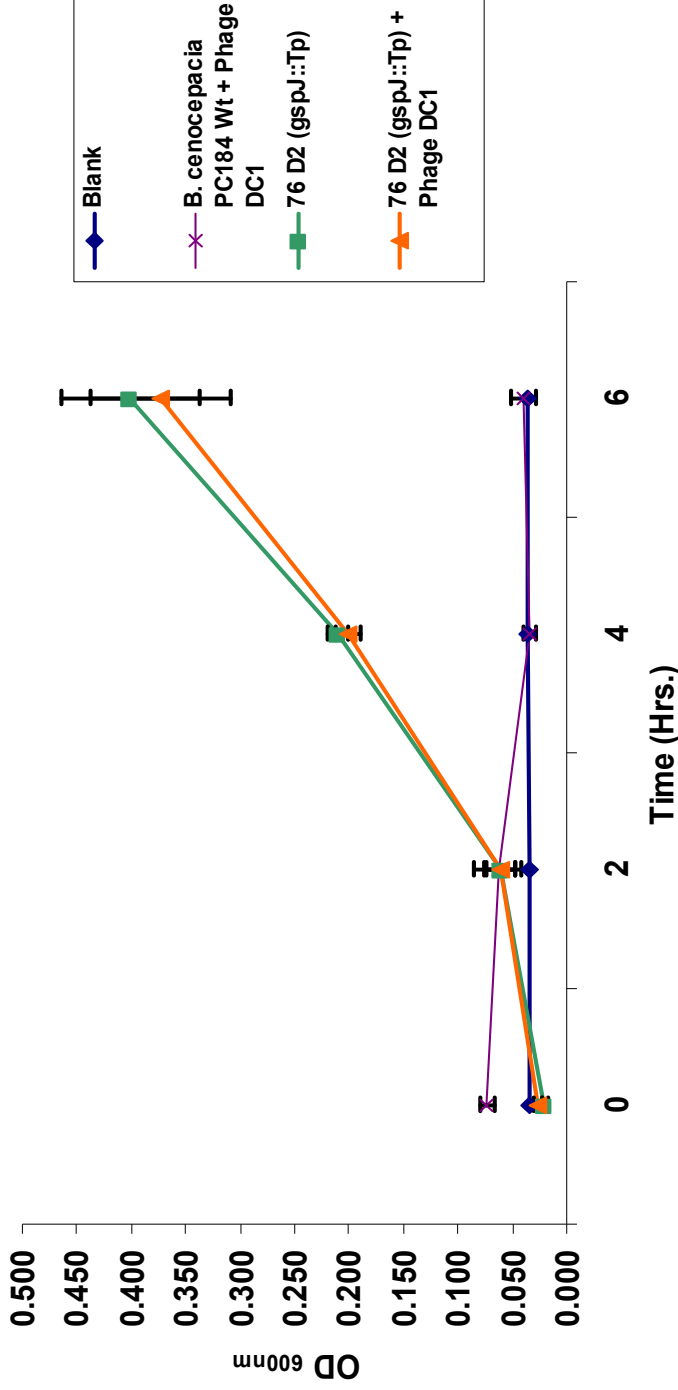


Figure 36: Growth curve of *B. cenocepacia* PC184::TnModluxOTp mutant 76 D2 (*gspJ::Tp^R*) exposed to phage DC1: Blue, blank control (200 μ L of $\frac{1}{2}$ LB broth), Purple, wt control (10 μ L of PC184 wt), (50 μ L of high titer phage stock) and (150 μ L of $\frac{1}{2}$ LB broth) mixed, Green, positive control (10 μ L of bacteria) and (190 μ L of $\frac{1}{2}$ LB broth), Orange, test group (10 μ L of bacteria), (50 μ L of high titer phage stock) and (150 μ L of $\frac{1}{2}$ LB broth) incubated at 37°C with continuous shaking (225 rpm). A_{600} measured every 2 hrs. for a period of 6 hrs in a Victor X3 2030 multilabel reader spectrophotometer. Mutant 76 D2 was previously grown on $\frac{1}{2}$ LB + 300 μ g of Tp/mL broth at 37°C with shaking (225 rpm) for ~16 hrs. Each point represents the mean of three independent experiments in triplicate; error bars indicate standard deviation. * Represents statistical significance between control (green) and test (orange) groups. A-Nova test (Tukey) ($P < 0.05$)

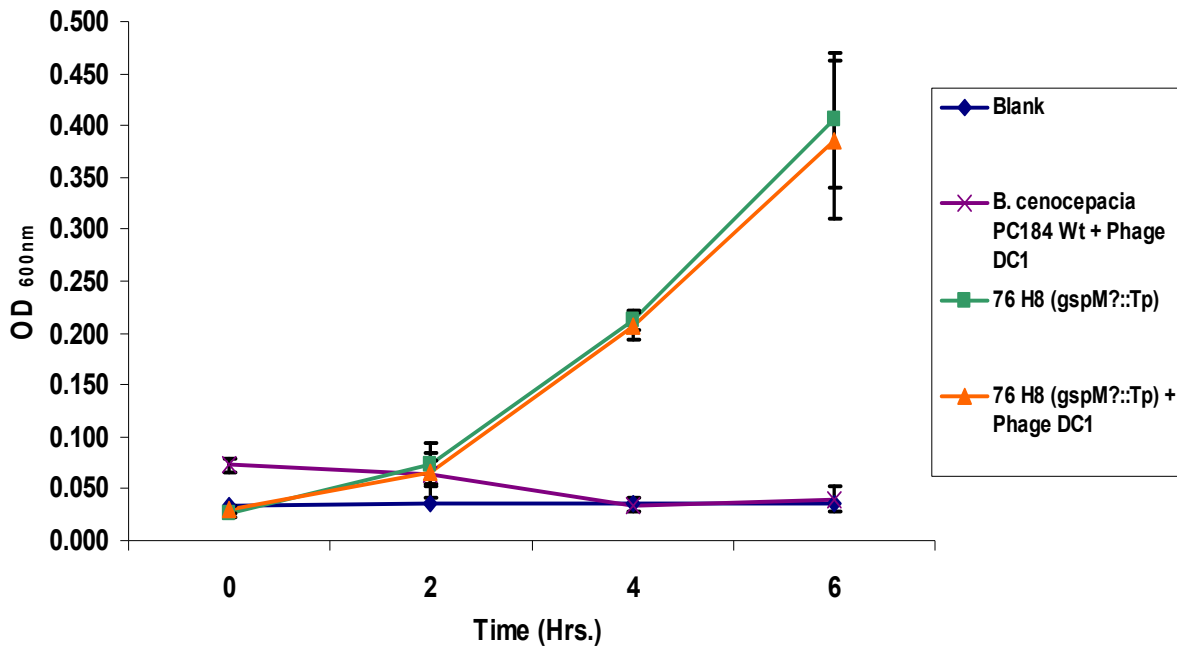


Figure 37: Growth curve of *B. cenocepacia* PC184::TnModluxOTp' mutant 76 H8 (*gspM?::Tp^R*) exposed to phage DC1: Blue, blank control (200 μ L of $\frac{1}{2}$ LB broth), Purple, wt control (10 μ L of PC184 wt), (50 μ L of high titer phage stock) and (150 μ L of $\frac{1}{2}$ LB broth) mixed, Green, positive control (10 μ L of bacteria) and (190 μ L of $\frac{1}{2}$ LB broth), Orange, test group (10 μ L of bacteria), (50 μ L of high titer phage stock) and (150 μ L of $\frac{1}{2}$ LB broth) incubated at 37°C with continuous shaking (225 rpm). A₆₀₀ measured every 2 hrs. for a period of 6 hrs in a Victor X3 2030 multilabel reader spectrophotometer. Mutant 76 H8 was previously grown on $\frac{1}{2}$ LB + 300 μ g of Tp/mL broth at 37°C with shaking (225 rpm) for ~16 hrs. Each point represents the mean of three independent experiments in triplicate; error bars indicate standard deviation. * Represents statistical significance between control (green) and test (orange) groups. A-Nova test (Tukey) ($P < 0.05$)

For the case of phage SR1 (a phage variant of phage KS10) (Routier, 2010), no resistant mutants were isolated after screening the entire library. I do not have an explanation for this, other than perhaps experimental error. For the case of related phage KS10, two resistant mutants were isolated [Table 9; Figs. 38 & 39]. These two mutants were subsequently tested against phage SR1 [Table 9; Figs. 40 & 41], and results revealed that both phages were unable to infect these

two mutants. These results were somewhat expected, since phage SR1 is a phage variant of KS10 (Routier, 2010).

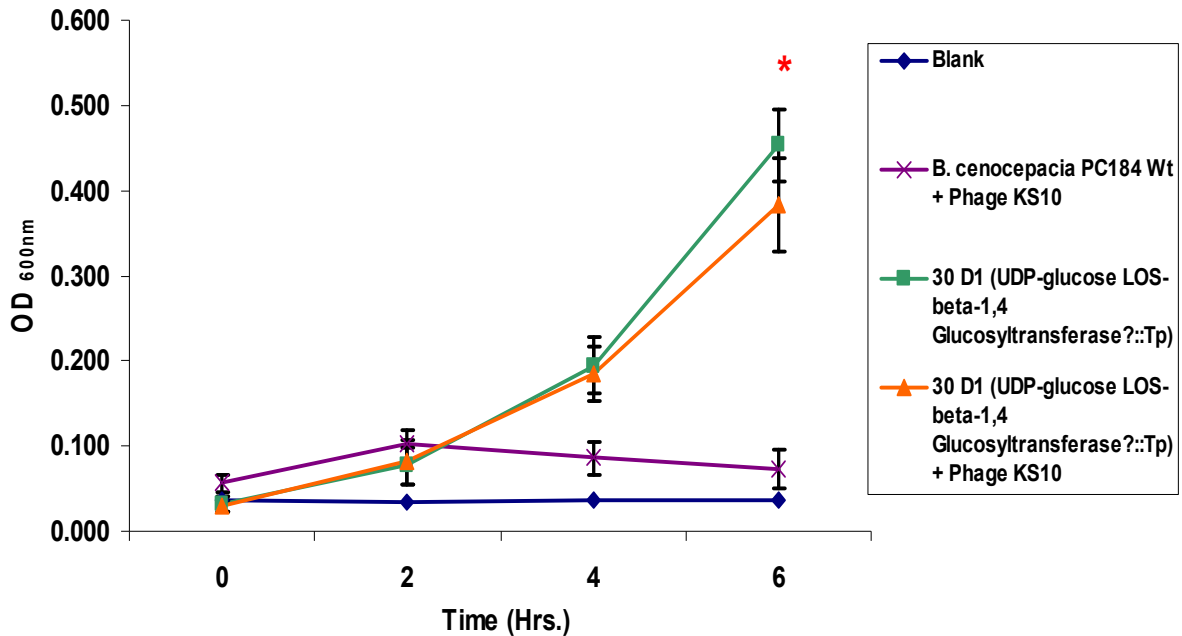


Figure 38: Growth curve of *B. cenocepacia* PC184::pTnModluxOTp' mutant 30 D1 (UDP-glucose LOS-beta-1,4 Glucosyltransferase *Bcenmc03_2331*::Tp^R) exposed to phage KS10: Blue, blank control (200 μ L of $\frac{1}{2}$ LB broth), Purple, wt control (10 μ L of PC184 wt), (50 μ L of high titer phage stock) and (150 μ L of $\frac{1}{2}$ LB broth) mixed, Green, positive control (10 μ L of bacteria) and (190 μ L of $\frac{1}{2}$ LB broth), Orange, test group (10 μ L of bacteria), (50 μ L of high titer phage stock) and (150 μ L of $\frac{1}{2}$ LB broth) incubated at 37°C with continuous shaking (225 rpm). A₆₀₀ measured every 2 hrs. for a period of 6 hrs in a Victor X3 2030 multilabel reader spectrophotometer. Mutant 30 D1 was previously grown on $\frac{1}{2}$ LB + 300 μ g of Tp/mL broth at 37°C with shaking (225 rpm) for ~16 hrs. Each point represents the mean of three independent experiments in triplicate; error bars indicate standard deviation. * Represents statistical significance between control (green) and test (orange) groups. A-Nova test (Tukey) (P < 0.05)

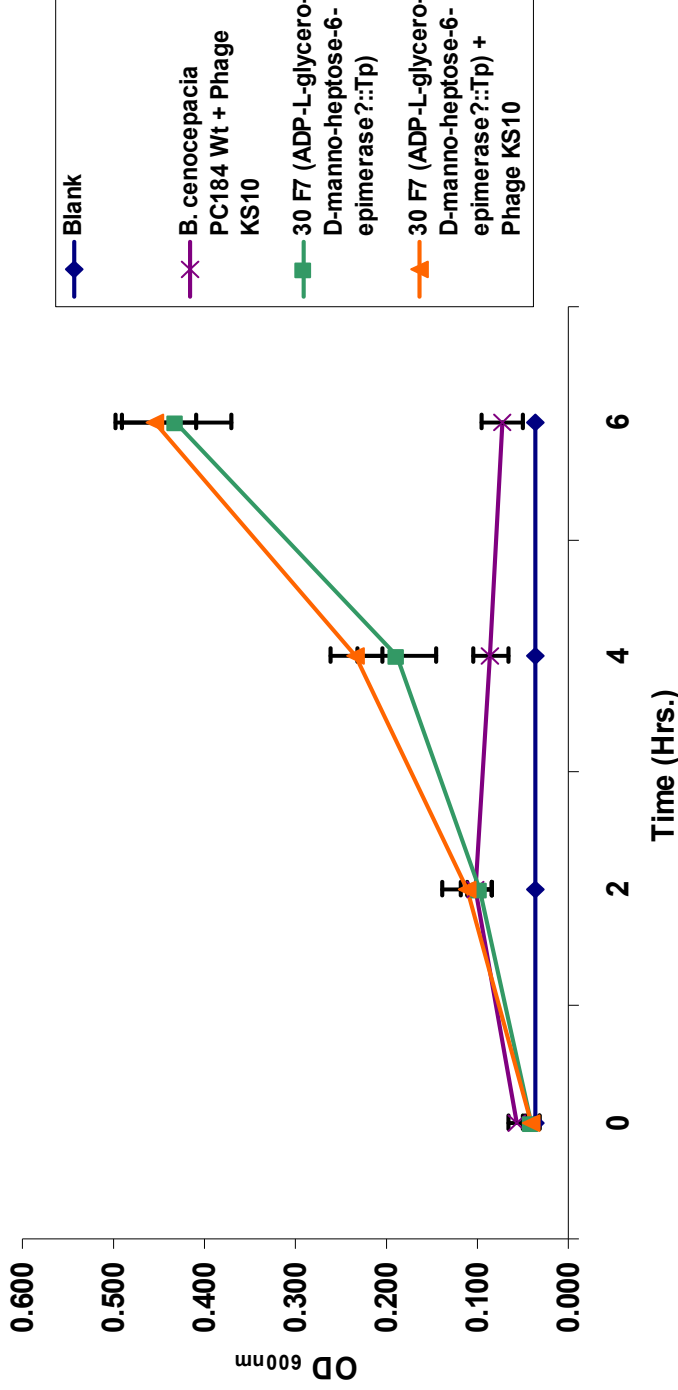


Figure 39: Growth curve of *B. cenocepacia* PC184::pTnModluxOTp' mutant 30 F7 (ADP-L-glycero-D-manno-heptose-6-epimerase? *Bcenmc03_1012::Tp^R*) exposed to phage KS10: Blue, blank control (200 μ L of $\frac{1}{2}$ LB broth), Purple, wt control (10 μ L of PC184 wt), (50 μ L of high titer phage stock) and (150 μ L of $\frac{1}{2}$ LB broth) mixed, Green, positive control (10 μ L of bacteria) and (190 μ L of $\frac{1}{2}$ LB broth), Orange, test group (10 μ L of bacteria), (50 μ L of high titer phage stock) and (150 μ L of $\frac{1}{2}$ LB broth) incubated at 37°C with continuous shaking (225 rpm). A_{600} measured every 2 hrs. for a period of 6 hrs in a Victor X3 2030 multilabel reader spectrophotometer. Mutant 30 F7 was previously grown on $\frac{1}{2}$ LB + 300 μ g of Tp/mL broth at 37°C with shaking (225 rpm) for ~16 hrs. Each point represents the mean of three independent experiments in triplicate; error bars indicate standard deviation. * Represents statistical significance between control (green) and test (orange) groups. A-Nova test (Tukey) ($P < 0.05$)

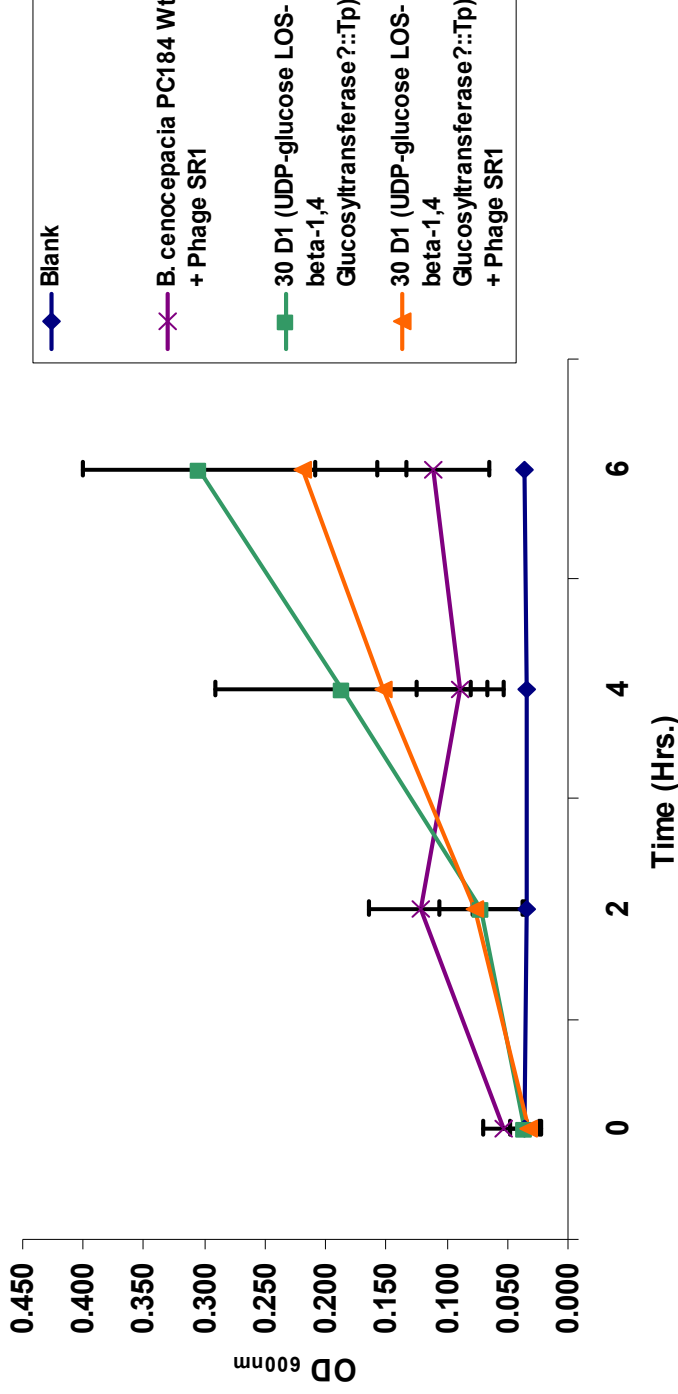


Figure 40: Growth curve of *B. cenocepacia* PC184::pTnModluxOTp' mutant 30 D1 (UDP-glucose LOS-beta-1,4 Glucosyltransferase *Bcenmc03_2331*::Tp^R) exposed to phage SR1: Blue, blank control (200 μ L of $\frac{1}{2}$ LB broth), Purple, wt control (10 μ L of PC184 wt), (50 μ L of high titer phage stock) and (150 μ L of $\frac{1}{2}$ LB broth) mixed, Green, positive control (10 μ L of bacteria) and (190 μ L of $\frac{1}{2}$ LB broth), Orange, test group (10 μ L of bacteria), (50 μ L of high titer phage stock) and (150 μ L of $\frac{1}{2}$ LB broth) incubated at 37°C with continuous shaking (225 rpm). A₆₀₀ measured every 2 hrs. for a period of 6 hrs in a Victor X3 2030 multilabel reader spectrophotometer. Mutant 30 D1 was previously grown on $\frac{1}{2}$ LB + 300 μ g of Tp/mL broth at 37°C with shaking (225 rpm) for ~16 hrs. Each point represents the mean of three independent experiments in triplicate; error bars indicate standard deviation. * Represents statistical significance between control (green) and test (orange) groups. A-Nova test (Tukey) (P < 0.05)

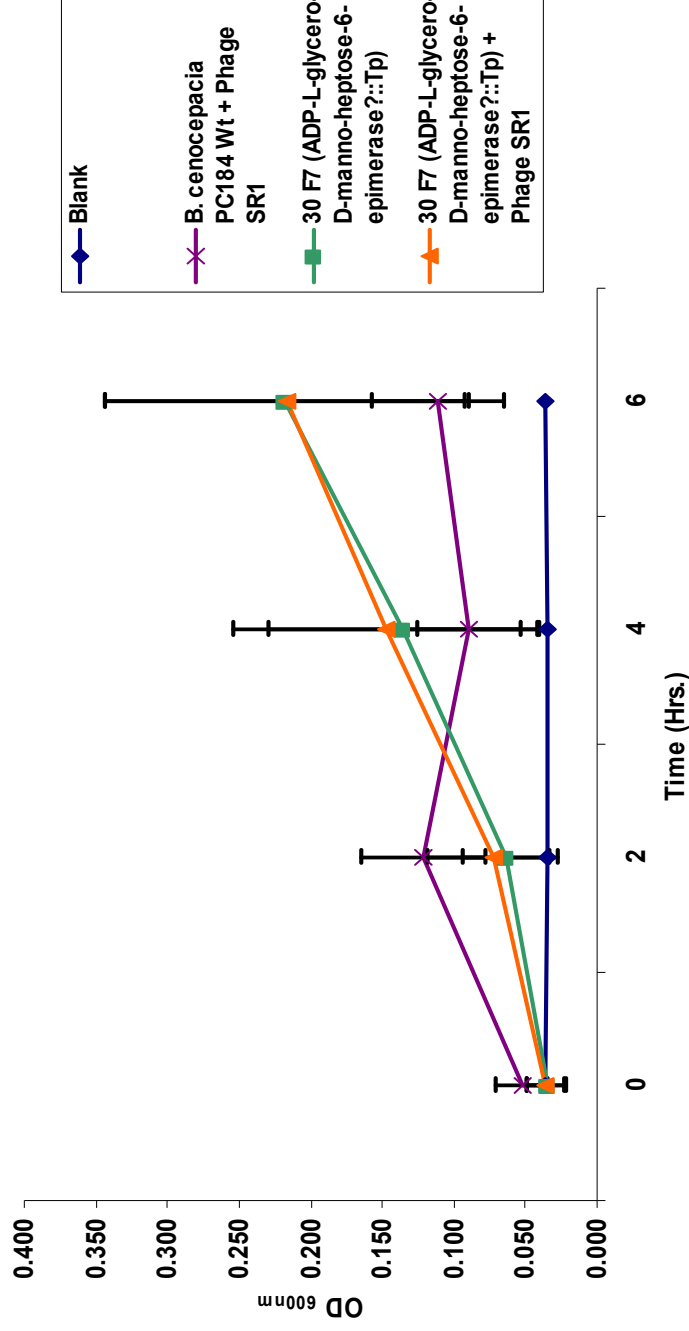


Figure 41: Growth curve of *B. cenocepacia* PC184::pTnModluxOTp' mutant 30 F7 (ADP-L-glycero-D-manno-heptose-6-epimerase? *Bcenmc03_1012::Tp^R*) exposed to phage SR1: Blue, blank control (200 μ L of $\frac{1}{2}$ LB broth), Purple, wt control (10 μ L of PC184 wt), (50 μ L of high titer phage stock) and (150 μ L of $\frac{1}{2}$ LB broth) mixed, Green, positive control (10 μ L of bacteria) and (190 μ L of $\frac{1}{2}$ LB broth), Orange, test group (10 μ L of bacteria), (50 μ L of high titer phage stock) and (150 μ L of $\frac{1}{2}$ LB broth) incubated at 37°C with continuous shaking (225 rpm). A_{600} measured every 2 hrs. for a period of 6 hrs in a Victor X3 2030 multilabel reader spectrophotometer. Mutant 30 F7 was previously grown on $\frac{1}{2}$ LB + 300 μ g of Tp/mL broth at 37°C with shaking (225 rpm) for ~16 hrs. Each point represents the mean of three independent experiments in triplicate; error bars indicate standard deviation. * Represents statistical significance between control (green) and test (orange) groups. A-Nova test (Tukey) ($P < 0.05$)

Plasposon mutant library screening confirmatory assays [Solid media]

To further confirm previous findings, we decided to test all of the resistant mutants from both libraries against their respective phages by the soft agar overlay method [data not shown]. The hypothesis was that the resistant mutants isolated in liquid cultures, would also be resistant to phage infection using solid media. The results revealed similarities to liquid clearing experiments, and were actually more consistent on agar plates than in liquid cultures. The ten K56-2::pTn*ModOTp*' mutants showed resistance to phages KS4-M and KS12 infection. However, there was one exception. Mutant 32 F4 showed partial sensitivity to phage KS12, as small, turbid plaques were detected on the plate (approximately 20-30 plaques). Interestingly, even though the phage is still infecting the host, the efficiency is greatly reduced as the control plate (K56-2 wt) showed confluent lysis, suggesting that there must be an alteration affecting phage binding or perhaps lysis for this particular mutant. For the case of phage KS9, all ten KS4-M resistant mutants also showed resistance to KS9 infection. Previous results contradict the results observed for mutants 22 G8, 67 B4, 72 D1 and 73 F6, which showed sensitivity in liquid cultures (but full resistance on agar plates). Unfortunately, we do not have an explanation for these contradictory results. For the case of phage KS5, the ten KS4-M resistant mutants were all sensitive to phage KS5 infection, and confluent lysis or several plaques were detected in all the plates. However, two out of the ten mutants showed reduced sensitivity to phage KS5 as compared to the full sensitivity detected for phage KS4-M. These mutants are 32 F4 and 67 F1. Perhaps similar to the results for phage KS12, an alteration affecting phage

binding or host lysis may be responsible for these non-identical results. We can however state that the results obtained on solid media are similar to and confirm the KS5 results observed in liquid cultures.

For the PC184::pTn*Modlux*OTp' mutants, data was similar to that found in liquid culture experiments. The six DC1 resistant mutants were also resistant to DC1 on agar plates, as no plaques were detected on the plates, confirming the results obtained from the liquid clearing assays. For the two KS10 and SR1 phage resistant mutants, they were also resistant on agar plates, and no differences were observed between the liquid and solid cultures.

There is an apparent difference in phage infection efficiency for some phage resistant mutants between liquid and solid media. We hypothesize that these differences cause the “contradictory” results between the liquid culture clearing assays and the results obtained from the agar plates. One reason may be that phages have higher chances to infect their host in liquid cultures, due continuous phage movement, which increases the chances of the phage colliding with the host. Since phage-bacteria infection is a random chance event (Rakhuba et al., 2010), this seems a reasonable explanation; however, we don't have data to prove it. Alternatively, it is possible that the differences observed are due to hydration affecting receptor structure. For some mutants, perhaps the phage receptor does not assume proper (phage-recognizable) conformation unless it is surrounded by water molecules, an environmental condition more frequently encountered in

liquid rather than solid media. Given the data, this may be the most probable explanation for the differences observed in liquid and solid media.

Plasposon mutant library screening in minimal media.

In order to determine whether we were not observing the expression of some receptors due to growth of the bacteria in rich media, a second screening of both libraries was carried out using minimal media (MM) [data not shown]. Because members of the Bcc are usually found in nutrient poor soils or environments (Mahenthiralingam et al., 2005), it was expected that this second screening might more accurately imitate natural environments where nutrients are limited. It was hypothesized that nutrient deprivation would force expression of alternative phage receptors by the host. Unfortunately, no alternative phage resistant mutants were isolated, the only observed difference between the use of ½ LB broth and MM was the slow and reduced growth of bacteria in MM.

Plasposon isolation and sequencing of disrupted genes

After the phage resistant mutants were isolated, purified, and stored for future use, we proceeded to identify the disrupted receptor gene from each of them. The bacterial DNA from ten K56-2::Tn*Mod*OTp' KS4-M, KS9 and KS12 resistant mutants [Table 7], six PC184::Tn*Modlux*OTp' DC1 resistant mutants [Table 8] and two PC184::pTn*Modlux*OTp' KS10 and SR1 resistant mutants [Table 9] was isolated and purified by the CTAB DNA precipitation protocol (Wilson, 1997), as described in materials and methods. Chromosomal DNA was

subsequently digested with an appropriate restriction enzyme, and the plasposon was recovered, religated, and transformed into a permissive host; in this case *E. coli* DH5- α cells were used. Only clones carrying the plasposon and providing T_p resistance were recovered, along with flanking DNA indicating where in the genome the plasposon had inserted.

Using this strategy, the plasposon insertion site and the genes surrounding it are isolated as a plasmid. Obtained DNA was sequenced with the specific primers JD28 5' Ori: 5'-GGGGAAACGCCTGGTATC and JD47 3' T_p: 5'-TTTATCCTGTGGCTGC which bind to specific regions inside the plasposon and allow for the sequencing of the regions surrounding the plasposon, which belong to the disrupted gene(s) of interest. These sequences are then analyzed using bioinformatics. The software 4peaks, DynamoDNA and the Basic Local Alignment Search Tool (BLAST, blast.ncbi.nlm.nih.gov/Blast.cgi) using the NCBI database were used to analyze all of the sequences. In the case of the KS4-M resistant mutants, sequences of four out of the ten isolated mutants (16 E1, 20 A12, 72 D1 and 73 F6) revealed that the plasposon inserted and disrupted two divergent genes (*wbxD-wbcE::T_p*) [Fig. 42] involved in LPS production. These genes were annotated as *wbxD* (a glycosyltransferase) and *wbcE* (a pseudo glycosyltransferase) in the most closely associated GenBank entry, *B. cenocepacia* strain J2315. In the case of *wbxD*, several important structural motifs were located on the predicted encoded protein. One of the motifs, located from amino acid (AA) 75 to 174 and also from AA 326 to 535, classified this protein as a glycosyltransferase belonging to Superfamily A of

glycosyltransferases. According to NCBI, glycosyltransferases adopt one of two possible folds. One is termed GT-A fold, the other one is GT-B fold. In this particular case, the protein product has a GT-A type structural fold, characterized by two tightly associated β - α - β domains that tend to form a continuous central sheet of at least eight β -strands. A second motif was located from AA 25 to 250. This motif, termed WcaA, is characteristic of glycosyltransferases involved in cell wall biogenesis (cell envelope and outer membrane biogenesis). Gene *wbcE* is annotated as a pseudoglycosyltransferase. This gene is interrupted by an IS element inserted after codon 84 in strain J2315, an IS element does not appear to interrupt this gene in K56-2 or PC184. No additional information is provided for *wbcE* on the NCBI website.

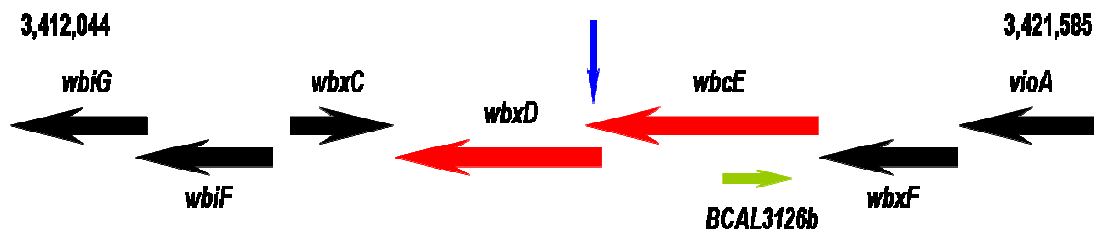


Figure 42: NCBI genomic context and organization of the *B. cenocepacia* J2315 region containing the disrupted genes (red) from the KS4-M resistant mutants (16 E1, 20 A12, 72 D1 and 73 F6). Plasposon insertion is illustrated as a blue vertical arrow. The IS element found in strain J2315 is depicted in green. It inserted after codon 84 of *wbcE*.

In the case of mutants 15 E11, 21 C7 and 67 B4, the sequence files retrieved a general match for glycosyltransferases and no specific genes were identified. However, in all cases the same GeneBank match (AAT48329.1) was given for the plasposon sequences, suggesting that the plasposon had inserted in the same gene in each case. Because a glycosyltransferase was disrupted by the

plasposon, we hypothesized that LPS was being used by these phages as a receptor to bind to and infect the host cell. Due to the polar mutation nature of the plasposon insertion, there is still a possibility that other LPS structures might be disrupted. No exact gene match was found for some resistant mutants, therefore it was difficult to determine whether LPS was the only phage receptor structure.

The plasposon sequences from the remaining three mutants (22 G8, 32 F4 and 67 F1) were all different. Sequence data from mutant 22 G8 matched gene *ESA_02316::Tp*, a hypothetical protein in *Cronobacter sakazakii* strain ATCC BAA-894 (GeneBank#: YP_001438401.1). No additional information was found in the NCBI database and all the genes surrounding *ESA_02316* are annotated as hypothetical proteins (Fig. 43).

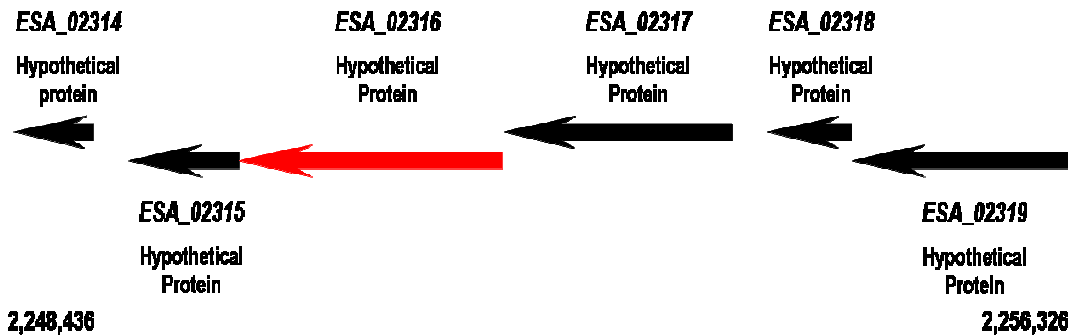


Figure 43: NCBI genomic context and organization of the *Cronobacter sakazakii* ATCC BAA-894 region containing the disrupted gene (red) from the KS4-M resistant mutant (22 G8). All the genes are annotated as hypothetical proteins.

Mutant 32 F4 sequence matched gene *BCAM1921::Tp*, a putative phage membrane protein found in *B. cenocepacia* strain J2315 (GeneBank#: YP_002234531.1). According to the NCBI website, this protein is predicted to be

a transmembrane helix due a structural motif, but no additional information is provided. Similar to mutant 22 G8, the genes surrounding *BCAM1921* are annotated as hypothetical proteins (Fig. 44).

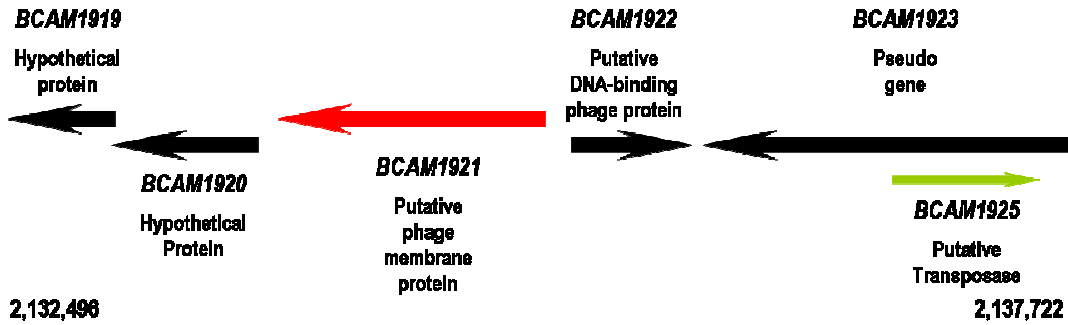


Figure 44: NCBI genomic context and organization of the *B. cenocepacia* J2315 region containing the disrupted gene (red) from the KS4-M resistant mutant (32 F4).

Finally, mutant 67 F1 sequence data matched the gene *BCAS0773A::Tp*, a hypothetical protein found in the chromosome 3 of strain J2315 (GeneBank#: YP_002154145.1)(Fig. 45). No additional information is found in the database, the gene itself is only 186 nucleotides making this a small gene.

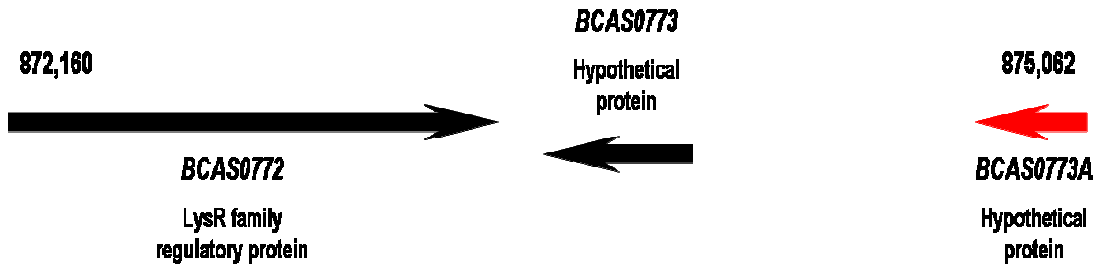


Figure 45: NCBI genomic context and organization of the *B. cenocepacia* J2315 region containing the disrupted gene (red) from the KS4-M resistant mutant (67 F1).

Mutant Plate & Well #	Match output	Amino acids	E Value	GeneBank #	Gene Symbol	Locus Tag
15 E11 3'	Glycosyltransferase (<i>B. cenocepacia</i>)	456	3e-106	AAT48329.1	No match	No match
15 E11 5'	Glycosyltransferase (<i>B. cenocepacia</i>)	“	4e-36	AAT48329.1	No match	No match
16 E1 3'	Glycosyltransferase (<i>B. cenocepacia</i> J2315)	655	3e-110	YP_002232235.1	<i>wbxD</i>	BCAL3124
16 E1 5'	Glycosyltransferase (<i>B. cenocepacia</i> J2315)	“	1e-38	YP_002232235.1	<i>wbxD</i>	BCAL3124
20 A12 3'	Glycosyltransferase (<i>B. cenocepacia</i>)	456	0.0	AAT48329.1	No match	
20 A12 5'	Glycosyltransferase (<i>B. cenocepacia</i> J2315)	655	2e-88	YP_002232235.1	<i>wbxD</i>	BCAL3124
21 C7 3'	Glycosyltransferase (<i>B. cenocepacia</i>)	456	1e-162	AAT48329.1	No match	No match
21 C7 5'	Glycosyltransferase (<i>B. cenocepacia</i>)	“	2e-59	AAT48329.1	No match	No match
22 G8 3'	Digested with <i>Xba</i> I cuts inside the Tp cassette	--	--	--	--	--
22 G8 5'	Hypothetical protein ESA_02316 (<i>Cronobacter sakazakii</i> ATCC BAA-894)	940	6e-09	YP_001438401.1	<i>ESA_02316</i>	ESA_02316
32 F4 3'	Putative phage membrane protein (<i>B. cenocepacia</i> J2315)	344	4e-45	YP_002234531.1	<i>BCAM1921</i>	BCAM1921
32 F4 5'	Digested with <i>Bg</i> /II cuts inside the Ori	--	--	--	--	--

67 B4 3'	Glycosyltransferase (<i>B. cenocepacia</i>)	456	2e-173	AAT48329.1	No match	No match
67 B4 5'	Glycosyltransferase (<i>B. cenocepacia</i>)	"	1e-17	AAT48329.1	No match	No match
67 F1 3'	Hypothetical protein BCAS0773A (<i>B. cenocepacia</i> J2315)	61	1e-34	YP_002154145.1	BCAS0773A	BCAS0773A
67 F1 5'	Digested with <i>Bgl</i> II cuts inside the Ori	--	--	--	--	--
72 D1 3'	Glycosyltransferase (<i>B. cenocepacia</i> J2315)	655	1e-134	YP_002232235.1	<i>wbxD</i>	BCAL3124
72 D1 5'	Digested with <i>Bgl</i> II cuts inside the Ori	--	--	--	--	--
73 F6 3'	Glycosyltransferase (<i>B. cenocepacia</i> J2315)	655	1e-180	YP_002232235.1	<i>wbxD</i>	BCAL3124
73 F6 5'	Glycosyltransferase (<i>B. cenocepacia</i>)	456	4e-76	AAT48329.1	No match	No match

Table 7: Ten *B. cenocepacia* K56-2::pTnModOTp' KS4-M resistant mutants. These mutants were also tested against phages KS5, KS9 and KS12.

The general secretory pathway (GSP) is a well-studied mechanism by which proteins, virulence factors, hydrolytic enzymes, pili, etc. are secreted into the extracellular environment. It is a two-step process requiring the Sec translocase in the IM and an alternative secretion apparatus (substrate-specific) that translocates the proteins across the OM (Stathopoulos, 2000). The Gsp proteins are part of this secretory pathway. Once the proteins (toxins, enzymes etc.) to be excreted have been translocated across the IM via the Sec translocase, the final step (translocation across the OM) can happen by different routes. The most common of these routes is known as the GSP main general branch, also known as the T2SS, which exports the majority of the bacterial exoenzymes and toxins and contributes to pathogenesis (Stathopoulos, 2000; Sandkvist, 2001). The T2SS apparatus [Fig. 43] is composed of at least 12 (and up to 15) gene products that form a multiprotein complex. This complex spans the periplasm and is essential for the translocation of proteins through the OM. Interestingly, this secretion system shares many features and components with the proteins required for the biogenesis of Type IV pili, which suggests that the two systems are evolutionary related (Sandkvist, 2001). The pullulanase (Pul) export system in *Klebsiella oxytoca* was the first T2SS characterized. In the case of *E. coli*, the T2SS genes were designated as *gsp*.

Two (possibly three) plasposon sequences from the PC184::pTn*Modlux*-OTp' DC1 resistant mutants match the general secretion protein T2SS protein M (*gspM*::Tp) as annotated in *B. cenocepacia* strain J2315. These mutants are 49 B12, 54 H3, and possibly 76 H8. In all cases, the sequence length obtained was short, less than 60 bases. However, we are confident that these sequences are accurate because the sequences from the remaining mutants also match elements that are part of the T2SS. GspM (or PulM) is one of the five integral GSP IM proteins, the others being C, N, K and F. It is predicted that these proteins are anchored to the IM and may be involved in the formation of the basal body of the T2SS apparatus, which is also anchored to the IM on the periplasmic side.

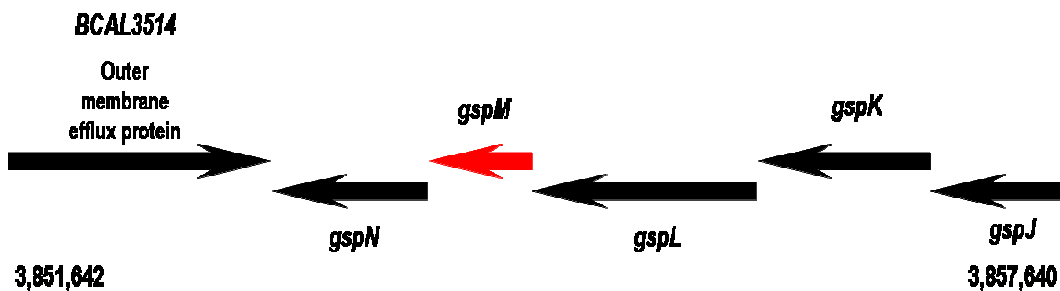


Figure 47: NCBI genomic context and organization of the *B. cenocepacia* J2315 region containing the disrupted gene (red) from the DC1 resistant mutants (49 B12, 54 H3 and 76 H8).

Plasposon sequence data from mutant 76 D2 matched GSP J (*gspJ*::Tp) with no specific strain annotation, but identified as part of *B. cenocepacia*. GspJ is one of the four type 4 pilin-like proteins or pseudopilins (the others being G, H and I), which are also similar to subunits of the type IV pili. These four proteins are created as precursor pilin subunits, contain a prepilin peptidase cleavage and

are methylated by the prepilin peptidase O (PulO) or (GspO). It is hypothesized that these four proteins are localized to the periplasm. Some researchers suggest that these proteins may assemble into a pilus-like structure (similar to a secretion tube) across the periplasm that allows the transport of proteins across the OM (Stathopoulos, 2000; Sandkvist, 2001). Plasposon sequence data from mutant 72 C12 matched the T2SS prepilin signal peptidase O (*pulO::Tp*) on strain PC184. As it was previously mentioned, PulO is a type 4 prepilin-like signal peptidase that methylates pseudopilins (G, H, I and J). Finally, the plasposon sequence from mutant 76 B3 matched an hypothetical protein (hypothetical protein BCPG_02344::Tp) on strain PC184. Unfortunately, no additional information is provided on the NCBI database for this particular product. Combining all the available data, we hypothesized that phage DC1 does not use LPS as a receptor like phages KS4-M, KS9 and KS12. However, we do not discard the possibility that LPS might serve as a co-receptor, as previously observed for other phages (Rakhuba *et al.*, 2010).

Due the fact that the T2SS and type IV pili share many features and components (Stathopoulos, 2000; Sandkvist, 2001), we hypothesized that phage DC1 is using type IV pili or a pili-like structure as a receptor in order to infect its host (Chibeu *et al.*, 2009). However, there remains the possibility that elements of the T2SS apparatus and not a pili structure serve as a receptor for phage DC1. To further confirm our hypothesis, a series of experiments were performed using these mutants, as described below.

Mutant Plate & Well #	Match output	Amino acids	E Value	GenBank #	Gene Symbol	Locus Tag
49 B12 5'	Type II secretion system protein M (<i>B. cenocepacia</i> J2315)	168	0.090	YP_002232619.1	<i>gspM</i>	BCAL3516
49 B12 3'	LuxE cloning vector	--	--	--	--	--
54 H3 5'	Type II secretion system protein M (<i>B. cenocepacia</i> J2315)	168	0.079	YP_002232619.1	<i>gspM</i>	BCAL3516
54 H3 3'	LuxE cloning vector	--	--	--	--	--
72 C12 5'	Type II secretory pathway, prepilin signal peptidase PulO (<i>B. cenocepacia</i> PC184)	303	9e-116	ZP_04939727.1	No Match	No Match
72 C12 3'	LuxE cloning vector	--	--	--	--	--
76 B3 5'	Hypothetical protein BCPG_02344 (<i>B. cenocepacia</i> PC184)	157	4e-108	ZP_04940865.1	No match	No match
76 B3 3'	LuxE cloning vector	--	--	--	--	--
76 D2 5'	General secretion protein J GspJ (<i>B. cenocepacia</i>)	92	9e-32	AAF36475.1	No Match	No Match
76 D2 3'	LuxE cloning vector	--	--	--	--	--
76 H8 5'	Type II secretion system protein M? (<i>B. cenocepacia</i> J2315)	168	0--	YP_002232619.1	<i>gspM?</i>	BCAL3516
76 H8 3'	LuxE cloning vector	--	--	--	--	--

Table 8: Six *B. cenocepacia* PC184::pTnModlux-OTp' DC1 resistant mutants.

Finally, in the case of the two *B. cenocepacia* PC184::pTnModlux-OTp' KS10 and SR1 resistant mutants, sequences revealed the disruption of the following genes: Mutant 30 D1 plasposon sequence matched a general Glycosyltransferase family 2 product (*Bcenmc03_2331*::Tp) on *B. cenocepacia* strain MC0-3. Further investigation revealed a conserved motif on the gene product that matched the UDP-glucose LOS-beta-1,4 glucosyltransferase. This motif extends from AA 5 to 230. This glycosyltransferase catalyzes the addition of the first glucose residue of the lacto-N-neotetrase structure to Heptose I (Hep I) of the lipooligosaccharide (LOS) inner core. LOS is the major constituent of the outer leaflet of the OM of gram-negative bacteria, and thus an essential component of bacterial LPS. In strain PC184, this exact gene can be found as *BCPG_02409*, but no genomic context is available for the genomic data for strain PC184, therefore we used the putative data available from strain MC0-3.

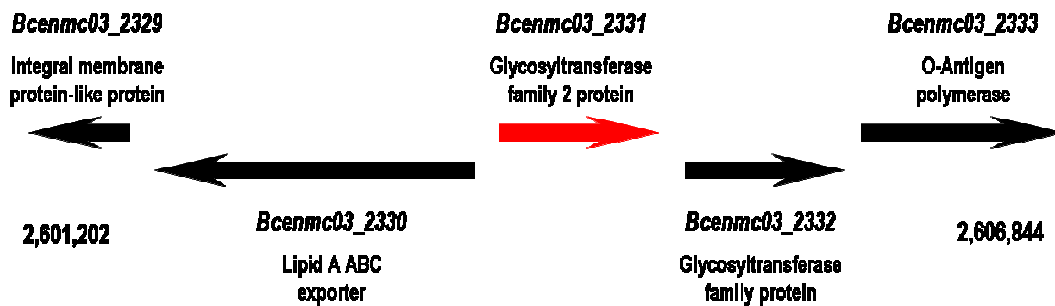


Figure 48: NCBI genomic context and organization of the *B. cenocepacia* MC0-3 region containing the disrupted gene (red) from the KS10, SR1 resistant mutant (30 D1).

The plasposon sequence data from mutant 30 F7 revealed that two divergent genes were disrupted. One of them was the hypothetical protein *Bcen_0575* (*Bcen_0575*::Tp) in *B. cenocepacia* strain AU1054. According to the

conserved motif located from AA 25 to 77, we determined that this gene possibly encodes the ComEA protein involved in DNA uptake and related to other DNA-binding proteins. Its possible function involves a role in DNA replication, recombination, and repair. A second motif, the helix-hairpin-helix motif or HhH domain (a short DNA-binding domain) was also located in the protein encoded by this gene. In strain PC184, this gene is annotated as *BCPG_00710*. If *Bcen_0575* does not encode some sort of regulator for the adjacent operon, we suspect that the disrupted gene causing phage resistance is the adjacent gene (*Bcen_0574::Tp*), because it encodes an ADP-L-glycero-D-manno-heptose-6-epimerase. A motif located from AA 3 to 326 matches this family of enzymes, which are involved in the biosynthesis of the LPS inner core OS in Gram-negative bacteria. According to NCBI, this enzyme is homologous to UDP-glucose 4-epimerase. In strain PC184, this gene is annotated as *BCPG_00711*, but no genomic context is provided for strain PC184 [Fig. 46]. Because many phages bind to LPS (Rakhuba et al., 2010), we hypothesize that the defect in *Bcen_0574* is altering the LPS core OS, which thereby affects phage binding. Previous data suggests that phages KS10 and SR1 may bind to the inner or outer core OS of their host.

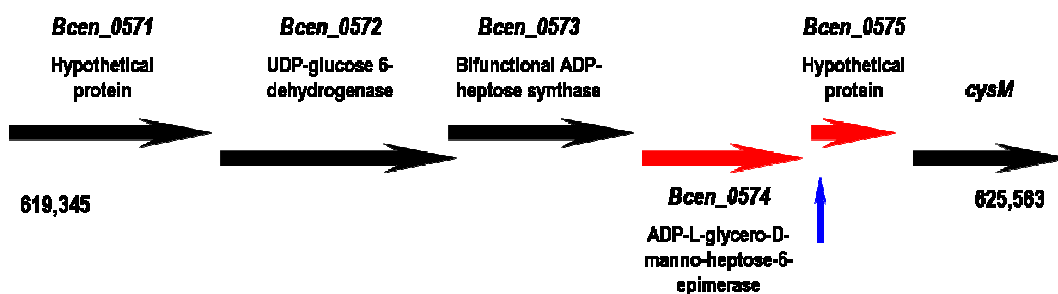


Figure 49: NCBI genomic context and organization of the *B. cenocepacia* AU 1054 region containing the disrupted genes (red) from the KS10, SR1 resistant mutant (30 F7).

Mutant Plate & Well #	Match output	Amino acids	E Value	GenBank #	Gene Symbol	Locus Tag
30 D1 5'	Glycosyltransferase family 2 (<i>B. cenocepacia</i> MC0-3) UDP-glucose LOS-beta-1,4 glucosyltransferase	250	9e-52	YP_001765614.1	<i>Bcenmc03_2331</i>	Bcenmc03_2331
30 D1 3'	LuxE cloning vector	--	--	--	--	--
30 F7 5'	Hypothetical protein Bcen_0575 (<i>B. cenocepacia</i> AU 1054)	115	7e-35	YP_620459.1	<i>Bcen_0575</i>	Bcen_0575
	ADP-L-glycero-D-manno-heptose-6-epimerase (<i>B. cenocepacia</i> AU 1054)	330		YP_620458.1	<i>Bcen_0574</i>	Bcen_0574
30 F7 3'	LuxE cloning vector	--	--	--	--	--

Table 9: Two *B. cenocepacia* PC184::pTnModlux-OTp' KS10 and SR1 resistant mutants.

Genes *wbxD* & *wbcE* and their function.

According to seven of the ten K56-2::pTnModOTp' KS4-M, KS9 and KS12 resistant mutant sequences, genes involved in LPS production were disrupted by the plasposon insertions. This led us to further investigate this possibility and to also elucidate the possible function of the disrupted genes *wbxD-wbcE*::Tp. Previous publications by Ortega et al. (2005, 2009) described a genomic region in strains K56-2 and J2315 containing genes involved in LPS production (inner and outer core OS and O-antigen biosynthesis) [Fig. 50]. According to their research, the function of *wbcE* (also termed *wbxE*) was determined to be a glycosyltransferase required for polymeric O-antigen assembly. This was determined after comparing the same region between strains K56-2, J2315, and other clonal isolates. In the case of strain J2315, an insertion sequence IS402 interrupting gene *wbcE* disrupted the visualization of O-antigen on Tris-Tricine LPS gels. Interestingly, of all the strains tested by Ortega, only K56-2 lacked the IS402 inserted within gene *wbcE*, thus the characteristic ladder-like O-antigen banding pattern LPS was present on K56-2 but not on strain J2315 (and others tested). The function of *wbcE* was further confirmed by cloning genes *wbxD-wbcE* (red box) in plasmid pXO3, where gene *wbxD* was included to avoid the possibility of a polar effect, and either *wbxD* was cloned in plasmid pXO7 (which revealed no restoration of O-antigen), or *wbcE* cloned in plasmid pXO4 (restoration of O-antigen). Results further confirmed the function of *wbcE* as a glycosyltransferase involved in O-antigen assembly. Additionally, it was determined that IS402 did not cause a polar mutation of *wbxD* and therefore its

expression was not affected. However, Ortega et al., (2005) did not identify the function of *wbxD*. Because several phages are known to recognize and attach to the O-antigen (e.g. phages P22, pb1, HK620) (Erikson & Lindberg, 1977; Heller, 1992; Rakhuba et al., 2010), we hypothesized that our phages (KS4-M, KS9 and KS12) require the presence of the LPS O-antigen in order to adsorb to the host cell.

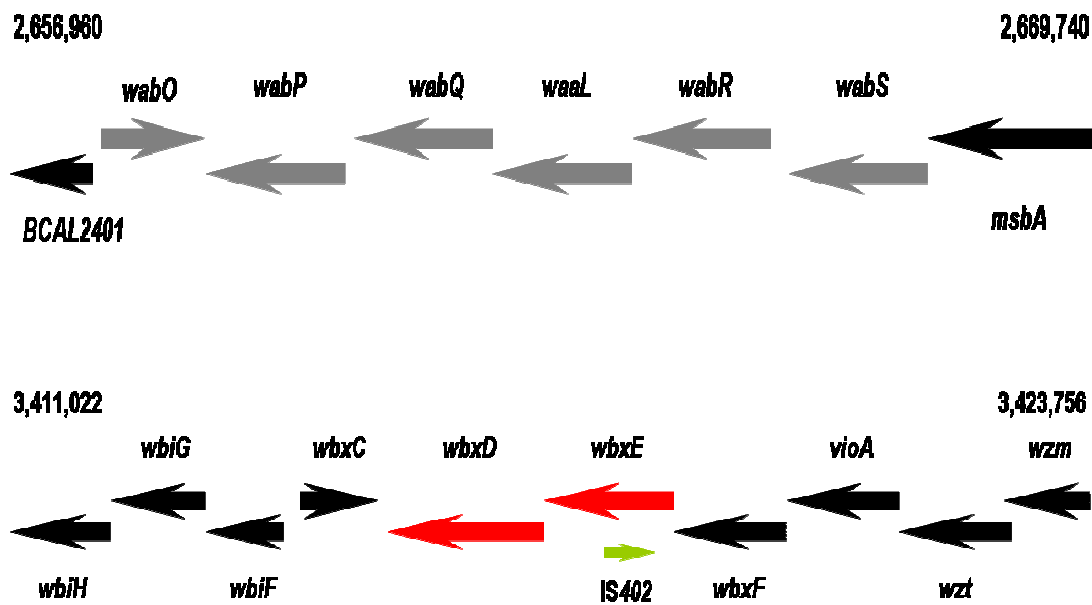


Figure 50: Genetic organization of the *B. cenocepacia* K56-2 region containing genes for core oligosaccharide (OS) and O antigen biosynthesis (Adapted from Ortega et al., 2009). The *IS402* is found on strain J2315 but not in K56-2. Genes disrupted in KS4-M resistant mutant in red.

Bacteriophage infection assays vs. LPS truncated mutants [Liquid culture clearing assays]

Taking together the results from the resistant mutants isolated by plasposon mutant library screening and the results from Ortega et al., (2005, 2009), we decided to perform a series of liquid clearing assays against a collection

of six K56-2 mutants in which the LPS is truncated at different levels; some mutants lack the O-antigen, while others lack the outer and inner core OS [Fig. 51]. These mutants were kindly provided by Dr. Miguel Valvano (Ortega et al., 2009; Loutet et al., 2006). A brief description of each one of these mutants is included in the following lines.

Mutant **XOA7** (*waaL*::pGPΩTp Tp^R) produces a complete Lipid A and core OS similar to the parental strain K56-2, however XOA7 does not produce O-antigen subunits. It was determined that *waaL* encodes a O-antigen ligase.

Mutant **XOA8** (*wabO*::pGPΩTp Tp^R) produces a complete Lipid A and a truncated outer core OS, no O-antigen subunits are produced by this strain. It was determined that *wabO* encodes a glucosyltransferase mediating the addition of β-D-glc to the HeptI (heptose I).

Mutant **RSF19** (*wbxE*::pRF201 Tp^R) produces a complete Lipid A and core (inner and outer) OS and a partial O-antigen subunit linked to the Lipid A-Core OS. *wbxE* encodes a glycosyltransferase necessary for O-antigen subunits assembly.

Mutant **CCB1** (*waaC*::pGPΩTp Tp^R) produces a complete Lipid A and inner core OS, no outer core OS or O-antigen subunits are produced by this strain. *waaC* encodes the Heptosyltransferase I enzyme.

Mutant **XOA15** (*wabR*::pGPΩTp Tp^R) produces a complete Lipid A and inner core OS, a partial outer core OS and no O-antigen subunits are produced by this strain. *wabR* function couldn't be determined however it seems to be involved in core OS production.

Finally, mutant **XOA17** (*wabS*::pGPAPp Tp^R) produces a complete Lipid A and inner core OS, a partial outer core OS and no O-antigen subunits are produced by this strain. *wabS* is involved in core OS production.

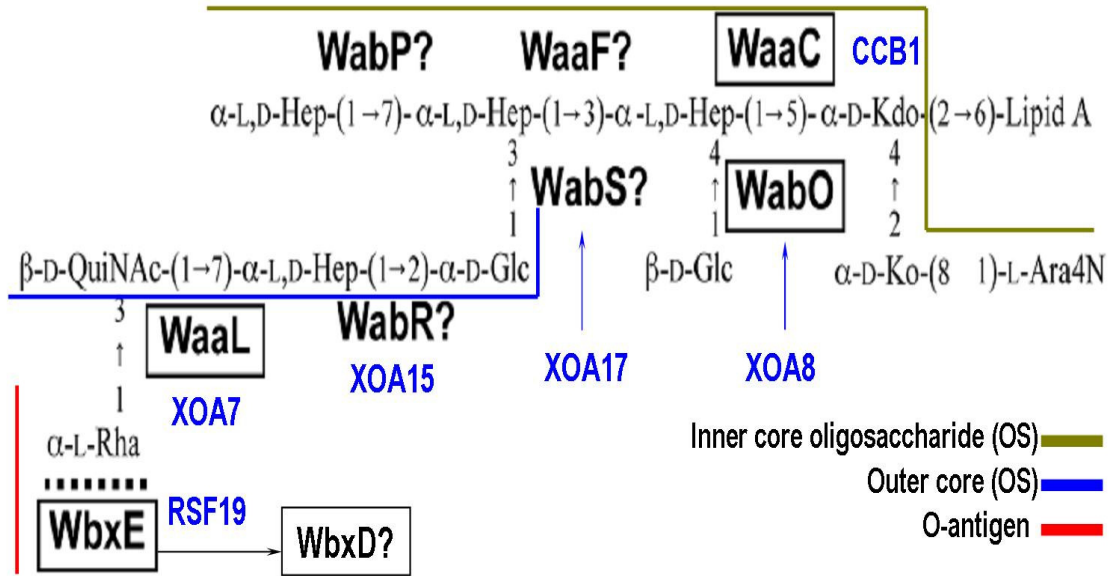


Figure 51: Structural assignments of the core OS and O-antigen subunit from *B. cenocepacia* K56-2 LPS truncated mutants. Each mutant name (blue) and the disrupted product (box) are indicated in the diagram. ? symbols indicate proposed functional assignments (Adapted from Ortega et al., 2009).

We attempted to compare and confirm whether (i) LPS was being used as a receptor by phages KS4-M, KS5, KS9 and KS12 and (ii) there was similarity between the phage resistant mutants isolated through mutant library screening and those constructed using inn vitro techniques. A similar approach to that performed for mutant library screening was used and similar controls were included. Results revealed that phages KS4-M and KS12 behaved in a similar manner, with some slight variations. It was demonstrated that phage KS12 [Figs.

52-57] was able to lyse the LPS mutants RSF19 (*wbxE*::pRF201 Tp^R), CCB1 (*waaC*::pGPΩTp Tp^R), XOA15 (*wabR*::pGPΩTp Tp^R) and XOA17 (*wabS*::pGPApTp Tp^R) after 6 hrs. of exposure, whereas mutants XOA7 (*waaL*::pGPΩTp Tp^R) and XOA8 (*wabO*::pGPΩTp Tp^R) showed resistance to KS12 throughout the entire exposure. Phage KS4-M showed similar results to those for KS12 when exposed to mutants XOA8, RSF19, CCB1, XOA15 and XOA17, the only difference being that mutant XOA7 (*waaL*::pGPΩTp Tp^R) was sensitive to phage KS4-M infection but resistant to KS12 infection [Fig. 58, compare with Fig. 52]. These were unexpected results. Our prior data suggested that LPS O-antigen serves as a receptor for phages KS4-M and KS12, thus in theory, all of the LPS mutants should be resistant to these two phages since O-antigen is impaired in all of the LPS mutants (Ortega *et al.*, 2009, Loutet *et al.*, 2006).

As previously mentioned, there is a difference in infection efficiency between liquid and solid media, and we observed that in some cases, phages are more effective at clearing bacterial liquid cultures. There may also be differences between the resistant mutants isolated from the library screening and the constructed LPS mutants, however we are unaware of how these differences may affect the assays. Given these results, it appears KS12 adheres to the O-antigen, whereas KS4-M adheres to the O-antigen, but also to the distal tip of the outer core oligosaccharide.

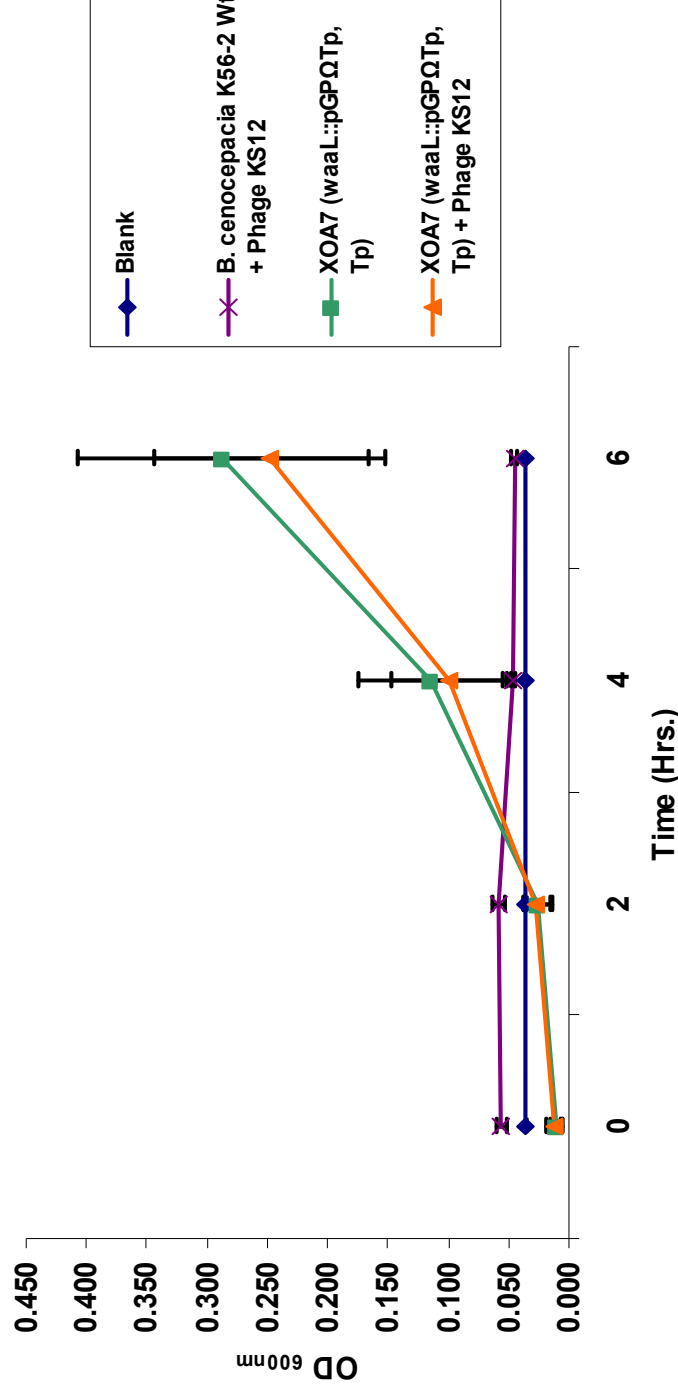


Figure 52: Growth curve of *B. cenocepacia* K56-2 LPS mutant XOA7 (*waaL*::pGPΩTp Tp^R) exposed to phage KS12: Blue, blank control (200 μL of ½ LB broth), Purple, wt control (10 μL of K56-2 wt), (50 μL of high titer phage stock) and (150 μL of ½ LB broth) mixed, Green, positive control (10 μL of bacteria) and (190 μL of ½ LB broth + 100 μg of Tp/mL), Orange, test group (10 μL of bacteria), (50 μL of high titer phage stock) and (150 μL of ½ LB broth + 100 μg of Tp/mL) incubated at 37°C with continuous shaking (225 rpm). A₆₀₀ measured every 2 hrs. for a period of 6 hrs in a Victor X3 2030 multilabel reader spectrophotometer. Mutant XOA7 was previously grown on ½ LB + 100 μg of Tp/mL broth at 37°C with shaking (225 rpm) for ~16 hrs. Each point represents the mean of three independent experiments in triplicate; error bars indicate standard deviation. * Represents statistical significance between control (green) and test (orange) groups. A-Nova test (Tukey) (P < 0.05)

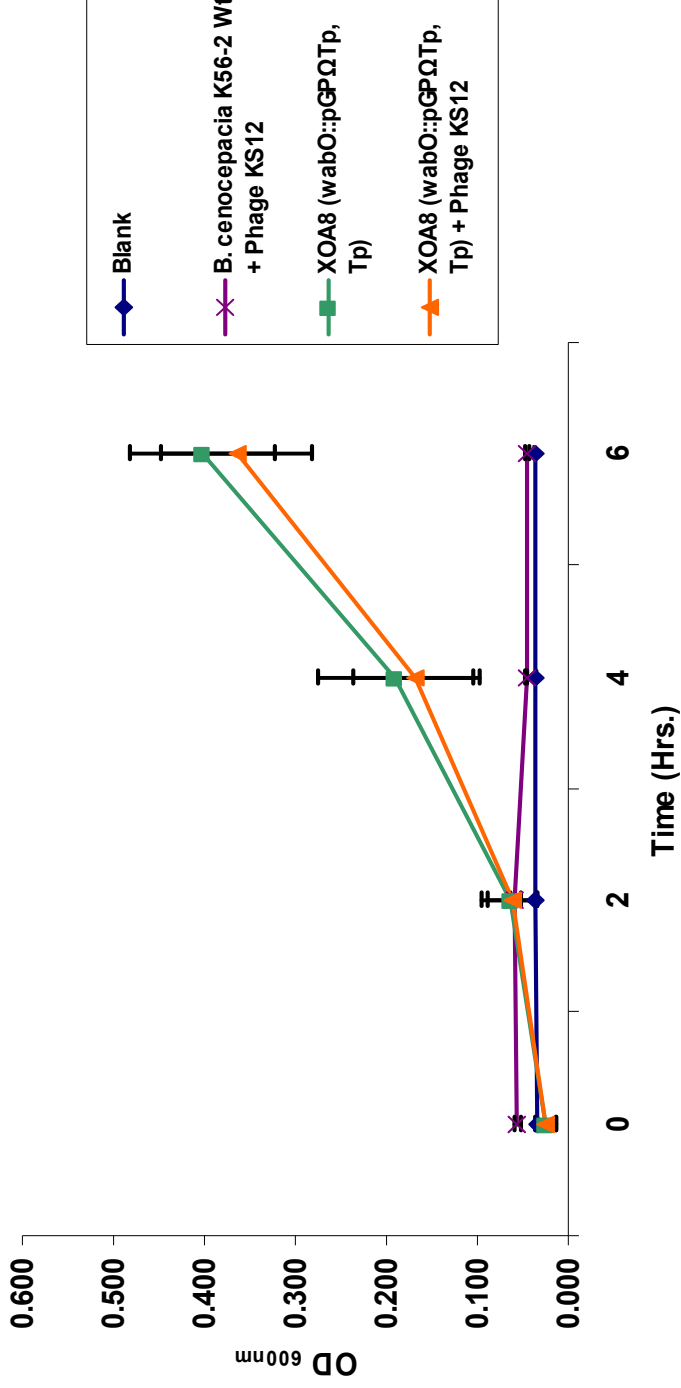


Figure 53: Growth curve of *B. cenocepacia* K56-2 LPS mutant XOA8 (*wabO::pGPOTp Tp^R*) exposed to phage KS12: Blue, blank control (200 μ L of $\frac{1}{2}$ LB broth), Purple, wt control (10 μ L of K56-2 wt), (50 μ L of high titer phage stock) and (150 μ L of $\frac{1}{2}$ LB broth) mixed, Green, positive control (10 μ L of bacteria) and (190 μ L of $\frac{1}{2}$ LB broth + 100 μ g of Tp/mL), Orange, test group (10 μ L of bacteria), (50 μ L of high titer phage stock) and (150 μ L of $\frac{1}{2}$ LB broth + 100 μ g of Tp/mL) incubated at 37°C with continuous shaking (225 rpm). A_{600} measured every 2 hrs. for a period of 6 hrs in a Victor X3 2030 multilabel reader spectrophotometer. Mutant XOA8 was previously grown on $\frac{1}{2}$ LB + 100 μ g of Tp/mL broth at 37°C with shaking (225 rpm) for ~16 hrs. Each point represents the mean of three independent experiments in triplicate; error bars indicate standard deviation. * Represents statistical significance between control (green) and test (orange) groups. A-Nova test (Tukey) ($P < 0.05$)

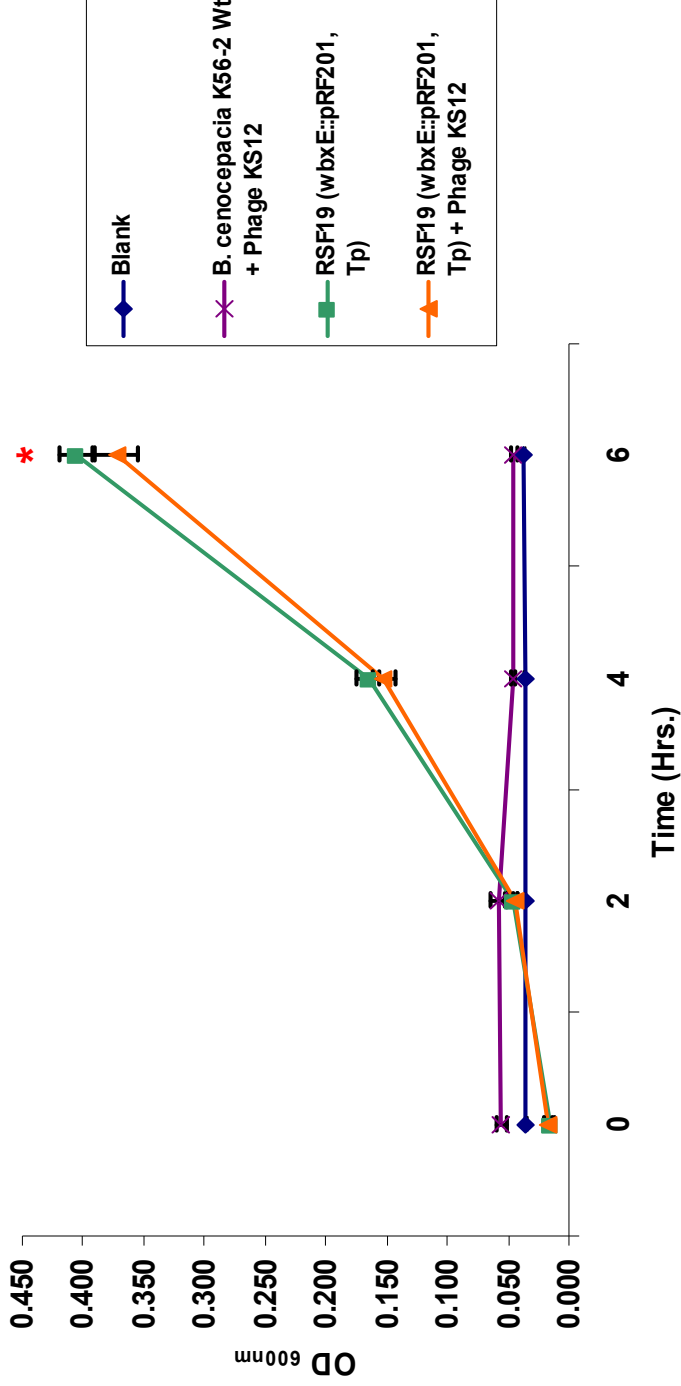


Figure 54: Growth curve of *B. cenocepacia* K56-2 LPS mutant RSF19 (*wbxE::pRF201 Tp^R*) exposed to phage KS12: Blue, blank control (200 μ L of $\frac{1}{2}$ LB broth), Purple, wt control (10 μ L of K56-2 wt), (50 μ L of high titer phage stock) and (150 μ L of $\frac{1}{2}$ LB broth) mixed, Green, positive control (10 μ L of bacteria) and (190 μ L of $\frac{1}{2}$ LB broth + 100 μ g of Tp/mL), Orange, test group (10 μ L of bacteria), (50 μ L of high titer phage stock) and (150 μ L of $\frac{1}{2}$ LB broth + 100 μ g of Tp/mL) incubated at 37°C with continuous shaking (225 rpm). A_{600} measured every 2 hrs. for a period of 6 hrs in a Victor X3 2030 multilabel reader spectrophotometer. Mutant RSF19 was previously grown on $\frac{1}{2}$ LB + 100 μ g of Tp/mL broth at 37°C with shaking (225 rpm) for ~16 hrs. Each point represents the mean of three independent experiments in triplicate; error bars indicate standard deviation. * Represents statistical significance between control (green) and test (orange) groups. A-Nova test (Tukey) ($P < 0.05$)

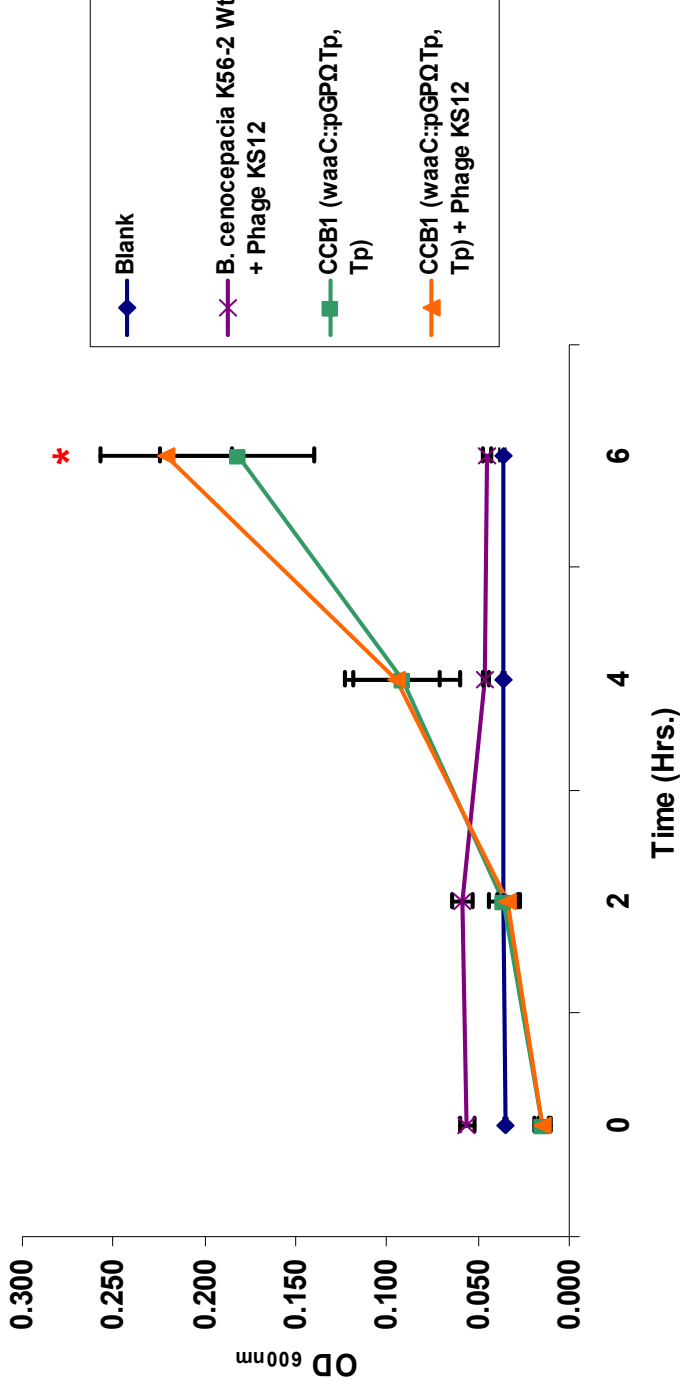


Figure 55: Growth curve of *B. cenocepacia* K56-2 LPS mutant CCB1 (*waaC::pGPQ Tp^R*) exposed to phage KS12: Blue, blank control (200 μ L of $\frac{1}{2}$ LB broth), Purple, wt control (10 μ L of K56-2 wt), (50 μ L of high titer phage stock) and (150 μ L of $\frac{1}{2}$ LB broth) mixed, Green, positive control (10 μ L of bacteria) and (190 μ L of $\frac{1}{2}$ LB broth + 100 μ g of Tp/mL), Orange, test group (10 μ L of bacteria), (50 μ L of high titer phage stock) and (150 μ L of $\frac{1}{2}$ LB broth + 100 μ g of Tp/mL) incubated at 37°C with continuous shaking (225 rpm). A_{600} measured every 2 hrs. for a period of 6 hrs in a Victor X3 2030 multilabel reader spectrophotometer. Mutant CCB1 was previously grown on $\frac{1}{2}$ LB + 100 μ g of Tp/mL broth at 37°C with shaking (225 rpm) for ~16 hrs. Each point represents the mean of three independent experiments in triplicate; error bars indicate standard deviation. * Represents statistical significance between control (green) and test (orange) groups. A-Nova test (Tukey) ($P < 0.05$)

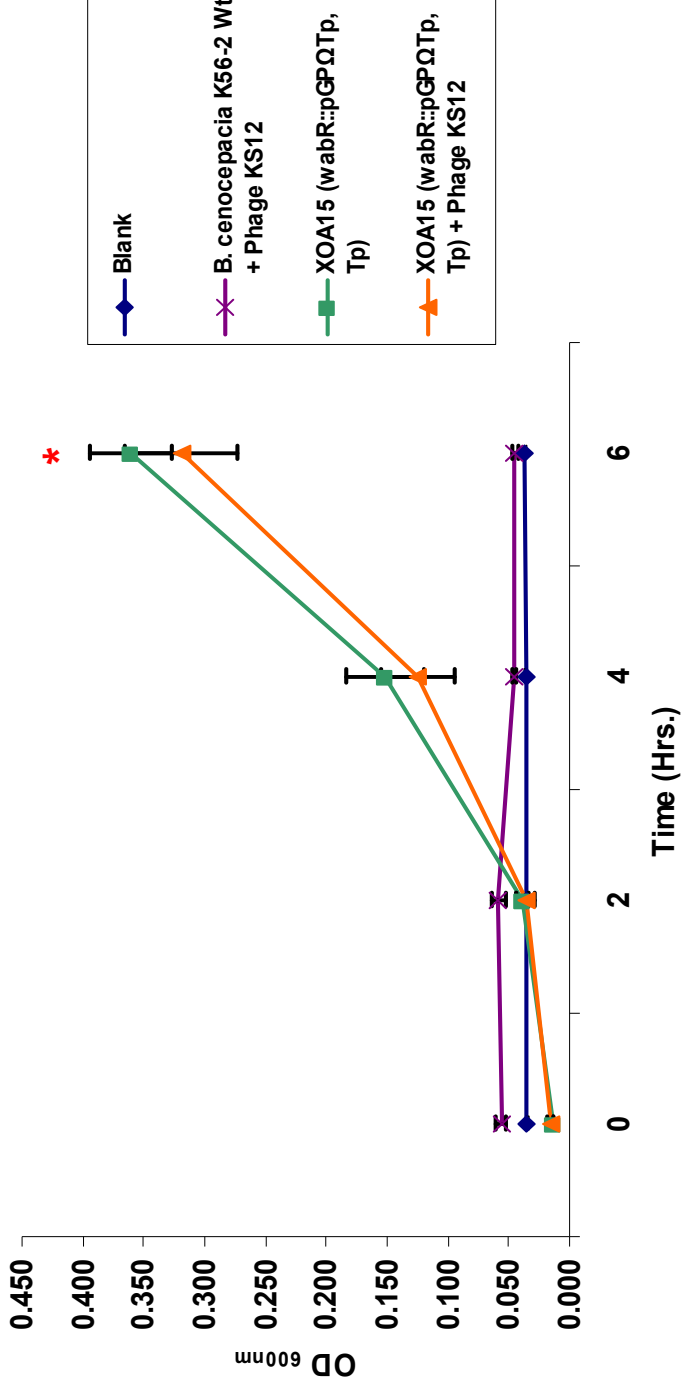


Figure 56: Growth curve of *B. cenocepacia* K56-2 LPS mutant XOA15 (*wabR::pGPΩTp Tp^R*) exposed to phage KS12: Blue, blank control (200 μ L of $\frac{1}{2}$ LB broth), Purple, wt control (10 μ L of K56-2 wt), (50 μ L of high titer phage stock) and (150 μ L of $\frac{1}{2}$ LB broth) mixed, Green, positive control (10 μ L of bacteria) and (190 μ L of $\frac{1}{2}$ LB broth + 100 μ g of Tp/mL), Orange, test group (10 μ L of bacteria), (50 μ L of high titer phage stock) and (150 μ L of $\frac{1}{2}$ LB broth + 100 μ g of Tp/mL) incubated at 37°C with continuous shaking (225 rpm). A_{600} measured every 2 hrs. for a period of 6 hrs in a Victor X3 2030 multilabel reader spectrophotometer. Mutant XOA15 was previously grown on $\frac{1}{2}$ LB + 100 μ g of Tp/mL broth at 37°C with shaking (225 rpm) for ~16 hrs. Each point represents the mean of three independent experiments in triplicate; error bars indicate standard deviation. * Represents statistical significance between control (green) and test (orange) groups. A-Nova test (Tukey) ($P < 0.05$)

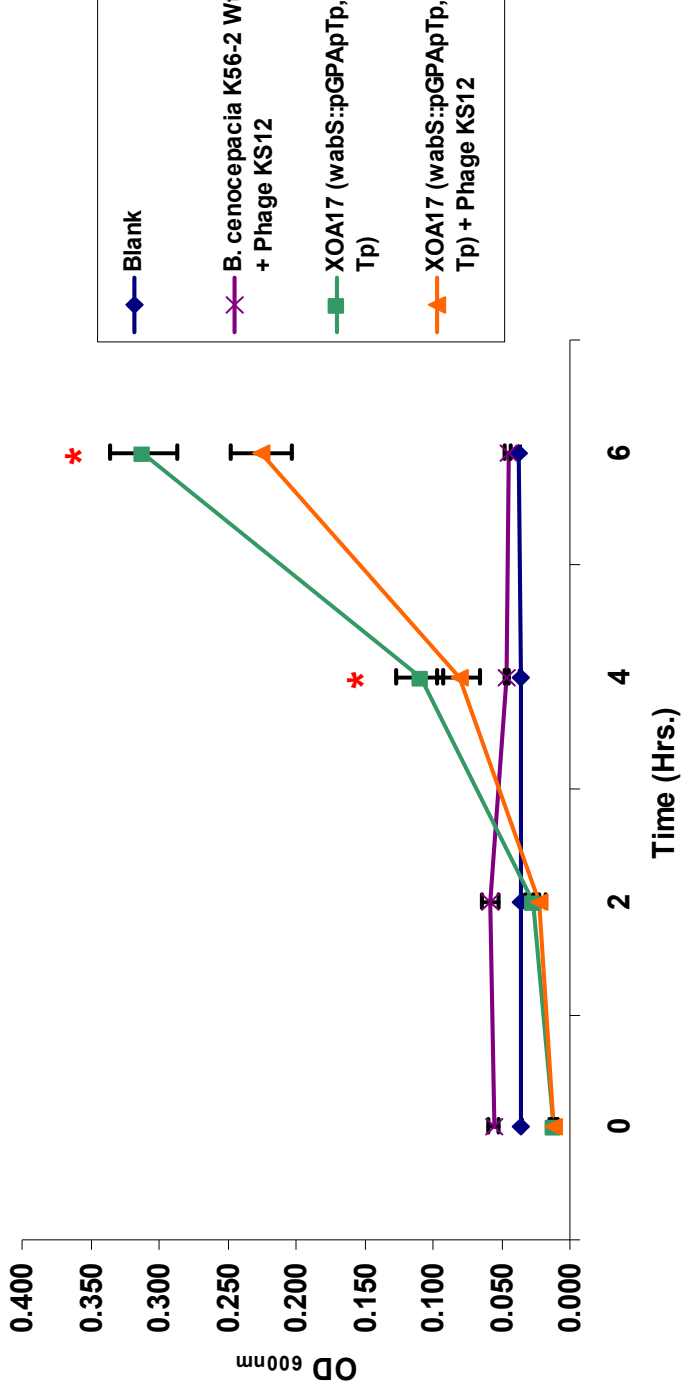


Figure 57: Growth curve of *B. cenocepacia* K56-2 LPS mutant XOA17 (*wabS::pGPAPtp Tp^R*) exposed to phage KS12: Blue, blank control (200 μ L of $\frac{1}{2}$ LB broth), Purple, wt control (10 μ L of K56-2 wt), (50 μ L of high titer phage stock) and (150 μ L of $\frac{1}{2}$ LB broth) mixed, Green, positive control (10 μ L of bacteria) and (190 μ L of $\frac{1}{2}$ LB broth + 100 μ g of Tp/mL), Orange, test group (10 μ L of bacteria), (50 μ L of high titer phage stock) and (150 μ L of $\frac{1}{2}$ LB broth + 100 μ g of Tp/mL) incubated at 37°C with continuous shaking (225 rpm). A_{600} measured every 2 hrs. for a period of 6 hrs in a Victor X3 2030 multilabel reader spectrophotometer. Mutant XOA17 was previously grown on $\frac{1}{2}$ LB + 100 μ g of Tp/mL broth at 37°C with shaking (225 rpm) for ~16 hrs. Each point represents the mean of three independent experiments in triplicate; error bars indicate standard deviation. * Represents statistical significance between control (green) and test (orange) groups. A-Nova test (Tukey) ($P < 0.05$)

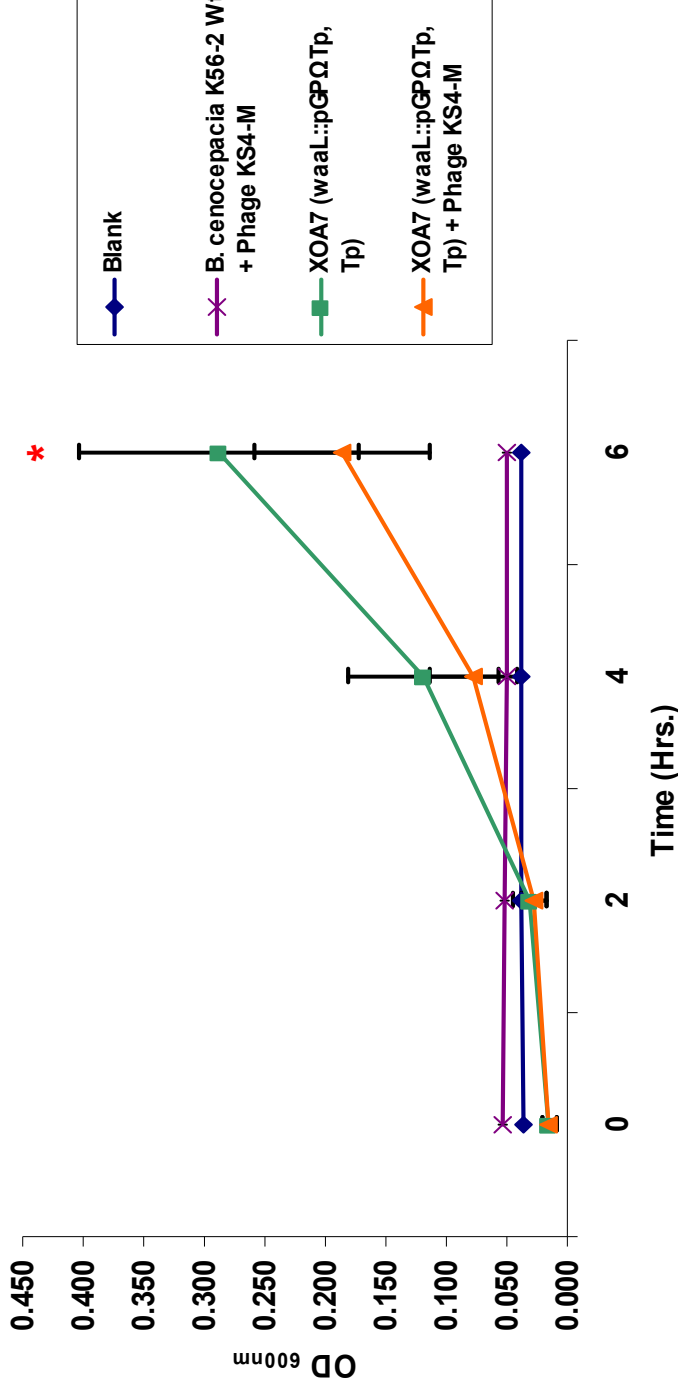


Figure 58: Growth curve of *B. cenocepacia* K56-2 LPS mutant XOA7 (*waaL::pGPΩTp Tp^R*) exposed to phage KS4-M: Blue, blank control (200 μ L of $\frac{1}{2}$ LB broth), Purple, wt control (10 μ L of K56-2 wt), (50 μ L of high titer phage stock) and (150 μ L of $\frac{1}{2}$ LB broth) mixed, Green, positive control (10 μ L of bacteria) and (190 μ L of $\frac{1}{2}$ LB broth + 100 μ g of Tp/mL), Orange, test group (10 μ L of bacteria), (50 μ L of high titer phage stock) and (150 μ L of $\frac{1}{2}$ LB broth + 100 μ g of Tp/mL) incubated at 37°C with continuous shaking (225 rpm). A_{600} measured every 2 hrs. for a period of 6 hrs in a Victor X3 2030 multilabel reader spectrophotometer. Mutant XOA7 was previously grown on $\frac{1}{2}$ LB + 100 μ g of Tp/mL broth at 37°C with shaking (225 rpm) for ~16 hrs. Each point represents the mean of three independent experiments in triplicate; error bars indicate standard deviation. * Represents statistical significance between control (green) and test (orange) groups. A-Nova test (Tukey) ($P < 0.05$)

In similar experiments, results revealed that phages KS5 [Figs. 59-64] and KS9 [data not shown] behaved similarly. Both phages were able to lyse LPS mutants XOA7 (*waaL*::pGPΩTp Tp^R), RSF19 (*wbxE*::pRF201 Tp^R), XOA15 (*wabR*::pGPΩTp Tp^R) and XOA17 (*wabS*::pGPAPpTp Tp^R). This suggests that LPS O-antigen and other structures away from the lipid A are not essential for these phages when infecting their host. On the other hand, both phages were unable to clear mutants XOA8 (*wabO*::pGPΩTp Tp^R) and CCB1 (*waaC*::pGPΩTp Tp^R), which further supports the adherence results reported by Lynch et al., 2010. The remaining four mutants showed sensitivity to phage KS9. Taken together, the data suggests that phages KS5 and KS9 bind deeper in the LPS structure (as compared to phages KS4-M and KS12), since mutants XOA8 and CCB1 were resistant to these phages and these LPS mutants lack the majority of the LPS (Ortega et al., 2009). To summarize, data suggest that phages KS4-M and KS12 require a complete LPS structure including O-antigen, in order to infect their host, whereas phages KS5 and KS9 bind deeper in the LPS at the inner or outer core OS.

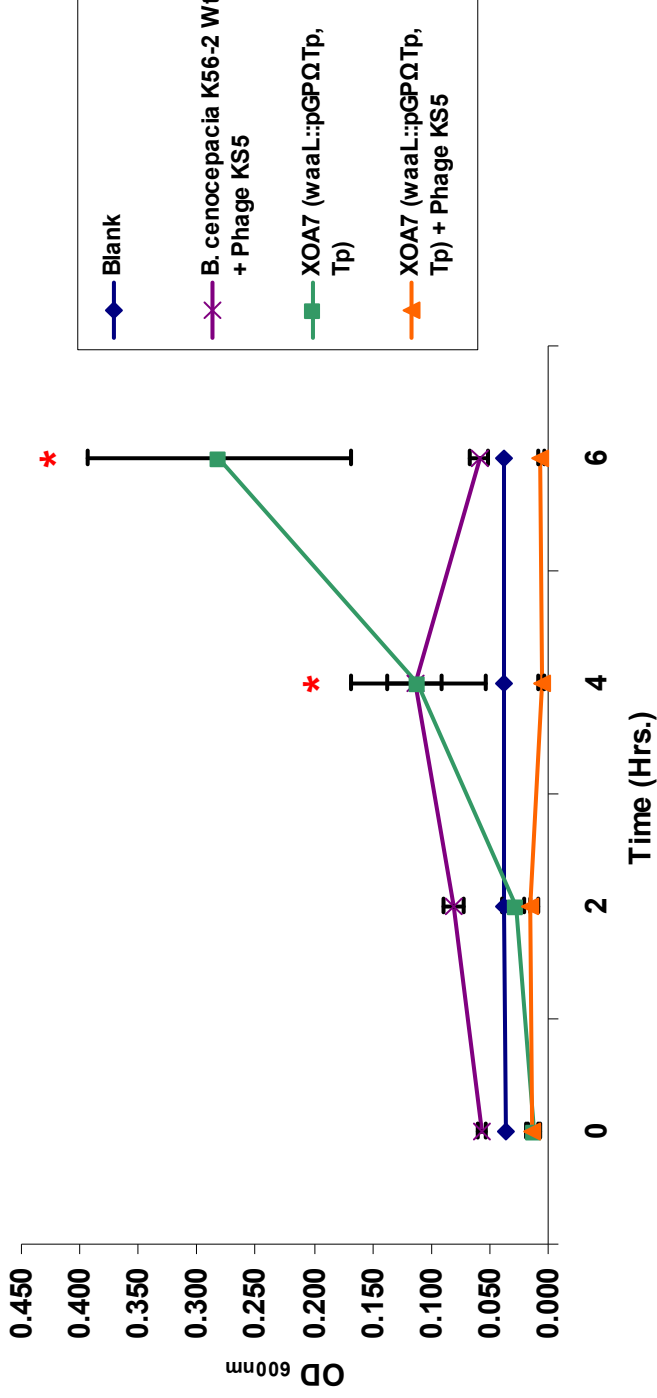


Figure 59: Growth curve of *B. cenocepacia* K56-2 LPS mutant XOA7 (*waaL::pGPΩTp Tp^R*) exposed to phage KS5: Blue, blank control (200 μ L of $\frac{1}{2}$ LB broth), Purple, wt control (10 μ L of K56-2 wt), (50 μ L of high titer phage stock) and (150 μ L of $\frac{1}{2}$ LB broth) mixed, Green, positive control (10 μ L of bacteria) and (190 μ L of $\frac{1}{2}$ LB broth + 100 μ g of Tp/mL), Orange, test group (10 μ L of bacteria), (50 μ L of high titer phage stock) and (150 μ L of $\frac{1}{2}$ LB broth + 100 μ g of Tp/mL) incubated at 37°C with continuous shaking (225 rpm). A_{600} measured every 2 hrs. for a period of 6 hrs in a Victor X3 2030 multilabel reader spectrophotometer. Mutant XOA7 was previously grown on $\frac{1}{2}$ LB + 100 μ g of Tp/mL broth at 37°C with shaking (225 rpm) for ~16 hrs. Each point represents the mean of three independent experiments in triplicate; error bars indicate standard deviation. * Represents statistical significance between control (green) and test (orange) groups. A-Nova test (Tukey) ($P < 0.05$)

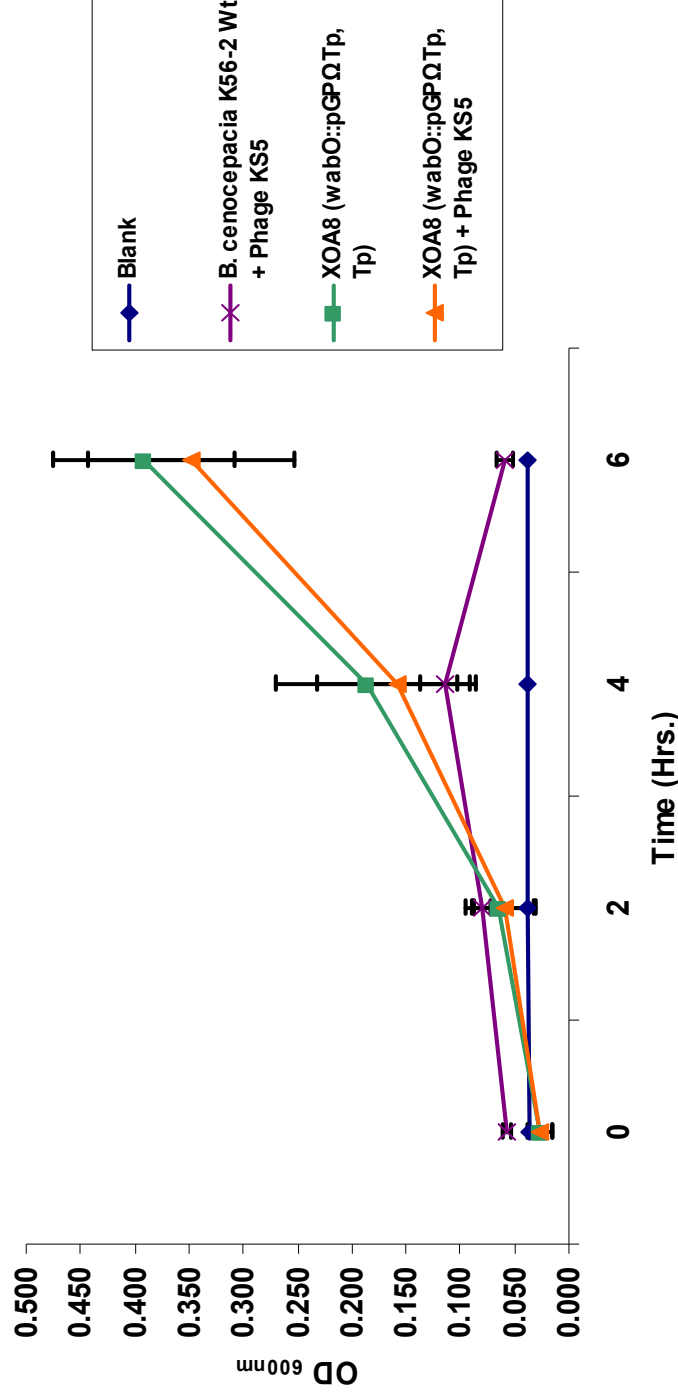


Figure 60: Growth curve of *B. cenocepacia* K56-2 LPS mutant XOA8 (*wabO::pGPO Tp^R*) exposed to phage KS5: Blue, blank control (200 μ L of $\frac{1}{2}$ LB broth), Purple, wt control (10 μ L of K56-2 wt), (50 μ L of high titer phage stock) and (150 μ L of $\frac{1}{2}$ LB broth) mixed, Green, positive control (10 μ L of bacteria) and (190 μ L of $\frac{1}{2}$ LB broth + 100 μ g of Tp/mL), Orange, test group (10 μ L of bacteria), (50 μ L of high titer phage stock) and (150 μ L of $\frac{1}{2}$ LB broth + 100 μ g of Tp/mL) incubated at 37°C with continuous shaking (225 rpm). A_{600} measured every 2 hrs. for a period of 6 hrs in a Victor X3 2030 multilabel reader spectrophotometer. Mutant XOA8 was previously grown on $\frac{1}{2}$ LB + 100 μ g of Tp/mL broth at 37°C with shaking (225 rpm) for ~16 hrs. Each point represents the mean of three independent experiments in triplicate; error bars indicate standard deviation. * Represents statistical significance between control (green) and test (orange) groups. A-Nova test (Tukey) ($P < 0.05$)

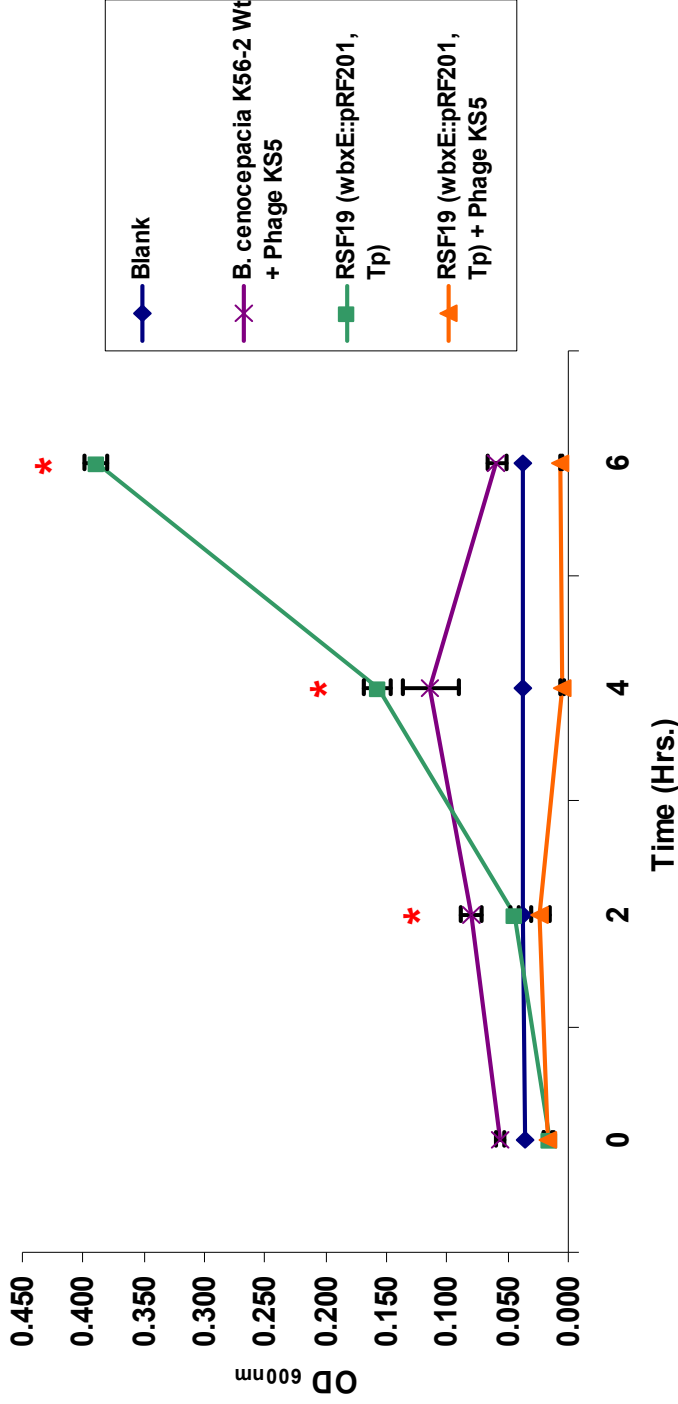


Figure 61: Growth curve of *B. cenocepacia* K56-2 LPS mutant RSF19 (*wbxE::pRF201 Tp^R*) exposed to phage KS5: Blue, blank control (200 μ L of $\frac{1}{2}$ LB broth), Purple, wt control (10 μ L of K56-2 wt), (50 μ L of high titer phage stock) and (150 μ L of $\frac{1}{2}$ LB broth) mixed, Green, positive control (10 μ L of bacteria) and (190 μ L of $\frac{1}{2}$ LB broth + 100 μ g of Tp/mL), Orange, test group (10 μ L of bacteria), (50 μ L of high titer phage stock) and (150 μ L of $\frac{1}{2}$ LB broth + 100 μ g of Tp/mL) incubated at 37°C with continuous shaking (225 rpm). A_{600} measured every 2 hrs. for a period of 6 hrs in a Victor X3 2030 multilabel reader spectrophotometer. Mutant RSF19 was previously grown on $\frac{1}{2}$ LB + 100 μ g of Tp/mL broth at 37°C with shaking (225 rpm) for ~16 hrs. Each point represents the mean of three independent experiments in triplicate; error bars indicate standard deviation. * Represents statistical significance between control (green) and test (orange) groups. A-Nova test (Tukey) ($P < 0.05$)

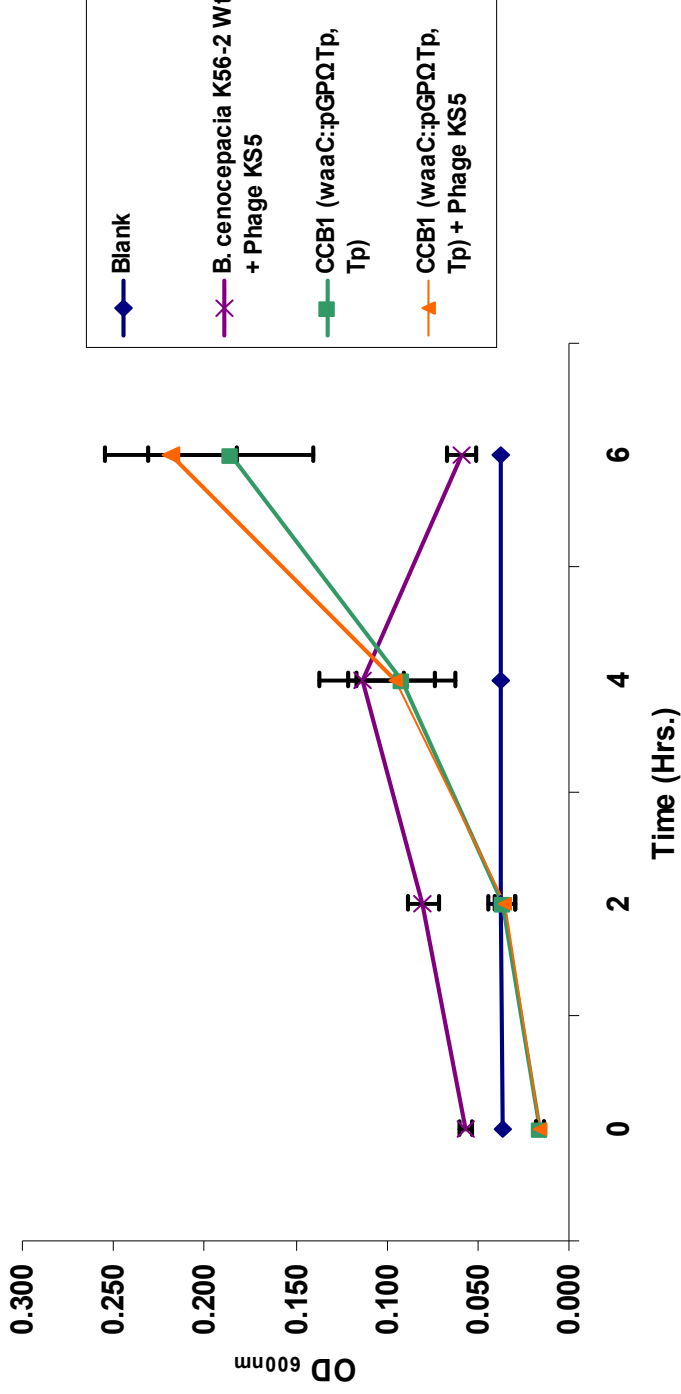


Figure 62: Growth curve of *B. cenocepacia* K56-2 LPS mutant CCB1 (*waaC::pGPΩTp Tp^R*) exposed to phage KS5: Blue, blank control (200 μ L of $\frac{1}{2}$ LB broth), Purple, wt control (10 μ L of K56-2 wt), (50 μ L of high titer phage stock) and (150 μ L of $\frac{1}{2}$ LB broth) mixed, Green, positive control (10 μ L of bacteria) and (190 μ L of $\frac{1}{2}$ LB broth + 100 μ g of Tp/mL), Orange, test group (10 μ L of bacteria), (50 μ L of high titer phage stock) and (150 μ L of $\frac{1}{2}$ LB broth + 100 μ g of Tp/mL) incubated at 37°C with continuous shaking (225 rpm). A_{600} measured every 2 hrs. for a period of 6 hrs in a Victor X3 2030 multilabel reader spectrophotometer. Mutant CCB1 was previously grown on $\frac{1}{2}$ LB + 100 μ g of Tp/mL broth at 37°C with shaking (225 rpm) for ~16 hrs. Each point represents the mean of three independent experiments in triplicate; error bars indicate standard deviation. * Represents statistical significance between control (green) and test (orange) groups. A-Nova test (Tukey) ($P < 0.05$)

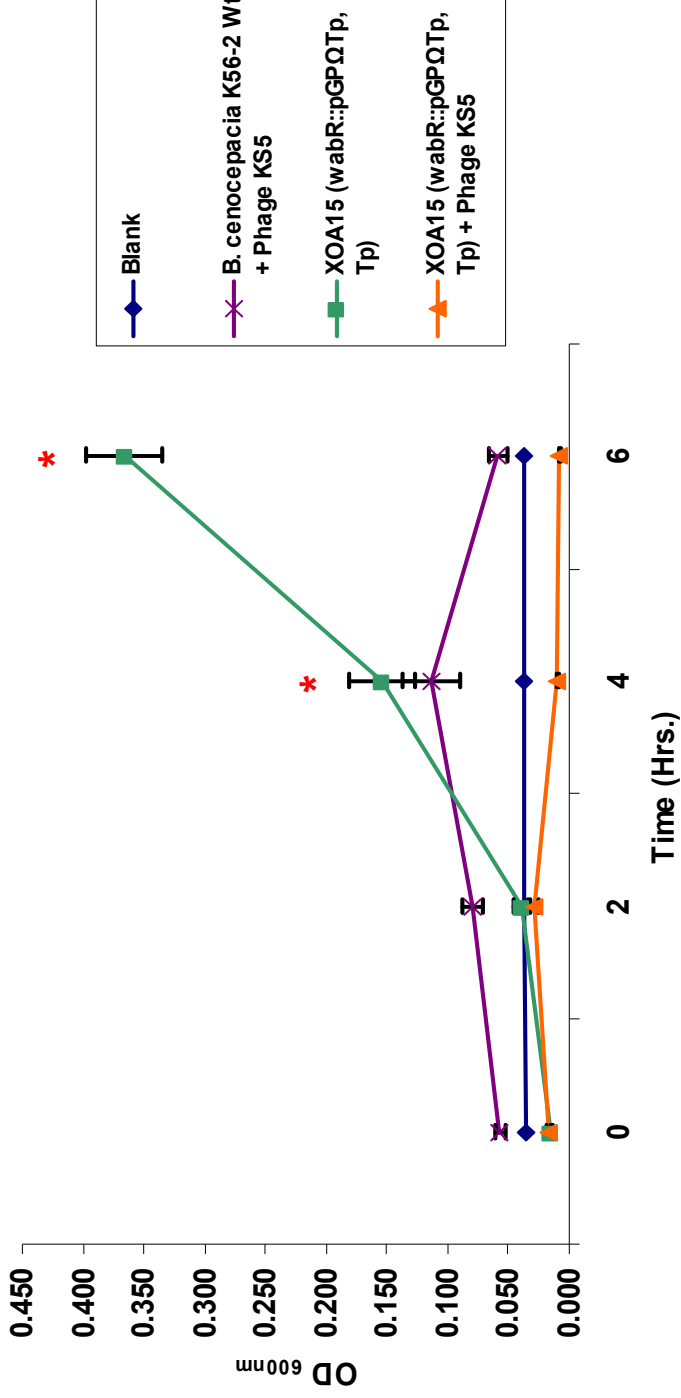


Figure 63: Growth curve of *B. cenocepacia* K56-2 LPS mutant XOA15 (*wabR::pGPΩTp Tp^R*) exposed to phage KS5: Blue, blank control (200 μ L of $\frac{1}{2}$ LB broth), Purple, wt control (10 μ L of K56-2 wt), (50 μ L of high titer phage stock) and (150 μ L of $\frac{1}{2}$ LB broth) mixed, Green, positive control (10 μ L of bacteria) and (190 μ L of $\frac{1}{2}$ LB broth + 100 μ g of Tp/mL), Orange, test group (10 μ L of bacteria), (50 μ L of high titer phage stock) and (150 μ L of $\frac{1}{2}$ LB broth + 100 μ g of Tp/mL) incubated at 37°C with continuous shaking (225 rpm). A_{600} measured every 2 hrs. for a period of 6 hrs in a Victor X3 2030 multilabel reader spectrophotometer. Mutant XOA15 was previously grown on $\frac{1}{2}$ LB + 100 μ g of Tp/mL broth at 37°C with shaking (225 rpm) for ~16 hrs. Each point represents the mean of three independent experiments in triplicate; error bars indicate standard deviation. * Represents statistical significance between control (green) and test (orange) groups. A-Nova test (Tukey) ($P < 0.05$)

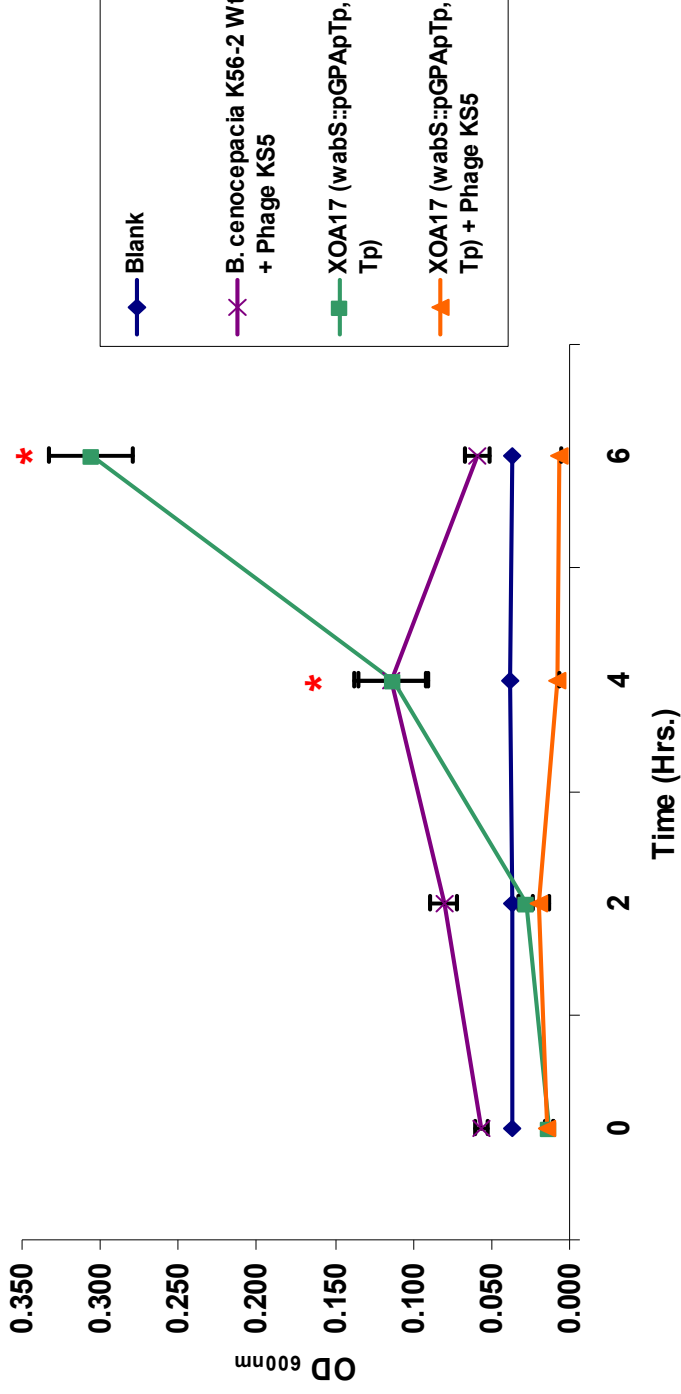


Figure 64: Growth curve of *B. cenocepacia* K56-2 LPS mutant XOA17 (*wabS::pGPApTp Tp^R*) exposed to phage KS5: Blue, blank control (200 μ L of $\frac{1}{2}$ LB broth), Purple, wt control (10 μ L of K56-2 wt), (50 μ L of high titer phage stock) and (150 μ L of $\frac{1}{2}$ LB broth) mixed, Green, positive control (10 μ L of bacteria) and (190 μ L of $\frac{1}{2}$ LB broth + 100 μ g of Tp/mL), Orange, test group (10 μ L of bacteria), (50 μ L of high titer phage stock) and (150 μ L of $\frac{1}{2}$ LB broth + 100 μ g of Tp/mL) incubated at 37°C with continuous shaking (225 rpm). A_{600} measured every 2 hrs. for a period of 6 hrs in a Victor X3 2030 multilabel reader spectrophotometer. Mutant XOA17 was previously grown on $\frac{1}{2}$ LB + 100 μ g of Tp/mL broth at 37°C with shaking (225 rpm) for ~16 hrs. Each point represents the mean of three independent experiments in triplicate; error bars indicate standard deviation. * Represents statistical significance between control (green) and test (orange) groups. A-Nova test (Tukey) ($P < 0.05$)

Bacteriophage infection assays vs. LPS truncated mutants [Efficiency of plating (EOP)]

A phage host range is defined by the bacterial genera, species, and strains the phage can lyse, and it can be affected by several factors including mutations that provide resistance (Labrie et al., 2010). For this reason, the efficiency of plating (EOP) is a useful tool for determining the efficiency of a phage forming plaques on a specific host. The EOP of a phage is defined as the titer of a phage for a given or specific bacterial cell line, in comparison to the phage's maximum titer. EOPs can vary considerably from host to host. It can be simply defined as the relative number of plaques a phage stock is able to produce relative to some other value used as control (Clokic & Kropinski, 2009). The EOPs of phages KS4, KS4-M and KS12 were determined to confirm that 1) LPS serves as a receptor for these phages, and 2), the six K56-2 LPS mutants are resistant to these phages. EOPs for phages KS5 and KS9 were previously reported by Lynch et al. (2010), therefore, these experiments were not performed again. ON cultures of the six K56-2 LPS mutants were standardized to an OD of ~ 2.0 . High titer phage stocks (and their corresponding serial dilutions from 10^{-1} up to 10^{-7}) and host were mixed as described in materials and methods. A total of nine plates per LPS truncated mutant (three independent cultures plated in triplicate) were incubated at 30°C for a period of ~ 16 hrs. The next day the plaques were counted. The hypothesis that K56-2 LPS mutants are resistant to phages KS4-M and KS12 was confirmed as the EOPs for phages KS4 [Fig. 65], KS4-M [Fig.66] and KS12 [Fig.67] was zero and no plaques were detected on any of the six mutants, even at

the highest phage concentration (undiluted phage stock). These results confirm that these three phages require a complete LPS structure, including O-antigen, in order to infect their host. Unfortunately, we are left without an explanation as to why Valvano LPS mutants and our mutants behave different in liquid cultures.

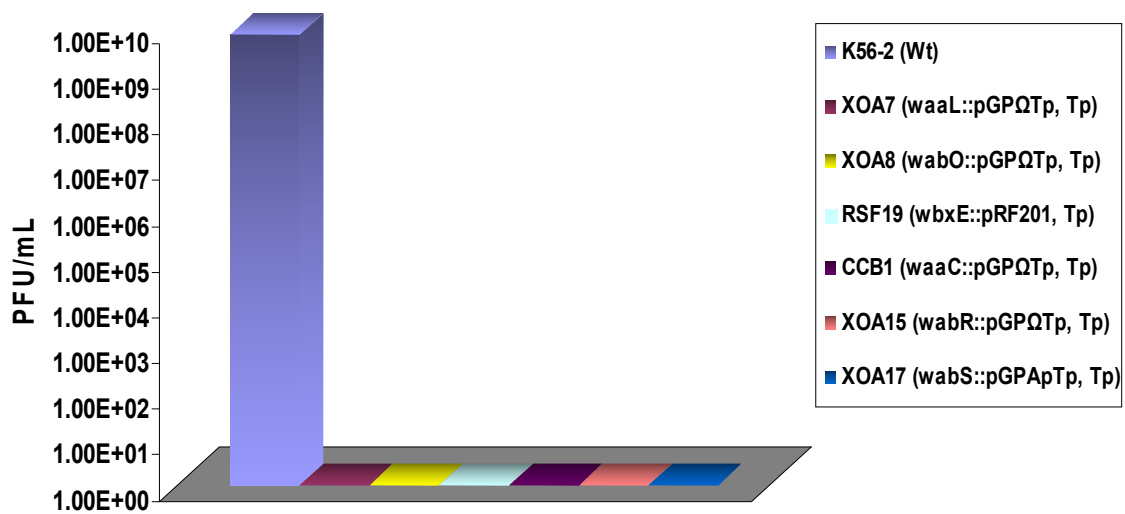


Figure 65: Efficiency of plating (EOP) of phage KS4 vs. *B. cenocepacia* K56-2 LPS mutants XOA7 (*waaL*::pGPΩTp Tp^R), XOA8 (*wabO*::pGPΩTp Tp^R), RSF19 (*wbxE*::pRF201 Tp^R), CCB1 (*waaC*::pGPΩTp Tp^R), XOA15 (*wabR*::pGPΩTp Tp^R) and XOA17 (*wabS*::pGPApTp Tp^R). Bacteria were previously grown on ½ LB + 100 µg of Tp/mL broth at 37°C with shaking (225 rpm) for ~16 hrs. The A₆₀₀ standardized (~2.0). Phage (100 µL) and mutants (100 µL) were mixed together in a sterile glass culture tube, incubated for 20 min. at room temp. and plated using the soft agar overlay method on ½ LB + 100 µg of Tp/mL agar plates. Plates were incubated at 30°C overnight. Each column represents the mean of three independent experiments in triplicate. Error bars (if visible) indicate standard deviation.

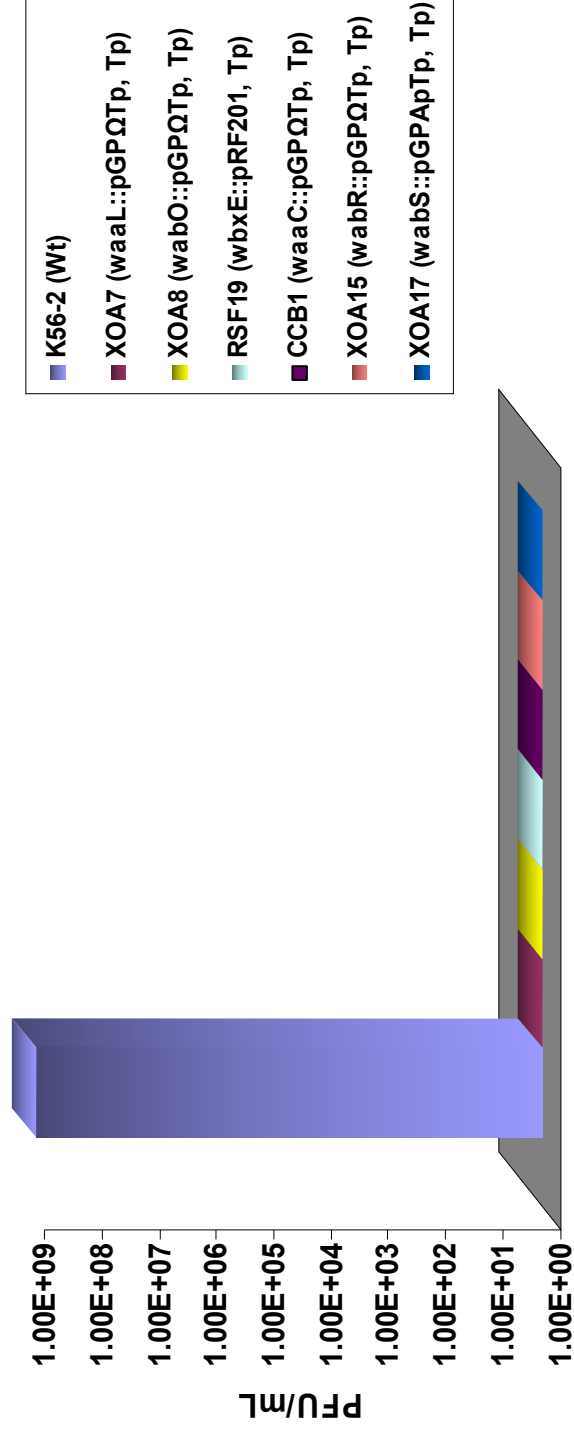


Figure 66: Efficiency of plating (EOP) of phage KS4-M vs. *B. cenocepacia* K56-2 LPS mutants XOA7 (*waaL*::pGPΩTp Tp^R), XOA8 (*wabO*::pGPΩTp Tp^R), RSF19 (*wbxE*::pRF201 Tp^R), CCB1 (*waaC*::pGPΩTp Tp^R), XOA15 (*wabR*::pGPΩTp Tp^R) and XOA17 (*wabS*::pGPAPTp Tp^R). Bacteria were previously grown on ½ LB + 100 µg of Tp/mL broth at 37°C with shaking (225 rpm) for ~16 hrs. The A₆₀₀ standardized (~2.0). Phage (100 µL) and mutants (100 µL) were mixed together in a sterile glass culture tube, incubated for 20 min. at room temp. and plated using the soft agar overlay method on ½ LB + 100 µg of Tp/mL agar plates. Plates were incubated at 30°C overnight. Each column represents the mean of three independent experiments in triplicate. Error bars (if visible) indicate standard deviation.

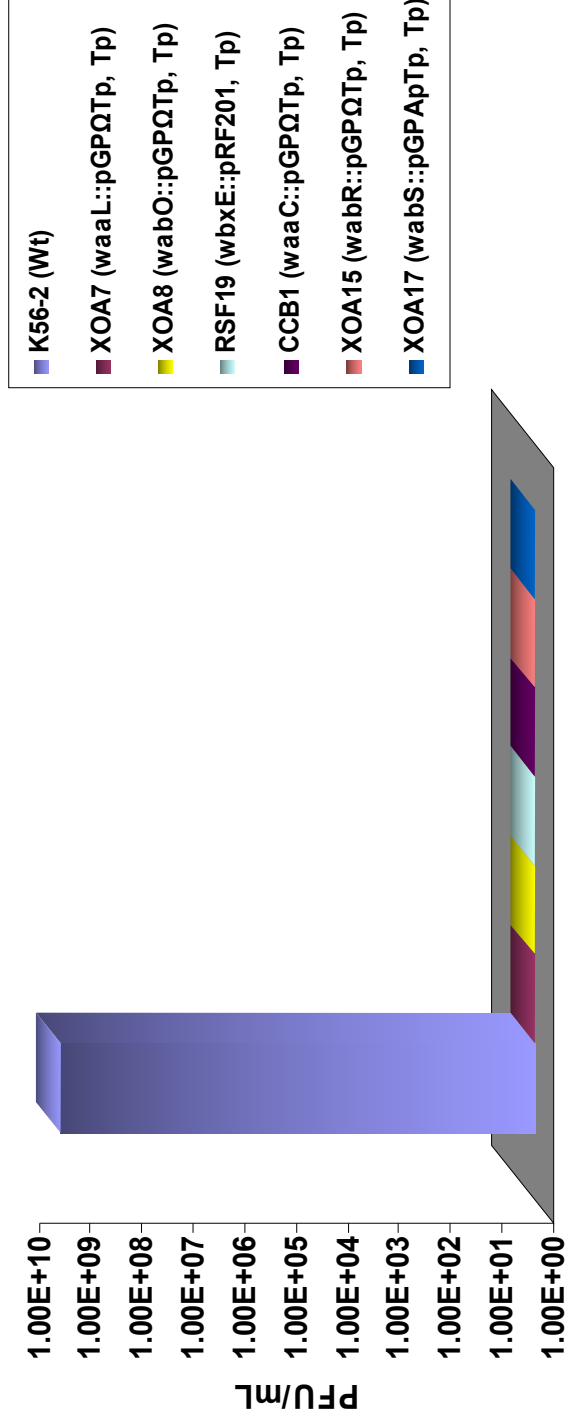


Figure 67: Efficiency of plating (EOP) of phage KS12 vs. *B. cenocepacia* K56-2 LPS mutants XOA7 (*waaL*::pGPΩTp Tp^R), XOA8 (*wabO*::pGPΩTp Tp^R), RSF19 (*wbxE*::pRF201 Tp^R), CCB1 (*waaC*::pGPΩTp Tp^R), XOA15 (*wabR*::pGPΩTp Tp^R) and XOA17 (*wabS*::pGPAPTp Tp^R). Bacteria were previously grown on ½ LB + 100 µg of Tp/mL broth at 37°C with shaking (225 rpm) for ~16 hrs. The A₆₀₀ standardized (~2.0). Phage (100 µL) and mutants (100 µL) were mixed together in a sterile glass culture tube, incubated for 20 min. at room temp. and plated using the soft agar overlay method on ½ LB + 100 µg of Tp/mL agar plates. Plates were incubated at 30°C overnight. Each column represents the mean of three independent experiments in triplicate. Error bars (if visible) indicate standard deviation.

Molecular cloning of *wbxD* & *wbcE* into pSCRhaB3 Tp-Tc and modification of pXO3 into pXO3 Tp-Tc

Taking together the data from the plasposon sequences, the assays performed on the K56-2 LPS truncated mutants, and the EOP determinations for these phages, we then proceeded to analyze the impact of genes *wbxD* and *wbcE* on phage adherence. As previously mentioned, plasmid pXO3 contains both genes *wbxD-wbcE* (Ortega et al., 2005). Unfortunately, this plasmid in its original form was not useable for our purposes due to the Tp^R marker found on the backbone plasmid pSCRhaB3. Therefore, a series of digestions and ligations were performed in order to obtain a plasmid with a functional antibiotic marker. The selected marker was Tetracycline (Tc), to which strain K56-2 is sensitive. To produce pSCRhaB3 with a Tc^R marker, plasmid pXO3 was first digested to eliminate *wbxD-wbcE* (~ 3.3 Kb), which resulted in the empty vector pSCRhaB3 [Fig. 68]. Further modifications allowed us to use *EcoRV* at basepair 158 to insert the Tc^R cassette (~1.4 Kb) that was extracted from p34S-Tc (Dennis & Zylstra, 1998).

After several attempts to construct a plasmid only carrying Tc^R, we constructed a plasmid carrying a Tc^R and Tp^R markers [Fig. 69], and this plasmid was named pSCRhaB3 Tp-Tc. The Tc^R cassette was inserted into the *EcoRV* site located 5 bases upstream of the stop codon of the Tp marker. Unfortunately, this not disrupt the Tp^R cassette, therefore the resulting plasmid carries both functional cassettes. To create the empty vector [Fig. 69], the *NdeI-XbaI* sticky ends were treated with mung bean nuclease, and the ends ligated back using T4 DNA ligase.

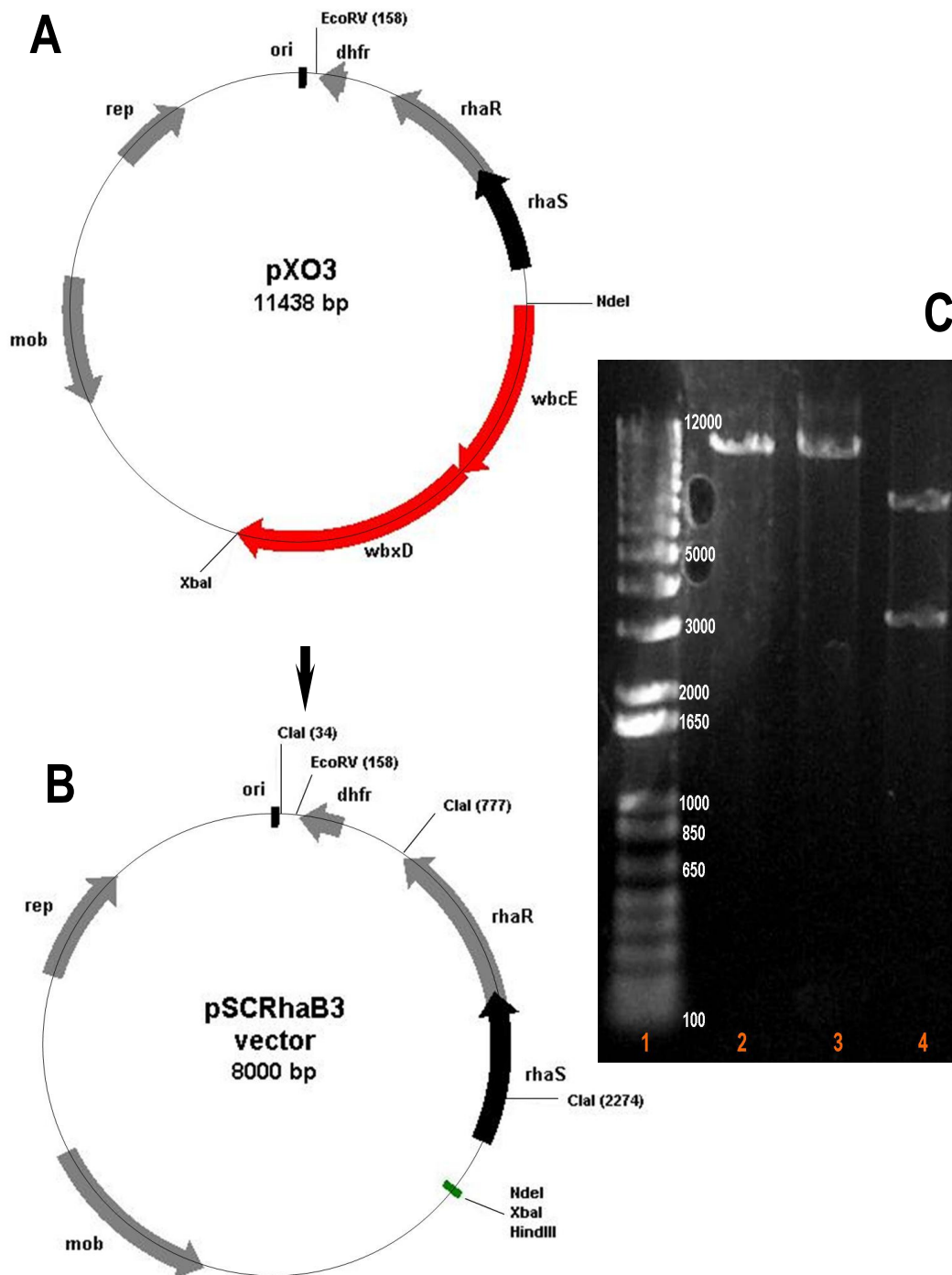


Figure 68: pDNA from *E. coli* DH5- α cells (Invitrogen): (A) Plasmid map of pXO3 (*wbxD-wbcE*) with the *dhfr*, dihydrofolate reductase gene encoding trimethoprim (Tp) resistance. (B) Plasmid map of pSCRhaB3 after elimination of insert (*wbxD-wbcE*), MCS depicted in green. (C) Gel image, 1: 1 Kb Plus DNA ladder, 2: pXO3 digested with *NdeI*, 3: digested with *XbaI*, 4: digested with *NdeI-XbaI*, insert (*wbxD-wbcE*) (~ 3.3 Kb) and empty vector (~ 8 Kb) seen on gel.

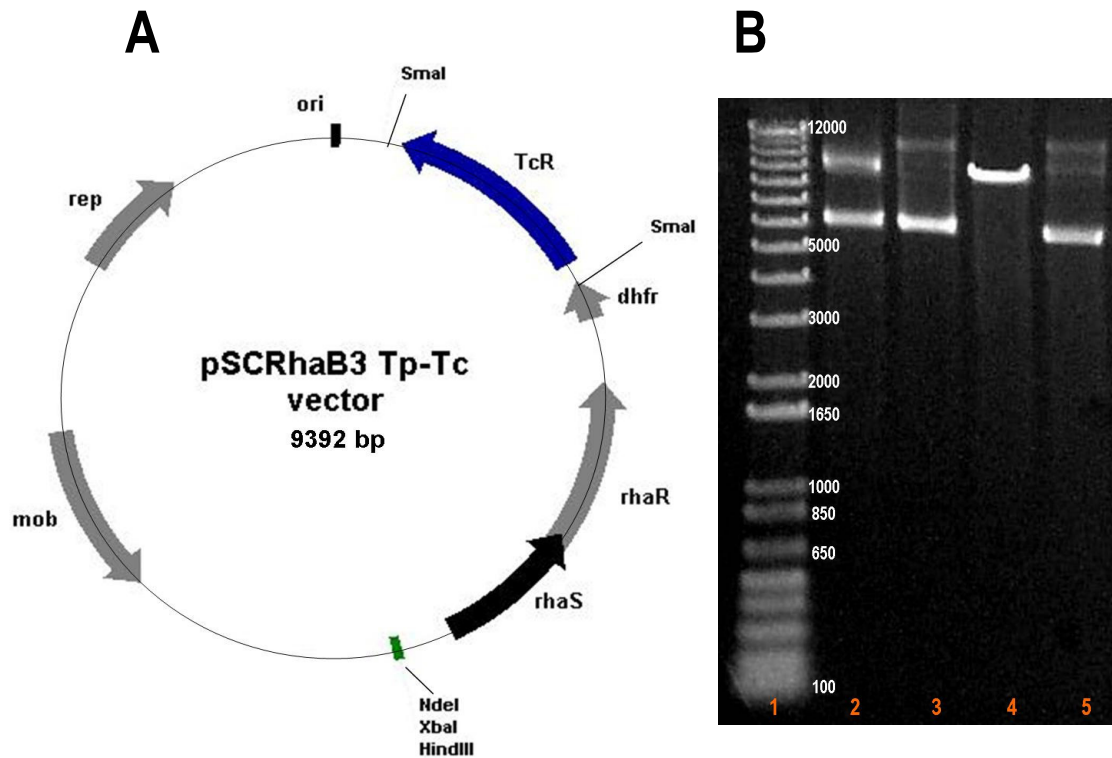


Figure 69: pDNA from *E. coli* DH5- α cells (Invitrogen): (A) Plasmid map from pSCRhaB3 Tp-Tc (empty vector) with the *dhfr*, dihydrofolate reductase gene encoding trimethoprim (Tp) resistance and the Tc^R cassette (*Sma*I) inserted at the *EcoRV* site (base 158) of pSCRhaB3. MCS depicted in green. (B) Gel image, 1: 1 Kb Plus DNA ladder, 2: pSCRhaB3 Tp-Tc digested with *Nde*I, 3: digested with *Xba*I, 4: digested with *Hind*III, 5: digested with *Nde*I-*Xba*I.

Once pSCRhaB3 Tp-Tc was constructed, genes *wbxD-wbcE* were cloned back into the vector, forming plasmid pXO3 Tp-Tc [Fig. 70]. Plasmid construction was confirmed by DNA digestion with the appropriate enzymes, and also by plasmid DNA sequencing. Both methods confirmed the correct insertion of the product.

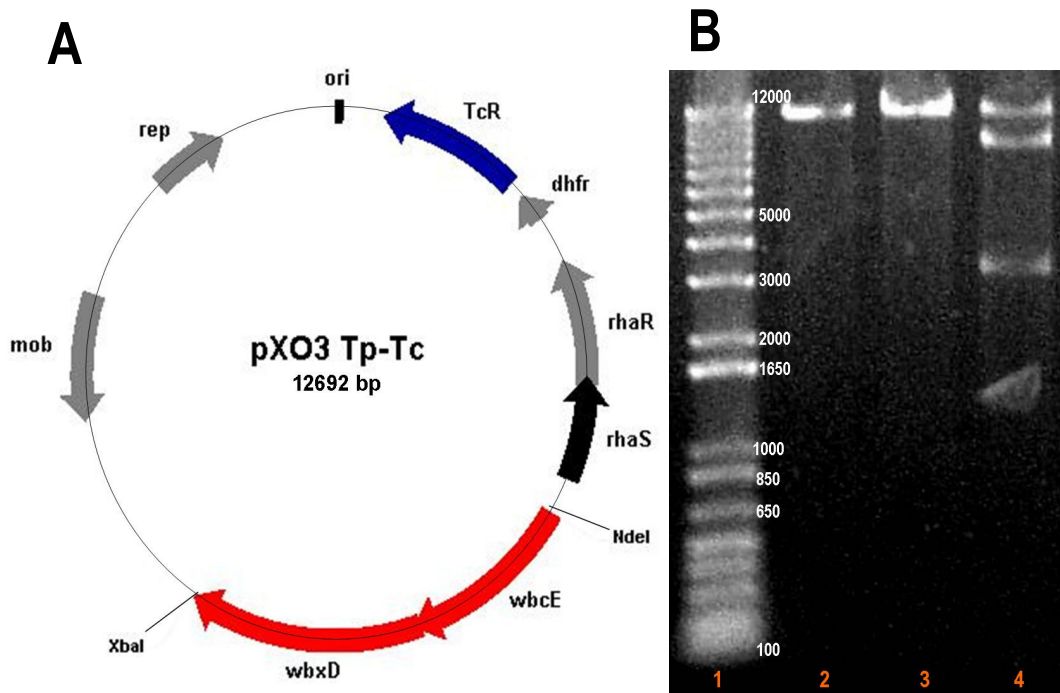


Figure 70: pDNA from *E. coli* DH5- α cells (Invitrogen): (A) Plasmid map from pXO3 Tp-Tc (*wbxD-wbcE*) with the *dhfr* and the Tc^R cassettes. (B) Gel image, 1: 1 Kb Plus DNA ladder, 2: pXO3 Tp-Tc digested with *NdeI*, 3: digested with *XbaI*, 4: digested with *NdeI-XbaI*, insert *wbxD-wbcE* (~ 3.3 Kb) and empty vector (~ 9 Kb) seen on gel.

In order to clone genes *wbcE* and *wbxD* separately [Fig. 71], TopTaq (Qiagen) polymerase chain reaction (PCR) was performed using the *wbxD-wbcE* fragment extracted from pXO3. A 6X His Tag sequence was included on both products for further analysis of protein expression.

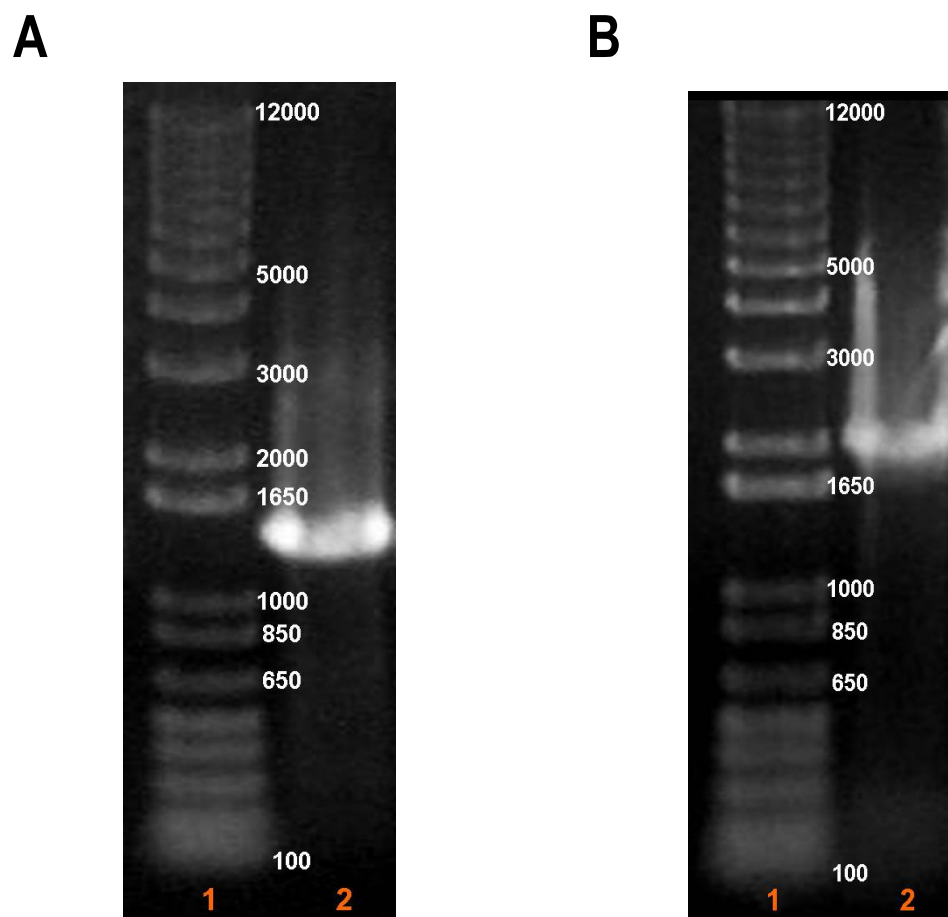


Figure 71: TopTaq PCR from DNA fragment *wbxD-wbcE* extracted from pXO3 Tp-Tc: (A) Gel image, 1: 1 Kb Plus DNA ladder, 2: *wbcE* product (~ 1.4 Kb) 3 min. extension time and 60°C annealing temp. (B) Gel Image, 1: 1 Kb Plus DNA ladder, 2: *wbxD* product (~ 2 Kb) 3 min. extension time and 64°C annealing temp.

Products were purified using the GeneClean III kit. Several attempts were made to insert the genes directly into pSCRhaB3 Tp-Tc, but these failed. Therefore, we decided to insert the products into pJET1.2/blunt (Fermentas) using a blunt end ligation protocol. To confirm the correct insertion of the products, plasmid DNA was extracted and digested with the appropriate restriction enzymes [Fig 72].

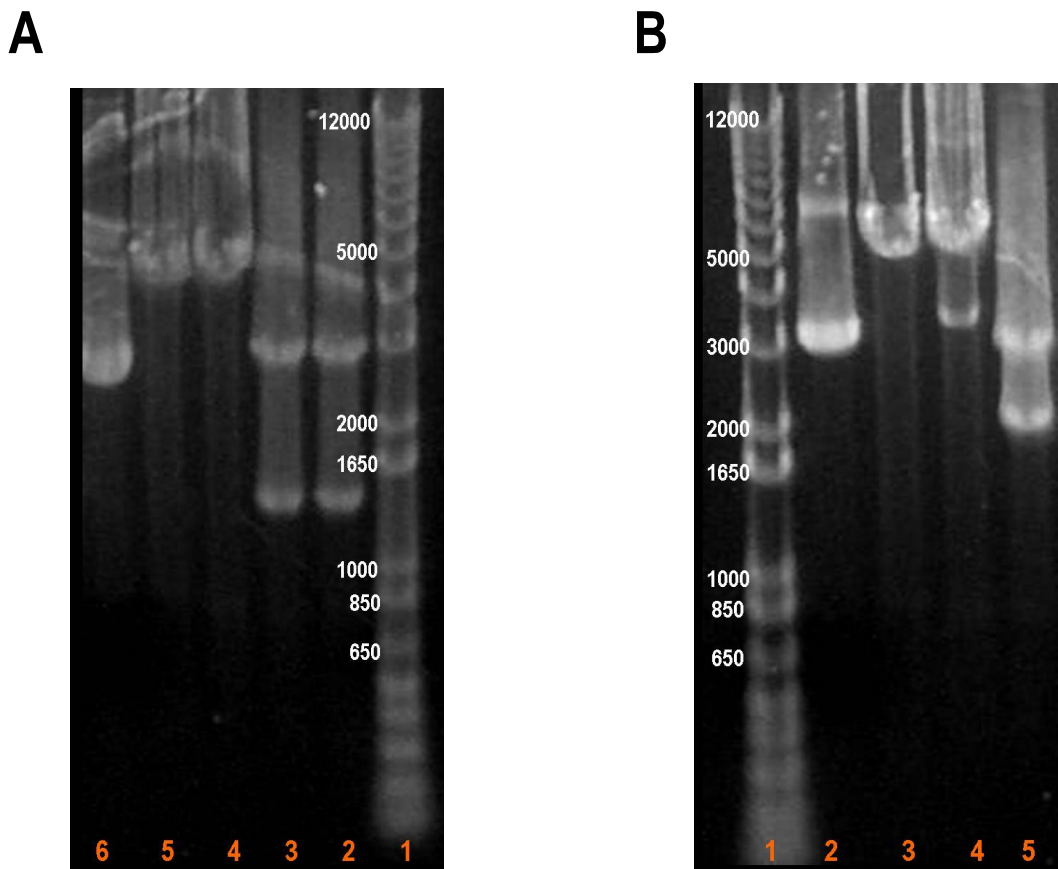


Figure 72: pDNA from *E. coli* DH5-*a* cells (Invitrogen): (A) Gel image, 1: 1 Kb Plus DNA ladder, 2 & 3: pJET1.2/blunt digested with *NdeI-XbaI*, insert *wbcE* (~ 1.4 Kb) and empty vector (~ 3 Kb) seen on gel, 4: pJET1.2/blunt digested with *XbaI*, 5: digested with *NdeI*, 6: undigested control. (B) Gel Image, 1: 1 Kb Plus DNA ladder, 2: pJET1.2/blunt undigested control, 3: digested with *NdeI*, 4: digested with *XbaI*, 5: digested with *NdeI-XbaI*, insert *wbxD* (~ 2 Kb) and empty vector (~ 3 Kb).

The gene products from pJET1.2/blunt were excised from the gel and purified using a GeneClean III kit. Products were subsequently cloned into pSCRhaB3 Tp-Tc. Resulting plasmids were named pXO4 Tp-Tc (*wbcE*) and pXO7 Tp-Tc (*wbxD*) [Fig. 73]. To confirm the correct insertion of the products, both plasmids were screened by DNA digestion with the appropriate enzymes and also by DNA sequencing.

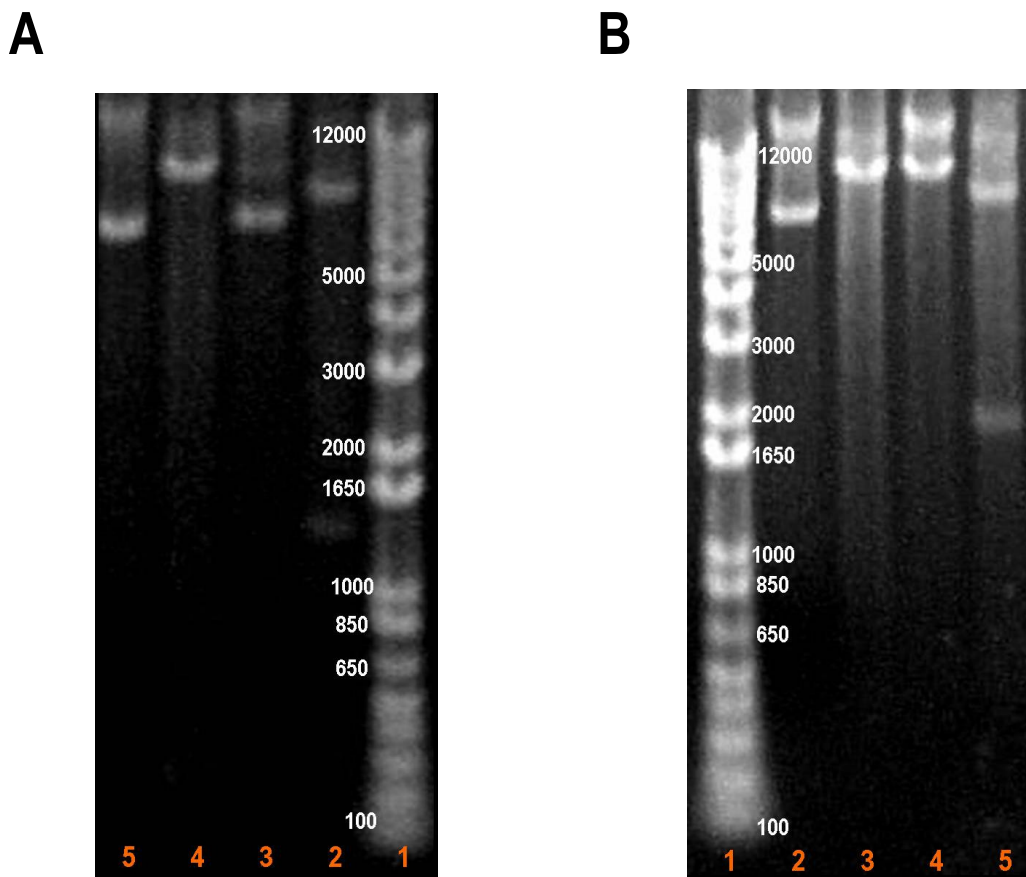


Figure 73: pDNA from *E. coli* DH5- α cells (Invitrogen): (A) Gel image, 1: 1 Kb Plus DNA ladder, 2: pXO4 Tp-Tc digested with *NdeI-XbaI*, insert *wbcE* (~ 1.4 Kb) and empty vector (~ 9 Kb), 3: digested with *XbaI*, 4: digested with *NdeI*, 5: undigested control. (B) Gel Image, 1: 1 Kb Plus DNA ladder, 2: pXO7 Tp-Tc undigested control, 3: digested with *NdeI*, 4: digested with *XbaI*, 5: digested with *NdeI-XbaI*, insert *wbxD* (~ 2 Kb) and empty vector (~ 9 Kb).

Complementation of pXO3 Tp-Tc, pXO4 Tp-Tc, pXO7 Tp-Tc and pSCRhaB3 Tp-Tc into the K56-2::pTnModOTp' KS4-M & KS12 resistant mutant 16 E1 (*wbxD-wbcE*::Tp^R) and into K56-2 wt

After constructing the four above-mentioned plasmids, it was essential to mobilize them into one of the KS4-M resistant mutants to confirm whether complementation of *wbxD* and *wbcE* would restore the wt phenotype or phage susceptibility. For this reason, mutant 16 E1 (*wbxD-wbcE*::Tp^R) was selected to continue with our research. Plasmids pXO3 Tp-Tc, pXO4 Tp-Tc, pXO7 Tp-Tc and pSCRhaB3 Tp-Tc were all mobilized into mutant 16 E1 (*wbxD-wbcE*::Tp^R) by tri-parental matings as described in materials and methods. To confirm the correct mobilization of the plasmids, exconjugants were subjected to colony PCR [Figs. 74-76], a technique used to amplify the desired DNA fragment without the isolation of plasmid DNA. In addition to complementing mutant 16 E1 (*wbxD-wbcE*::Tp^R), the K56-2 wt strain was also complemented with the same set of

plasmids [figures not shown]. These clones were used as controls in the LPS silver stain gels.

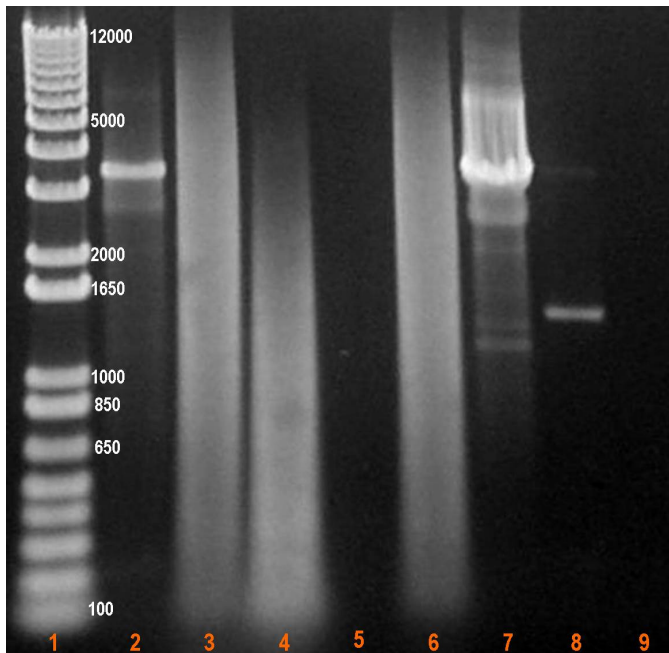


Figure 74: Colony PCR from mutant 16 E1 (*wbxD-wbcE*) complemented with pXO3 Tp-Tc. Gel image, 1: 1 Kb Plus DNA ladder, 2: Mutant 16 E1 + pXO3 Tp-Tc colony number 4, insert (~ 3.3 Kb), 3: 16 E1 + pXO3 Tp-Tc colony

number 5, 4: 16 E1 + pXO3 Tp-Tc colony number 6, 5: K56-2 wt (control), 6: mutant 16 E1 (control), 7: pXO3 (control), 8: pBBR1MCS (control), 9: mQH2O (control).

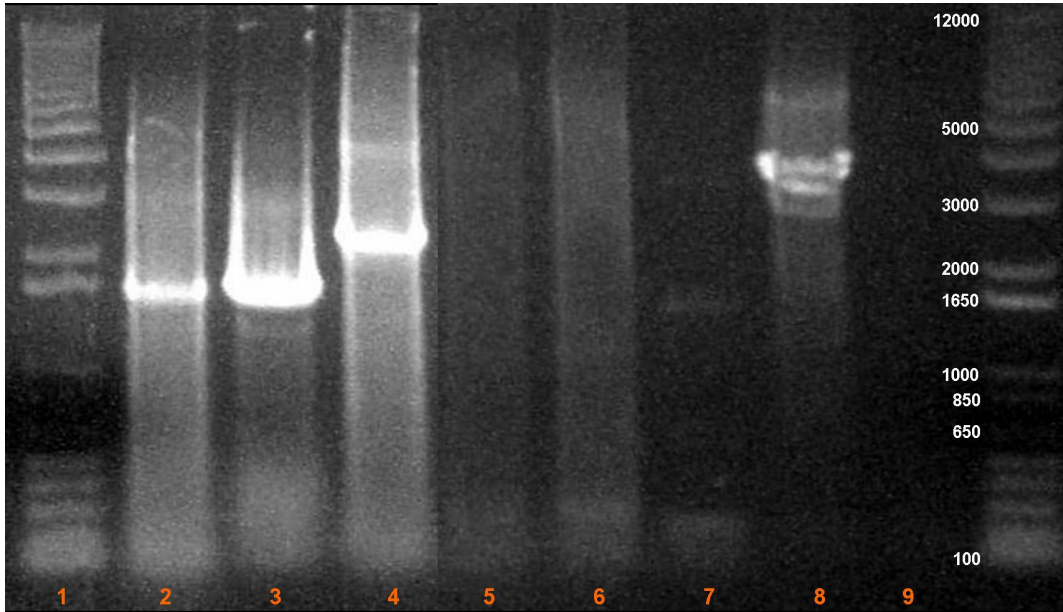


Figure 75: Colony PCR from mutant 16 E1 (*wbxD-wbcE*) complemented with pXO4 Tp-Tc and pXO7 Tp-Tc. Gel image, 1: 1 Kb Plus DNA ladder, 2: Mutant 16 E1 + pXO4 Tp-Tc colony number 2, insert (~ 1.4 Kb), 3: 16 E1 + pXO4 Tp-Tc colony number 4, 4: 16 E1 + pXO7 Tp-Tc colony number 8, 5: K56-2 wt (control), 6: mutant 16 E1 (control), 7: pBBR1MCS (control), 8: pXO3 (control), 9: mQH2O (control).

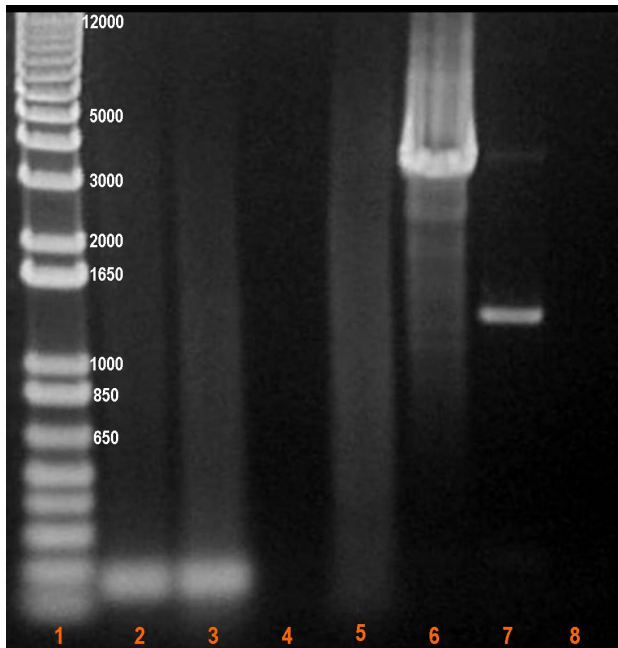


Figure 76: Colony PCR from mutant 16 E1 (*wbxD-wbcE*) complemented with pSCRhaB3 Tp-Tc. Gel image, 1: 1 Kb Plus DNA ladder, 2: Mutant 16 E1 + pSCRhaB3 Tp-Tc colony number 21, no insert (~ 150 bp), 3: 16 E1 + pSCRhaB3 Tp-Tc colony number 24, 4: K56-2 wt (control), 5: mutant 16 E1 (control), 6: pXO3 (control), 7: pBBR1MCS (control), 9: mQH2O (control).

Bacteriophage infection assays vs. K56-2::pTnMod-OTp' mutant 16 E1 (*wbxD-wbcE*::Tp^R) complemented with pXO3 Tp-Tc, pXO4 Tp-Tc, pXO7 Tp-Tc and pSCRhaB3 Tp-Tc [Liquid culture clearing assays]

To further confirm whether complementation of *wbxD* and *wbcE* in mutant 16 E1 would restore the wt phenotype (phage susceptibility), we performed a series of liquid culture clearing assays similar to those performed with the LPS truncated mutants. Similar control groups and test groups were analyzed, however, in this particular case, the complemented mutant 16 E1 was exposed only to phages KS4-M and KS12, since previous data suggests that these are the only two phages in our collection that utilize LPS O-antigen as a receptor. Because pSCRhaB3 carries a rhamnose-inducible P_{RHA} promoter, the expression of the genes can be tightly regulated by the addition of rhamnose to the media. Therefore, a set of bacterial strains containing different plasmids was induced with 0.2% rhamnose, while a second set was assayed under non-inducing conditions. Results revealed that 16 E1 (*wbxD-wbcE*::Tp^R) complemented with pXO3 Tp-Tc (*wbxD-wbcE*) was again sensitive to phage infection, the plasmid fully restoring the phenotype to wt levels, and both phages were able to lyse the bacterial host [Figs. 77 & 79]. This suggested that one (or perhaps) both genes were encoding the protein(s) used as a receptor for phage binding. In comparison, 16 E1 (*wbxD-wbcE*::Tp^R) complemented with pSCRhaB3 Tp-Tc (empty vector) showed continued resistance to phage infection [Figs. 78 & 80], as expected. Similar results were observed in the non-induced assays [data not shown]. Because *wbcE* was previously described as an O-antigen assembly

glycosyltransferase (Ortega et al., 2005), we hypothesized that O-antigen is the receptor for these phages. This data appears to support our hypothesis.

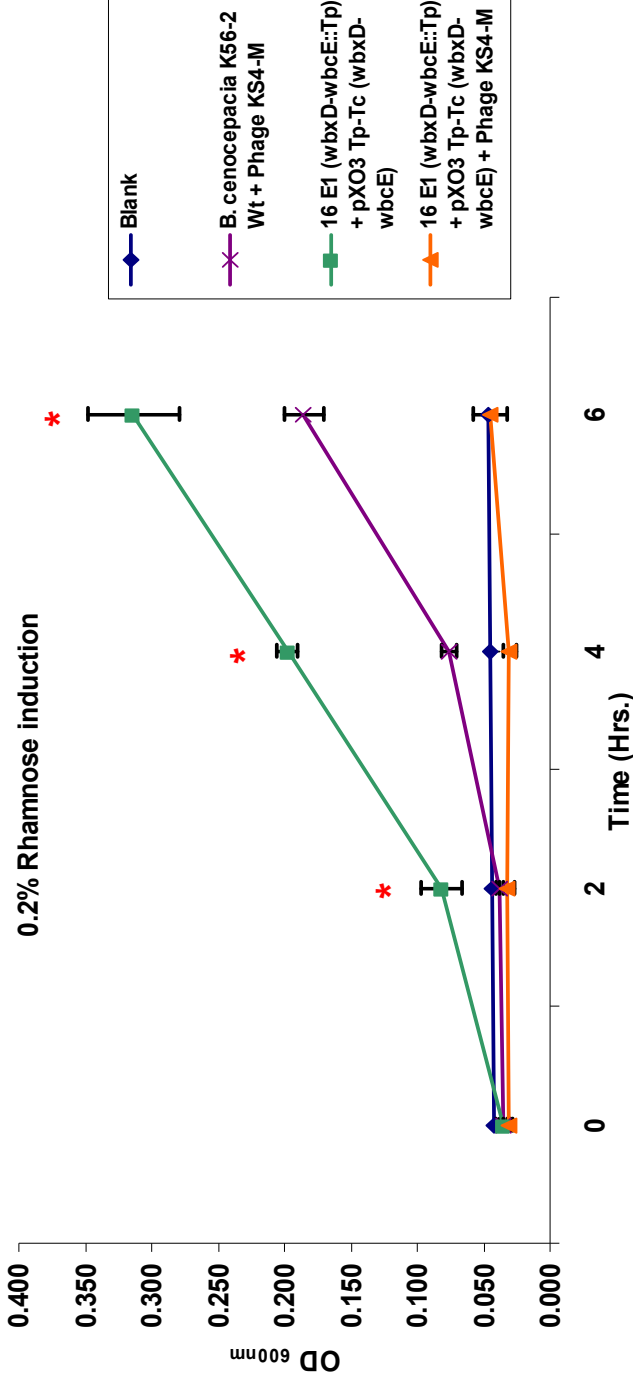


Figure 77: Growth curve of *B. cenocepacia* K56-2::pTnModOTp' mutant 16 E1 (*wbxD-wbcE::Tp^R*) complemented with pXO3 Tp-Tc (*wbxD-wbcE*) exposed to phage KS4-M: Blue, blank control (200 μ L of $\frac{1}{2}$ LB broth), Purple, wt control (10 μ L of K56-2 wt), (50 μ L of high titer phage stock) and (150 μ L of $\frac{1}{2}$ LB broth), Green, positive control (10 μ L of bacteria) and (190 μ L of $\frac{1}{2}$ LB broth + 100 μ g of Tp/mL + 100 μ g of Tc/mL + 0.2% Rha), Orange, test group (10 μ L of bacteria), (50 μ L of high titer phage stock) and (150 μ L of $\frac{1}{2}$ LB broth + 100 μ g of Tp/mL + 100 μ g of Tc/mL + 0.2% Rha). Incubation at 37°C with continuous shaking (225 rpm). A₆₀₀ measured every 2 hrs. for a period of 6 hrs in a Victor X3 2030 multilabel reader spectrophotometer. Mutant 16 E1 (*wbxD-wbcE::Tp^R*) + pXO3 Tp-Tc was previously grown on $\frac{1}{2}$ LB broth + 100 μ g of Tp/mL + 100 μ g of Tc/mL + 0.2% Rha at 37°C with shaking (225 rpm) for ~16 hrs. Each point represents the mean of three independent experiments in triplicate; error bars indicate standard deviation. * Represents statistical significance between control (green) and test (orange) groups. A-Nova test (Tukey) (P < 0.05)

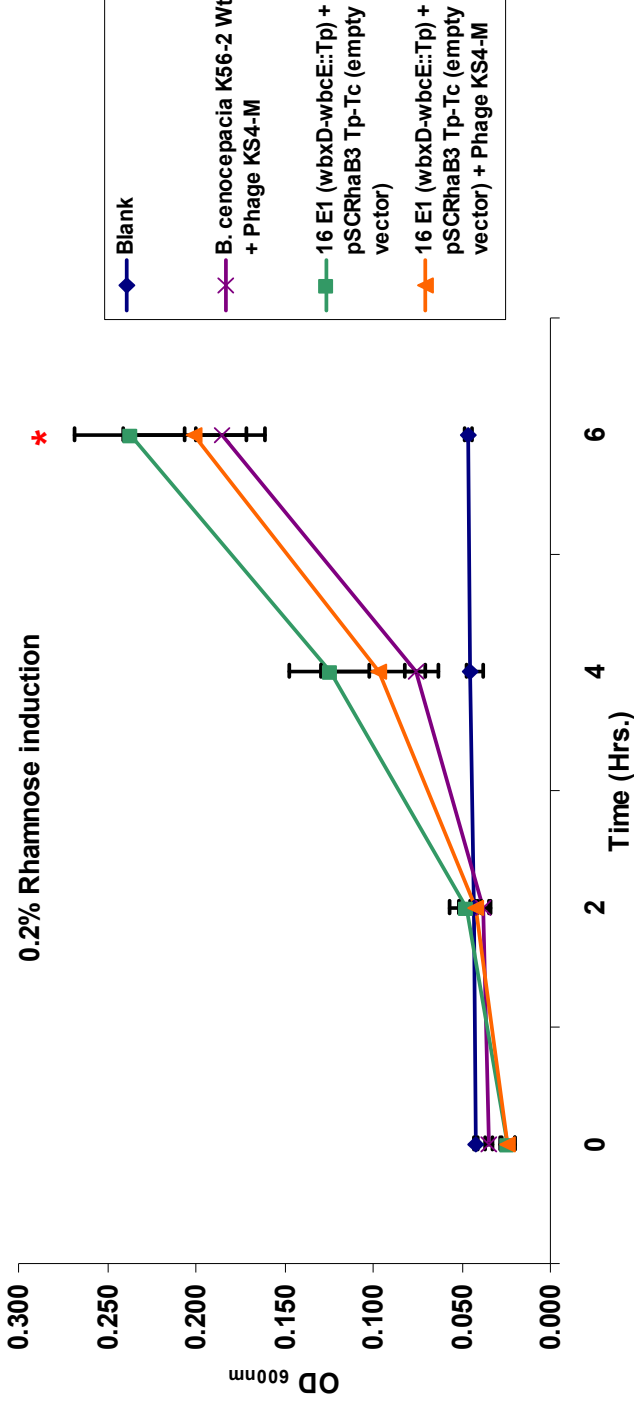


Figure 78: Growth curve of *B. cenocepacia* K56-2::pTnModOTp' mutant 16 E1 (*wbxD-wbcE::Tp^R*) complemented with pSCRhaB3 Tp-Tc (empty vector) exposed to phage KS4-M: Blue, blank control (200 μ L of $\frac{1}{2}$ LB broth), Purple, wt control (10 μ L of K56-2 wt), (50 μ L of high titer phage stock) and (150 μ L of $\frac{1}{2}$ LB broth), Green, positive control (10 μ L of bacteria) and (190 μ L of $\frac{1}{2}$ LB broth + 100 μ g of Tp/mL + 100 μ g of Tc/mL + 0.2% Rha), Orange, test group (10 μ L of bacteria), (50 μ L of high titer phage stock) and (150 μ L of $\frac{1}{2}$ LB broth + 100 μ g of Tp/mL + 100 μ g of Tc/mL + 0.2% Rha). Incubation at 37°C with continuous shaking (225 rpm). A_{600} measured every 2 hrs. for a period of 6 hrs in a Victor X3 2030 multilabel reader spectrophotometer. Mutant 16 E1 (*wbxD-wbcE::Tp^R*) + pSCRhaB3 Tp-Tc was previously grown on $\frac{1}{2}$ LB broth + 100 μ g of Tp/mL + 100 μ g of Tc/mL + 0.2% Rha at 37°C with shaking (225 rpm) for ~16 hrs. Each point represents the mean of three independent experiments in triplicate; error bars indicate standard deviation. * Represents statistical significance between control (green) and test (orange) groups. A-Nova test (Tukey) ($P < 0.05$)

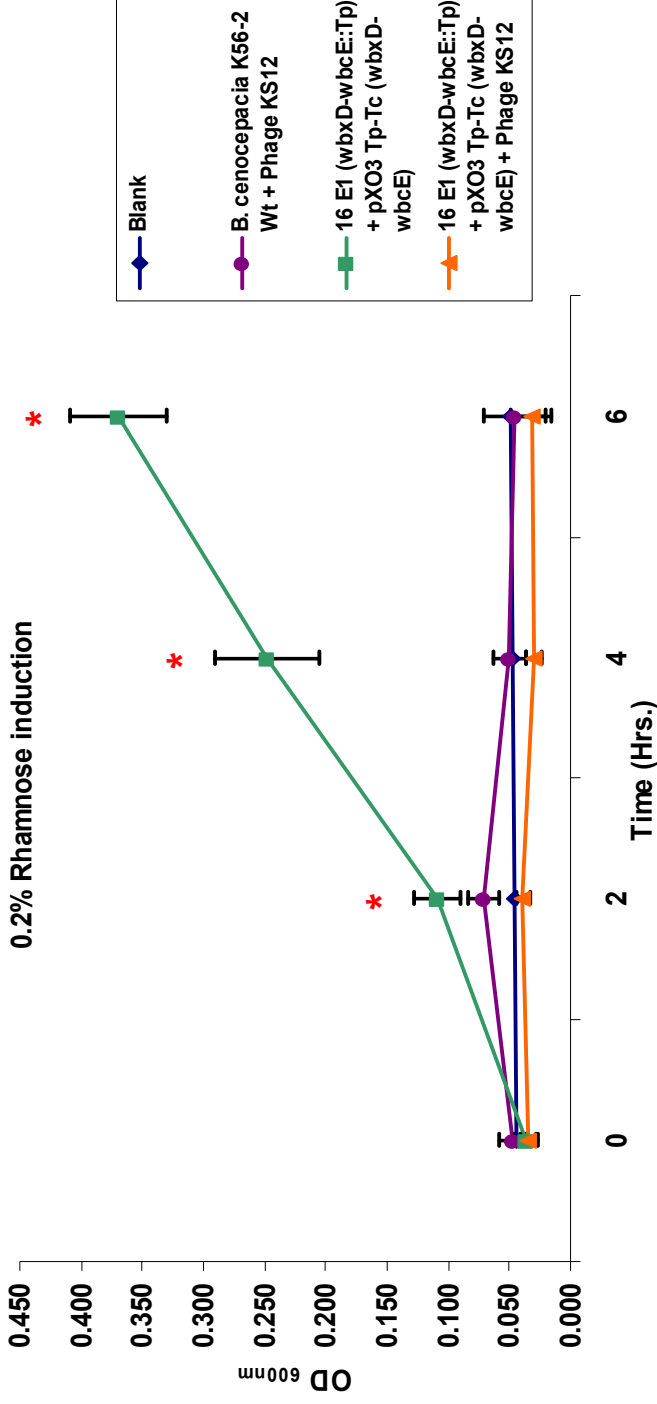


Figure 79: Growth curve of *B. cenocepacia* K56-2::pTnModOTp' mutant 16 E1 (*wbxD-wbcE::Tp^R*) complemented with pXO3 Tp-Tc (*wbxD-wbcE*) exposed to phage KS12: Blue, blank control (200 μ L of $\frac{1}{2}$ LB broth), Purple, wt control (10 μ L of K56-2 wt), (50 μ L of high titer phage stock) and (150 μ L of $\frac{1}{2}$ LB broth), Green, positive control (10 μ L of bacteria) and (190 μ L of $\frac{1}{2}$ LB broth + 100 μ g of Tp/mL + 100 μ g of Tc/mL + 0.2% Rha), Orange, test group (10 μ L of bacteria), (50 μ L of high titer phage stock) and (150 μ L of $\frac{1}{2}$ LB broth + 100 μ g of Tp/mL + 100 μ g of Tc/mL + 0.2% Rha). Incubation at 37°C with continuous shaking (225 rpm). A_{600} measured every 2 hrs. for a period of 6 hrs in a Victor X3 2030 multilabel reader spectrophotometer. Mutant 16 E1 (*wbxD-wbcE::Tp^R*) + pXO3 Tp-Tc was previously grown on $\frac{1}{2}$ LB broth + 100 μ g of Tp/mL + 100 μ g of Tc/mL + 0.2% Rha at 37°C with shaking (225 rpm) for ~16 hrs. Each point represents the mean of three independent experiments in triplicate; error bars indicate standard deviation. * Represents statistical significance between control (green) and test (orange) groups. A-Nova test (Tukey) ($P < 0.05$)

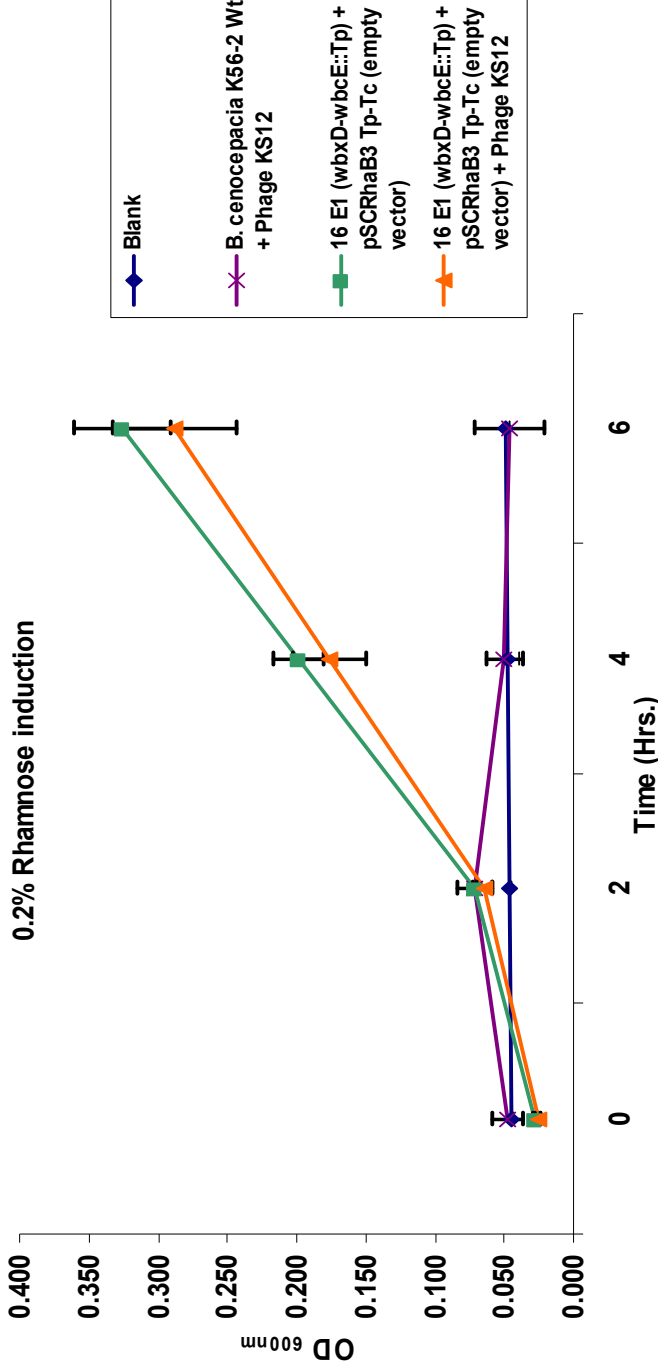


Figure 80: Growth curve of *B. cenocepacia* K56-2::pTnModOTp' mutant 16 E1 (*wbxD-wbcE::Tp^R*) complemented with pSCRhaB3 Tp-Tc (empty vector) exposed to phage KS12: Blue, blank control (200 μ L of $\frac{1}{2}$ LB broth), Purple, wt control (10 μ L of K56-2 wt), (50 μ L of high titer phage stock) and (150 μ L of $\frac{1}{2}$ LB broth), Green, positive control (10 μ L of bacteria) and (190 μ L of $\frac{1}{2}$ LB broth + 100 μ g of Tp/mL + 100 μ g of Tc/mL + 0.2% Rha), Orange, test group (10 μ L of bacteria), (50 μ L of high titer phage stock) and (150 μ L of $\frac{1}{2}$ LB broth + 100 μ g of Tp/mL + 100 μ g of Tc/mL + 0.2% Rha). Incubation at 37°C with continuous shaking (225 rpm). A_{600} measured every 2 hrs. for a period of 6 hrs in a Victor X3 2030 multilabel reader spectrophotometer. Mutant 16 E1 (*wbxD-wbcE::Tp^R*) + pSCRhaB3 Tp-Tc was previously grown on $\frac{1}{2}$ LB broth + 100 μ g of Tp/mL + 100 μ g of Tc/mL + 0.2% Rha at 37°C with shaking (225 rpm) for ~16 hrs. Each point represents the mean of three independent experiments in triplicate; error bars indicate standard deviation. * Represents statistical significance between control (green) and test (orange) groups. A-Nova test (Tukey) ($P < 0.05$)

After mutant 16 E1 complemented with pXO3 Tp-Tc revealed phage sensitivity in liquid clearing assays, it was imperative to determine which of the two gene products was essential for phage infection, *wbxD* or *wbcE*. Thus, strain 16 E1 was separately complemented with pXO4 Tp-Tc (*wbcE*) and pXO7 Tp-Tc (*wbxD*). Results revealed that when 16 E1 was complemented with pXO4 Tp-Tc, the wt phenotype was not restored and the mutant was still resistant to phage infection [Figs. 81 & 83]. Similar results were observed for both the induced and non-induced conditions [data not shown]. This was somewhat surprising since Ortega et al. (2005) reported *wbcE* as the gene encoding the glycosyltransferase involved in O-antigen assembly. Initially, we hypothesized that disruption of this gene would result in resistance to phage infection. However, our data revealed a different result.

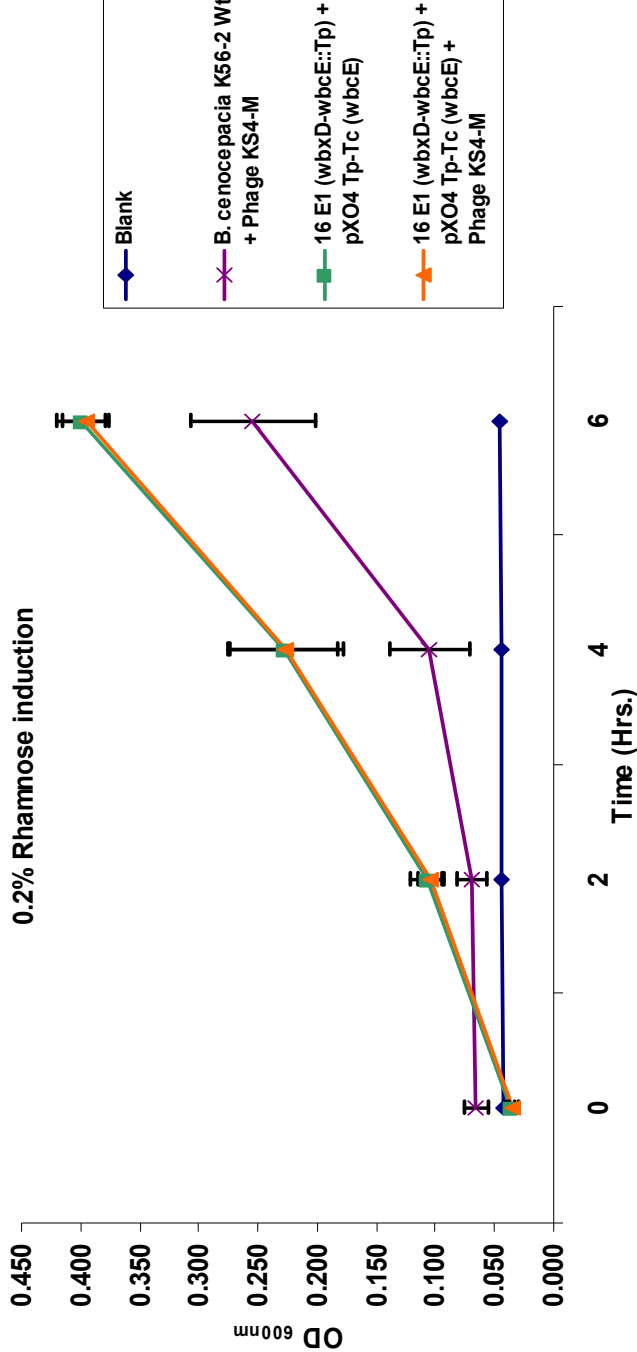


Figure 81: Growth curve of *B. cenocepacia* K56-2::pTnModOTp' mutant 16 E1 (*wbxD-wbcE::Tp^R*) complemented with pXO4 Tp-Tc (*wbcE*) exposed to phage KS4-M: Blue, blank control (200 μ L of $\frac{1}{2}$ LB broth), Purple, wt control (10 μ L of K56-2 wt), (50 μ L of high titer phage stock) and (150 μ L of $\frac{1}{2}$ LB broth), Green, positive control (10 μ L of bacteria) and (190 μ L of $\frac{1}{2}$ LB broth + 100 μ g of Tp/mL + 100 μ g of Tc/mL + 0.2% Rha), Orange, test group (10 μ L of bacteria), (50 μ L of high titer phage stock) and (150 μ L of $\frac{1}{2}$ LB broth + 100 μ g of Tp/mL + 100 μ g of Tc/mL + 0.2% Rha). Incubation was performed at 37°C with continuous shaking (225 rpm). A_{600} measured every 2 hrs. for a period of 6 hrs in a Victor X3 2030 multilabel reader spectrophotometer. Mutant 16 E1 (*wbxD-wbcE::Tp^R*) + pXO4 Tp-Tc was previously grown on $\frac{1}{2}$ LB broth + 100 μ g of Tp/mL + 100 μ g of Tc/mL + 0.2% Rha at 37°C with shaking (225 rpm) for ~16 hrs. Each point represents the mean of three independent experiments in triplicate; error bars indicate standard deviation. * Represents statistical significance between control (green) and test (orange) groups. A-Nova test (Tukey) ($P < 0.05$)

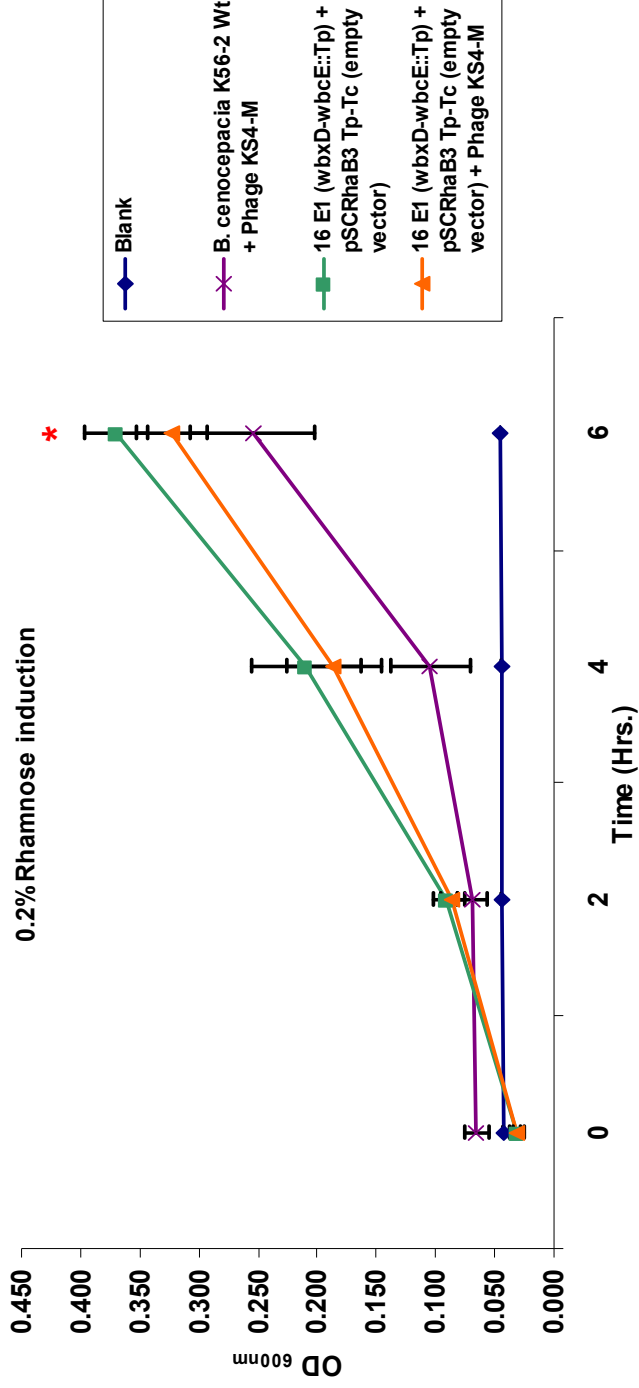


Figure 82: Growth curve of *B. cenocepacia* K56-2::pTnModOTp' mutant 16 E1 (*wbxD-wbcE::Tp^R*) complemented with pSCRhaB3 Tp-Tc (empty vector) exposed to phage KS4-M: Blue, blank control (200 μ L of $\frac{1}{2}$ LB broth), Purple, wt control (10 μ L of K56-2 wt), (50 μ L of high titer phage stock) and (150 μ L of $\frac{1}{2}$ LB broth), Green, positive control (10 μ L of bacteria) and (190 μ L of $\frac{1}{2}$ LB broth + 100 μ g of Tp/mL + 100 μ g of Tc/mL + 0.2% Rha), Orange, test group (10 μ L of bacteria), (50 μ L of high titer phage stock) and (150 μ L of $\frac{1}{2}$ LB broth + 100 μ g of Tp/mL + 100 μ g of Tc/mL + 0.2% Rha). Incubation was performed at 37°C with continuous shaking (225 rpm). A_{600} measured every 2 hrs. for a period of 6 hrs in a Victor X3 2030 multilabel reader spectrophotometer. Mutant 16 E1 (*wbxD-wbcE::Tp^R*) + pSCRhaB3 Tp-Tc was previously grown on $\frac{1}{2}$ LB broth + 100 μ g of Tp/mL + 100 μ g of Tc/mL + 0.2% Rha at 37°C with shaking (225 rpm) for ~16 hrs. Each point represents the mean of three independent experiments in triplicate; error bars indicate standard deviation. * Represents statistical significance between control (green) and test (orange) groups. A-Nova test (Tukey) ($P < 0.05$)

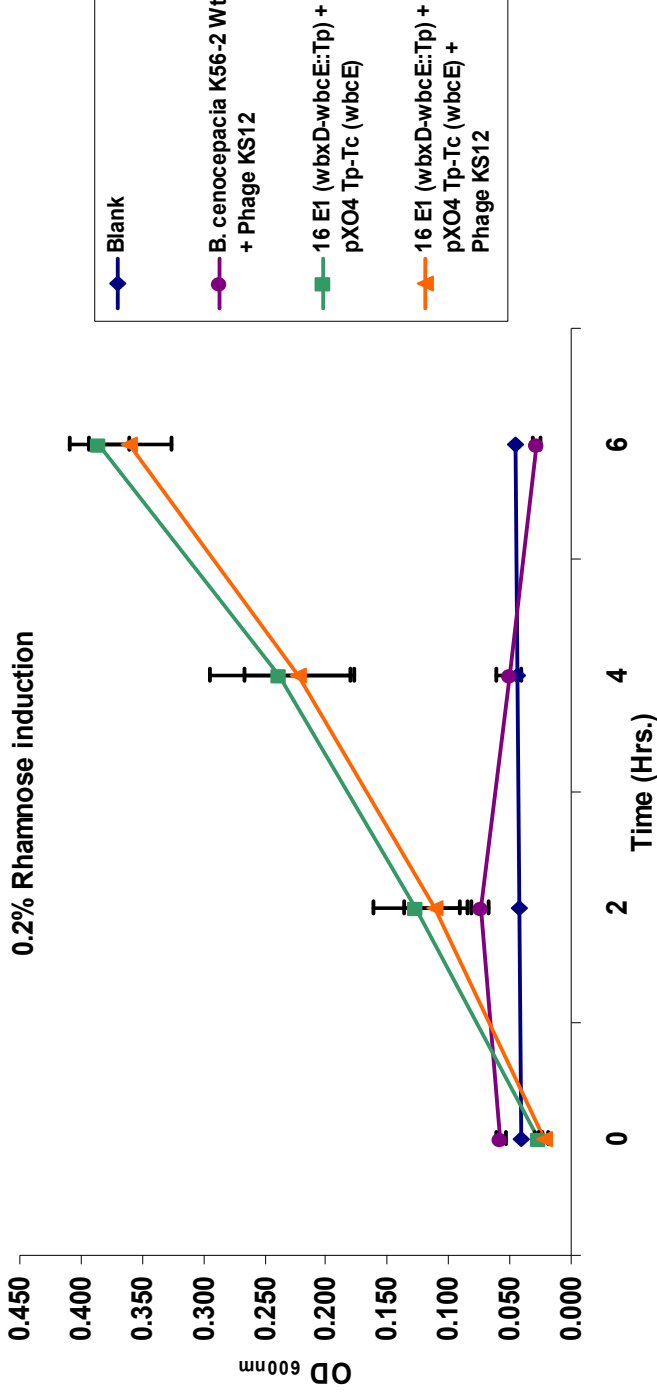


Figure 83: Growth curve of *B. cenocepacia* K56-2::pTnModOTp' mutant 16 E1 (*wbxD-wbcE::Tp^R*) complemented with pXO4 Tp-Tc (*wbcE*) exposed to phage KS12: Blue, blank control (200 μ L of $\frac{1}{2}$ LB broth), Purple, wt control (10 μ L of K56-2 wt), (50 μ L of high titer phage stock) and (150 μ L of $\frac{1}{2}$ LB broth), Green, positive control (10 μ L of bacteria) and (190 μ L of $\frac{1}{2}$ LB broth + 100 μ g of Tp/mL + 100 μ g of Tc/mL + 0.2% Rha), Orange, test group (10 μ L of bacteria), (50 μ L of high titer phage stock) and (150 μ L of $\frac{1}{2}$ LB broth + 100 μ g of Tp/mL + 100 μ g of Tc/mL + 0.2% Rha). Incubation was performed at 37°C with continuous shaking (225 rpm). A_{600} measured every 2 hrs. for a period of 6 hrs in a Victor X3 2030 multilabel reader spectrophotometer. Mutant 16 E1 (*wbxD-wbcE::Tp^R*) + pXO4 Tp-Tc was previously grown on $\frac{1}{2}$ LB broth + 100 μ g of Tp/mL + 100 μ g of Tc/mL + 0.2% Rha at 37°C with shaking (225 rpm) for ~16 hrs. Each point represents the mean of three independent experiments in triplicate; error bars indicate standard deviation. * Represents statistical significance between control (green) and test (orange) groups. A-Nova test (Tukey) ($P < 0.05$)

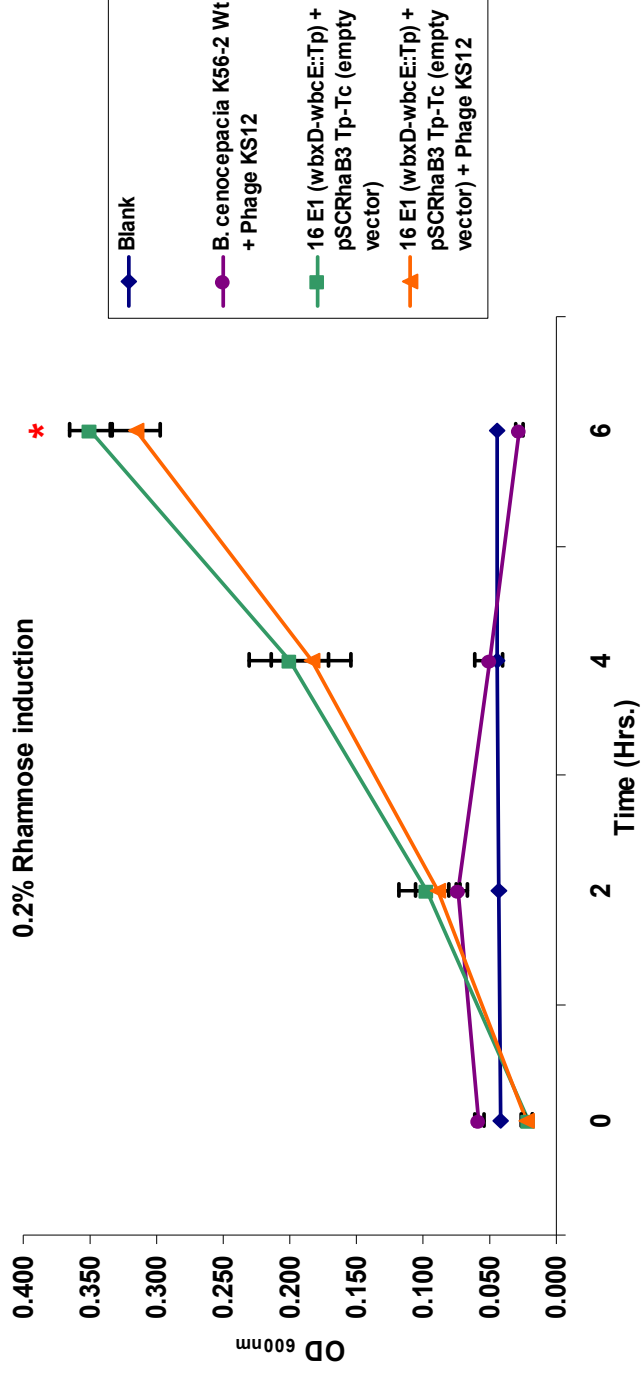


Figure 84: Growth curve of *B. cenocepacia* K56-2::pTnModOTp' mutant 16 E1 (*wbxD-wbcE::Tp^R*) complemented with pSCRhaB3 Tp-Tc (empty vector) exposed to phage KS12: Blue, blank control (200 μ L of $\frac{1}{2}$ LB broth), Purple, wt control (10 μ L of K56-2 wt), (50 μ L of high titer phage stock) and (150 μ L of $\frac{1}{2}$ LB broth), Green, positive control (10 μ L of bacteria) and (190 μ L of $\frac{1}{2}$ LB broth + 100 μ g of Tp/mL + 100 μ g of Tc/mL + 0.2% Rha), Orange, test group (10 μ L of bacteria), (50 μ L of high titer phage stock) and (150 μ L of $\frac{1}{2}$ LB broth + 100 μ g of Tp/mL + 100 μ g of Tc/mL + 0.2% Rha). Incubation was performed at 37°C with continuous shaking (225 rpm). A_{600} measured every 2 hrs. for a period of 6 hrs in a Victor X3 2030 multilabel reader spectrophotometer. Mutant 16 E1 (*wbxD-wbcE::Tp^R*) + pSCRhaB3 Tp-Tc was previously grown on $\frac{1}{2}$ LB broth + 100 μ g of Tp/mL + 100 μ g of Tc/mL + 0.2% Rha at 37°C with shaking (225 rpm) for ~16 hrs. Each point represents the mean of three independent experiments in triplicate; error bars indicate standard deviation. * Represents statistical significance between control (green) and test (orange) groups. A-Nova test (Tukey) ($P < 0.05$)

Conversely, mutant 16 E1 carrying pXO7 Tp-Tc showed partial sensitivity to phage infection, and the wt phenotype was partially restored [Figs. 85 & 87]. Phages were able to lyse the bacterial host, but not as effectively as observed with 16 E1 complemented with pXO3 Tp-Tc (*wbxD* and *wbcE*). Therefore, it appears that both genes and their encoded products are required for full KS4-M and KS12 phage infection. Ortega et al. (2005) only mentions the function of *wbcE* and doesn't give detail about the function of *wbxD*. There still exists the possibility that *wbxD* encodes an enzyme that attaches additional O-antigen subunits. An image from a recent publication by Kotrange et al. (2011) reveals that an O-antigen LPS mutant named XOA3 (*wbxE*::pGPΩTp Tp^R), which shares similarity with mutant RSF19 used in this study (*wbxE*::pRF201 Tp^R), produces a complete lipid A, complete core OS, and partial O-antigen subunit [Fig. 89]. Perhaps the remaining O-antigen subunits, which are essential for full phage infection, are produced and assembled by *wbxD*.

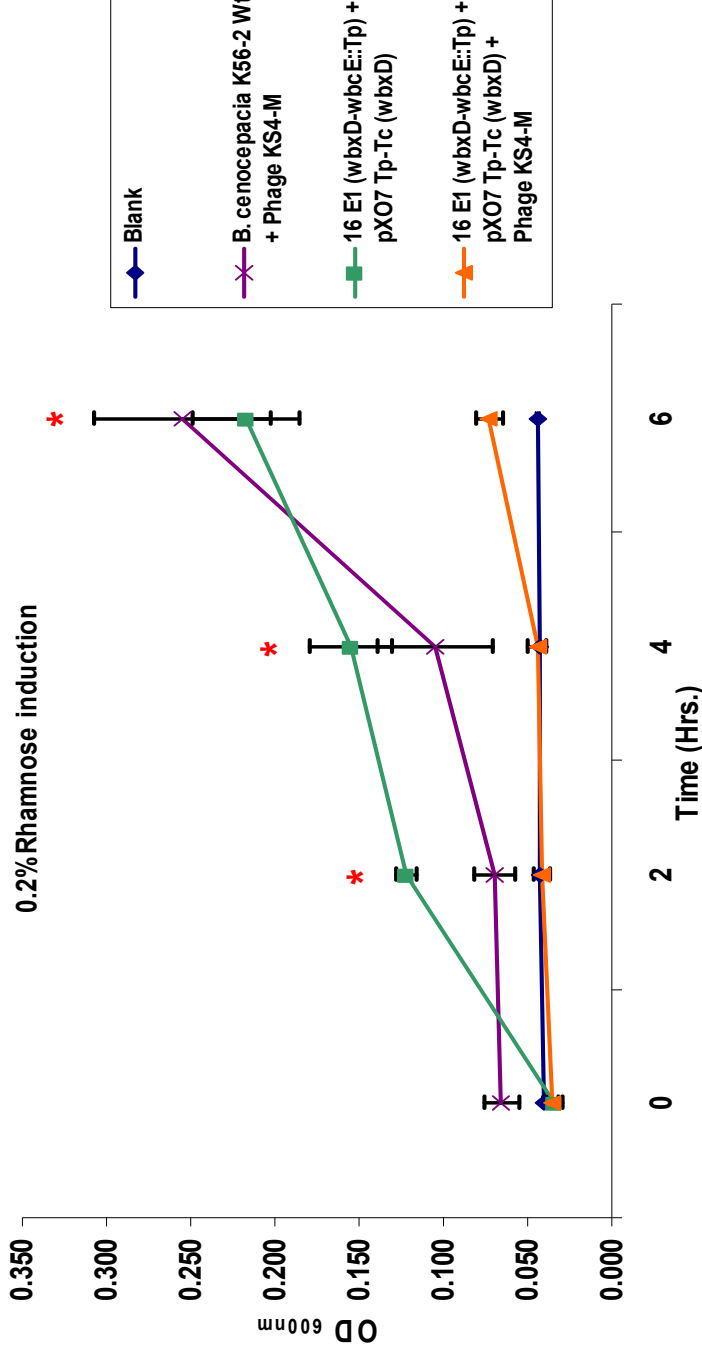


Figure 85: Growth curve of *B. cenocepacia* K56-2::pTnModOTp' mutant 16 E1 (*wbxD-wbcE::Tp^R*) complemented with pXO7 Tp-Tc (*wbxD*) exposed to phage KS4-M: Blue, blank control (200 μ L of $\frac{1}{2}$ LB broth), Purple, wt control (10 μ L of K56-2 wt), (50 μ L of high titer phage stock) and (150 μ L of $\frac{1}{2}$ LB broth), Green, positive control (10 μ L of bacteria) and (190 μ L of $\frac{1}{2}$ LB broth + 100 μ g of Tp/mL + 100 μ g of Tc/mL + 0.2% Rha), Orange, test group (10 μ L of bacteria), (50 μ L of high titer phage stock) and (150 μ L of $\frac{1}{2}$ LB broth + 100 μ g of Tp/mL + 100 μ g of Tc/mL + 0.2% Rha). Incubation was performed at 37°C with continuous shaking (225 rpm). A_{600} measured every 2 hrs. for a period of 6 hrs in a Victor X3 2030 multilabel reader spectrophotometer. Mutant 16 E1 (*wbxD-wbcE::Tp^R*) + pXO7 Tp-Tc was previously grown on $\frac{1}{2}$ LB broth + 100 μ g of Tp/mL + 100 μ g of Tc/mL + 0.2% Rha at 37°C with shaking (225 rpm) for ~16 hrs. Each point represents the mean of three independent experiments in triplicate; error bars indicate standard deviation. * Represents statistical significance between control (green) and test (orange) groups. A-Nova test (Tukey) ($P < 0.05$)

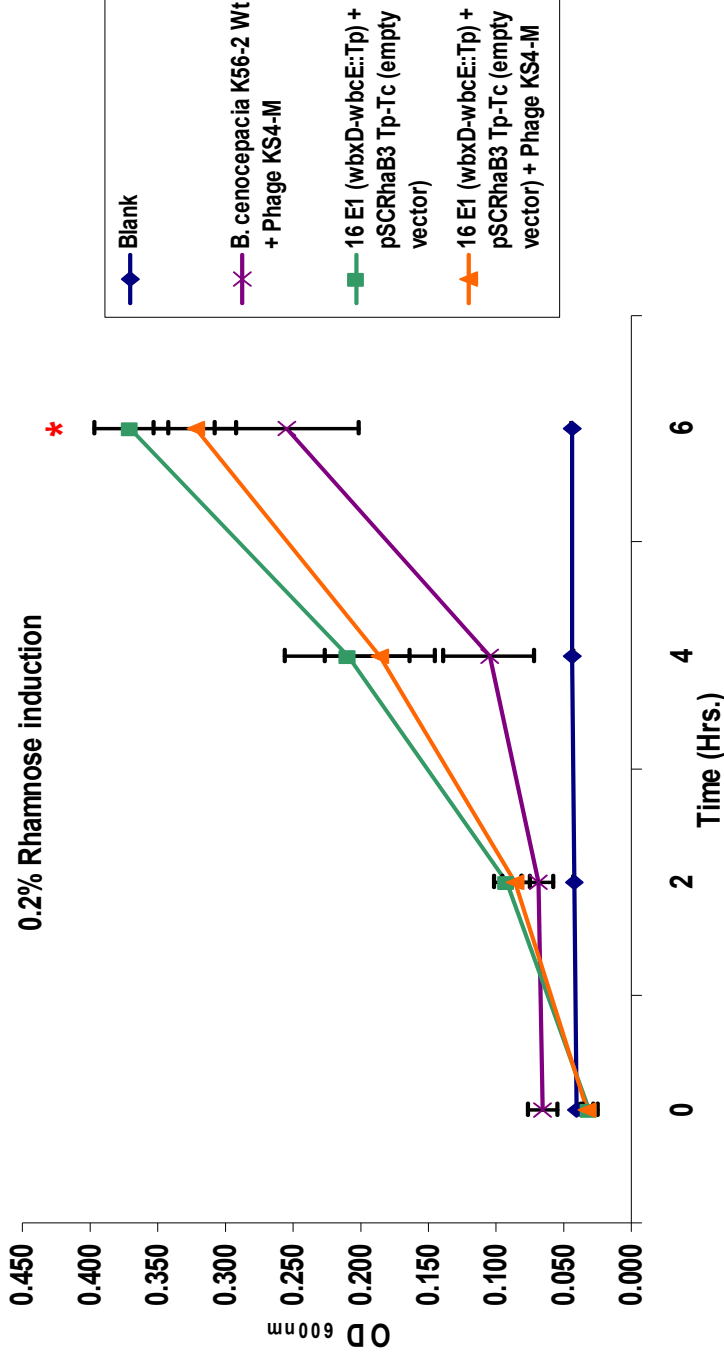


Figure 86: Growth curve of *B. cenocepacia* K56-2::pTnModOTp' mutant 16 E1 (*wbxD-wbcE::Tp^R*) complemented with pSCRhaB3 Tp-Tc (empty vector) exposed to phage KS4-M: Blue, blank control (200 μ L of $\frac{1}{2}$ LB broth), Purple, wt control (10 μ L of K56-2 wt), (50 μ L of high titer phage stock) and (150 μ L of $\frac{1}{2}$ LB broth), Green, positive control (10 μ L of bacteria) and (190 μ L of $\frac{1}{2}$ LB broth + 100 μ g of Tp/mL + 100 μ g of Tc/mL + 0.2% Rha), Orange, test group (10 μ L of bacteria), (50 μ L of high titer phage stock) and (150 μ L of $\frac{1}{2}$ LB broth + 100 μ g of Tp/mL + 100 μ g of Tc/mL + 0.2% Rha). Incubation was performed at 37°C with continuous shaking (225 rpm). A_{600} measured every 2 hrs. for a period of 6 hrs in a Victor X3 2030 multilabel reader spectrophotometer. Mutant 16 E1 (*wbxD-wbcE::Tp^R*) + pSCRhaB3 Tp-Tc was previously grown on $\frac{1}{2}$ LB broth + 100 μ g of Tp/mL + 100 μ g of Tc/mL + 0.2% Rha at 37°C with shaking (225 rpm) for ~16 hrs. Each point represents the mean of three independent experiments in triplicate; error bars indicate standard deviation. * Represents statistical significance between control (green) and test (orange) groups. A-Nova test (Tukey) ($P < 0.05$)

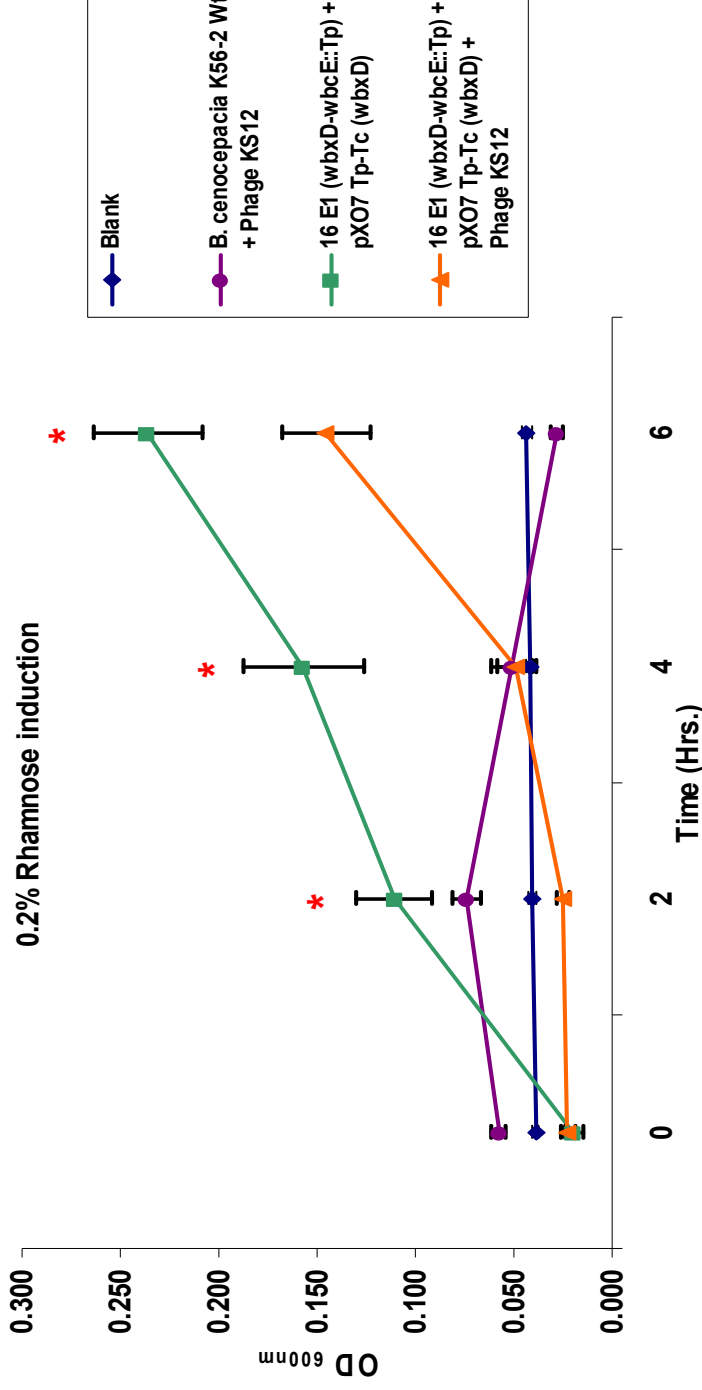


Figure 87: Growth curve of *B. cenocepacia* K56-2::pTnModOTp' mutant 16 E1 (*wbxD-wbcE::Tp^R*) complemented with pXO7 Tp-Tc (*wbxD*) exposed to phage KS12: Blue, blank control (200 μ L of $\frac{1}{2}$ LB broth), Purple, wt control (10 μ L of K56-2 wt), (50 μ L of high titer phage stock) and (150 μ L of $\frac{1}{2}$ LB broth), Green, positive control (10 μ L of bacteria) and (190 μ L of $\frac{1}{2}$ LB broth + 100 μ g of Tp/mL + 100 μ g of Tc/mL + 0.2% Rha), Orange, test group (10 μ L of bacteria), (50 μ L of high titer phage stock) and (150 μ L of $\frac{1}{2}$ LB broth + 100 μ g of Tp/mL + 100 μ g of Tc/mL + 0.2% Rha). Incubation was performed at 37°C with continuous shaking (225 rpm). A_{600} measured every 2 hrs. for a period of 6 hrs in a Victor X3 2030 multilabel reader spectrophotometer. Mutant 16 E1 (*wbxD-wbcE::Tp^R*) + pXO7 Tp-Tc was previously grown on $\frac{1}{2}$ LB broth + 100 μ g of Tp/mL + 100 μ g of Tc/mL + 0.2% Rha at 37°C with shaking (225 rpm) for ~16 hrs. Each point represents the mean of three independent experiments in triplicate; error bars indicate standard deviation. * Represents statistical significance between control (green) and test (orange) groups. A-Nova test (Tukey) ($P < 0.05$)

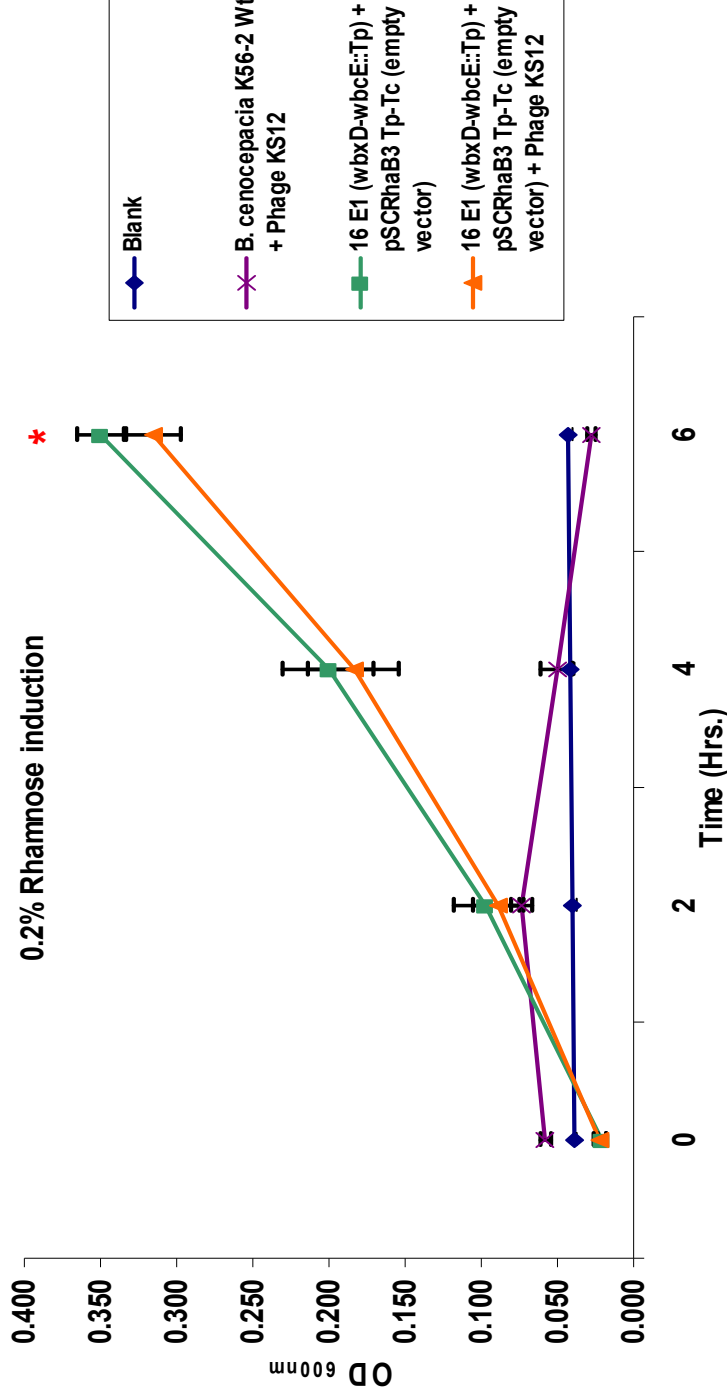


Figure 88: Growth curve of *B. cenocepacia* K56-2::pTnModOTp' mutant 16 E1 (*wbxD-wbcE::Tp^B*) complemented with pSCRhaB3 Tp-Tc (empty vector) exposed to phage KS12: Blue, blank control (200 μ L of $\frac{1}{2}$ LB broth), Purple, wt control (10 μ L of K56-2 wt), (50 μ L of high titer phage stock) and (150 μ L of $\frac{1}{2}$ LB broth), Green, positive control (10 μ L of bacteria) and (190 μ L of $\frac{1}{2}$ LB broth + 100 μ g of Tp/mL + 100 μ g of Tc/mL + 0.2% Rha), Orange, test group (10 μ L of bacteria), (50 μ L of high titer phage stock) and (150 μ L of $\frac{1}{2}$ LB broth + 100 μ g of Tp/mL + 100 μ g of Tc/mL + 0.2% Rha). Incubation was performed at 37°C with continuous shaking (225 rpm). A_{600} measured every 2 hrs. for a period of 6 hrs in a Victor X3 2030 multilabel reader spectrophotometer. Mutant 16 E1 (*wbxD-wbcE::Tp^B*) + pSCRhaB3 Tp-Tc was previously grown on $\frac{1}{2}$ LB broth + 100 μ g of Tp/mL + 100 μ g of Tc/mL + 0.2% Rha at 37°C with shaking (225 rpm) for ~16 hrs. Each point represents the mean of three independent experiments in triplicate; error bars indicate standard deviation. * Represents statistical significance between control (green) and test (orange) groups. A-Nova test (Tukey) ($P < 0.05$)

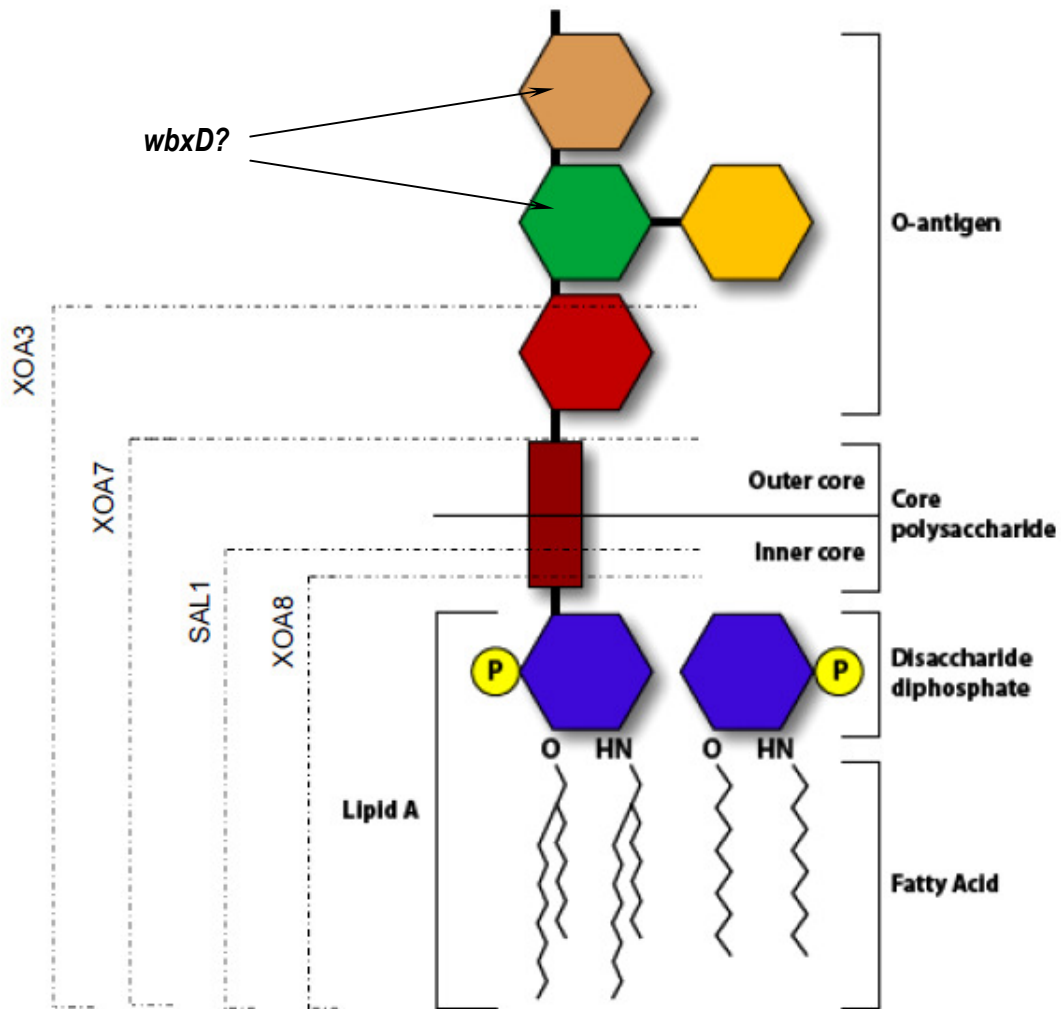


Figure 89: LPS diagram from four LPS truncated mutants. Mutant XOA3 (*wbxE*::pGPΩTp, Tp^R) similar to mutant RSF19 (*wbxE*::pRF201 Tp^R) produces a complete Lipid A, core (OS) and a partial O-antigen subunit. Dotted lines represent the level of LPS truncation on each of the four mutants. *wbxD* perhaps encodes the remaining O-antigen subunits essential for phage KS4-M and KS12 binding. (Adapted from Kotrange et al., 2011)

LPS extraction, purification and visualization from mutant 16 E1 complemented with pXO3 Tp-Tc, pXO4 Tp-Tc, pXO7 Tp-Tc and pSCRhaB3 Tp-Tc, and from K56-2 wt complemented with same set of plasmids

To further identify the possible differences in LPS structure between the strains K56-2 wt, 16 E1 (*wbxD-wbcE::Tp^R*), and 16 E1 complemented with pXOs plasmids, and to determine if the O-antigen subunits were restored on the complemented mutants, we extracted and visualized the LPS from various strains including controls. In addition, we determined whether there was an obvious difference in LPS production between cells grown under inducing and non-inducing conditions, with and without rhamnose. Following LPS extraction using a proteinase K, samples were run on a Tri-Tricine system and visualized by silver staining. Results revealed no apparent differences between the LPS isolated from 0.2% rhamnose-induced overnight cultures and non-induced cultures. Strain K56-2 wt complemented with the set of plasmids showed in general no difference than the wt strain without plasmids. The only difference was two additional bands (red arrows) detected in all of the complemented strains [Fig. 90]. Ortega et al. (2005) previously reported that these bands probably corresponded to Lipid A-Core OS replaced by partial O-antigen subunits.

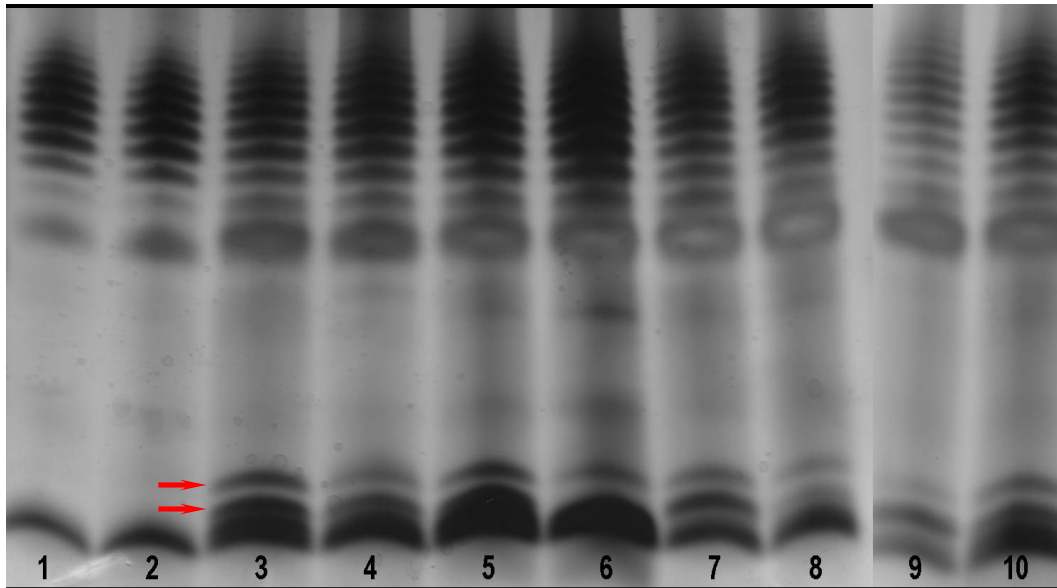


Figure 90: LPS electrophoretic profiles from *B. cenocepacia* K56-2 wt: 1: K56-2 wt induced with 0.2% Rha, 2: K56-2 wt non-induced, 3: K56-2 wt + pXO3 Tp-Tc + 0.2% Rha, 4: K56-2 wt + pXO3 Tp-Tc, 5: K56-2 wt + pXO4 Tp-Tc + 0.2% Rha, 6: K56-2 wt + pXO4 Tp-Tc, 7: K56-2 wt + pXO7 Tp-Tc + 0.2% Rha, 8: K56-2 wt + pXO7 Tp-Tc, 9: K56-2 wt + pSCRhaB3 Tp-Tc + 0.2% Rha, 10: K56-2 wt + pSCRhaB3 Tp-Tc.

As expected, an obvious difference was detected between mutant 16 E1 (*wbxD-wbcE::Tp^R*) when compared to K56-2 wt and the complemented mutant with either pXO3 Tp-Tc, which showed a similar banding pattern to that of the wt strain, and pXO7 Tp-Tc revealing faint O-antigen bands [Fig 91]. The intensity of the O-antigen bands seems to correlate with the efficiency of phage infection. Strain 16 E1 + pXO3 Tp-Tc showed intense O-antigen bands and phages are highly efficient when infecting this strain, whereas the faint O-antigen bands seen on the LPS profile of 16 E1 + pXO7 Tp-Tc correlate well with the reduced efficiency of phages KS4-M and KS12 infecting this host. This further supports the hypothesis that both genes are essential during phage binding. In the case of

16 E1 complemented with pXO4 Tp-Tc, the banding pattern was similar to 16 E1 with no plasmid. Thus, no complementation of O-antigen assembly (or at least none visible on the gel) seems to occur [Fig. 91]. Similar results from the liquid clearing assays also support this finding.

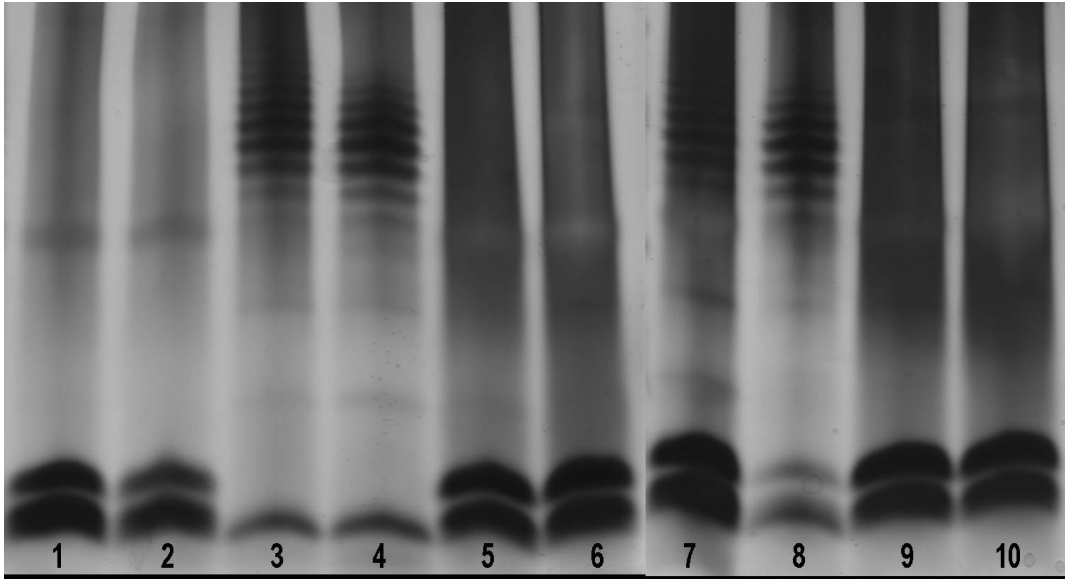


Figure 91: LPS electrophoretic profiles from *B. cenocepacia* K56-2::pTnModOTp' mutant 16 E1 (*wbxD-wbcE::Tp^R*): 1: 16 E1 (*wbxD-wbcE::Tp^R*) induced with 0.2% Rha, 2: 16 E1 (*wbxD-wbcE::Tp^R*) non-induced, 3: 16 E1 + pXO3 Tp-Tc + 0.2% Rha, 4: 16 E1 + pXO3 Tp-Tc, 5: 16 E1 + pXO4 Tp-Tc + 0.2% Rha, 6: 16 E1 + pXO4 Tp-Tc, 7: 16 E1 + pXO7 Tp-Tc + 0.2% Rha, 8: 16 E1 + pXO7 Tp-Tc, 9: 16 E1 + pSCRhaB3 Tp-Tc + 0.2% Rha, 10: 16 E1 + pSCRhaB3 Tp-Tc.

To summarize, after a series of different experiments, we were able to determine that phages KS4-M, KS4 and KS12 bind to the LPS O-antigen units (smooth LPS phenotype) in order to infect their bacterial host. LPS is the most common phage receptor (Nikaido, 2003; Bos & Tommassen, 2004) thus, these

results are unsurprising. Several phages have been reported in the past that utilize O-antigen subunits as a receptor, such as phages P22 (Eriksson & Lindberg, 1977), HK620 (Barbirz et al., 2008), Sf6, $\phi 1$, $\Omega 8$, ϵ^{15} and many more (Rakhuba et al., 2010). Phages KS4, KS4-M and KS12 can also be included in this category.

It is important to highlight that we haven't discarded the possibility that O-antigen subunits serve as a secondary receptor where reversible binding occurs, and that a primary receptor (where irreversible binding occurs) is still required for these phages to infect. At least three of the isolated KS4-M resistant mutants have plasposon insertions in genes that appear unrelated to LPS biosynthesis. Perhaps the construction of double mutants in LPS biosynthesis related genes will be helpful in order to further examine this idea. However, we are confident that our current results are correct due to the confirmatory nature of the evidence collected. It has been suggested that some phages require the presence of O-antigen subunits in order to infect their host and that the O-antigen serves as both the secondary and primary receptor (Letellier et al., 2004; Steinbacher et al., 1997). It might also be useful to determine whether the presence of sugar depolymerase enzymes like those reported for the degradation of O-antigen subunits are present in the phage tails of any of these three phages (Eriksson & Lindberg, 1977). Furthermore, LPS phage-neutralization assays can be performed to further confirm the involvement of LPS O-antigen as the receptor for these phages. A known concentration of phage is mixed with purified LPS, this mixture is incubated for a certain amount of time before serial dilutions are plated against the specific host. Phage inhibition can be compared with a control group (without

added LPS); phages inactivated to LPS should produce less plaque numbers than the control group.

Finally, the three KS4-M resistant mutants with plasposon insertions in non-LPS related genes should be analyzed. Isolation and comparison of the LPS to that of the parental strain K56-2, along with complementation of the disrupted genes, may provide additional information about the authentic phage receptor.

Molecular cloning and modification of pSCRhaB2 into pSCRhaB2-Tc

Similar to pSCRhaB3, plasmid pSCRhaB2 carries a Tp^R marker for plasmid selection (Cardona & Valvano, 2005). Thus a series of digestions and ligations were performed in order to obtain a plasmid with a functional antibiotic marker. The selected marker was tetracycline (Tc), to which strain K56-2 is sensitive. This modification was performed prior the cloning of *waaC* and *wabO* into the plasmid.

pSCRhaB2 was first digested with *SacI*, thus eliminating a section (base 447 to 772) of the Tp^R promoter region, greatly disrupting the function of the cassette [Fig. 92]. The Tc^R cassette (~1.4 Kb) was extracted from p34S-Tc (Dennis & Zylstra, 1998) digesting it with *SacI* [Fig. 92]. After ligating both products, the resulting plasmid was named pSCRhaB2-Tc [Fig. 93]. Only the clones with the Tc^R cassette inserted in the opposite (reverse) orientation of the MCS were stored for future use [Fig. 93]. Testing revealed that cells carrying pSCRhaB2-Tc were highly resistant to Tc and not resistant to Tp , thus confirming

that the plasmid was modified properly and the new antibiotic cassette was functional [Fig. 94].

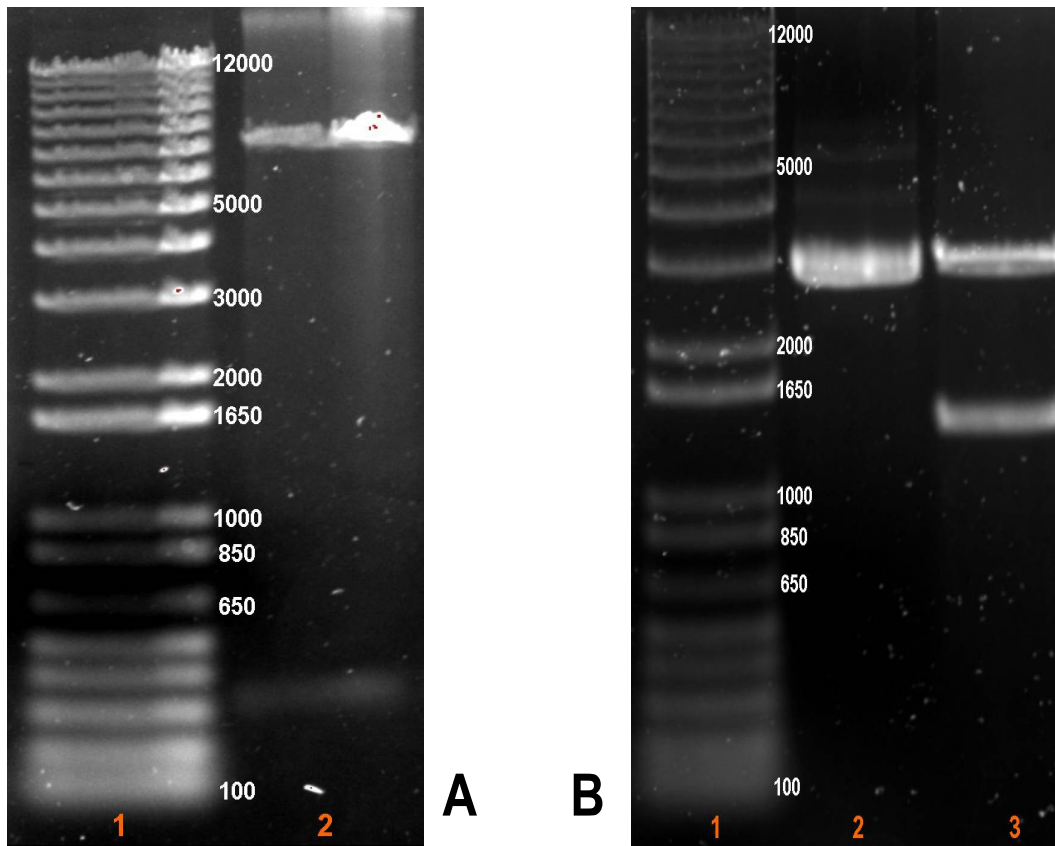


Figure 92: pDNA from *E. coli* DH5- α cells (Invitrogen): (A) Gel image, 1: 1 Kb Plus DNA ladder, 2: pSCRhaB2 digested with *SacI*, Tp^R promoter region (~320 bp) eliminated from plasmid. (B) Gel image, 1: 1 Kb Plus DNA ladder, 2: p34S-Tc undigested (control), 3: digested with *SacI*, Tc^R cassette (~1.4 Kb).

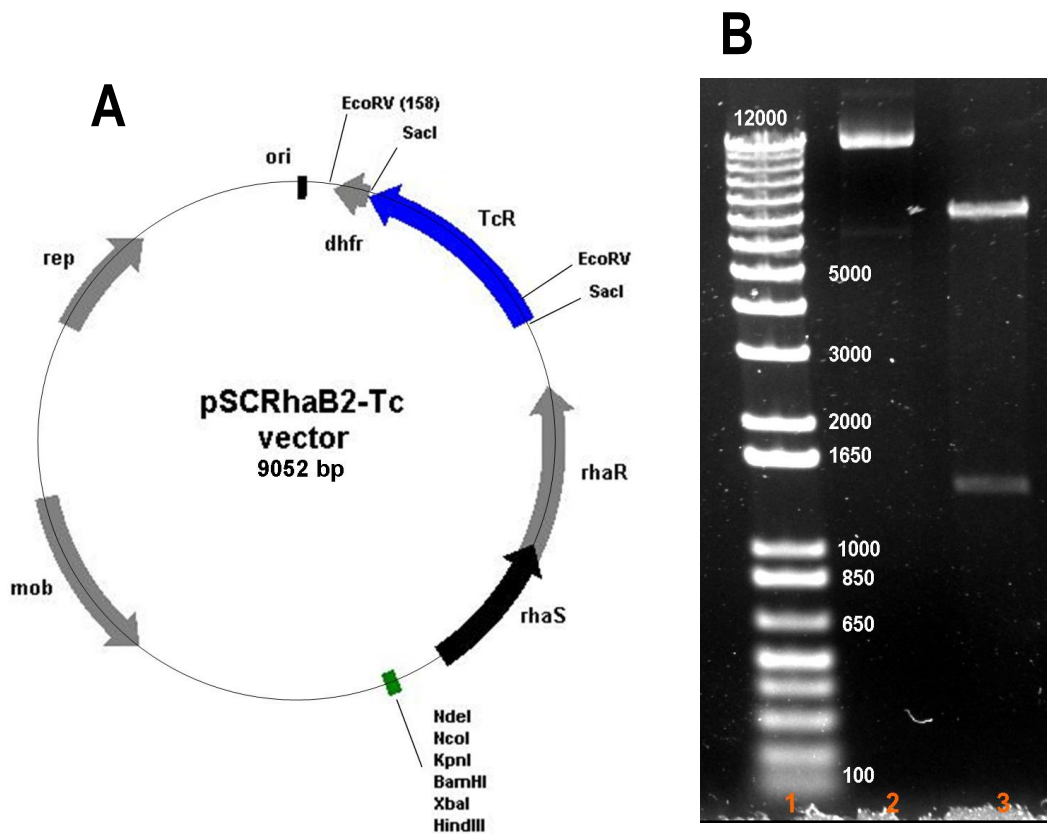


Figure 93: pDNA from *E. coli* DH5- α cells (Invitrogen): (A) Plasmid map from pSCRhaB2-Tc (empty vector) with the non functional *dhfr*, dihydrofolate reductase gene and the Tc^R cassette (*SacI*) inserted at the *SacI* sites (bases 447 to 772) of pSCRhaB2. MCS depicted in green. (B) Gel image, 1: 1 Kb Plus DNA ladder, 2: pSCRhaB2-Tc undigested (control), 3: digested with *EcoRV*.

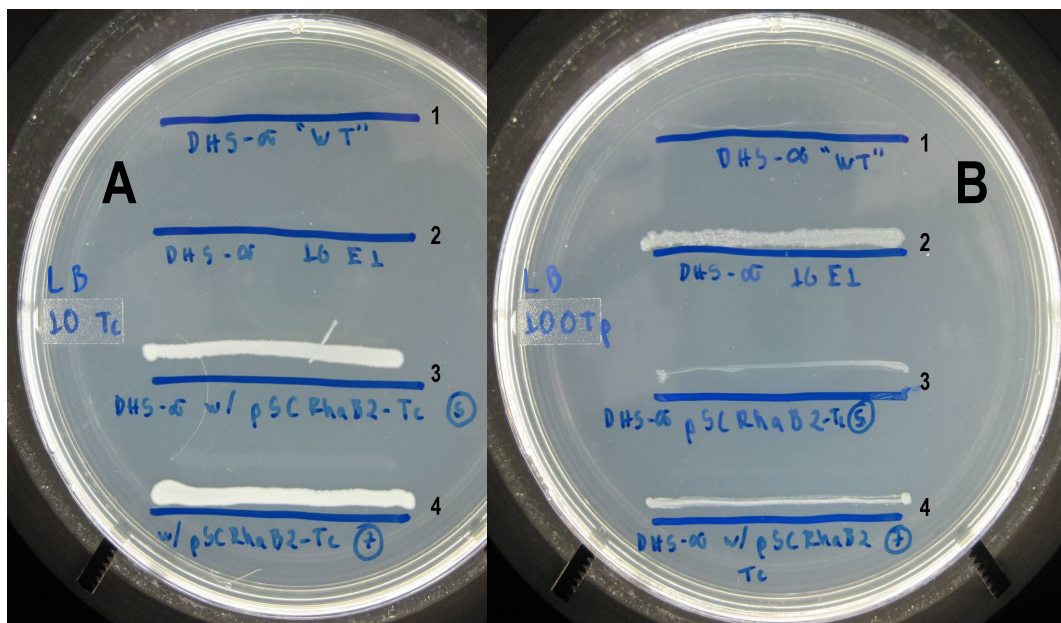


Figure 94: (A) *E. coli* DH5- α cells (Invitrogen) plated on LB + 10 μ g of Tc/mL. 1: With no plasmid (control), 2: Mutant 16 E1 (*wbxD-wbcE::Tp^R*) (control) carrying pTnModOTp', 3: Complemented with pSCRhaB2-Tc (empty vector) clone 5, 4: complemented with pSCRhaB2-Tc (empty vector) clone 7. (B) *E. coli* DH5- α cells (Invitrogen) plated on LB + 100 μ g of Tp/mL. 1: With no plasmid (control), 2: Mutant 16 E1 (*wbxD-wbcE::Tp^R*) (control) carrying pTnModOTp', 3: Complemented with pSCRhaB2-Tc (empty vector) clone 5, 4: complemented with pSCRhaB2-Tc (empty vector) clone 7.

Molecular cloning of *waaC* & *wabO* into pSCRhaB2-Tc

After pSCRhaB2-Tc was constructed, genes *waaC* and *wabO* [Fig. 95] were amplified by TopTaq (Qiagen) PCR using the *B. cenocepacia* K56-2 wt genomic DNA as a template. A 10X His Tag sequence was included on both products for analysis of protein expression.

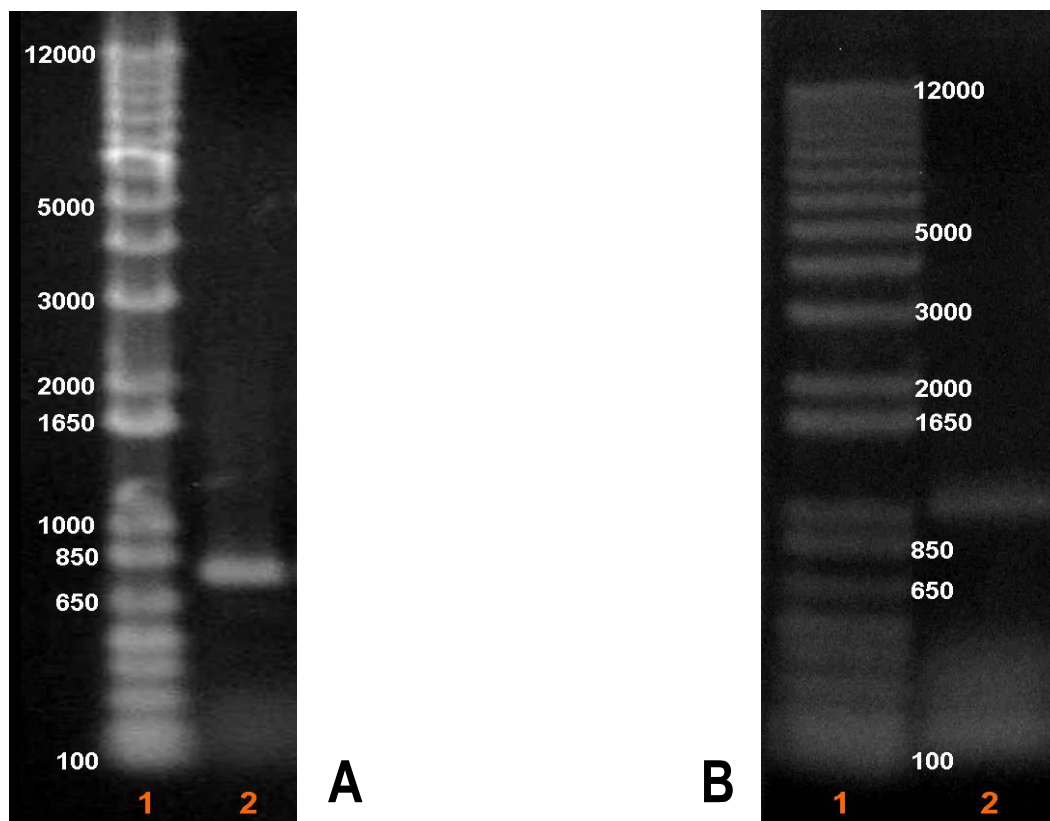


Figure 95: TopTaq PCR from *B. cenocepacia* K56-2 cDNA: (A) Gel image, 1: 1 Kb Plus DNA ladder, 2: *wabO* product (770 bp) 1 min. extension time and 69.5°C annealing temp. (B) Gel Image, 1: 1 Kb Plus DNA ladder, 2: *waaC* product (996 bp) 1:20 min. extension time and 56.5°C annealing temp.

Products were purified using a GeneClean III kit. PCR products were subsequently cloned into pJET1.2/blunt (Fermentas) using a blunt end cloning protocol following the manufacturer's instructions. To confirm the correct insertion of the product plasmid DNA was extracted from DH5- α (Invitrogen) cells carrying the plasmids and digested with the appropriate restriction enzymes [Fig. 96].

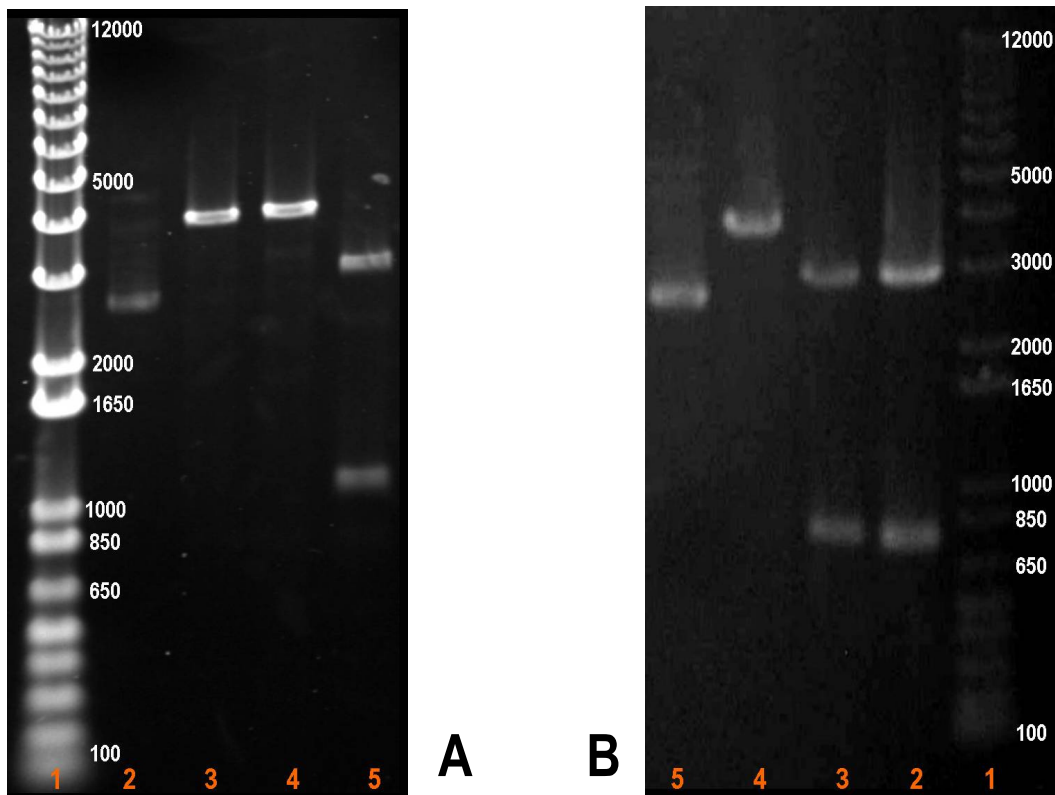


Figure 96: pDNA from *E. coli* DH5- α cells (Invitrogen): (A) Gel image, 1: 1 Kb Plus DNA ladder, 2: pJET1.2/blunt undigested (control), 3: pJET1.2/blunt digested with *Nde*I, 4: digested with *Bam*HI, 5: digested with *Nde*I-*Bam*HI, insert *waaC* (~ 1 Kb) and empty vector (~ 3 Kb). (B) Gel Image, 1: 1 Kb Plus DNA ladder, 2: pJET1.2/blunt digested with *Nde*I-*Xba*I, insert *wabO* (770 bp) and

empty vector (~ 3 Kb), 3: digested with *Xba*I, 4: digested with *Nde*I, 5: undigested (control).

To clone *wabO*, PCR products cloned in pJET1.2/blunt were excised from the gel and purified using GeneClean III. The products were subsequently cloned into pSCRhaB2-Tc. Resulting plasmids were named pSC*wabO*-Tc and pSC*waaC*-Tc [Fig. 97]. To confirm the correct insertion of the products both plasmids were screened by DNA digestion with the appropriate enzymes and also by sequencing; sequences revealed that genes were inserted properly.

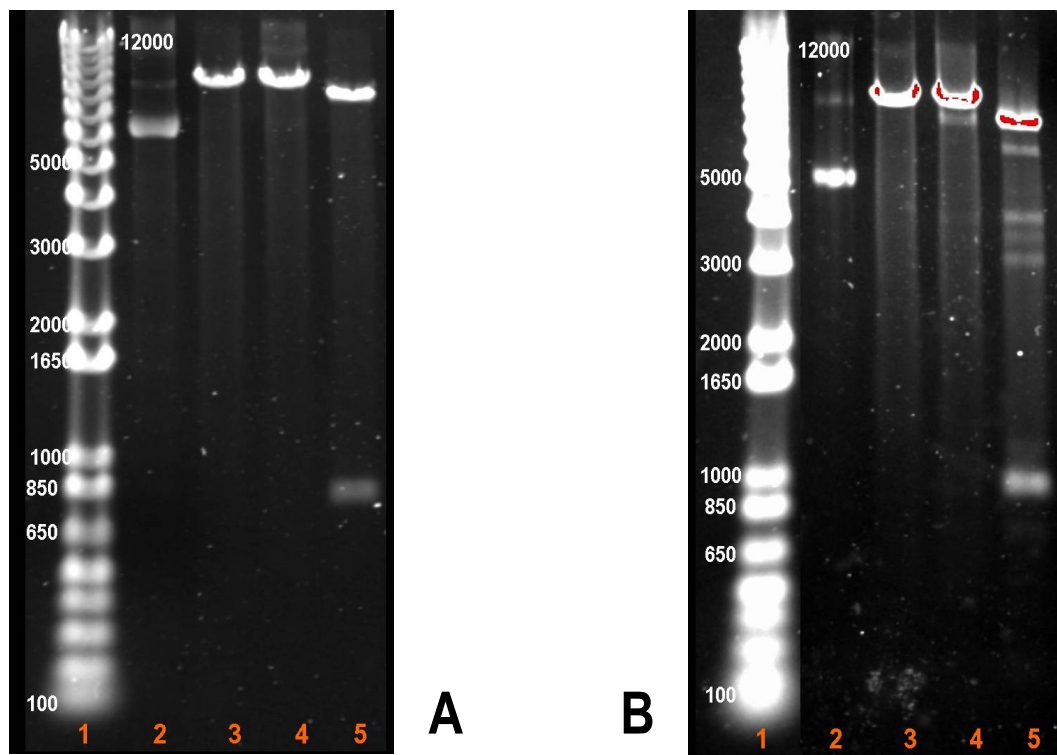


Figure 97: pDNA from *E. coli* DH5- α cells (Invitrogen): (A) Gel image, 1: 1 Kb Plus DNA ladder, 2: pSC*wabO*-Tc undigested (control), 3: digested with *Nde*I, 4: digested with *Xba*I, 5: digested with *Nde*I-*Xba*I, insert *wabO* (770 bp) and empty vector (~ 9 Kb). (B) Gel Image, 1: 1 Kb Plus DNA ladder, 2: pSC*waaC*-Tc undigested control, 3: digested with *Nde*I, 4: digested with *Xba*I, 5: digested with *Nde*I-*Xba*I, insert *waaC* (~ 1 Kb) and empty vector (~ 9 Kb).

Complementation of pSC*wabO*-Tc, pSC*waaC*-Tc, and pSCRhaB2-Tc into the K56-2 LPS truncated mutants XOA8 (*wabO*::pGPΩTp Tp^R) and CCB1 (*waaC*::pGPΩTp Tp^R)

After confirming the correct construction of previous plasmids, we mobilize them into the LPS truncated mutants XOA8 (*wabO*::pGPΩTp Tp^R) and CCB1 (*waaC*::pGPΩTp Tp^R). To further confirm if complementation of *wabO* and *waaC* would restore the wt phenotype. pSC*wabO*-Tc and pSCRhaB2-Tc were mobilized into mutant XOA8, and pSC*waaC*-Tc and pSCRhaB2-Tc into mutant CCB1 by tri-parental matings as previously described. Similar to mutant 16 E1 complemented with pXOs plasmids, mutants XOA8 [Fig. 98] and CCB1 [Fig. 99] complemented with the appropriate plasmid were subjected to colony PCR.

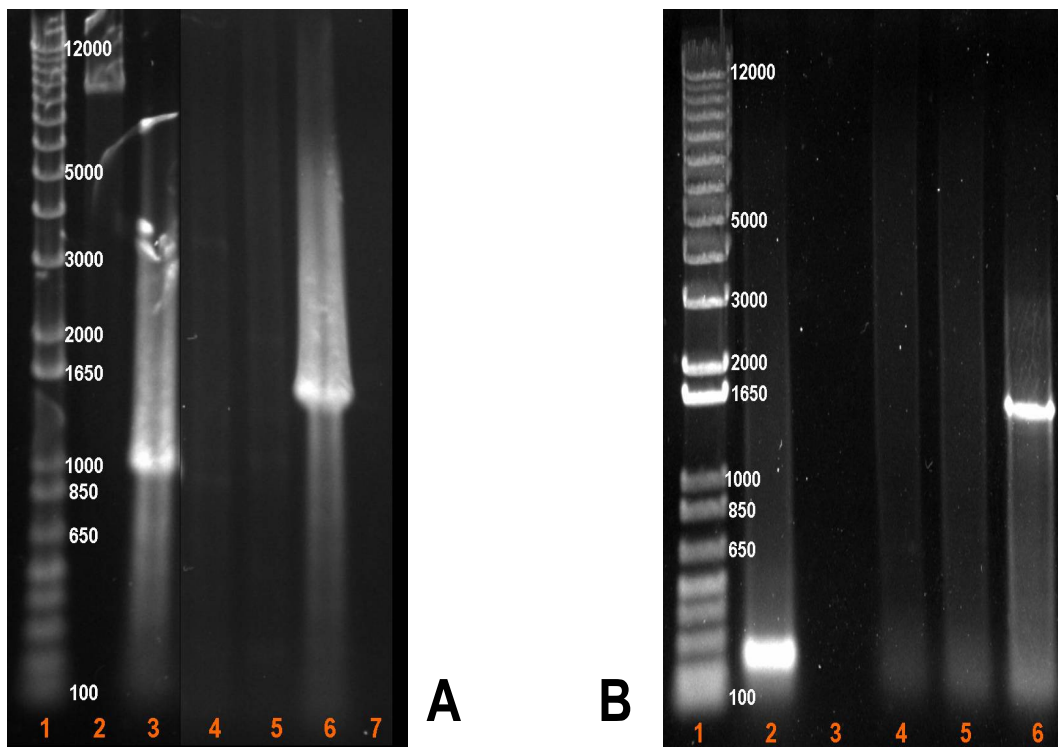


Figure 98: Colony PCR from mutant XOA8 (*wabO*::pGPΩTp Tp^R) complemented with pSC*wabO*-Tc and pSCRhaB2-Tc. (A) Gel image, 1: 1 Kb Plus DNA ladder,

2: Mutant XOA8 + pSC*wabO*-Tc colony number 1, 3: XOA8 + pSC*wabO*-Tc colony number 3, insert (~ 770 bp), 4: K56-2 wt (control), 5: mutant XOA8 (control), 6: pXO4 Tp-Tc (control), 7: mQH₂O (control). (B) Gel image, 1: 1 Kb Plus DNA ladder, 2: Mutant XOA8 + pSCRhaB2-Tc colony number 1, no insert (~ 150 bp), 3: mQH₂O (Control), 4: K56-2 wt (control), 5: mutant XOA8 (control), 6: pXO4 Tp-Tc (control).

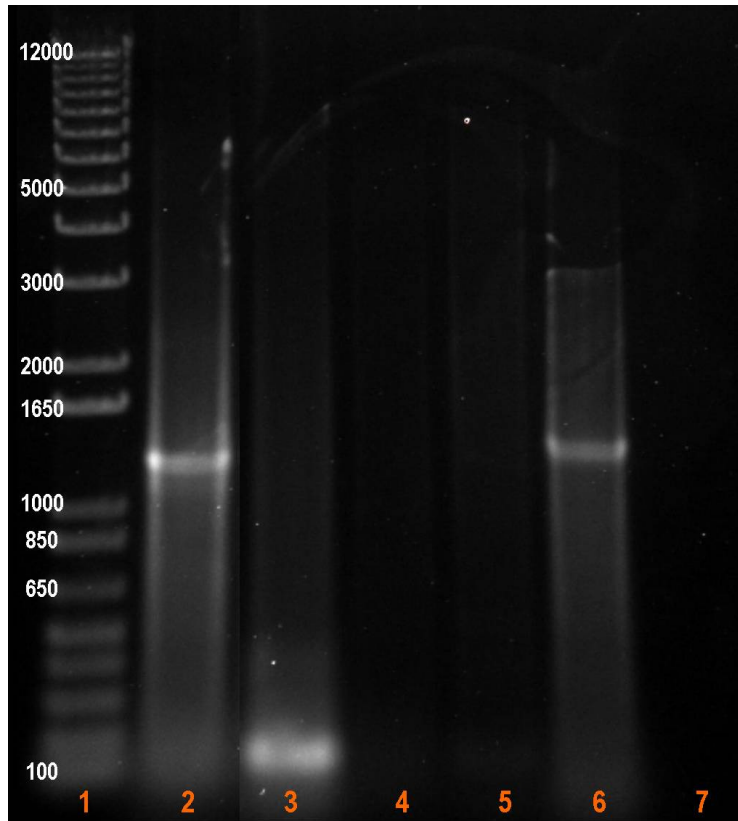


Figure 99: Colony PCR from mutant CCB1 (*waaC*::pGPΩTp Tp^R) complemented with pSC*waaC*-Tc and pSCRhaB2-Tc. Gel image, 1: 1 Kb Plus DNA ladder, 2: Mutant CCB1 + pSC*waaC*-Tc colony number 2, insert (~ 1 Kb), 3: mutant CCB1 + pSCRhaB2-Tc colony number 1, no insert (~ 150 bp), 4: K56-2 wt (control), 5: mutant CCB1 (control), 6: pXO4 Tp-Tc (control), 7: mQH₂O (control).

Bacteriophage infection assays vs. K56-2 LPS truncated mutants XOA8 (*wabO*::pGPΩTp Tp^R) complemented with pSC*wabO*-Tc and pSCRhaB2-Tc and CCB1 (*waaC*::pGPΩTp Tp^R) complemented with pSC*waaC*-Tc and pSCRhaB2-Tc [Liquid culture clearing assays]

To further confirm whether complementation of *wabO* and *waaC* in mutants XOA8 and CCB1 respectively would restore the wt phenotype (phage susceptibility), we performed a series of liquid culture clearing assays similar to those performed with the LPS truncated mutants and in mutant 16 E1 complemented with the pXOs plasmids. Similar control groups and test groups were analyzed, however for this particular case, complemented mutants XOA8 and CCB1 were exposed to phages KS5 and KS9. Previous data, including that from Lynch et al. (2010) suggested to us that these two phages utilize the LPS core OS as a receptor. pSCRhaB2-Tc also carries a rhamnose-inducible P_{RHA} promoter and the expression of the genes can be tightly regulated by the addition of rhamnose into the media. A plasmid set was induced with 0.2% rhamnose, while a second set was assayed under non-inducing conditions. Results revealed that strain XOA8 (*wabO*::pGPΩTp Tp^R) complemented with pSC*wabO*-Tc was sensitive to phages KS5 and KS9 infection; the plasmid fully restored the phenotype to wt levels [Figs. 100 & 102]. This suggests that the gene encoding the glucosyltransferase mediating the addition of β -D-glc to the HeptI appears to be essential for phage binding, further confirming the involvement of the outer core OS as a receptor for these phages.

Conversely, XOA8 complemented with pSCRhaB2-Tc (empty vector) showed partial resistance to phage infection [Figs. 101 & 103]. To confirm that this mutant was indeed resistant, we decided to plate phages (KS5 and KS9) and host (XOA8 + pSCRhaB2-Tc) by the soft agar overlay method. Results revealed that XOA8 + pSCRhaB2-Tc was resistant to phage infection, as no plaques were detected on the plates [data not shown]. This result was expected, however, we have no explanation as to why the control group in liquid cultures exhibit some sensitivity to phage infection. Similar results were observed in the non-induced conditions [data not shown].

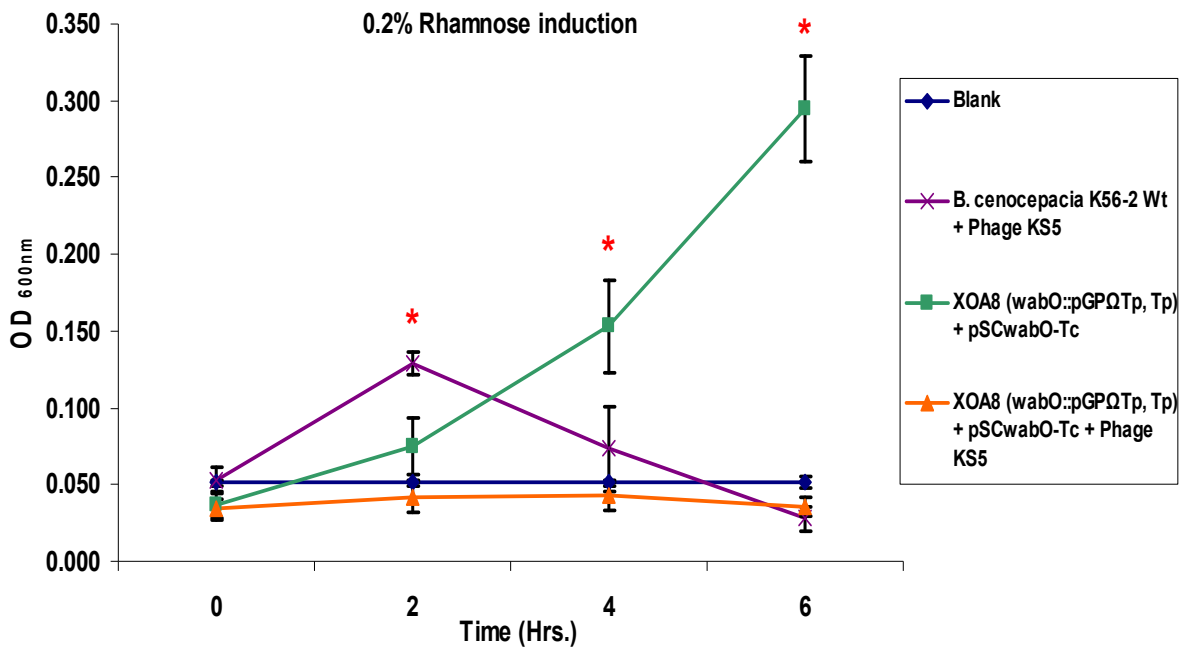


Figure 100: Growth curve of *B. cenocepacia* K56-2 LPS mutant XOA8 (*wabO::pGPΩTp Tp^R*) complemented with pSCwabO-Tc exposed to phage KS5: Blue, blank control (200 μ L of $\frac{1}{2}$ LB broth), Purple, wt control (10 μ L of K56-2 wt), (50 μ L of high titer phage stock) and (150 μ L of $\frac{1}{2}$ LB broth), Green, positive control (10 μ L of bacteria) and (190 μ L of $\frac{1}{2}$ LB broth + 100 μ g of Tp/mL + 100 μ g of Tc/mL + 0.2% Rha), Orange, test group (10 μ L of bacteria), (50 μ L of high titer phage stock) and (150 μ L of $\frac{1}{2}$ LB broth + 100 μ g of Tp/mL + 100 μ g of

Tc/mL + 0.2% Rha). Incubation at 37°C with continuous shaking (225 rpm). A_{600} measured every 2 hrs. for a period of 6 hrs in a Victor X3 2030 multilabel reader spectrophotometer. Mutant XOA8 (*wabO::pGPΩTp Tp^R*) + pSC*wabO*-Tc was previously grown on ½ LB broth + 100 µg of Tp/mL + 100 µg of Tc/mL + 0.2% Rha at 37°C with shaking (225 rpm) for ~16 hrs. Each point represents the mean of three independent experiments in triplicate; error bars indicate standard deviation. * Represents statistical significance between control (green) and test (orange) groups. A-Nova test (Tukey) ($P < 0.05$)

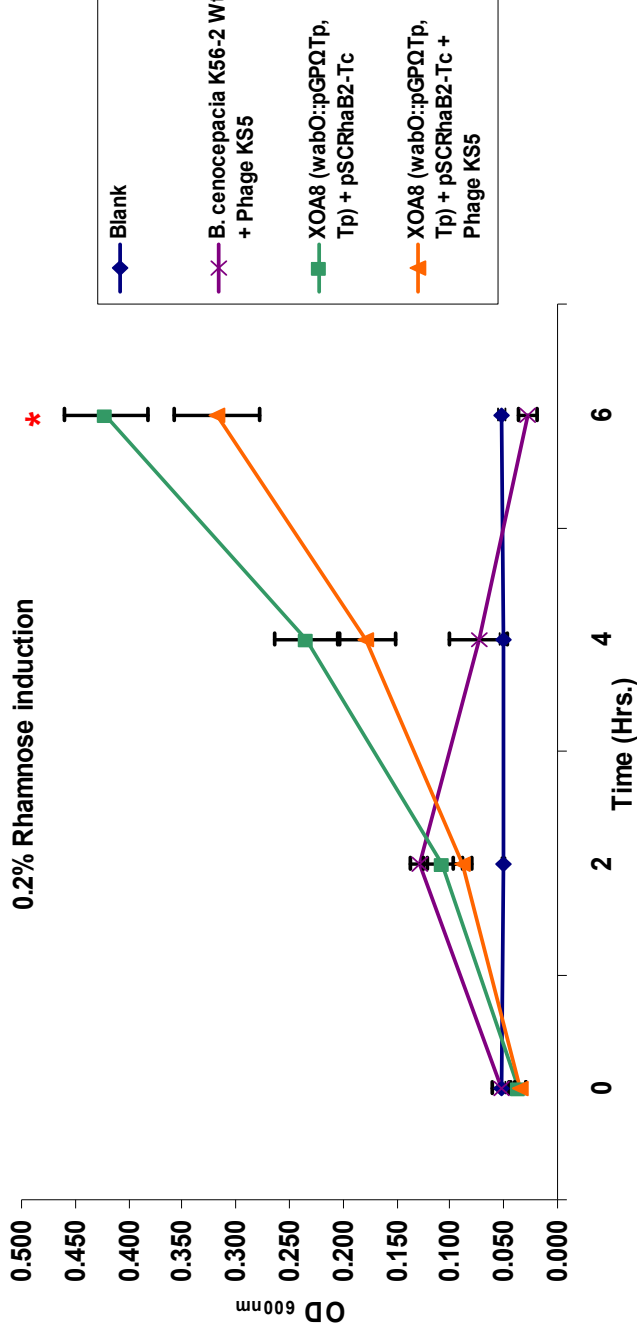


Figure 101: Growth curve of *B. cenocepacia* K56-2 LPS mutant XOA8 (*wabO*::pGPQTP Tp^R) complemented with pSCRhaB2-Tc exposed to phage KS5: Blue, blank control (200 μ L of $\frac{1}{2}$ LB broth), Purple, wt control (10 μ L of K56-2 wt), (50 μ L of high titer phage stock) and (150 μ L of $\frac{1}{2}$ LB broth), Green, positive control (10 μ L of bacteria) and (190 μ L of $\frac{1}{2}$ LB broth + 100 μ g of Tp/mL + 100 μ g of Tc/mL + 0.2% Rha), Orange, test group (10 μ L of bacteria), (50 μ L of high titer phage stock) and (150 μ L of $\frac{1}{2}$ LB broth + 100 μ g of Tc/mL + 100 μ g of Tp/mL + 0.2% Rha). Incubation at 37°C with continuous shaking (225 rpm). A₆₀₀ measured every 2 hrs. for a period of 6 hrs in a Victor X3 2030 multilabel reader spectrophotometer. Mutant XOA8 (*wabO*::pGPQTP Tp^R) + pSCRhaB2-Tc was previously grown on $\frac{1}{2}$ LB broth + 100 μ g of Tp/mL + 100 μ g of Tc/mL + 0.2% Rha at 37°C with shaking (225 rpm) for ~16 hrs. Each point represents the mean of three independent experiments in triplicate; error bars indicate standard deviation. * Represents statistical significance between control (green) and test (orange) groups. A-Nova test (Tukey) (P < 0.05)

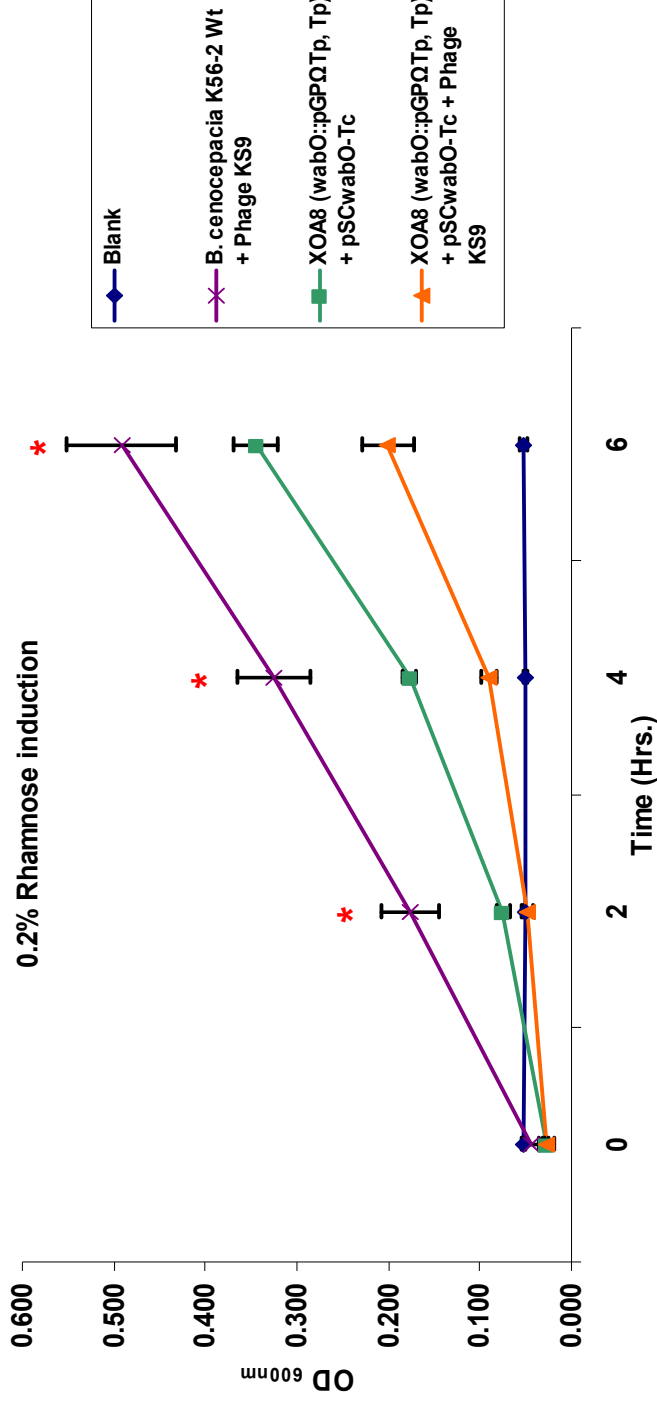


Figure 102: Growth curve of *B. cenocepacia* K56-2 LPS mutant XOA8 (*wabO*::pGPΩTp Tp^R) complemented with pSCwabO-Tc exposed to phage KS9: Blue, blank control (200 μL of ½ LB broth), Purple, wt control (10 μL of K56-2 wt), (50 μL of high titer phage stock) and (150 μL of ½ LB broth), Green, positive control (10 μL of bacteria) and (190 μL of ½ LB broth + 100 μg of Tp/mL + 100 μg of Tc/mL + 0.2% Rha), Orange, test group (10 μL of bacteria), (50 μL of high titer phage stock) and (150 μL of ½ LB broth + 100 μg of Tp/mL + 100 μg of Tc/mL + 0.2% Rha). Incubation at 37°C with continuous shaking (225 rpm). A₆₀₀ measured every 2 hrs. for a period of 6 hrs in a Victor X3 2030 multilabel reader spectrophotometer. Mutant XOA8 (*wabO*::pGPΩTp Tp^R) + pSCwabO-Tc was previously grown on ½ LB broth + 100 μg of Tp/mL + 100 μg of Tc/mL + 0.2% Rha at 37°C with shaking (225 rpm) for ~16 hrs. Each point represents the mean of three independent experiments in triplicate; error bars indicate standard deviation. * Represents statistical significance between control (green) and test (orange) groups. A-Nova test (Tukey) (P < 0.05)

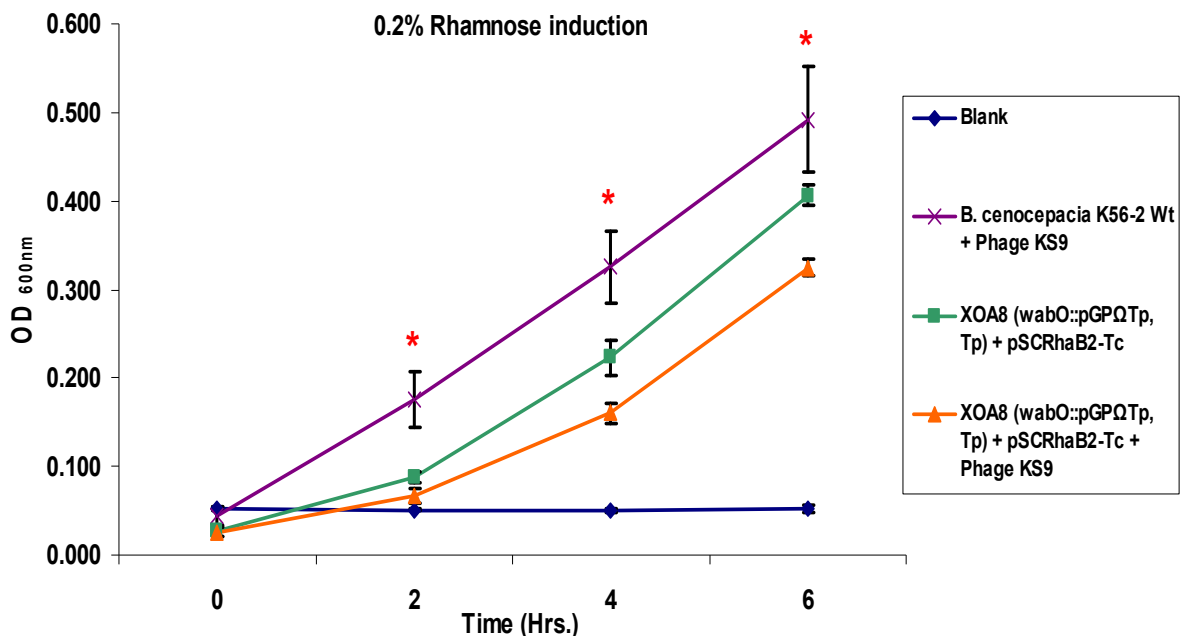


Figure 103: Growth curve of *B. cenocepacia* K56-2 LPS mutant XOA8 (*wabO*::pGPΩTp Tp^R) complemented with pSCRhaB2-Tc exposed to phage KS9: Blue, blank control (200 μL of ½ LB broth), Purple, wt control (10 μL of K56-2 wt), (50 μL of high titer phage stock) and (150 μL of ½ LB broth), Green, positive control (10 μL of bacteria) and (190 μL of ½ LB broth + 100 μg of Tp/mL + 100 μg of Tc/mL + 0.2% Rha), Orange, test group (10 μL of bacteria), (50 μL of high titer phage stock) and (150 μL of ½ LB broth + 100 μg of Tp/mL + 100 μg of Tc/mL + 0.2% Rha). Incubation at 37°C with continuous shaking (225 rpm). A₆₀₀ measured every 2 hrs. for a period of 6 hrs in a Victor X3 2030 multilabel reader spectrophotometer. Mutant XOA8 (*wabO*::pGPΩTp Tp^R) + pSCRhaB2-Tc was previously grown on ½ LB broth + 100 μg of Tp/mL + 100 μg of Tc/mL + 0.2% Rha at 37°C with shaking (225 rpm) for ~16 hrs. Each point represents the mean of three independent experiments in triplicate; error bars indicate standard deviation. * Represents statistical significance between control (green) and test (orange) groups. A-Nova test (Tukey) (P < 0.05)

In the case of mutant CCB1 (*waaC*::pGPΩTp Tp^R) complemented with pSCwaaC-Tc, an interesting phenomenon was observed. When the plasmid was induced with 0.2% rhamnose the growth levels of both the test (CCB1 + pSCwaaC-Tc) [Fig. 101] and the control (CCB1 + pSCRhaB2-Tc) [Fig. 102] groups were greatly reduced and after six hours the bacteria barely grew.

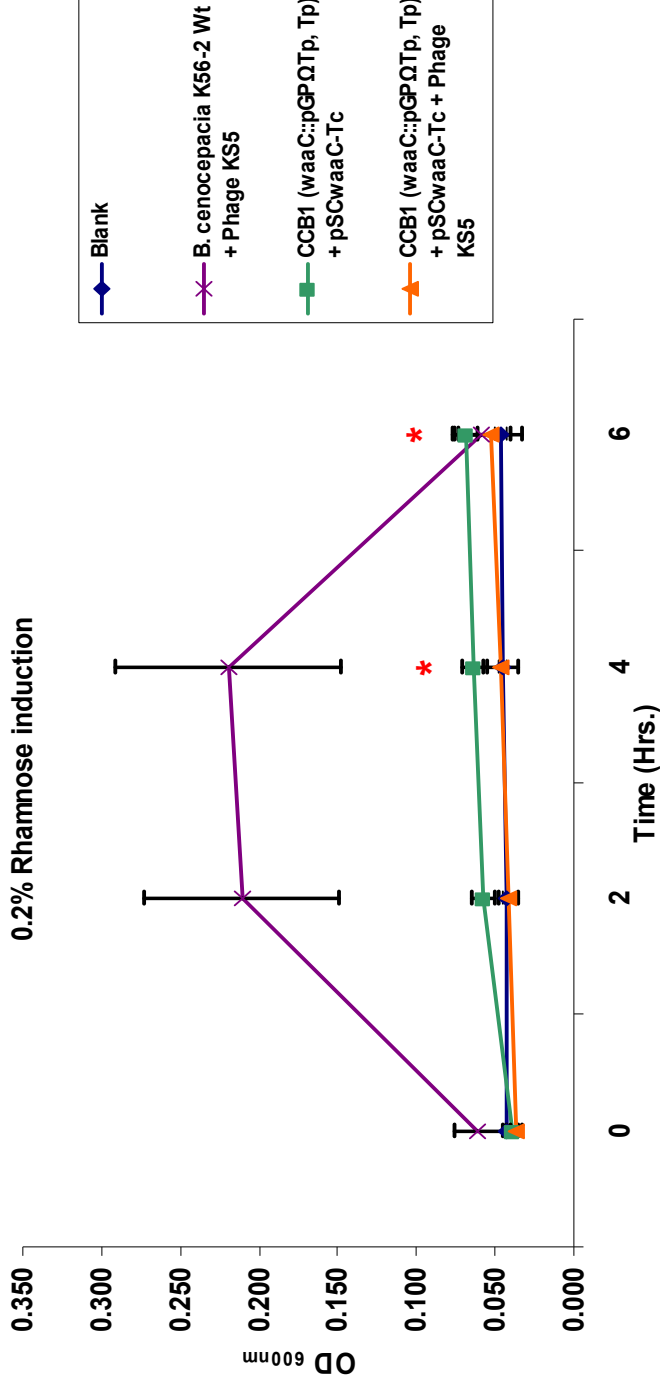


Figure 104: Growth curve of *B. cenocepacia* K56-2 LPS mutant CCB1 (*waaC*::pGP Ω Tp Tp^R) complemented with pSCwaaC-Tc exposed to phage KS5: Blue, blank control (200 μ L of $\frac{1}{2}$ LB broth), Purple, wt control (10 μ L of K56-2 wt), (50 μ L of high titer phage stock) and (150 μ L of $\frac{1}{2}$ LB broth), Green, positive control (10 μ L of bacteria) and (190 μ L of $\frac{1}{2}$ LB broth + 100 μ g of Tp/mL + 100 μ g of Tc/mL + 0.2% Rha), Orange, test group (10 μ L of bacteria), (50 μ L of high titer phage stock) and (150 μ L of $\frac{1}{2}$ LB broth + 100 μ g of Tc/mL + 100 μ g of Tp/mL + 0.2% Rha). Incubation at 37°C with continuous shaking (225 rpm). A₆₀₀ measured every 2 hrs. for a period of 6 hrs in a Victor X3 2030 multilabel reader spectrophotometer. Mutant CCB1 (*waaC*::pGP Ω Tp Tp^R) + pSCwaaC-Tc was previously grown on $\frac{1}{2}$ LB broth + 100 μ g of Tp/mL + 100 μ g of Tc/mL + 0.2% Rha at 37°C with shaking (225 rpm) for ~16 hrs. Each point represents the mean of three independent experiments in triplicate; error bars indicate standard deviation. * Represents statistical significance between control (green) and test (orange) groups. A-Nova test (Tukey) (P < 0.05)

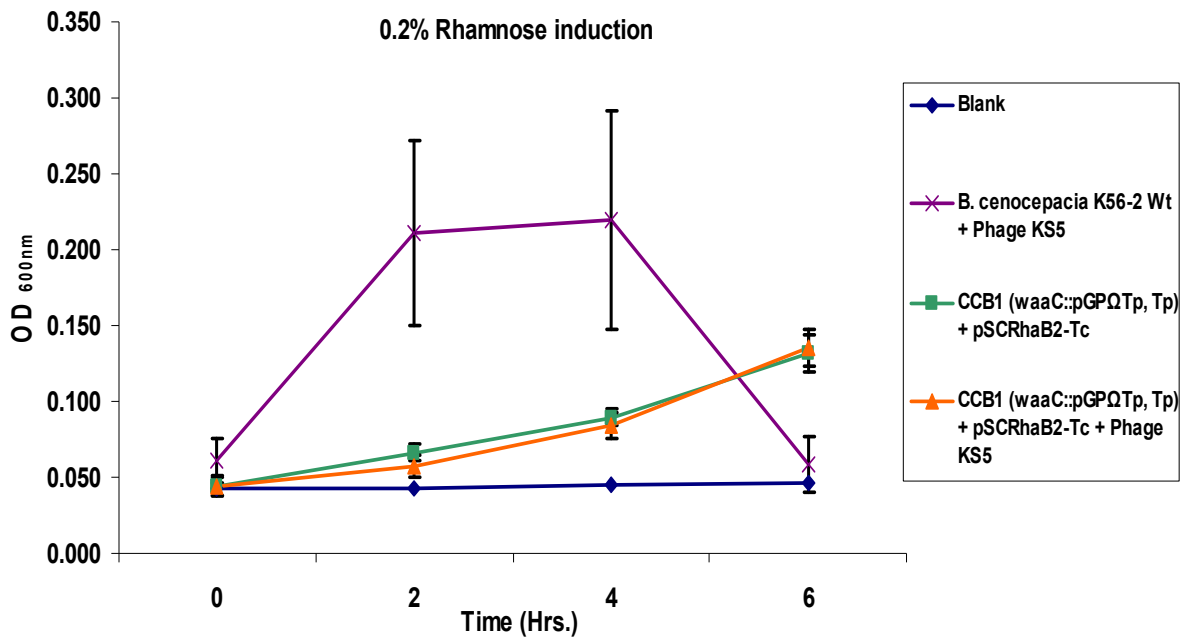


Figure 105: Growth curve of *B. cenocepacia* K56-2 LPS mutant CCB1 (*waaC*::pGPΩTp Tp^R) complemented with pSCRhaB2-Tc exposed to phage KS5: Blue, blank control (200 μL of ½ LB broth), Purple, wt control (10 μL of K56-2 wt), (50 μL of high titer phage stock) and (150 μL of ½ LB broth), Green, positive control (10 μL of bacteria) and (190 μL of ½ LB broth + 100 μg of Tp/mL + 100 μg of Tc/mL + 0.2% Rha), Orange, test group (10 μL of bacteria), (50 μL of high titer phage stock) and (150 μL of ½ LB broth + 100 μg of Tp/mL + 100 μg of Tc/mL + 0.2% Rha). Incubation at 37°C with continuous shaking (225 rpm). A₆₀₀ measured every 2 hrs. for a period of 6 hrs in a Victor X3 2030 multilabel reader spectrophotometer. Mutant CCB1 (*waaC*::pGPΩTp Tp^R) + pSCRhaB2-Tc was previously grown on ½ LB broth + 100 μg of Tp/mL + 100 μg of Tc/mL + 0.2% Rha at 37°C with shaking (225 rpm) for ~16 hrs. Each point represents the mean of three independent experiments in triplicate; error bars indicate standard deviation. * Represents statistical significance between control (green) and test (orange) groups. A-Nova test (Tukey) (P < 0.05)

We hypothesized that because *waaC* is one of the first genes involved in the synthesis of the inner core OS, the overexpression of the gene plus the antibiotics in the media overcome the low copy plasmid efficiency, thus greatly affecting the growth levels. In addition, the cell wall in mutant CCB1 may be less efficient at protecting the host from external elements, such as antibiotics, due to the deep

LPS truncation and this might contribute to the reduced growth levels observed. Further, when mutant CCB1 is streaked on an agar plate, the colonies are usually smaller in size than the rest of the LPS truncated mutants after a 16 hr. incubation [data not shown]. Interestingly, the liquid ON culture of CCB1 + pSC*waaC*-Tc and CCB1 + pSCRhaB2-Tc after a 16 hr. incubation have a normal growth level; only when the bacteria is subcultured into fresh media do we see this reduced growth. For this reason, we performed the assays adding only 0.02% rhamnose, which had been previously demonstrated to be functional for gene induction (Cardona & Valvano, 2005). Results revealed that growth levels improved, although they did not reach the wt growth levels, or those observed for the non-induced group [Fig. 106 & 107]. However, it was possible to determine that CCB1 + pSC*waaC*-Tc was sensitive to phages KS5 [Fig. 108] and KS9 infection as well [data not shown], confirming that the plasmid restored the phenotype.

Results suggests that 1) *wabO* is indeed the gene required for phage binding, further confirming the involvement of the outer core OS as the receptor for these phages 2) complementation of *waaC* undoubtedly restores the wt phenotype, and complementation of this gene permits the rest of the LPS genes (including *wabO*) to be expressed. Recently, another student in our lab working with the same gene, performed a series of liquid clearing assays against phage KS10, with the assay extended for a period of 10 hrs. After 10 hrs. the growth levels were comparable to those for the non-induced group (Abdu, personal communication).

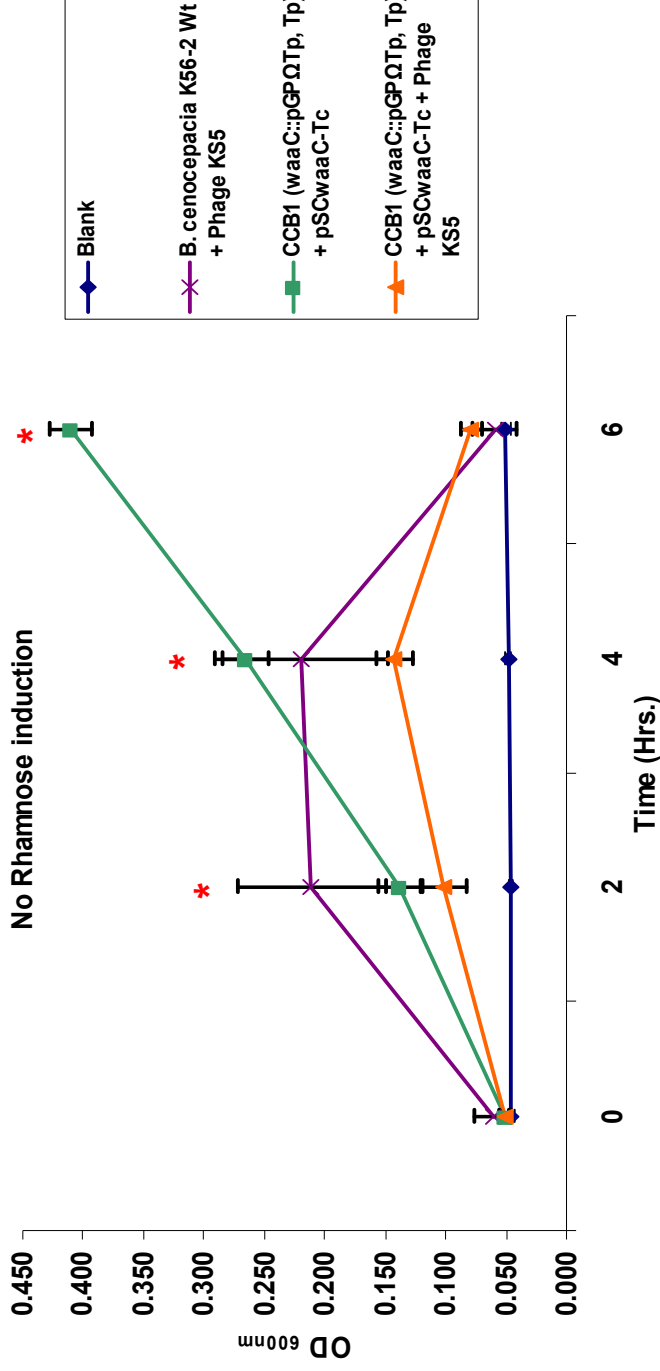


Figure 106: Growth curve of *B. cenocepacia* K56-2 LPS mutant CCB1 (*waaC*::pGPΩTp Tp^R) complemented with pSC*waaC*-Tc exposed to phage KS5: Blue, blank control (200 μL of ½ LB broth), Purple, wt control (10 μL of K56-2 wt), (50 μL of high titer phage stock) and (150 μL of ½ LB broth), Green, positive control (10 μL of bacteria) and (190 μL of ½ LB broth + 100 μg of Tp/mL + 100 μg of Tc/mL), Orange, test group (10 μL of bacteria), (50 μL of high titer phage stock) and (150 μL of ½ LB broth + 100 μg of Tp/mL + 100 μg of Tc/mL). Incubation at 37°C with continuous shaking (225 rpm). A₆₀₀ measured every 2 hrs. for a period of 6 hrs in a Victor X3 2030 multilabel reader spectrophotometer. Mutant CCB1 (*waaC*::pGPΩTp Tp^R) + pSC*waaC*-Tc was previously grown on ½ LB broth + 100 μg of Tp/mL + 100 μg of Tc/mL at 37°C with shaking (225 rpm) for ~16 hrs. Each point represents the mean of three independent experiments in triplicate; error bars indicate standard deviation. * Represents statistical significance between control (green) and test (orange) groups. A-Nova test (Tukey) (P < 0.05)

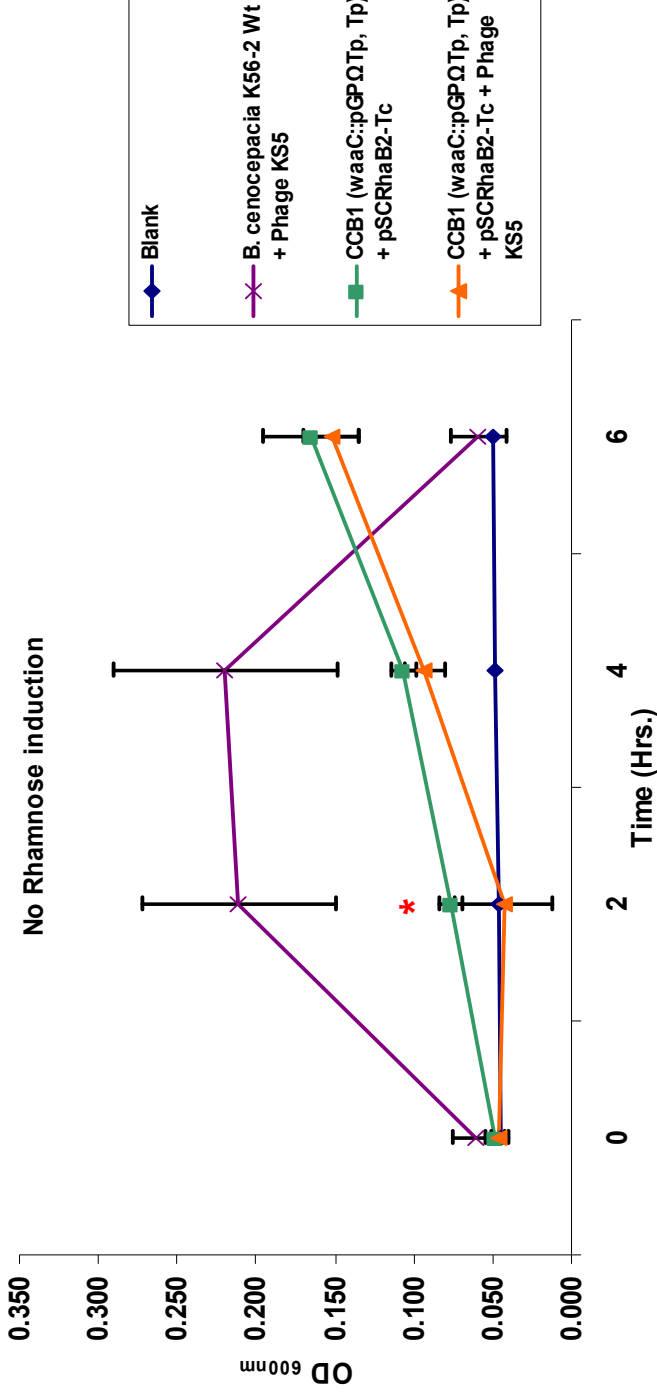


Figure 107: Growth curve of *B. cenocepacia* K56-2 LPS mutant CCB1 (*waaC*::pGPΩTp Tp^R) complemented with pSCRhaB2-Tc exposed to phage KS5: Blue, blank control (200 μL of ½ LB broth), Purple, wt control (10 μL of K56-2 wt), (50 μL of high titer phage stock) and (150 μL of ½ LB broth), Green, positive control (10 μL of bacteria) and (190 μL of ½ LB broth + 100 μg of Tp/mL + 100 μg of Tc/mL), Orange, test group (10 μL of bacteria), (50 μL of high titer phage stock) and (150 μL of ½ LB broth + 100 μg of Tp/mL + 100 μg of Tc/mL). Incubation at 37°C with continuous shaking (225 rpm). A₆₀₀ measured every 2 hrs. for a period of 6 hrs in a Victor X3 2030 multilabel reader spectrophotometer. Mutant CCB1 (*waaC*::pGPΩTp Tp^R) + pSCRhaB2-Tc was previously grown on ½ LB broth + 100 μg of Tp/mL + 100 μg of Tc/mL at 37°C with shaking (225 rpm) for ~16 hrs. Each point represents the mean of three independent experiments in triplicate; error bars indicate standard deviation. * Represents statistical significance between control (green) and test (orange) groups. A-Nova test (Tukey) (P < 0.05)

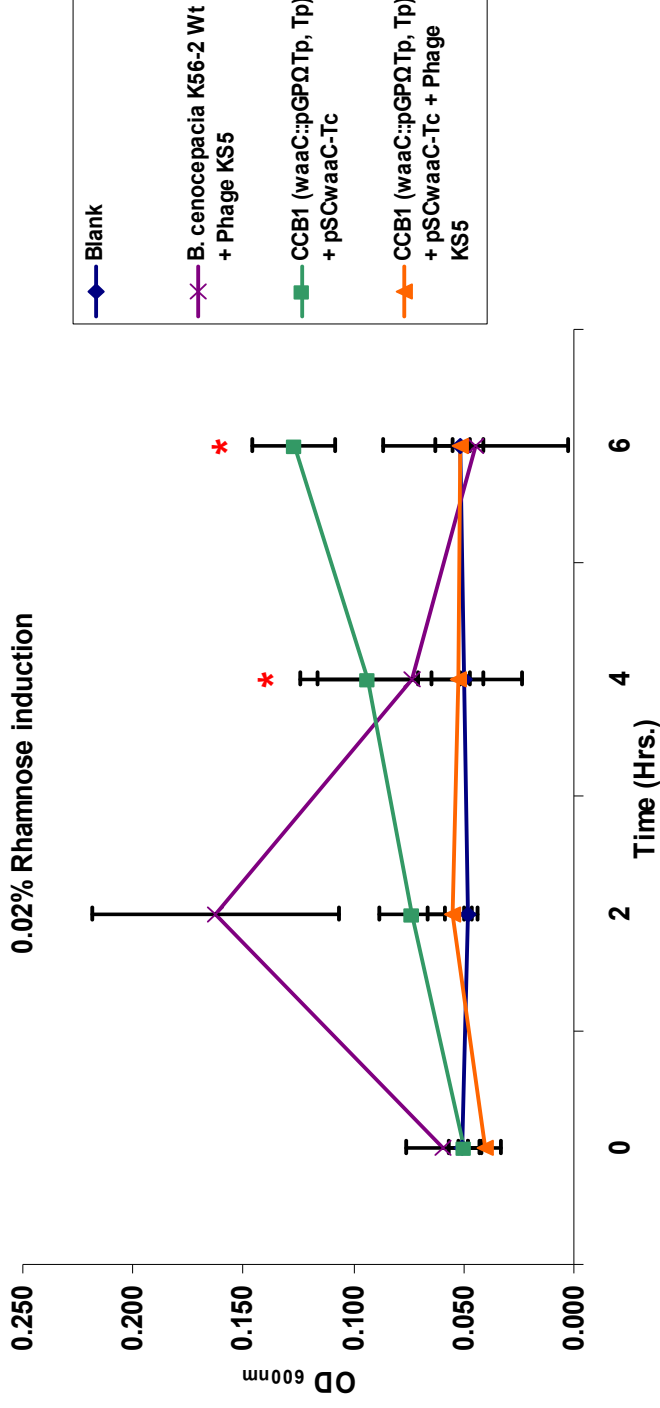


Figure 108: Growth curve of *B. cenocepacia* K56-2 LPS mutant CCB1 (*waaC*::pGPO Tp^R) complemented with pSCwaaC-Tc exposed to phage KS5: Blue, blank control (200 μ L of $\frac{1}{2}$ LB broth), Purple, wt control (10 μ L of K56-2 wt), (50 μ L of high titer phage stock) and (150 μ L of $\frac{1}{2}$ LB broth), Green, positive control (10 μ L of bacteria) and (190 μ L of $\frac{1}{2}$ LB broth + 100 μ g of Tp/mL + 100 μ g of Tc/mL + 0.02% Rha), Orange, test group (10 μ L of bacteria), (50 μ L of high titer phage stock) and (150 μ L of $\frac{1}{2}$ LB broth + 100 μ g of Tp/mL + 100 μ g of Tc/mL + 0.02% Rha). Incubation at 37°C with continuous shaking (225 rpm). A₆₀₀ measured every 2 hrs. for a period of 6 hrs in a Victor X3 2030 multilabel reader spectrophotometer. Mutant CCB1 (*waaC*::pGPO Tp^R) + pSCwaaC-Tc was previously grown on $\frac{1}{2}$ LB broth + 100 μ g of Tp/mL + 100 μ g of Tc/mL + 0.02% Rha at 37°C with shaking (225 rpm) for ~16 hrs. Each point represents the mean of three independent experiments in triplicate; error bars indicate standard deviation. * Represents statistical significance between control (green) and test (orange) groups. A-Nova test (Tukey) (P < 0.05)

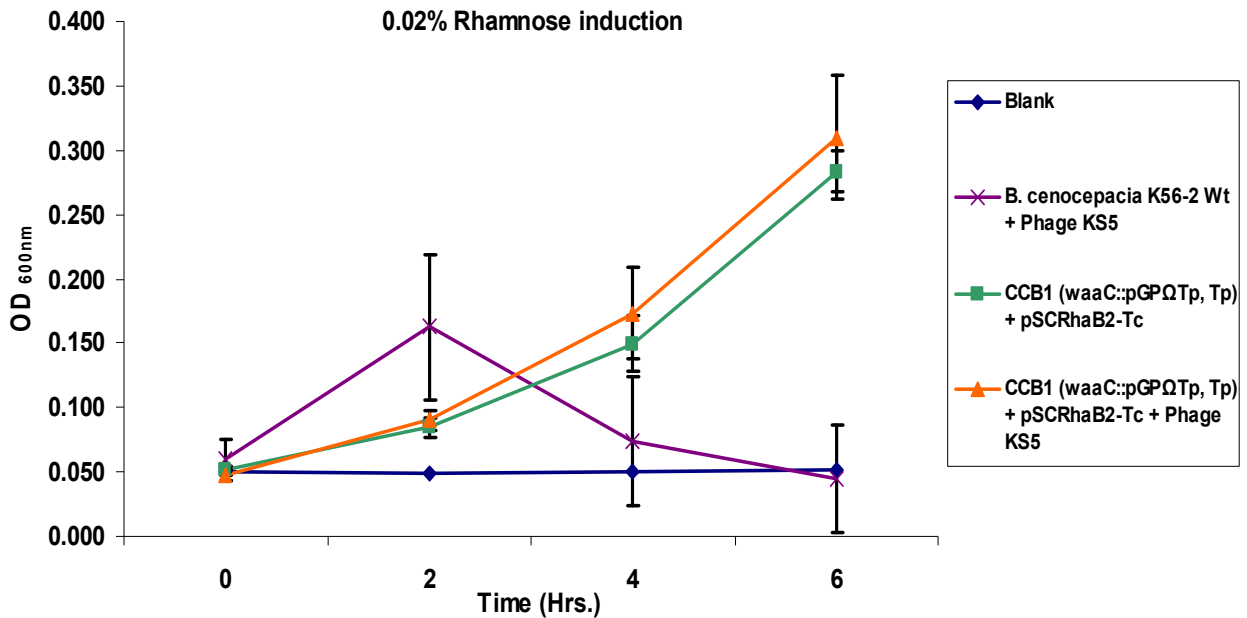


Figure 109: Growth curve of *B. cenocepacia* K56-2 LPS mutant CCB1 (*waaC*::pGPΩTp Tp^R) complemented with pSCRhaB2-Tc exposed to phage KS5: Blue, blank control (200 μL of ½ LB broth), Purple, wt control (10 μL of K56-2 wt), (50 μL of high titer phage stock) and (150 μL of ½ LB broth), Green, positive control (10 μL of bacteria) and (190 μL of ½ LB broth + 100 μg of Tp/mL + 100 μg of Tc/mL + 0.02% Rha), Orange, test group (10 μL of bacteria), (50 μL of high titer phage stock) and (150 μL of ½ LB broth + 100 μg of Tp/mL + 100 μg of Tc/mL + 0.02% Rha). Incubation at 37°C with continuous shaking (225 rpm). A₆₀₀ measured every 2 hrs. for a period of 6 hrs in a Victor X3 2030 multilabel reader spectrophotometer. Mutant CCB1 (*waaC*::pGPΩTp Tp^R) + pSCRhaB2-Tc was previously grown on ½ LB broth + 100 μg of Tp/mL + 100 μg of Tc/mL + 0.02% Rha at 37°C with shaking (225 rpm) for ~16 hrs. Each point represents the mean of three independent experiments in triplicate; error bars indicate standard deviation. * Represents statistical significance between control (green) and test (orange) groups. A-Nova test (Tukey) (P < 0.05)

To confirm that CCB1 + pSCRhaB2-Tc was resistant to phages KS5 and KS9 infection, we plated phages and bacterial hosts using the soft agar overlay method. Results revealed that CCB1 + pSCRhaB2-Tc was resistant to phage infection, and no plaques were detected on the plates [data not shown].

LPS extraction, purification and visualization from XOA8 (*wabO*::pGPΩTp Tp^R) complemented with pSC*wabO*-Tc and pSCRhaB2-Tc and from CCB1 (*waaC*::pGPΩTp Tp^R) complemented with pSC*waaC*-Tc and pSCRhaB2-Tc

To further identify a possible difference in LPS structure between the strains K56-2 wt, XOA8 (*wabO*::pGPΩTp Tp^R), CCB1 (*waaC*::pGPΩTp Tp^R) and the same mutants complemented with the appropriate plasmids, we extracted and visualized the LPS from each strain. In addition, we wanted to determine if there was an obvious difference in LPS production between plasmid induction versus no induction with rhamnose. The LPS was extracted using proteinase K, and samples were visualized on Tri-Tricine gels with silver staining. Both attempts using this approach failed and no LPS was detected. The conditions were the same as those performed on mutant 16 E1 + pXOs plasmids, therefore we can not explain why LPS was not present for mutants XOA8 and CCB1.

Subsequently, the samples were tested on a Tris-Glycine system [Figs. 110 & 111]. Similar to previous attempts, staining revealed no apparent differences between the 0.2%, 0.02% rhamnose induced overnight cultures and the uninduced cultures, with the exception of CCB1 (*waaC*::pGPΩTp Tp^R) + pSC*waaC*-Tc [Fig. 111, lanes 7 & 8]. The uninduced lane shows slightly stronger staining, perhaps because the growth levels were higher in this culture, as was observed in the liquid clearing assays. Another interesting phenomenon detected was that all samples contained thin Lipid A-core OS bands, and no additional bands were detected, opposite to the case of mutant 16 E1 complemented with pXOs plasmids

where several additional bands were observed. Perhaps this is the reason why XOA8 and CCB1 Lipid A-core OS bands were not visualized on Tricine gels.

However, an obvious difference was detected between mutants XOA8 and CCB1 when compared to K56-2 wt and the complemented mutants with either pSC*wabO*-Tc or pSC*waaC*-Tc, which both produced a similar LPS banding pattern to the wt strain [Figs. 110 & 111, lanes 1-4]. As we previously mentioned, because XOA8 and CCB1 carry single mutations, once the disrupted gene is complemented (with either *wabO* or *waaC*), the complete LPS structure (Lipid A, core OS and O-antigen) should be produced and is detectable on the gels. For XOA8 and CCB1 complemented with pSCRhaB2-Tc (negative control), the LPS banding pattern is similar to that seen for the mutants since no complementing gene is present on the plasmid [Figs. 110 & 111, lanes 9 & 10].

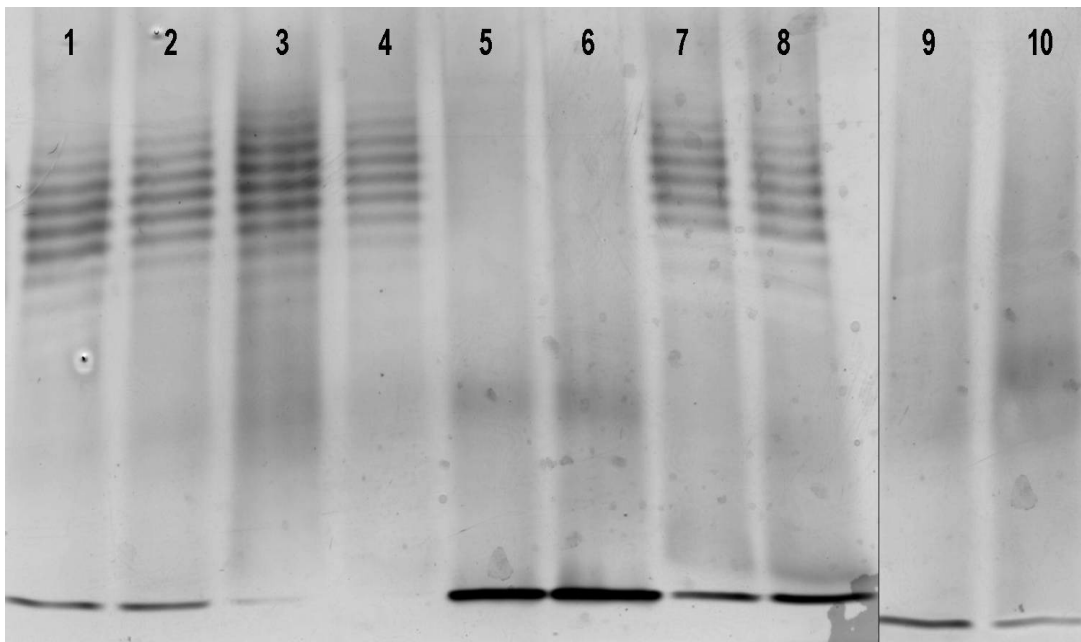


Figure 110: LPS electrophoretic profiles from *B. cenocepacia* K56-2 wt and K56-2 LPS truncated mutant XOA8 (*wabO*::pGPΩTp Tp^R): 1: K56-2 wt induced with 0.2% Rha, 2: K56-2 wt non-induced, 3: K56-2 wt + pSCRhaB2-Tc + 0.2% Rha,

4: K56-2 wt + pSCRhaB2-Tc, 5: XOA8 (*wabO*::pGPΩTp Tp^R) + 0.2% Rha, 6: XOA8 (*wabO*::pGPΩTp Tp^R), 7: XOA8 (*wabO*::pGPΩTp Tp^R) + pSC*wabO*-Tc + 0.2% Rha, 8: XOA8 (*wabO*::pGPΩTp Tp^R) + pSC*wabO*-Tc, 9: XOA8 (*wabO*::pGPΩTp Tp^R) + pSCRhaB2-Tc + 0.2% Rha, 10: XOA8 (*wabO*::pGPΩTp Tp^R) + pSCRhaB2-Tc.

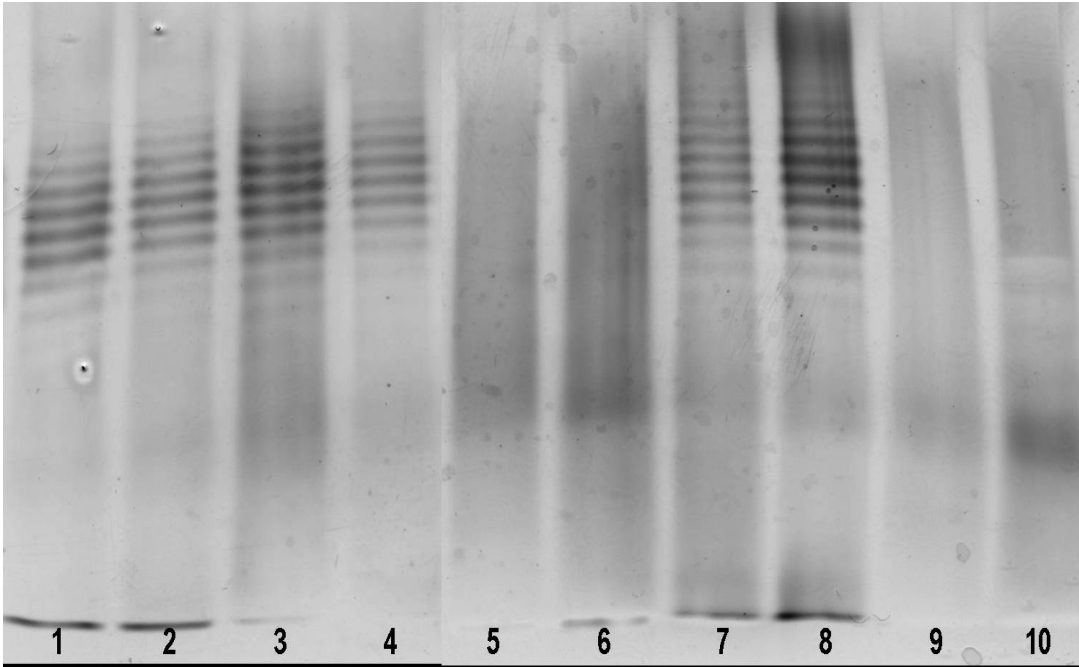


Figure 111: LPS electrophoretic profiles from *B. cenocepacia* K56-2 wt and K56-2 LPS truncated mutant CCB1 (*waaC*::pGPΩTp Tp^R): 1: K56-2 wt induced with 0.2% Rha, 2: K56-2 wt noninduced, 3: K56-2 wt + pSCRhaB2-Tc + 0.2% Rha, 4: K56-2 wt + pSCRhaB2-Tc, 5: CCB1 (*waaC*::pGPΩTp Tp^R) + 0.2% Rha, 6: CCB1 (*waaC*::pGPΩTp Tp^R), 7: CCB1 (*waaC*::pGPΩTp Tp^R) + pSC*waaC*-Tc + 0.2% Rha, 8: CCB1 (*waaC*::pGPΩTp Tp^R) + pSC*waaC*-Tc, 9: CCB1 (*waaC*::pGPΩTp Tp^R) + pSCRhaB2-Tc + 0.2% Rha, 10: CCB1 (*waaC*::pGPΩTp Tp^R) + pSCRhaB2-Tc.

To summarize we were able to determine after a series of experiments that phages KS5 and KS9 bind to the outer core OS (rough LPS phenotype) in order to infect their host. Our results are similar to those reported by Lynch et al. (2010). Phages binding to a host with R-type LPS (Lipid A, core OS) have been previously described. Some of the well-studied examples include phage T7 (Molineux, 2001; Kemp et al., 2005) and phages F0, S13, 6SR and PhiX174

(Rakhuba et al., 2010). Phages KS5 and KS9 can also be included in this category. Based upon these results, we are confident that the LPS core OS serves as a receptor during phage infection.

Western Blots from mutant 16 E1 complemented with pXO4 Tp-Tc, pXO7 Tp-Tc and pSCRhaB3 Tp-Tc and from K56-2 LPS mutants XOA8 complemented with pSCwabO-Tc and pSCRhaB2-Tc and from CCB1 (*waaC::pGPΩTp Tp^R*) complemented with pSCwaaC-Tc and pSCRhaB2-Tc

To further confirm protein expression and the results from the LPS silver stained gels and liquid culture clearing assays, we performed a series of western blots. Results revealed that for the case of mutant 16 E1 complemented with pXO4 Tp-Tc and pXO7 Tp-Tc, the bands indicating the presence of WbcE_{His} (~54.87 kD) and WbxD_{His} (~73.86 kD) were not clearly detected by western blot [Red box], thus making it difficult to determine if the bands correspond to the predicted product. Several attempts were made to detect the bands on the membranes but I was not able to get clear bands [Fig. 112]. However, Coomassie gels run in parallel to the western blots appear to show these proteins [Fig. 113], suggesting a problem with the immunoblotting process. We know that the plasmid is present in the mutant, as confirmed by the liquid culture clearing assays (restoration of the wt phenotype) and colony PCR. The problem, however, seems to be the type of polyhistidine tag used. 6xHis tags are known to cause detection problems (according to members of the Feldman and Raivio labs, personal

communication). Therefore, to solve this problem a 10X His tag could be included on the PCR constructs; because of time constraints this was not possible.

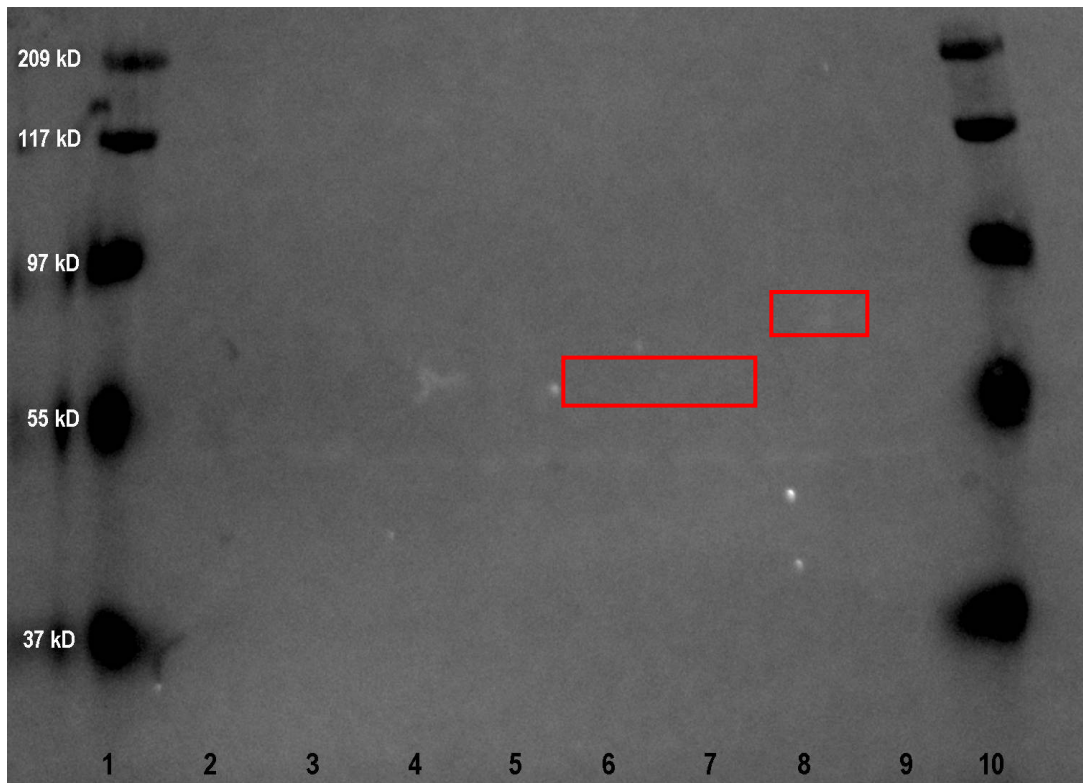


Figure 112: Western blot from *B. cenocepacia* K56-2 wt and mutant 16 E1 (*wbxD-wbcE::Tp*): 1, 10: Prestained SDS-PAGE standards ladder, 2: K56-2 wt + pSCRhaB3 Tp-Tc induced with 0.2% Rha, 3: K56-2 wt + pSCRhaB3 Tp-Tc non-induced, 4: 16 E1 (*wbxD-wbcE::Tp*) + pSCRhaB3 Tp-Tc + 0.2% Rha, 5: 16 E1 (*wbxD-wbcE::Tp*) + pSCRhaB3 Tp-Tc, 6: 16 E1 (*wbxD-wbcE::Tp*) + pXO4 Tp-Tc + 0.2% Rha, 7: 16 E1 (*wbxD-wbcE::Tp*) + pXO4 Tp-Tc, 8: 16 E1 (*wbxD-wbcE::Tp*) + pXO7 Tp-Tc + 0.2% Rha, 9: 16 E1 (*wbxD-wbcE::Tp*) + pXO7 Tp-Tc.

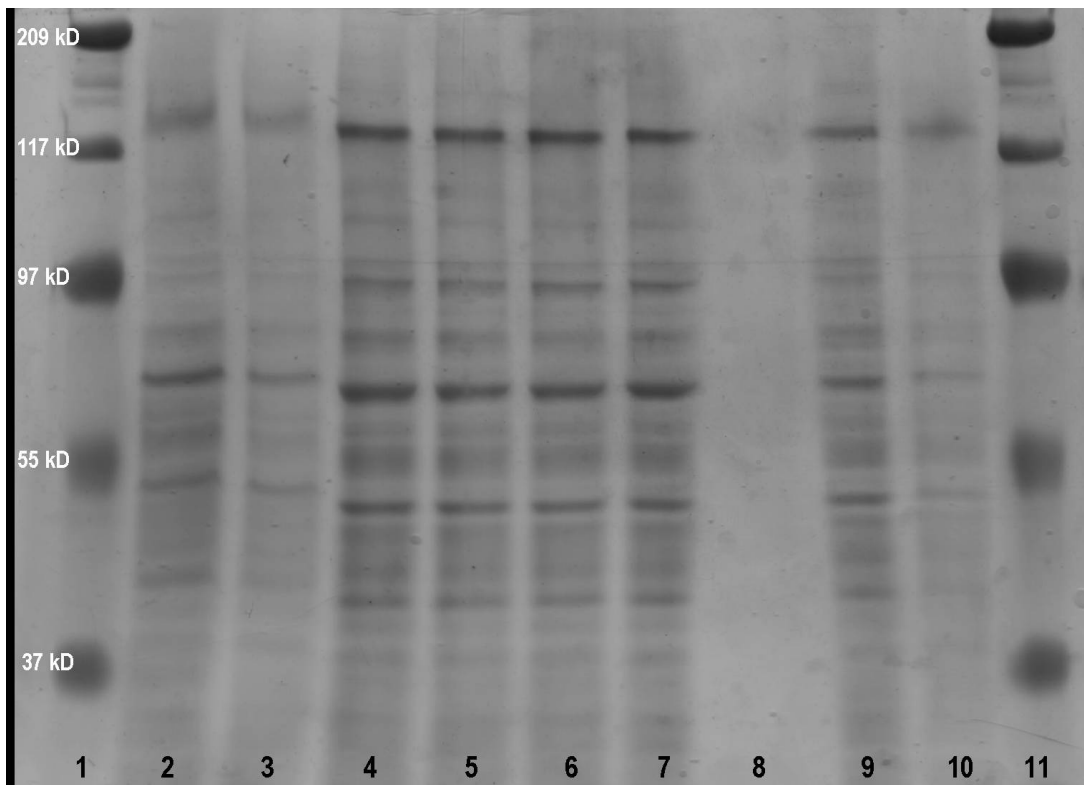


Figure 113: Coomassie blue-stained gel from *B. cenocepacia* K56-2 wt and mutant 16 E1 (*wbxD-wbcE::Tp*): 1, 11: Prestained SDS-PAGE standards ladder, 2: K56-2 wt + pSCRhaB3 Tp-Tc induced with 0.2% Rha, 3: K56-2 wt + pSCRhaB3 Tp-Tc non-induced, 4: 16 E1 (*wbxD-wbcE::Tp*) + pSCRhaB3 Tp-Tc + 0.2% Rha, 5: 16 E1 (*wbxD-wbcE::Tp*) + pSCRhaB3 Tp-Tc, 6: 16 E1 (*wbxD-wbcE::Tp*) + pXO4 Tp-Tc + 0.2% Rha, 7: 16 E1 (*wbxD-wbcE::Tp*) + pXO4 Tp-Tc, 8: empty lane, 9: 16 E1 (*wbxD-wbcE::Tp*) + pXO7 Tp-Tc + 0.2% Rha, 10: 16 E1 (*wbxD-wbcE::Tp*) + pXO7 Tp-Tc.

For the case of mutant XOA8 complemented with pSC*wabO*-Tc and CCB1 complemented with pSC*waaC*-Tc, immunoblotting revealed both gene products. As expected, the 0.2% and 0.02% Rha-induced samples revealed a bright band, which further confirms that WabO_{His} (~ 29.96 kD) and WaaC_{His} (~ 38.58 kD) are

being expressed under the P_{RHA} promoter [Figs. 114, 115]. Contrasting the previously-discussed undetectable $WbcE_{His}$ and $WbxD_{His}$, $WabO_{His}$ and $WaaC_{His}$ were modified with 10X His tags.

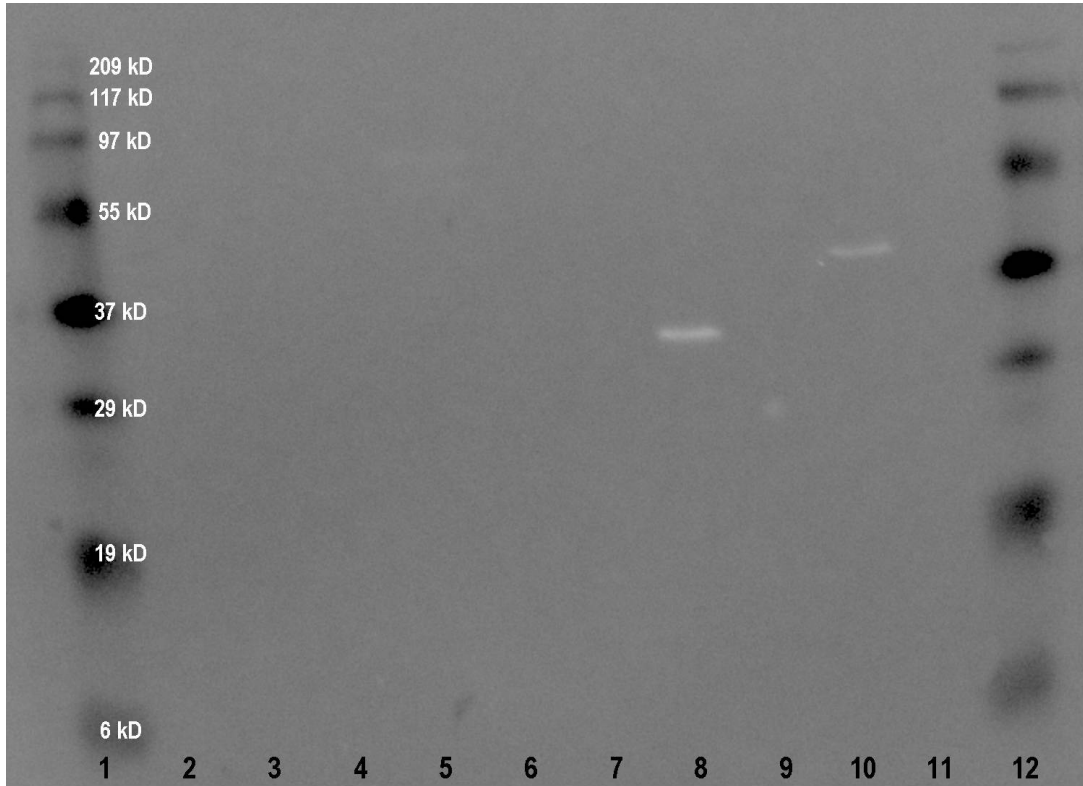


Figure 114: Western blot from *B. cenocepacia* K56-2 wt and K56-2 LPS truncated mutants XOA8 ($wabO::pGP\Omega Tp^R$) and CCB1 ($waaC::pGP\Omega Tp^R$): 1, 12: Prestained SDS-PAGE standards ladder, 2: K56-2 wt + pSCRhaB2-Tc induced with 0.2% Rha, 3: K56-2 wt + pSCRhaB2-Tc non-induced, 4: XOA8 ($wabO::pGP\Omega Tp^R$) + pSCRhaB2-Tc + 0.2% Rha, 5: XOA8 ($wabO::pGP\Omega Tp^R$) + pSCRhaB2-Tc, 6: CCB1 ($waaC::pGP\Omega Tp^R$) + pSCRhaB2-Tc + 0.02% Rha, 7: CCB1 ($waaC::pGP\Omega Tp^R$) + pSCRhaB2-Tc, 8: XOA8 ($wabO::pGP\Omega Tp^R$) + pSCwabO-Tc + 0.2% Rha, 9: XOA8 ($wabO::pGP\Omega Tp^R$) + pSCwabO-Tc, 10: CCB1 ($waaC::pGP\Omega Tp^R$) + pSCwaaC-Tc + 0.02% Rha, 11: CCB1 ($waaC::pGP\Omega Tp^R$) + pSCwaaC-Tc.

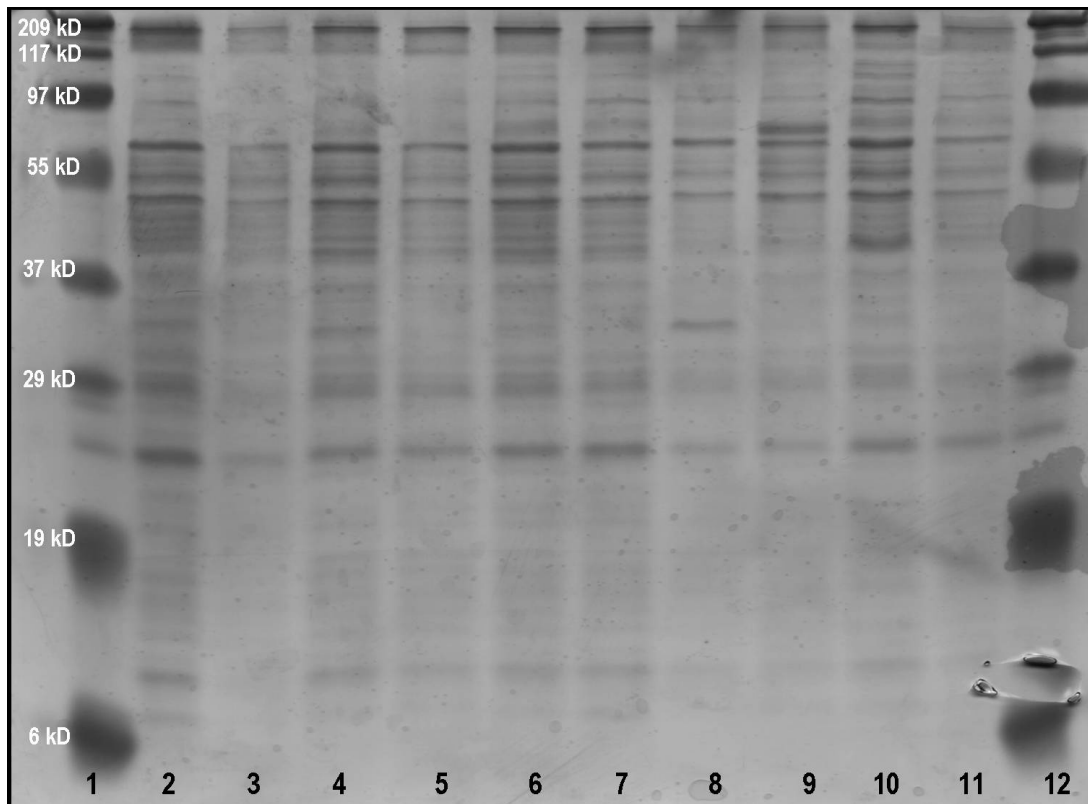


Figure 115: Coomassie blue stained gel from *B. cenocepacia* K56-2 wt and K56-2 LPS truncated mutants XOA8 (*wabO*:: pGPΩTp Tp^R) and CCB1 (*waaC*::pGPΩTp Tp^R): 1, 12: Prestained SDS-PAGE standards ladder, 2: K56-2 wt + pSCRhaB2-Tc induced with 0.2% Rha, 3: K56-2 wt + pSCRhaB2-Tc non-induced, 4: XOA8 (*wabO*:: pGPΩTp Tp^R) + pSCRhaB2-Tc + 0.2% Rha, 5: XOA8 (*wabO*:: pGPΩTp Tp^R) + pSCRhaB2-Tc, 6: CCB1 (*waaC*::pGPΩTp Tp^R) + pSCRhaB2-Tc + 0.02% Rha, 7: CCB1 (*waaC*::pGPΩTp Tp^R) + pSCRhaB2-Tc, 8: XOA8 (*wabO*:: pGPΩTp Tp^R) + pSC*wabO*-Tc + 0.2% Rha, 9: XOA8 (*wabO*:: pGPΩTp Tp^R) + pSC*wabO*-Tc, 10: CCB1 (*waaC*::pGPΩTp Tp^R) + pSC*waaC*-Tc + 0.02% Rha, 11: CCB1 (*waaC*::pGPΩTp Tp^R) + pSC*waaC*-Tc.

**Transmission electron microscopy (TEM) from PC184 pTn*Modlux*-OTp'
DC1 resistant mutant 72 C12 (*pulO*::Tp^R), PC184 wt and 72 C12 (*pulO*::Tp^R)
incubated with phage DC1**

As previously described, DNA sequences from five of six PC184::pTn*Modlux*-OTp' DC1 resistant mutants detected genes encoding proteins that assemble the T2SS. These included mutants 49 B12, 54 H3, 76 H8 (*gspM*::Tp^R), mutant 76 D1 (*gspJ*::Tp^R) and mutant 72 C12 (*pulO*::Tp^R). The latter mutant was of particular interest because the affected gene encodes a prepilin signal peptidase, a type IV prepilin-like peptidase (Sandkvist, 2001). Because several genes required for pili assembly are homologous in the T2SS and type IV pili (Stathopoulos, 2000; Sandkvist, 2001; Mattick, 2002), we hypothesized that perhaps type IV pili or a pili-like structure might be used by DC1 as a receptor to infect its host. Type IV pili are usually located at one or both poles of the bacterium and can be easily detectable by TEMs (Bahar et al., 2009; Shan et al., 2004; Chibeu et al., 2009; Rashid & Kornberg, 2000). In addition, other phages binding to type IV pili have been previously described (Chibeu et al., 2009; Mattick, 2002). Thus, a series of transmission electron micrographs were taken to provide evidence of the possible involvement of type IV pili during phage DC1 infection.

We had hoped to visualize a possible defect in type IV pili expression on mutant 72 C12 (*pulO*::Tp^R) as compared to *B. cenocepacia* PC184 wt [Figs. 116 & 117]. However, after several attempts using different types of media, no apparent differences were observed. In fact, no type IV pili, pili-like structure, or

other pili were observed in the wt strain. Therefore, the TEMs did not provide any evidence to support our theory.

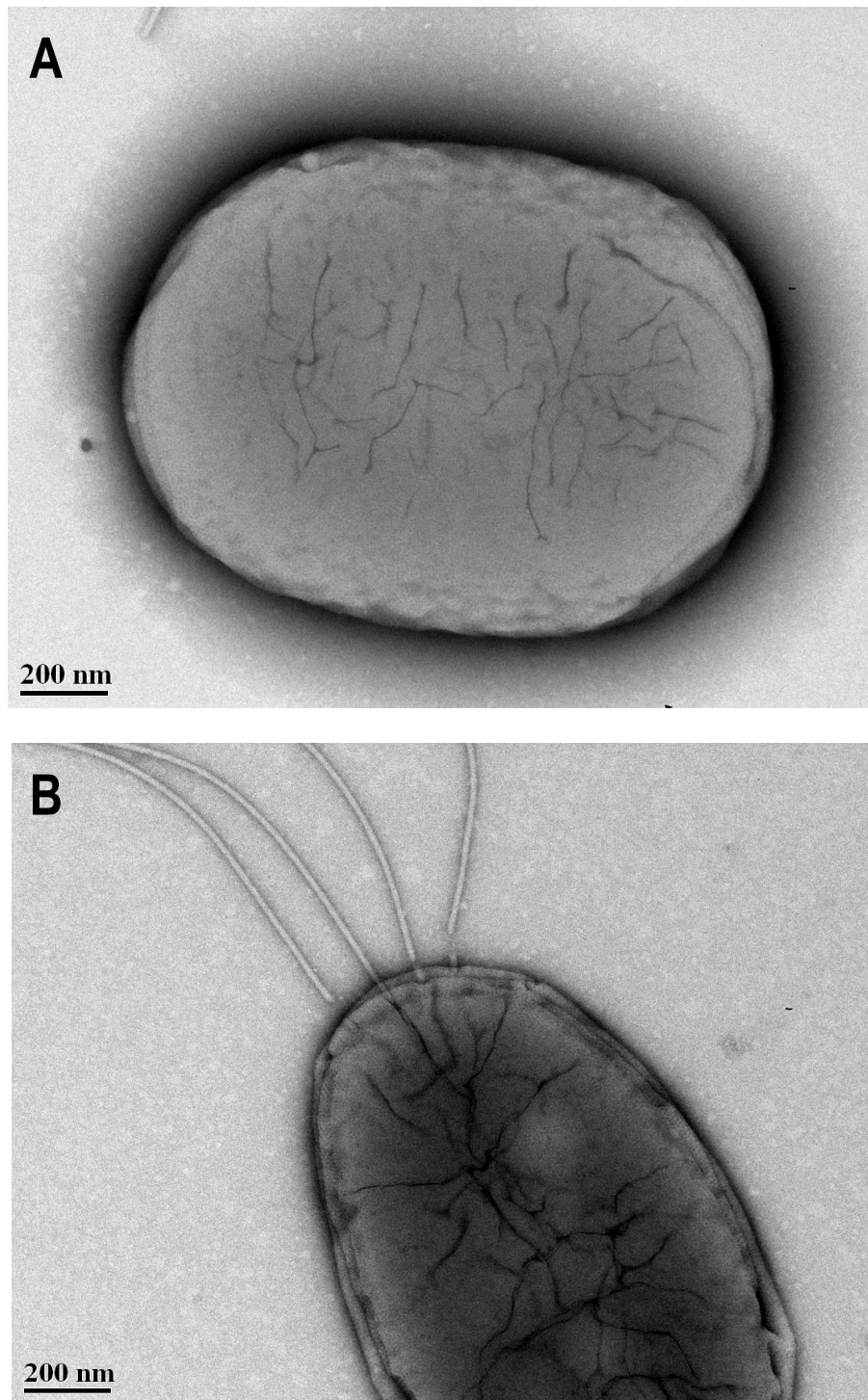


Figure 116: Electron micrographs of negatively stained (2% PTA) *B. cenocepacia* PC184 wt (A) and mutant 72 C12 (*pulO::Tp^R*) (B). Bacteria previously grown on

$\frac{1}{2}$ LB and $\frac{1}{2}$ LB + 300 μ g of Tp/mL broth respectively at 30°C with shaking (225 rpm) for 16 hrs.

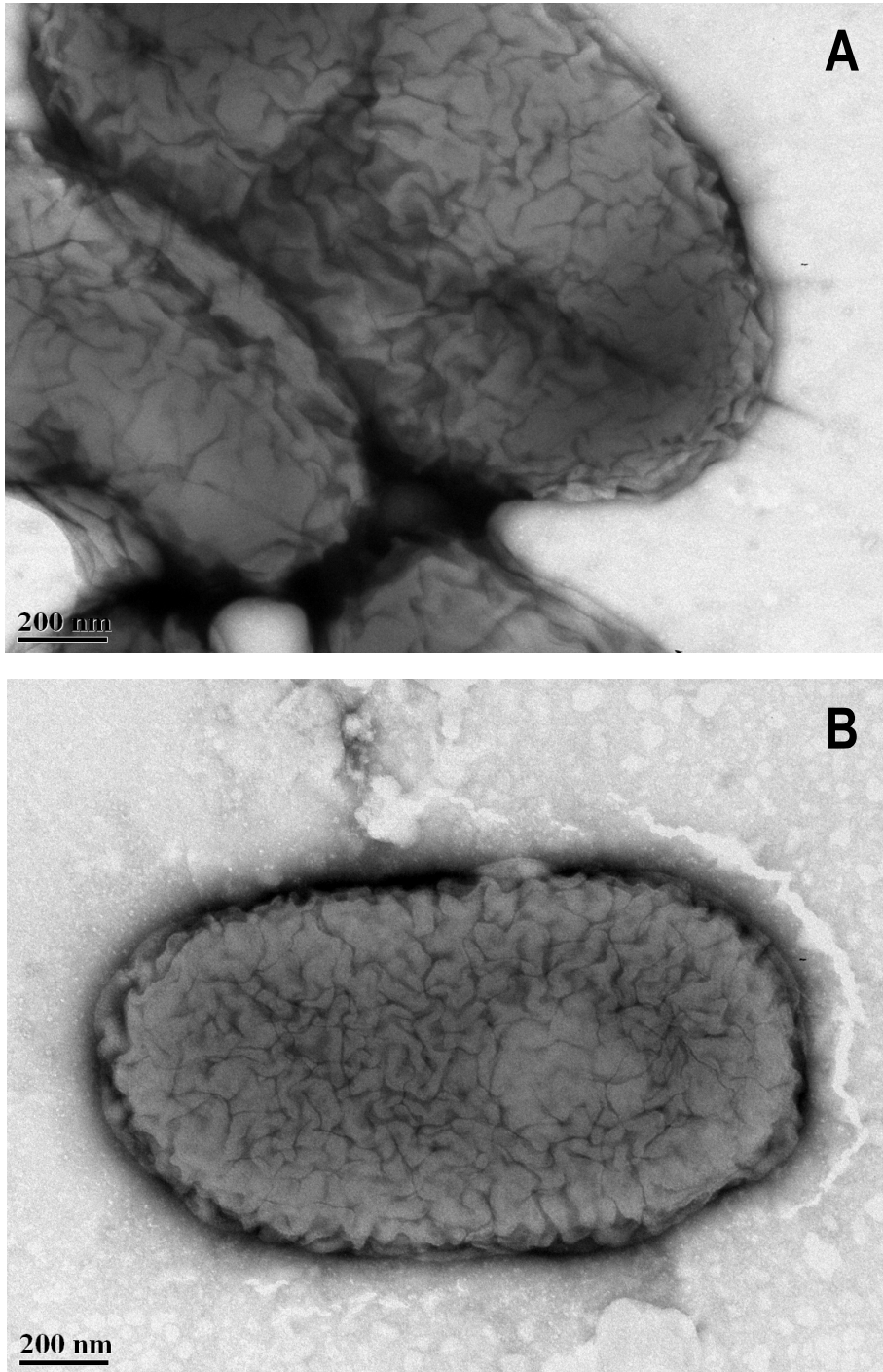


Figure 117: Electron micrographs of negatively stained (2% PTA) *B. cenocepacia* PC184 wt (A) and mutant 72 C12 (*pulO*::Tp^R) (B). Bacteria grown on tryptic soy agar (TSA) and TSA + 300 μ g of Tp/mL respectively at 30°C for 16 hrs.

Due the lack of pili in all TEMs, we included phage DC1 in the preparation, to compare possible difference between mutant 72 C12 and PC184 wt [Fig. 118]. We hypothesized that perhaps phages would be visible and attached to any pilus structure on the wt strain, but not on the plasposon mutant.

Unfortunately similar to previous TEMs, no obvious structure was detected on the TEMs, even though phages seem to be attached to the cell surface in the wt TEM.

A possible alternative method to determine whether a type IV pili or a pili-like structure is absent on mutant 72 C12 would be the use of pili immunogold labeling followed by TEM (Vignon et al., 2003). Specific pili antibodies are used to label pili, and gold beads serve as a secondary antibody that bind to the primary antibody and allow for the detection of pili in the TEMs. However, since we have already detected no pili on the wt strain, this approach may be of little value.

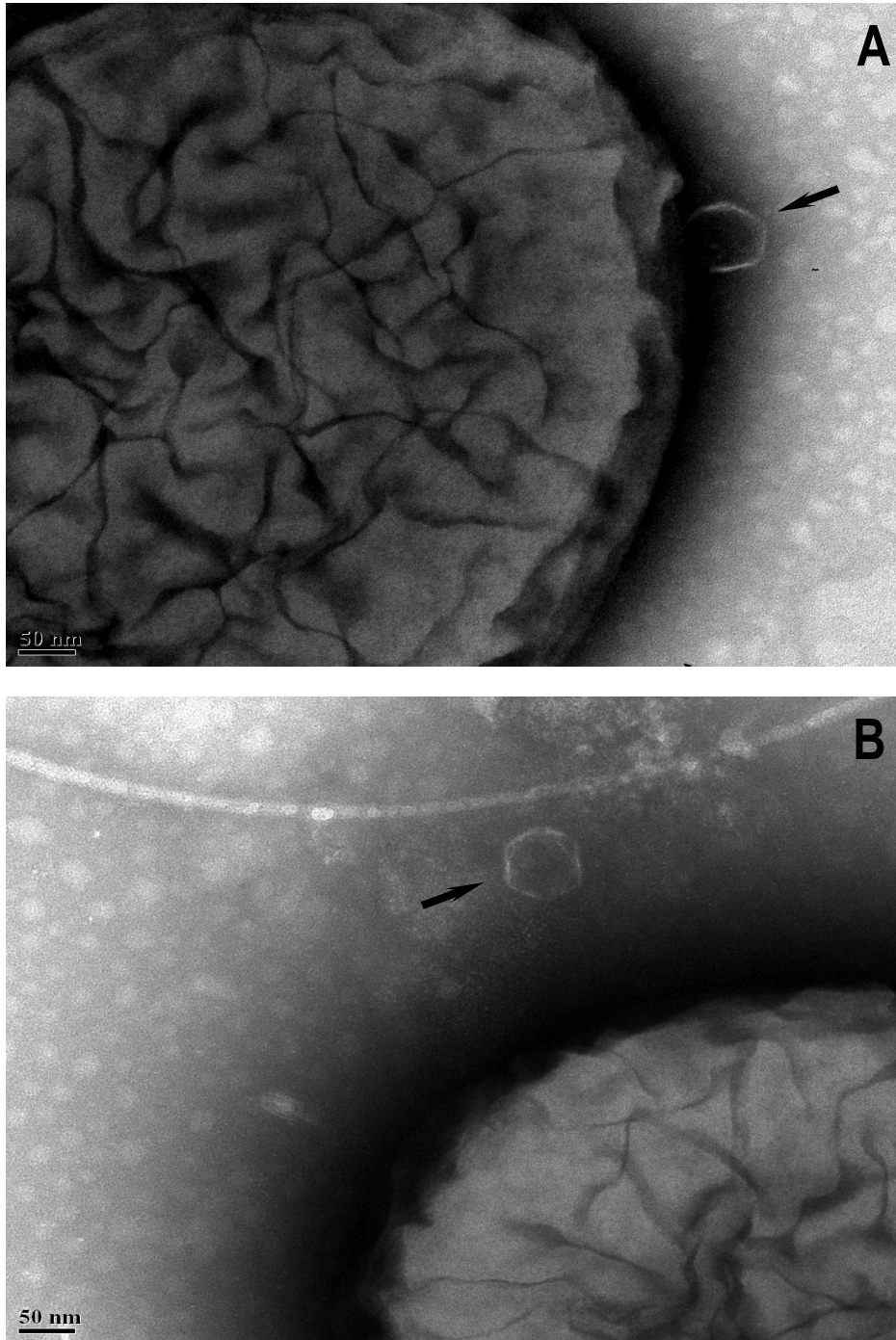


Figure 118: Electron micrographs of negatively stained (2% PTA) *B. cenocepacia* PC184 wt + phage DC1 (A) and mutant 72 C12 (*pulO*::Tp^R) + phage DC1 (B). Bacteria grown on ½ LB and ½ LB + 300 µg of Tp/mL agar plates respectively at 30°C for 16 hrs. Bacteria was resuspended on 1 mL of ½ LB broth. 100 µL of previous suspension was mixed with 100 µL of high titer phage stock (DC1) and

incubated for 20 minutes at room temp. prior the samples staining. Arrows indicate location of phage DC1.

Swarming and Twitching Motility assays from PC184::pTn*Modlux*-OTp'

DC1 resistant mutants, PC184 wt and *Pseudomonas aeruginosa* strain PAO1

As it was mentioned in the previous section type IV pili is usually located at one or both poles of the bacterium. In some species like *P. aeruginosa* or *Acidovorax avenae* subsp. *citrulli* type IV pili is essential for twitching motility, a flagella-independent form of bacterial motility that occurs mainly over moist surfaces and has also been linked to plant and animal host colonization and biofilm and fruiting bodies formation (Bahar et al.,2009; Chibeu et al.,2009; Rashid & Kornberg, 2000). Because the lack of evidence in detecting type IV pili, pili or a pili-like structure by TEMs we decided to perform an alternative assay that indirectly tests for the presence of type IV pili and twitching motility.

The six PC184::pTn*Modlux*-OTp' DC1 resistant mutants, PC184 wt and *P. aeruginosa* PAO1 were stab inoculated (Shan et al.,2004; Rashid & Kornberg, 2000) on the appropriate plates as described in materials and methods.

After incubation the zone of motility characterized by a hazy halo formed at the agar/Petri dish interface surrounding the point of inoculation was measured and compared between the six DC1 resistant mutants, PC184 wt and *P. aeruginosa* strain PAO1 [Figs. 119] A total of three plates were measured for each strain.

Unfortunately no difference in twitching motility was detected between PC184 wt [Figs 119A] and the six DC1 resistant mutants [Fig. 119C]. For example the

average halo diameter in mm between PC184 wt and mutant 72 C12 (*pulO*::Tp^R) was 9.5 ± 0.866 and 8.333 ± 0.577 respectively.

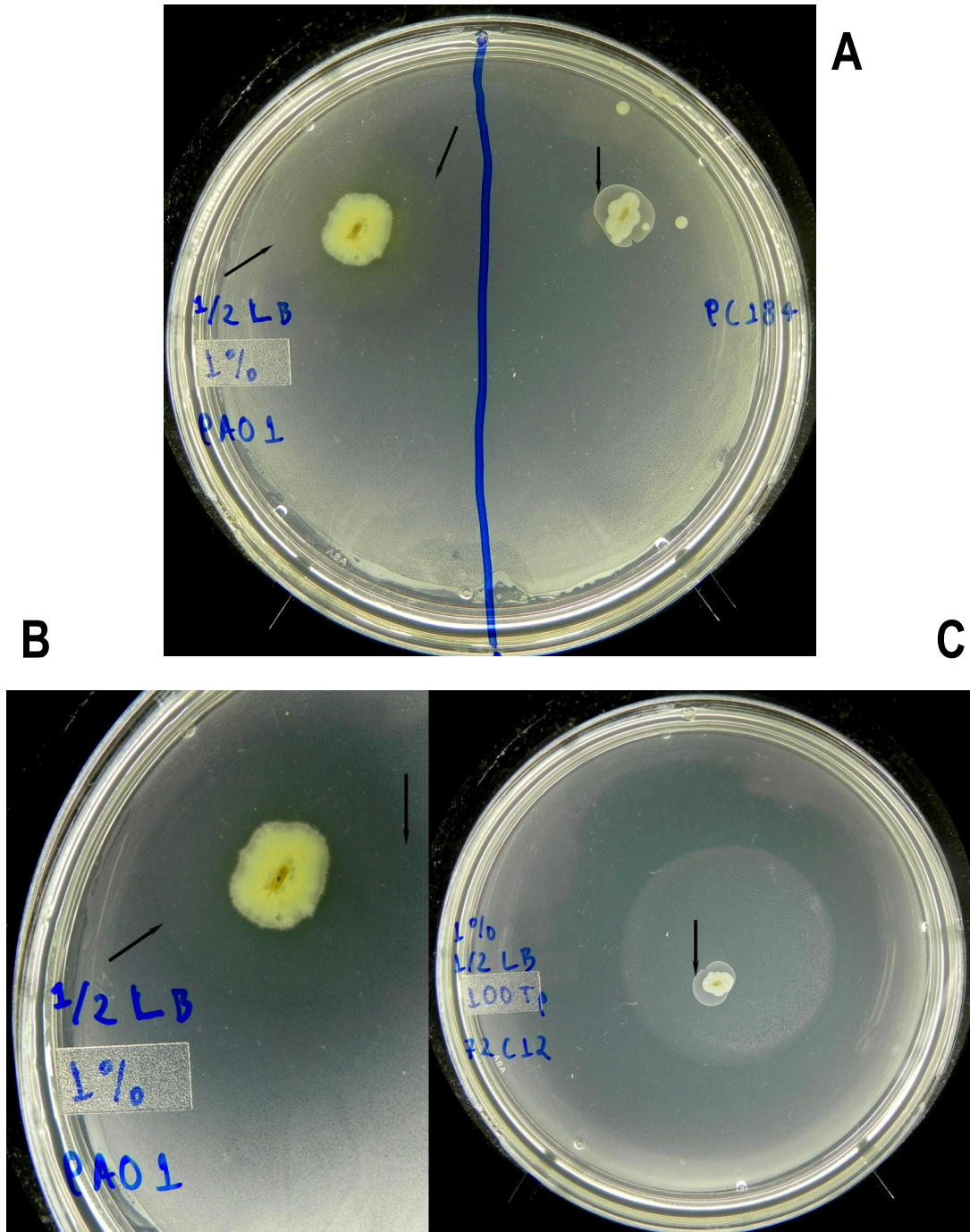


Figure 119: Stab assay for twitching motility on 1% agar plates with antibiotics were needed. (A) *P. aeruginosa* PAO1, left (positive control) and *B. cenocepacia*

PC184 wt, right (control). (B) Closer look from *P. aeruginosa* PAO1 (positive control). (C) Mutant 72 C12 (*pulO::Tp^R*). Bacteria grown on ½ LB and ½ LB + 100 µg of Tp/mL agar plates at 37°C for 16-24 hrs (Pictures show 24 hr. growth). Arrows indicate twitching motility zone. Previous results support the fact that no type IV pili was visible on the TEMs.

An obvious difference in twitching motility is observed between *P. aeruginosa* PAO1 with an average halo diameter of 28.667 ± 1.527 , *B. cenocepacia* PC184 wt 9.5 ± 0.866 and the above described plasposon mutants. Since type IV pili were not seen on TEMs and no twitching motility seems to occur, evidence suggests that perhaps phage DC1 does not utilize type IV pili, pili or a pili-like structure to infect its host. Based on a report that links type IV pili and swarming motility in *P. aeruginosa* (but not in other swarmer cells) (Köhler et al., 2000), swarming motility was analyzed in the six DC1 resistant mutants and compared with that of PC184 wt and *P. aeruginosa* PAO1. Swarming motility is a flagellum-dependent type of motility characterized by elongated and hyperflagellated bacteria that move in a coordinated manner (Mattick, 2002; Rashid & Kornberg, 2000). However, Köhler's research also suggests a requirement for type IV pili in the case of *P. aeruginosa*.

The six PC184::pTn*Modlux*-OTp' DC1 resistant mutants, PC184 wt and *P. aeruginosa* PAO1 were inoculated with a sterile toothpick (Rashid & Kornberg, 2000) on the appropriate plates. After incubation, the zone of motility, characterized by either a motility en masse at the colony edge, as rafts of migrating cells leaving the colony behind (moving from point of inoculation to the edges of the plate), or the characteristic production of extracellular slime

(polysaccharide and/or biosurfactant), was measured and compared between the six DC1 resistant mutants, PC184 wt and *P. aeruginosa* strain PAO1 [Fig. 120]. A total of three plates for each strain were measured. Similar to previous tests, no differences in swarming motility were observed between PC184 wt and the six DC1 resistant mutants [Fig. 120]. For example, the average halo diameter between PC184 wt and mutant 72 C12 (*pulO::Tp^R*) was 4.667 ± 0.577 , identical in both cases. An obvious difference in swarming motility was observed between *P. aeruginosa* PAO1, with an average halo diameter of 13.667 ± 1.527 , and *B. cenocepacia* PC184 wt 4.667 ± 0.577 .

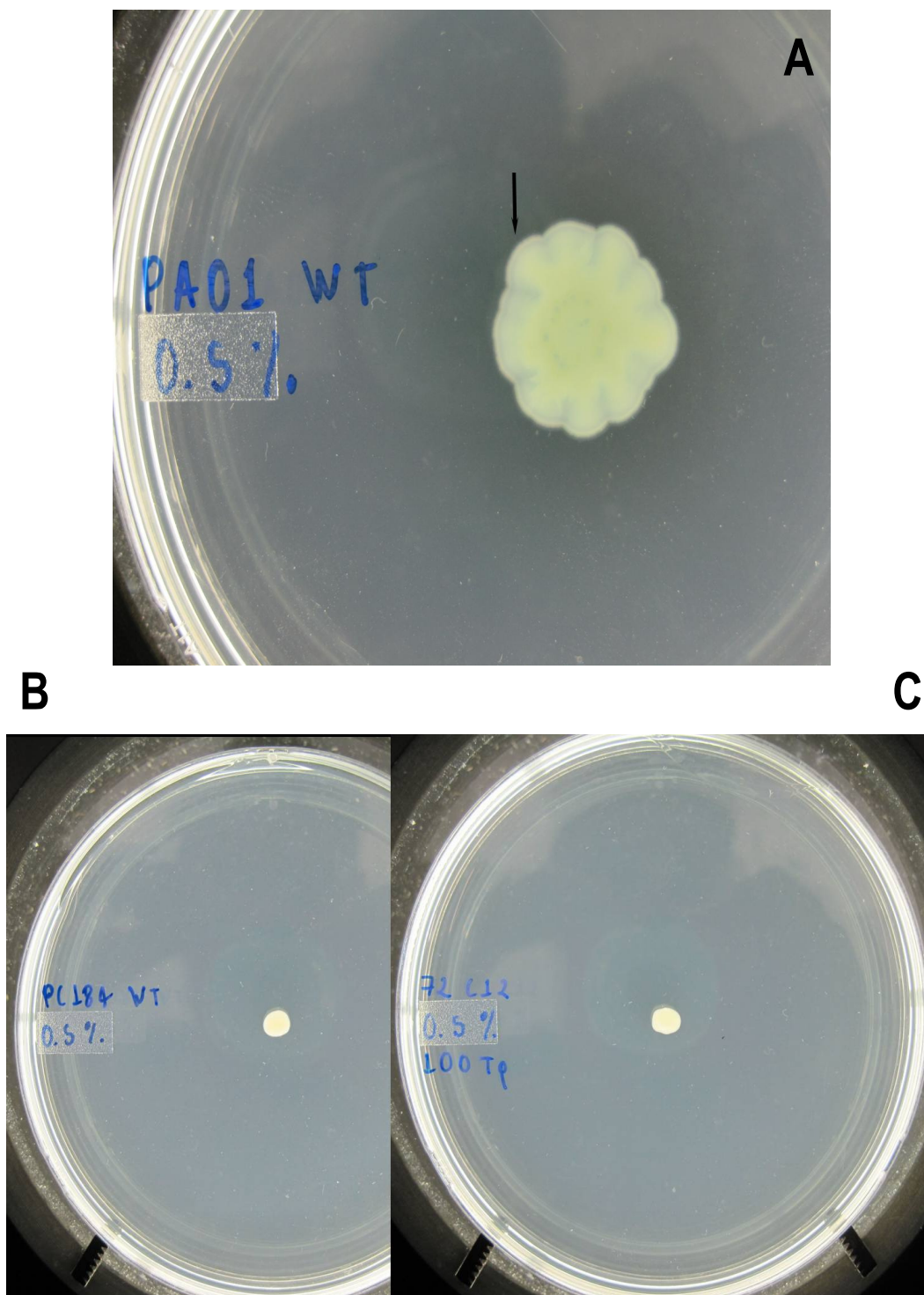


Figure 120: Swarming motility on 0.5% agar plates with antibiotics were needed. (A) *P. aeruginosa* PAO1 (positive control) (B) *B. cenocepacia* PC184 wt (control). (C) Mutant 72 C12 (*pulO::Tp^R*). Bacteria grown on $\frac{1}{2}$ LB and $\frac{1}{2}$ LB + 100 μ g of Tp/mL agar plates at 30°C for 16-24 hrs (Pictures show 24 hr. growth). Arrows indicate swarming motility zone.

To summarize, evidence from the TEMs and the twitching and swarming motility assays suggest that *B. cenocepacia* PC184 wt does not produce type IV pili, at least under the conditions tested. For this reason, we can conclude that phage DC1 does not seem to utilize type IV pili, pili or a pili-like structure to infect its host. It is possible that DC1 utilizes some other surface structure that is assembled by the T2SS machinery. Further investigation is needed to support this argument. Currently we are attempting to genetically complement DC1 mutant 72 C12 (*pulO::Tp^R*) in order to demonstrate restoration of the wt phenotype (phage susceptibility), and prove that the plasposon insertion is solely responsible for mutant phenotype observed. An interesting case is reported by Chibeu et al. (2009), in which their evidence suggests that *P. aeruginosa* phage Φ KMV infectivity requires the presence of both the *pilMNOPQ* operon and the *ponA* product; if some of these genes are missing, phage infectivity and twitching motility are diminished. Interestingly, phage Φ KMV is a member of the *Podoviridae* family, as is phage DC1.

Previous work in the Dennis lab has shown that phage DC1 putatively carries an exopolysaccharide (EPS) depolymerase enzyme. The activity of depolymerases is characterized by large expanding haloes surrounding the phage plaques on agar plates. Perhaps phage DC1 infectivity is governed not only by the presence of a specific receptor, but also by enzymatic modification of the receptor before phage binding. Phages exhibiting depolymerase activity have been described in the past, and interestingly, many of these are members of the

Podoviridae family (Rakhuba et al., 2010; Labrie et al., 2010; Glonti et al., 2010; Nimmich et al., 1991).

Table 10: Bcc specific bacteriophages tested in this study and their receptors.
Legends: ? represents unconfirmed receptor.

Phage	Host	Putative receptor
DC1	<i>B. cenocepacia</i> PC184	T2SS machinery?
KS4 & KS4-M	<i>B. cenocepacia</i> K56-2	LPS O-antigen
KS5	<i>B. cenocepacia</i> K56-2	LPS Inner core OS
KS9	<i>B. cenocepacia</i> K56-2	LPS Inner core OS
KS10	<i>B. cenocepacia</i> PC184	LPS Inner core OS?
KS12	<i>B. cenocepacia</i> K56-2	LPS O-antigen
KS14	<i>B. cenocepacia</i> PC184	?
KL1	<i>B. cenocepacia</i> K56-2	?
AH2	<i>B. cenocepacia</i> K56-2	?
SR1	<i>B. cenocepacia</i> PC184	LPS Inner core OS?

CONCLUSION

Bacteriophage receptors and their implications in phage therapy

In order to utilize phage therapy as an alternative method to treat infectious diseases, especially in infections caused by highly antibiotic resistant bacteria, it is important to understand phage-bacteria interactions. It has been proposed that the majority of past failures regarding phage therapy were due to a lack of knowledge about phage biology and how phage and bacteria interact (O'Flaherty et al., 2004). One potential disadvantage when using phages is that host bacteria can mutate to prevent phage infection (Labrie et al., 2010). In addition, phages typically have a narrow host range, often a specific phage can only infect a specific bacterial host strain (Chibeu et al., 2009). However, combinations of different phages with different host specificities, or “phage cocktails”, have been proposed as a way to increase the effectiveness of phage therapy (Chibeu et al., 2009; Tanji et al., 2004; McVay et al., 2007). Additionally, genetic engineering may also be a useful tool, with the potential to eliminate, add, or control genes of interest in a specific phage.

Through genetic approaches it has been possible to identify, isolate and purify several phage receptors from the cell surfaces and membranes of bacteria. *In vitro* studies have provided substantial information about how specific and strong interactions occur utilizing purified receptors and complete or partial phage particles. The tertiary structure, chemical composition, concentration in bacteria of receptors, and even external factors such as pH, temperature, and ions, play important roles during phage infection.

The Dennis lab currently possesses a collection of at least 10 Bcc specific phages with the potential to be used in phage cocktail preparations. Future studies should work toward creating broad spectrum phage cocktails by combining specific phages that target distinct bacterial receptors, thus greatly increasing the chances to infect the host, but also reducing the potential appearance of phage resistant mutants (Tanji et al., 2004). In order to develop rational phage cocktails, it will be important to identify the specific receptor(s) each phage uses.

Through the research presented, we were able to determine at least one of the receptors utilized by the Bcc specific phages KS4, KS4-M, KS5, KS9 and KS12, and identify a putative receptor for phages KS10, SR1 and DC1. In the majority of cases, LPS appears to play an important role during phage adsorption to the host, perhaps because LPS is the first bacterial element a phage might encounter when colliding with a host cell. Phages KS4, KS4-M and KS12 require the presence of the entire LPS structure (Lipid A, core OS and O-antigen subunits) or S-type LPS, in order to infect their host. If one of these elements is missing the phage will not be able to initiate its infection cycle. Even if the majority of the LPS structure is intact but the O-antigen subunits are missing, phages KS4, KS4-M and KS12 will not infect the host. This indicates that LPS O-antigen specifically serves as a binding receptor for these three phages.

For phages KS5 and KS9, the experimental evidence suggests that these phages do not require a complete LPS structure to infect their host. An R-type LPS structure (Lipid A and core OS) is enough to allow infection of the host. Results suggest that these phages bind to the outer core OS. Phages binding to the

core OS are particularly advantageous for use in phage therapy because in general, mutations modifying the core OS of bacteria are less common than those occurring at the O-antigen (Nikaido, 2003; Bos & Tommassen, 2004). As in phages KS4, KS4-M and KS12, we do not discount the possibility that KS5 and KS9 require the presence of a primary or secondary receptor to infect their host. The other two phages from our collection that appear to utilize LPS as a receptor are phages KS10 and SR1, and preliminary evidence suggests that these phages probably bind to the core OS. This is supported by the fact that one of the resistant mutants 30 D1 (*Bcenmc03_233::Tp^R*) gene products has the conserved domain UDP-glucose LOS-beta-1,4 glucosyltransferase running from AA 5 to 230. This domain is the same as that found in *wabO*, and both genes are approximately 750 basepairs long, and the surrounding genes are LPS related. Current work in the lab will determine the function of this gene product, and its effect on phage adherence to core OS.

Finally, phage DC1 is the only phage in our current collection that appears to utilize a receptor other than LPS. Several attempts to elucidate the receptor for this phage have provided little information. What evidence we have, suggests that a product secreted by the T2SS machinery serves as a receptor for this phage. Initially, we hypothesized that perhaps type IV pili or a pili-like structure was the receptor due the disruption of a prepilin peptidase (*pulO*) in one of the isolated mutants. However, TEMs and motility assays did not provide evidence to support this hypothesis, as a pili structure was never detected. There is also the possibility that phage DC1 requires a protein of the T2SS to directly bind and infect its host.

A similar phenomenon has been reported in other *Podoviridae* viruses (Chibeu et al., 2009).

The utilization of phages as a therapeutic strategy to treat bacterial infectious diseases is a viable alternative to traditional chemical antibiotics. Modern technologies have greatly increased our knowledge of the phage-bacteria biology resulting in a deeper comprehension of their interactions. Thus, the possibility now exists to use phages as a feasible treatment option.

LITERATURE CITED

- Ackermann, H.W., Kropinski, A.M. 2007. Curated list of prokaryote viruses with fully sequenced genomes. *Res. Microbiol.* **158**(7):555-66.
- Arisaka, F. 2005. Assembly and infection process of bacteriophage T4. *Chaos.* **15**(4):047502.
- Bahar, O., Goffer, T. & Burdman. S. 2009. Type IV pili are required for virulence, twitching motility, and biofilm formation of *Acidovorax avenae* subsp. *citrulli* *Mol. Plant-Microbe Interact.* **22**: 909-920.
- Barbirz, S., Muller, J.J. *et al.*,2008. Crystal structure of Escherichia coli phage HK620 tailspike: podoviral tailspike endoglycosidase modules are evolutionarily related. *Mol. Microbiol.* **69**(2):303-16.
- Barrow, P.A. & Soothill, J.S. 1997. Bacteriophage therapy and prophylaxis: rediscovery and renewed assessment of potential., *Trends. Microbiol.* **5**(7):268-71.
- Bergh, O., Borsheim, K.Y., Bratbak, G. & Heldal, M. 1989. High abundance of viruses found in aquatic environments. *Nature.* **340**(6233):467-8.
- Berkane, E., Orlik, F. *et al.*,2006. Interaction of bacteriophage lambda with its cell surface receptor: an in vitro study of binding of the viral tail protein gpJ to LamB (Maltoporin). *Biochemistry.* **45**(8):2708-20.
- Biswas, B., Adhya, S., Washart, P., Paul, B., Trostel, A.N., Powell, B., Carlton, R. & Merrill, C.R. 2002. Bacteriophage therapy rescues mice bacteremic from a clinical isolate of vancomycin-resistant *Enterococcus faecium*. *Infect. Immun.* **70**:204-210.
- Bonhivers, M., Ghazi, A., Boulanger, P. & Letellier, L. 1996. FhuA, a transporter of the *Escherichia coli* outer membrane, is converted into a channel upon binding of bacteriophage T5. *EMBO J.* **15**(8):1850-6.
- Bos, M.P. & Tommassen, J. 2004. Biogenesis of the Gram-negative bacterial outer membrane. *Curr. Opin. Microbiol.* **7**(6):610-6.
- Burns, J.L., Lien, D.M. & Hedin, L.A. 1989a. Isolation and characterization of dihydrofolate reductase from trimethoprim-susceptible and trimethoprim-resistant *Pseudomonas cepacia*. *Antimicrob. Agents Chemother.* **33**:1247-1251.
- Burns, J.L., Hedin, L.A. & Lien, D.M. 1989b. Chloramphenicol resistance in *Pseudomonas cepacia* because of decreased permeability *Antimicrob. Agents*

- Chemother **33**: 136-141.
- Campbell, A. 2003. The future of bacteriophage biology. *Nat. Rev. Genet.* **4**(6):471-7.
- Cardona, S.T. & Valvano, M.A. 2005. An expression vector containing a rhamnose-inducible promoter provides tightly regulated gene expression in *Burkholderia cenocepacia*. *Plasmid.* **54**:219-228.
- Carlton, R.M. 1999. Phage therapy: past history and future prospects. *Arch. Immunol. Ther. Exp.* **47**(5):267-74.
- Cascales, E., Lloubes, R. & Sturgis, J.N. 2001. The TolQ-TolR proteins energize TolA and share homologies with the flagellar motor proteins MotA-MotB. *Mol. Microbiol.* **42**(3):795-807.
- Casjens, S.R. 2008. Diversity among the tailed-bacteriophages that infect the *Enterobacteriaceae*. *Res. Microbiol.* **159**(5):340-8.
- Chibeu, A., Ceysens, P. *et al.*, 2009. The adsorption of *Pseudomonas aeruginosa* bacteriophage phiKMV is dependent on expression regulation of type IV pili genes. *FEMS Microbiol. Lett.* **296**(2):210-8.
- Chiesa, C., Labrozzi, P.H. & Aronoff, S.C. 1986. Decreased baseline β -lactamase production and inducibility associated with increased piperacillin susceptibility of *Pseudomonas cepacia* isolated from children with cystic fibrosis. *Pediatr. Res.* **20**:1174-1177.
- Clokie, M.R.J. & Kropinski, A.M. 2009. *Phage host range and Efficiency of plating, chapter 14*. In *Bacteriophages methods and protocols*, Vol. 1. Humana Press. New York, USA. pp. 141-9.
- Coenye, T., Vandamme, P., Govan, J.R.W. & Lipuma, J.J. 2001. Taxonomy and identification of the *Burkholderia cepacia* complex. *J. Clin. Microbiol.* **39**:3427-3436.
- Conway, B.D., Venu, V. & Speert, D.P. 2002. Biofilm formation and acyl homoserine lactone production in the *Burkholderia cepacia* complex. *J. Bacteriol.* **184**:5678-5685.
- Coward, C., Grant, A.J. *et al.*, 2006. Phase-variable surface structures are required for infection of *Campylobacter jejuni* by bacteriophages. *Appl. Environ. Microbiol.* **72**(7):4638-47.
- Cvirkaite-Krupovic, V., Poranen, M.M. & Bamford, D.H. 2010a. Phospholipids act as secondary receptor during the entry of the enveloped, double-stranded

- RNA bacteriophage phi6. *J. Gen. Virol.* **91**(8):2116-20
- Cvirkaite-Krupovic, V., Krupovic, M., Daugelavicius, R. & Bamford, D.H. 2010b. Calcium ion-dependent entry of the membrane-containing bacteriophage PM2 into its *Pseudoalteromonas* host. *Virology.* **405**(1):120-8.
- Das, P. 2001. Bacteriophage therapy offers new hope for streptococcal infections. *The Lancet.* **9260**: 938.
- Datta, D.B., Arden, B. & Henning, U. 1977. Major proteins of the *Escherichia coli* outer cell envelope membrane as bacteriophage receptors. *J. Bacteriol.* **131**(3):821-9.
- Daugelavicius, R., Cvirkaite, V. *et al.*, 2005. Penetration of enveloped double-stranded RNA bacteriophages phi13 and phi6 into *Pseudomonas syringae* cells. *J. Virol.* **79**(8):5017-26.
- Dennis, J.J. & Zylstra, G.J. 1998. Plasposons: Modular self-cloning minitransposon derivatives for rapid genetic analysis of gram-negative bacterial genomes. *Appl. Environ. Microbiol.* **64**:2710-2715.
- Desai, M., Bühler, T., Weller, P.H. & Brown, M.R.W. 1998. Increasing resistance of planktonic and biofilm cultures of *Burkholderia cepacia* to ciprofloxacin and ceftazidime during exponential growth. *J. Antimicrob. Chemother.* **42**:153-160.
- Duckworth, D.H. & Gulig, P.A. 2002. Bacteriophages: potential treatment for bacterial infections. *BioDrugs.* **16**(1):57-62.
- Eriksson, U. & Lindberg, A.A. 1977. Adsorption of phage P22 to *Salmonella typhimurium*. *J. Gen. Virol.* **34**(2):207-21.
- Evans, T.J., Trauner, A., Komitopoulou, E., & Salmond, G.P. 2010. Exploitation of a new flagellatropic phage of *Erwinia* for positive selection of bacterial mutants attenuated in plant virulence: towards phage therapy. *J. Appl. Microbiol.* **108**(2):676-85.
- Figurski, D.H. & Helinski, D.R. 1979. Replication of an origin-containing derivative of plasmid RK2 dependent on a plasmid function provided in trans. *Proc. Natl. Acad. Sci. USA* **76**:1648-1652.
- Fomsgaard, A., Freudenberg, M.A. & Galanos, C. 1990. Modification of the silver staining technique to detect lipopolysaccharide in polyacrylamide gels. *J. Clin. Microbiol.* **28**: 2627-2631.
- Frangolias, D.D., Mahenthiralingam, E., Rae, S., Raboud, J.M., Davidson, A.G.F., Wittmann, R. & Wilcox, P.G. 1999. *Burkholderia cepacia* in cystic fibrosis:

- Variable disease course. *Am. J. Respir. Crit. Care Med.* **160**:1572-1577.
- Glonti, T., Chanishvili, N. & Taylor, P.W. 2010. Bacteriophage-derived enzyme that depolymerizes the alginic acid capsule associated with cystic fibrosis isolates of *Pseudomonas aeruginosa*. *J. Appl. Microbiol.* **108**(2):695-702.
- Gowen, B., Bamford, J.K.H., Bamford, D.H. & Fuller, S.D. 2003. The tailless icosahedral membrane virus PRD1 localizes the proteins involved in genome packaging and injection at a unique vertex. *J. Virol.* **77**(14):7863-71.
- Grahn, A.M., Daugelavicius, R. & Bamford, D.H. 2002. Sequential model of phage PRD1 DNA delivery: active involvement of the viral membrane. *Mol. Microbiol.* **46**(5):1199-209.
- Grahn, A.M., Caldentey, J., Bamford, J.K. & Bamford, D.H. 1999. Stable packaging of phage PRD1 DNA requires adsorption protein P2, which binds to the IncP plasmid-encoded conjugative transfer complex. *J. Bacteriol.* **181**(21):6689-96.
- Hanlon, G.W. 2007. Bacteriophages: an appraisal of their role in the treatment of bacterial infections. *Int. J. Antimicrob. Agents.* **30**(2):118-28.
- Hashemolhosseini, S., Holmes, Z., Mutschler, B. & Henning, U. 1994. Alterations of receptor specificities of coliphages of the T2 family. *J. Mol. Biol.* **240**(2):105-10.
- Heller, K.J. 1992. Molecular interaction between bacteriophage and the gram-negative cell envelope. *Arch. Microbiol.* **158**(4):235-48.
- Jeannin, P., Magistrelli, G. *et al.*, 2002. Outer membrane protein A (OmpA): a new pathogen-associated molecular pattern that interacts with antigen presenting cells-impact on vaccine strategies. *Vaccine.* **20** Suppl 4:A23-7.
- Kemp, P., Garcia, L.R. & Molineux, I.J. 2005. Changes in bacteriophage T7 virion structure at the initiation of infection. *Virology.* **340**(2):307-17.
- Köhler, T., Curty, L.K., Barja, F., Van Delden, C. & Pechere, J. 2000. Swarming of *Pseudomonas aeruginosa* is dependent on cell-to-cell signaling and requires flagella and pili. *J. Bacteriol.* **182**:5990-5996.
- Kotranga, S., Kopp, B., Akhter, A. *et al.*, 2011. *Burkholderia cenocepacia* O polysaccharide chain contributes to caspase-1-dependent IL-1 β production in macrophages. *J. Leukoc. Biol.* **89**:481-488.
- Labrie, S.J., Samson, J.E. & Moineau, S. 2010. Bacteriophage resistance mechanisms. *Nat. Rev. Microbiol.* **8**(5):317-27

- Leiman, P.G., Kanamaru, S., Mesyanzhinov, V.V., Arisaka, F. & Rossmann, M.G. 2003. Structure and morphogenesis of bacteriophage T4. *Cell Mol. Life Sci.* **60**(11):2356-70.
- Letellier, L., Boulanger, P., Plancon, L., Jacquot, P. & Santamaria, M. 2004. Main features on tailed phage, host recognition and DNA uptake. *Front. Biosci.* **9**:1228-339.
- Lorenz, S.H., Jakob, R.P. *et al.*, 2011. The filamentous phages fd and IF1 use different mechanisms to infect *Escherichia coli*. *J. Mol. Biol.* **405**(4):989-1003.
- Loutet, S.A., Flannagan, R.S., Kooi, C., Sokol, P.A. & Valvano, M.A. 2006. A complete lipopolysaccharide inner core oligosaccharide is required for resistance of *Burkholderia cenocepacia* to antimicrobial peptides and bacterial survival in vivo. *J. Bacteriol.* **188**:2073-2080.
- Lynch, K.H., Stothard, P. & Dennis, J.J. 2012. Comparative analysis of two phenotypically-similar but genomically-distinct *Burkholderia cenocepacia*-specific bacteriophages. *BMC Genomics.* 223.
- Lynch, K.H., Seed, K.D., Stothard, P. & Dennis, J.J. 2010. Inactivation of *Burkholderia cepacia* complex phage KS9 gp41 identifies the phage repressor and generates lytic virions. *J. Virol.* 84:1276-1288.
- Madigan, M.T. & Martinko, J.M. 2006. Cell membranes and cell walls. In *Brock biology of microorganisms*. Pearson Prentice Hall. pp. 66-81.
- Mahenthiralingam, E., Urban, T.A. & Goldberg, J.B. 2005. The multifarious, multireplicon *Burkholderia cepacia* complex. *Nat. Revs. Microbiol.* 3:144-156.
- Mahenthiralingam, E., Bischof, J., Byrne, S.K., Radomski, C., Davies, J.E., Av-Gay, Y. & Vandamme, P. 2000. DNA-based diagnostic approaches for identification of *Burkholderia cepacia* complex, *Burkholderia vietnamiensis*, *Burkholderia multivorans*, *Burkholderia stabilis*, and *Burkholderia cepacia* genomovars I and III. *J. Clin. Microbiol.* **38**:3165-3173.
- Marolda, C.L., Welsh, J., Dafoe, L. & Valvano, M.A. 1990. Genetic analysis of the O7-polysaccharide biosynthesis region from the *Escherichia coli* O7:K1 strain VW187. *J. Bacteriol.* **172**:3590-3599.
- Matsuzaki, S., Rashel, M., Uchiyama, J. *et al.*, 2005. Bacteriophage therapy: A revitalized therapy against bacterial infectious diseases. *J. Infect. Chemothera.* **11**:211-219.

- Mattick, J.S. 2002. Type IV pili and twitching motility. *Annu. Rev. Microbiol.* **56**:289-314.
- May, T., Tsuruta, K. & Okabe, S. 2011. Exposure of conjugative plasmid carrying *Escherichia coli* biofilms to male-specific bacteriophages. *ISME J.* **5**(4):771-5.
- McVay, C.S., Velásquez, M. & Fralick, J.A. 2007. Phage therapy of *Pseudomonas aeruginosa* infection in a mouse burn wound model. *Antimicrob. Agents Chemother.* **51**:1934-1938.
- Merril, C.R., Biswas, B. *et al.*, 1996. Long-circulating bacteriophage as antibacterial agents. *Proc. Natl. Acad. Sci. USA.* **93**(8):3188-92.
- Molineux, I.J. 2001. No syringes please, ejection of phage T7 DNA from the virion is enzyme driven. *Mol. Microbiol.* **40**(1):1-8.
- Nikaido, H. 1993. Transport across the bacterial outer membrane. *J. Bioenerg. Biomembr.* **25**(6):581-9.
- Nikaido, H. 2003. Molecular basis of bacterial outer membrane permeability revisited. *Microbiol. Mol. Biol. Rev.* **67**(4):593-656.
- Nimmich, W., Schmidt, G. & Krallmann-Wenzel, U. 1991. Two different *Escherichia coli* capsular polysaccharide depolymerases each associated with one of the coliphage phi K5 and phi K20. *FEMS Microbiol. Lett.* **66**(2):137-41.
- Nishikawa, H., Yasuda, M. *et al.*, 2008. T-even-related bacteriophages as candidates for treatment of *Escherichia coli* urinary tract infections. *Arch. Virol.* **153**(3):507-15.
- Ochs, H.D., Davis, S.D. & Wedgwood, R.J. 1971. Immunologic responses to bacteriophage phi-X 174 in immunodeficiency diseases. *J. Clin. Invest.* **50**:2559-2568.
- O'Flaherty, S., Ross, R.P. & Coffey, A. 2009. Bacteriophage and their lysins for elimination of infectious bacteria. *FEMS Microbiol. Rev.* **33**(4):801-19.
- Ortega, X., Silipo, A., Saldas, M.S., Bates, C.C., Molinaro, A. & Valvano, M.A. 2009. Biosynthesis and structure of the *Burkholderia cenocepacia* K56-2 lipopolysaccharide core oligosaccharide: Truncation of the core oligosaccharide leads to increased binding and sensitivity to polymyxin B. *J. Biol. Chem.* **284**:21738-21751.

- Ortega, X., Hunt, T.A., Loutet, S., Vinion-Dubiel, A.D., Datta, A., Choudhury, B., Goldberg, J.B., Carlson, R. & Valvano, M.A. 2005. Reconstitution of O-specific lipopolysaccharide expression in *Burkholderia cenocepacia* strain J2315, which is associated with transmissible infections in patients with cystic fibrosis. *J. Bacteriol.* **187**:1324-1333.
- Parke, J.L. & Gurian-Sherman, D. 2001. Diversity of the *Burkholderia cepacia* complex and implications for risk assessment of biological control strains. *Annu. Rev. Phytopath.* **39**:225-258.
- Plançon, L., Janmot, C. *et al.*, 2002. Characterization of a high-affinity complex between the bacterial outer membrane protein FhuA and the phage T5 protein pb5. *J. Mol. Biol.* **318**(2):557-69.
- Power, M.L., Ferrari, B.C. *et al.*, 2006. A naturally occurring novel allele of *Escherichia coli* outer membrane protein A reduces sensitivity to bacteriophage. *Appl. Environ. Microbiol.* **72**(12):7930-2.
- Rabsch, W., Ma, L. *et al.*, 2007. FepA- and TonB-dependent bacteriophage H8: receptor binding and genomic sequence. *J. Bacteriol.* **189**(15):5658-74.
- Raetz, C.R.H. & Whitfield, C. 2002. Lipopolysaccharide endotoxins. *Annu. Rev. Biochem.* **71**:635-700.
- Rakhuba, D.V., Kolomiets, E.I., Dey, E.S. & Novik, G.I. 2010. Bacteriophage receptors, mechanisms of phage adsorption and penetration into host cell. *Pol. J. Microbiol.* **59**(3):145-55.
- Rashid, M.H. & Kornberg, A. 2000. Inorganic polyphosphate is needed for swimming, swarming, and twitching motilities of *Pseudomonas aeruginosa*. *Proc. Natl. Acad. Sci. USA.* **97**:4885-4890.
- Routier, S.J.M. 2010. DC1, a podoviridae with a putative cepacian depolymerase enzyme. MSc thesis. University of Alberta. Edmonton, Alberta, Canada.
- Sambrook, J., Fritsch, E.F., & Maniatis, T. 1989. *Molecular cloning: a laboratory manual.*, Cold Springs Harbor Laboratory Press, Cold Springs Harbor, New York.
- Sandkvist, M. 2001. Biology of type II secretion. *Mol. Microbiol.* **40**:271-283.
- Schägger, H. & Von Jagow, G. 1987. Tricine-sodium dodecyl sulfate-polyacrylamide gel electrophoresis for the separation of proteins in the range from 1 to 100 kDa. *Anal., Biochem.* **166**:368-379.
- Schägger, H. 2006. Tricine-SDS-PAGE. *Nature Protocols* **1**:16-22.

- Seed, K.D. & Dennis, J.J. 2009. Experimental bacteriophage therapy increases survival of *Galleria mellonella* larvae infected with clinically relevant strains of the *Burkholderia cepacia* complex. *Antimicrob. Agents Chemother.* **53**:2205-2208.
- Seed, K.D. & Dennis, J.J. 2005. Isolation and characterization of bacteriophages of the *Burkholderia cepacia* complex. *FEMS Microbiol. Lett.* **251**:273-280.
- Shan, Z., Xu, H., Shi, X., Yu, Y., Yao, H., Zhang, X., Bai, Y., Gao, C., Saris, P.E.J. & Qiao, M. 2004. Identification of two new genes involved in twitching motility in *Pseudomonas aeruginosa*. *Microbiology.* **150**:2653-2661.
- Sillankorva, S., Oliveira, R., Vieira, M.J., Sutherland, I. & Azeredo, J. 2004. *Pseudomonas fluorescens* infection by bacteriophage PhiS1: the influence of temperature, host growth phase and media. *FEMS Microbiol. Lett.* **241**(1):13-20.
- Srivastava, M., Tucker, M.S., Gulig, P.A. & Wright, A.C. 2009. Phase variation, capsular polysaccharide, pilus and flagella contribute to uptake of *Vibrio vulnificus* by the Eastern oyster (*Crassostrea virginica*). *Environ. Microbiol.* **11**(8):1934-44.
- Stathopoulos, C., Hendrixson, D.R., Thanassi, D.G., Hultgren, S.J., St. Geme III, J.W. & Curtiss III, R. 2000. Secretion of virulence determinants by the general secretory pathway in Gram-negative pathogens: An evolving story. *Microb. Infect.* **2**:1061-1072.
- Steinbacher, S., Miller, S. *et al.*, 1997. Phage P22 tailspike protein: crystal structure of the head-binding domain at 2.3 Å, fully refined structure of the endorhamnosidase at 1.56 Å resolution, and the molecular basis of O-antigen recognition and cleavage. *J. Mol. Biol.* **267**(4):865-80.
- Summers, W.C. 2001. Bacteriophage therapy. *Annu. Rev. Microbiol.* **55**:437-51.
- Suttle, C.A. 2005. Viruses in the sea. *Nature.* **437**(7057):356-61.
- Tanji, Y., Shimada, T., Yoichi, M., Miyanaga, K., Hori, K. & Unno, H. 2004. Toward rational control of *Escherichia coli* O157:H7 by a phage cocktail. *Appl. Microbiol. Biotechnol.* **64**:270-274.
- Traurig, M. & Misra, R. 1999. Identification of bacteriophage K20 binding regions of OmpF and lipopolysaccharide in *Escherichia coli* K-12. *FEMS Microbiol. Lett.* **181**(1):101-8.
- Vignon, G., Köhler, R., Larquet, E., Giroux, S., Prévost, M., Roux, P. & Pugsley, A.P. 2003. Type IV-like pili formed by the type II secretin: Specificity,

- composition, bundling, polar localization, and surface presentation of peptides. *J. Bacteriol.* **185**: 3416-3428.
- Vinion-Dubiel, A.D. & Goldberg, J.B. 2003. Lipopolysaccharide of *Burkholderia cepacia* Complex. *J. Endotoxin. Res.* **9**:201-213.
- Wang, J., Hofnung, M., & Charbit, A. 2000. The C-terminal portion of the tail fiber protein of bacteriophage lambda is responsible for binding to LamB, its receptor at the surface of *Escherichia coli* K-12. *J. Bacteriol.* **182**(2):508-12.
- Wang, J., Michel, V., Hofnung, M. & Charbit, A. 1998. Cloning of the J gene of bacteriophage lambda, expression and solubilization of the J protein: first in vitro studies on the interactions between J and LamB, its cell surface receptor. *Res. Microbiol.* **149**(9):611-24.
- Wilson, K. 2001. Preparation of genomic DNA from bacteria. In *Current protocols in molecular biology.* **2**.
- Yoichi, M., Abe, M., Miyanaga, K., Unno, H. & Tanji, Y. 2005. Alteration of tail fiber protein gp38 enables T2 phage to infect *Escherichia coli* O157:H7. *J. Biotechnol.* **115**(1):101-7.
- Yu, F. & Mizushima, S. 1982. Roles of lipopolysaccharide and outer membrane protein OmpC of *Escherichia coli* K-12 in the receptor function for bacteriophage T4. *J. Bacteriol.* **151**(2):718-22.
- Zayas, M. & Villafane, R. 2006. Identification of the *Salmonella* phage epsilon 34 tailspike gene. *Gene.* **386**(1-2):211-7.
- Zhilenkov, E.L., Popova, V.M. *et al.*, 2006. The ability of flagellum-specific *Proteus vulgaris* bacteriophage PV22 to interact with *Campylobacter jejuni* flagella in culture. *Virol. J.* **27**;3:50.